# MIND THE TIME:
## 24-hour rhythms in drug exposure and effect

Laura Kervezee

# Mind the time:
# 24-hour rhythms in drug exposure and effect

Laura Kervezee

# Mind the time:
# 24-hour rhythms in drug exposure and effect

Proefschrift

ter verkrijging van
de graad van Doctor aan de Universiteit Leiden,
op gezag van Rector Magnificus prof.mr. C.J.J.M. Stolker,
volgens besluit van het College voor Promoties
te verdedigen op dinsdag 10 januari 2017
klokke 16:15 uur

door

Laura Kervezee

geboren te 's Gravenhage
in 1989

*Each time I study an organism under controlled, timeless conditions and watch it wake with a rising sun that it cannot see or feel, I am enthralled and filled with the wonder of nature.*

- J.D. Palmer, Cycles of nature (1990)

# TABLE OF CONTENTS

# CHAPTER

## General introduction

# 1

A thorough understanding of the underlying physiological processes that determine a drug's exposure and effect is required to address the challenges encountered during the development or optimisation of new and existing drug therapies. A ubiquitous feature of many physiological processes is their systematic variation over the course of the 24-hour day. As a result of the rhythmic nature of physiology, the exposure and effect of drugs could be influenced by the time of day that they are administered. In this chapter, the origin of these 24-hour rhythms will be discussed first. Next, an overview is given of the 24-hour variation in physiological processes and how these impact the exposure and effect of drugs. The current approaches of chronopharmacology, the branch of chronobiology that studies the effect of dosing time on drug treatments, will be summarized and some of the challenges will be identified. Finally, it will be discussed how the tools that have been developed within the field of pharmacometrics can be applied to benefit chronopharmacological research. This chapter lays the foundation for the research presented in this thesis.

## THE ORGANISATION OF THE BIOLOGICAL CLOCK

Organisms across all kingdoms of life, from bacteria to mammals, possess an endogenous timing system that generates daily variations in biological processes. This timing system, termed the circadian clock, is thought to have emerged early in evolutionary history as an adaptation to the cyclic changes in light, temperature and food availability present on Earth (Schibler and Sassone-Corsi, 2002). The current understanding of the complex organisation of the circadian clock will be briefly summarised here.

As shown in Figure 1A, the circadian timing system consists of an input pathway that detects cyclic changes in the environment, a central clock where this input is integrated and an output pathway that conveys this information from the central clock to the periphery. A major input signal of the circadian timing system in mammals is light, which is transmitted from the retina to the central clock located in the suprachiasmatic nuclei (SCN) of the hypothalamus (Dibner et al., 2010).

Cells in the SCN show a self-sustained circadian rhythm. These rhythms are generated by a molecular transcriptional/translational feedback loop that consists of positive and negative limbs (Mohawk et al., 2012). In short, a heterodimer consisting of CLOCK and BMAL1 proteins binds to E-box domains of *per* and *cry* genes (among others), thereby activating the transcription of these genes. After translation, PER and CRY proteins dimerize, translocate to the nucleus and suppress the activity of CLOCK and BMAL1, thereby effectively inhibiting their own transcription. PER and CRY are degraded and, as a results of their declining levels, the CLOCK:BMAL1 dimer can resume its transcriptional activity. A variety of auxiliary core clock components and post-translational modifications add to the robustness of this mechanism, creating a molecular feedback loop in each SCN neuron that autonomously sustains a rhythm with a period of approximately 24 hours (Figure 1B).

The translational/transcriptional feedback loop is not unique to the cells of the SCN. In fact, most cell types in the body express a similar set of clock genes (Balsalobre et al., 1998; Zylka et al., 1998) that can oscillate autonomously (Welsh et al., 2004). However,
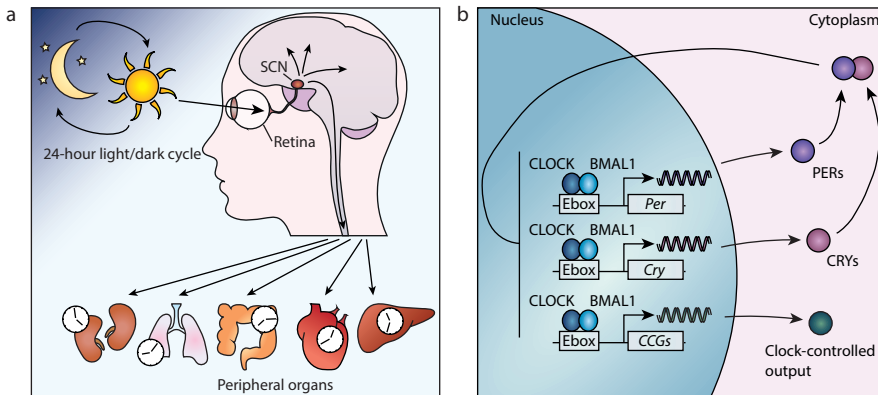
**Figure 1** Organisation of the circadian timing system at (A) the level of the organism and (B) of the cell. **(A)** The biological clock is located in the suprachiasmatic nuclei (SCN). Light information from the environment is transmitted from the retina to the SCN in the hypothalamus. Neuronal and humoral signals from the SCN synchronize the circadian oscillators in peripheral organs. **(B)** At the cellular level, a 24-hour rhythm is generated by a translational/transcriptional feedback loop. The transcription factors CLOCK and BMAL1 bind to E-box elements in the promotor of other clock genes (period1,2 and cryptochrome1,2) and of clock-controlled genes (CCGs), thereby activating their transcription. After translation in the cytoplasm, PER and CRY dimerize and translocate to the nucleus, where they inhibit the transcriptional activity of CLOCK and BMAL1. Hereby, they downregulate their own transcription. This (simplified) process creates oscillations in gene expression with a period of approximately 24 hours.

three properties unique to SCN cells have led to the distinction of the central clock in the SCN and peripheral clocks in other brain regions and organs (Welsh et al., 2010). Firstly, the phase of SCN neurons is directly modulated by photic input; that is, these cells can be entrained by environmental light information that is conveyed from the retina via the retinohypothalamic tract to the SCN. Secondly, SCN neurons are tightly coupled, so their rhythm remains synchronized even in the absence of any oscillating input. Thirdly, their firing rate shows pronounced circadian variation, by which they directly and indirectly synchronize other cells in the body (Welsh et al., 2010). Other cell types in the body do not share these properties. Instead, synchronisation among cells within a tissue, and of a tissue with the external light/dark cycle, relies on the rhythmic output generated by the SCN, which is transmitted via various mechanisms, including neuronal connections, endocrine signalling and indirect cues conveyed by oscillations in body temperature or behaviour (Dibner et al., 2010). In the absence of synchronizing signals, tissues as a whole rapidly lose their rhythmicity due to subtle differences in the period length between the individual cells (Nagoshi et al., 2004; Welsh et al., 2004).

The core clock genes do not only regulate their own expression, but also that of clock controlled genes. Early microarray studies revealed that up to 10% of genes in the SCN and the liver show circadian expression patterns (Panda et al., 2002). More recently, it was shown that 43% of all genes in mice are rhythmically transcribed in at least one organ (Zhang et al., 2014). Through these fluctuations in gene expression, the circadian timing system controls a wide range of physiological processes, such as metabolism, heart rate, renal function and hormone levels (Duguay and Cermakian, 2009).

In the context of this thesis, it is important to emphasize the correct use of the word "circadian". Although frequently used more loosely outside the field of chronobiology, a circadian rhythm refers, by definition, to a rhythm with a period of approximately 24 hours that is autonomous and therefore persists under constant conditions. The terms "diurnal", "daily" or "24-hour" can be used to describe any rhythm with a period of 24 hours, regardless of whether it is endogenously generated or caused by rhythms in light exposure, social cues, or activity (Klerman, 2005). Therefore, research on the effect of time of day in any biological process that is conducted in the presence of environmental cues that exhibit a 24-hour variation, like most clinical trials, do not study circadian rhythmicity, but rather 24-hour, diurnal or daily rhythmicity. This distinction is important for the correct understanding and interpretation of chronobiological research (Klerman, 2005).

## THE EFFECT OF PHYSIOLOGICAL RHYTHMS ON DRUG TREATMENTS

Twenty-four hour rhythms in physiological processes are known to influence the exposure and effect of numerous drugs (Dallmann et al., 2014). The existence of these rhythms implies that the effectiveness of a drug may depend on dosing time and that there may be an optimal time of administration for any given drug. Therefore, although often overlooked, the rhythmic nature of mammalian physiology is a source of variation that could have
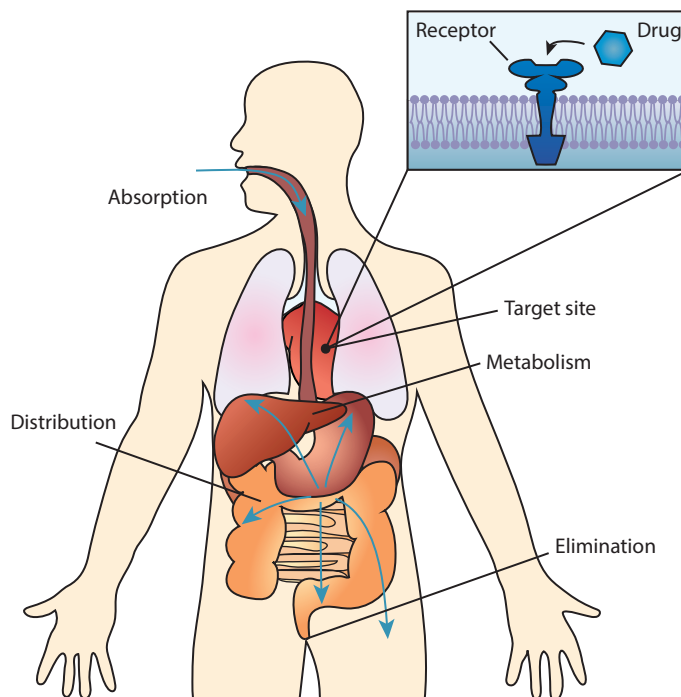


**Figure 2** Overview of the processes that determine the exposure (pharmacokinetics) and effect (pharmacodynamics) of a drug. The exposure to a drug in the body is determined by the rate and extent of absorption, distribution, metabolism and elimination. The effect is determined by the interaction between the drug and its receptor at the target site.

important implications for the design of new and existing drug therapies. This section will give an overview of the rhythms in physiological processes and provide some examples of how the exposure (pharmacokinetics) and effect (pharmacodynamics) of a drug (Figure 2) are influenced by the time of day.

**Pharmacokinetics**

Pharmacokinetics refers to the fate of a drug in the body from the moment it is administered until it is eliminated. The pharmacokinetics of a drug is defined by its absorption, distribution, metabolism and elimination. Collectively known as ADME, these properties determine the exposure and the shape of the concentration-time profile of a drug in the body. The four ADME properties and the extent to which they show 24-hour variation will be briefly discussed here.

*Absorption*
Depending on the route of administration, a drug needs to be absorbed before it reaches the systemic circulation. Following oral administration, a compound passes through the gastrointestinal tract, crosses the intestinal wall and reaches the liver via the portal vein, after which it enters the bloodstream. Absorption is affected by system- and drug-specific factors, such as gastric emptying time, the pH of the gastrointestinal tract, gastrointestinal blood flow, intestinal motility, function of transporter enzymes, first-pass effects, as well as the solubility and permeability of the compound (Martinez and Amidon, 2002).

Many processes involved in drug absorption show 24-hour or circadian variation (Baraldo, 2008). For example, in humans, intestinal motility (Keller et al., 2001; Kumar et al., 1986; Rao et al., 2001), gastric emptying rate (Goo et al., 1987) and hepatic blood flow (Lemmer and Nold, 1991) are higher in the morning than in the evening or night. In line with these findings, many drugs, including roflumilast, nifedipine, cilostazol, and paracetamol, are absorbed most rapidly in the morning (Bethke et al., 2010; Kamali et al., 1987; Lee et al., 2014; Lemmer et al., 1991). Daily variation in the rate of drug absorption influences the peak concentration ($C_{max}$) and the time to the peak concentration ($T_{max}$) (Baraldo, 2008). This could be relevant for drugs with a narrow therapeutic window, or for drugs whose effect depends on the $C_{max}$ or the period of time that the concentration is above a critical concentration, as is the case for many antibiotics (Drusano, 2004). Additionally, there is some evidence that dosing time affects the bioavailability of a drug after oral administration. The bioavailability of an immediate-release formulation of nifedipine, a calcium channel blocker used for the treatment of hypertension, was 40% lower after administration in the evening compared to the morning (Lemmer et al., 1991). This reduction was attributed to diurnal variation in the absorption of the drug, because neither a sustained-release formulation nor an intravenous solution of nifedipine showed dosing time dependent variations in exposure, excluding the effect of rhythmic metabolism (Lemmer et al., 1991). In theory, daily variations in the extent or rate of absorption may provide a rationale to adapt the dose depending on the time of day, but this has not been applied clinically.
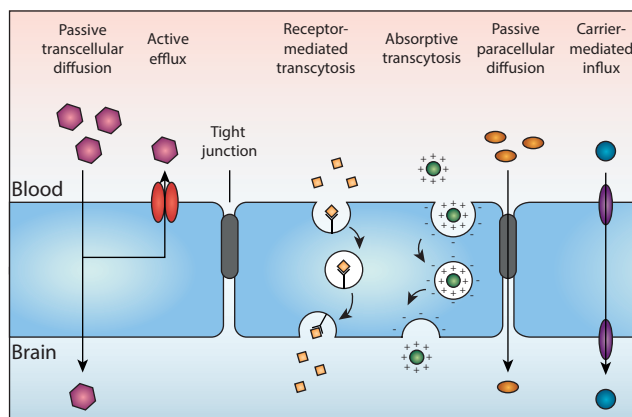
**Figure 3 Routes of transport across the blood-brain barrier.** Molecules, including therapeutic drugs, may enter the brain via passive transcellular or paracellular diffusion. Efflux transporters actively pump their substrates out of the brain through an energy-dependent process. Molecules, including hormones and albumin, also enter via receptor-mediated or absorptive transcytosis. Specialized influx transporters facilitate the entry of their substrates to the brain.

*Distribution*

After reaching the circulation, a drug travels through the bloodstream and moves into and out of the various sites of the body, a process known as distribution. The distribution of a drug is a critical determinant of its concentration at the target site and thereby, ultimately, of its effectiveness. Whether a drug is primarily retained in the blood or whether it mainly concentrates in organs or tissues depends partly on its physicochemical properties, like lipophilicity and molecular size. However, physiological processes such as organ blood flow, active transport and plasma protein binding, also play an important role in the rate and extent of distribution (Danhof et al., 2007). Given the focus of this thesis, the importance of 24-hour variation in drug distribution will be discussed here in the context of drugs targeted at the central nervous system (CNS).

A better understanding of the underlying mechanisms that regulate the transport of drugs between the blood to the brain is required to increase the success rate of treatments targeted at CNS disorders (de Lange and Hammarlund-Udenaes, 2015). More specifically, knowledge on 24-hour variation in the processes that regulate drug distribution in the CNS may lead to better informed dosing decisions by providing insight into the effect of dosing time on the concentration at the target site.

Unlike most peripheral tissues, the distribution of drugs and other potentially toxic compounds to and within the brain is limited because of the existence of a specialized barrier called the blood-brain barrier (BBB). The BBB is made up of a layer of endothelial cells that line the wall of the brain capillaries and that are connected by tight junctions. Tight junctions are multiprotein complexes that effectively restrict the paracellular diffusion of drugs and other molecules (Keaney and Campbell, 2015). Therefore, the transport of molecules to and from the brain takes place primarily via transcellular pathways (Figure 3). These pathways include passive or facilitated diffusion, active influx and efflux by membrane transporters

and receptor- or adsorptive-mediated transcytosis (Abbott, 2013). Active efflux transport involves the movement of molecules from the CNS back into the circulation by specialized transporter proteins. One of the best-studied efflux transporters is P-glycoprotein (P-gp), which is expressed in the BBB as well as in the blood-cerebral spinal fluid (BCSFB) and in various parenchymal cell types such as neurons and glial cells (de Lange, 2013; Stieger and Gao, 2015). P-gp has broad substrate specificity and restricts the distribution of a wide variety of drugs to the brain, forming a major challenge for the development of effective therapies for neurological disorders (Miller, 2010).

It is becoming increasingly clear that the transport across the BBB is highly dynamic and is influenced by both physiological processes such as the sleep-wake cycle and aging as well as pathophysiological conditions such as ischaemic stroke and infection (Keaney and Campbell, 2015). However, it is unknown if, and to what extent, the transport of drugs and endogenous compounds to and within the CNS is influenced by 24-hour variation in the mechanisms that regulate transport across this barrier.

The possibility that the transport of molecules, including therapeutic drugs, across of the BBB is influenced by the time of day is largely unexplored, but is not fully unsupported. For example, it has been shown that the effect of mannitol-induced osmotic opening of the BBB on the exposure to intravenously administered atenolol in brain extracellular fluid is 10x higher in the afternoon compared to the morning (de Lange et al., 1995). Other processes showing 24-hour variation that could conceivably influence drug distribution to the CNS depending on the time of day include cerebral blood flow (Conroy et al., 2005; Endo et al., 1990) and the production of cerebral spinal fluid (CSF) (Nilsson et al., 1992, 1994). Additionally, it has been shown in several *in vitro* and *in vivo* studies that that the expression and activity of P-gp in the liver and intestine exhibits 24-hour variation (Ando et al., 2005; Ballesta et al., 2011; Hayashi et al., 2010; Murakami et al., 2008; Okyar et al., 2012). However, it is unknown whether this applies to P-gp expression and activity in the CNS as well. Considering the large number of drugs that are a substrate for this and other efflux transporters, this question warrants further investigation.

*Metabolism*

Xenobiotic metabolism is mediated by two groups of enzymes that have distinct functional roles (Xu et al., 2005). The first group of enzymes activate or inactivate drugs through oxidation, reduction or hydroxylation. The cytochrome P450 (CYP) microsomal enzymes, which are mainly found in the liver, gastrointestinal tract, lung and kidney, are an important family of this group. The second group of enzymes catalyses conjugation reactions. This makes lipophilic compounds more hydrophilic, thereby facilitating their excretion into urine, faeces or bile. The expression of many of these metabolizing enzymes in the liver shows profound 24-hour variation, which is regulated by clock-controlled transcription factors (Gachon et al., 2006; Takiguchi et al., 2007). As a result, the metabolism of many drugs is influenced by the time of day (Dallmann et al., 2014). For example, acetaminophen (paracetamol) bioactivation and toxicity in mice, which is controlled by CYP enzymes,

shows 24-hour variation that appears to be at least partly regulated by the autonomous hepatocyte circadian clock (DeBruyne et al., 2014; Johnson et al., 2014). Also in humans, CYP3A activity, as measured by 6β-hydroxycortisol to cortisol ratio in urine, shows 24-hour variation with 2.8 fold higher activity between 17:00 and 21:00 than between 9:00 and 13:00 (Ohno et al., 2000).

*Elimination*
Drugs, and their metabolites, are excreted from the body through renal, biliary, pulmonary or faecal elimination. Diurnal rhythms have been found in many physiological processes that underlie renal elimination, the predominant route of drug excretion, including glomerular filtration rate, renal plasma flow, urine volume and the excretion of electrolytes in urine (Stow and Gumz, 2011). Of note, the variation in glomerular filtration rate and renal plasma flow persist when food and fluid intake as well as posture kept constant for the entire study duration, indicating the endogenous nature of these rhythms (Buijsen et al., 1994; Koopman et al., 1989; Voogel et al., 2001). In line with these findings, the renal clearance of various antibiotics, including amikacin and gentamicin, has been reported to depend on the time of day, with generally higher clearance during the day and lower clearance during the night in human subjects (Beauchamp and Labrecque, 2007). However, mechanistic links between the 24-hour variation in renal physiology and drug clearance at different times of the day have not been reported (Paschos et al., 2010).

**Pharmacodynamics**

Pharmacodynamics is the result of the interaction of a drug with its target. Recently, it was reported that the majority of best-selling drugs directly target the product of a gene that is rhythmically transcribed, suggesting that the effect of these drugs could depend on the time of day (Zhang et al., 2014). Indeed, the most successful examples of chronopharmacological interventions involve rhythmic targets and/or symptoms (Dallmann et al., 2014). For example, blood pressure shows clear 24-hour variation with a marked decrease during the night. In patients with hypertension, the absence of this night-time dip is associated with an increased risk of cardiac events (Ohkubo et al., 2002; Staessen, 1999; Verdecchia et al., 1994). It has been shown that patients that take at least one antihypertensive medication at bedtime, instead of upon awakening, have better blood pressure control and lower risk of developing cardiovascular events (Hermida et al., 2008, 2010).

The chronopharmacology of pain management has also received considerable attention due to the rhythmic nature of pain intensity (Junker and Wirz, 2010). Indeed, numerous studies have reported an effect of time-of-day on the action of analgesic drugs in humans, although the results with regards to the timing of these effects has been conflicting (Potts et al., 2011). Furthermore, the translation of these findings to clinical practice is difficult due to the heterogeneity in the nature and causes of pain, the large variation in pain among individuals as well as the difficulty to obtain an objective measure.

**Toxicity**

The toxicity of many types of drugs, such as aminoglycosides, anti-cancer drugs and acetaminophen (paracetamol), also varies over the 24-hour period, which should be considered when determining the most optimal time of drug administration (Paschos et al., 2010). Time-of-day dependent toxicity may arise from variation in the exposure to a drug or its toxic metabolites or from variation in the sensitivity of target cells. To discriminate between these two possibilities with regard to the anticancer drug cyclophosphamide, Gorbacheva et al (2005) combined pharmacokinetic analysis of this drug and its metabolites with measurements of the sensitivity of the hematopoietic system, the main target of cyclophosphamide toxicity, at different dosing times (Gorbacheva et al., 2005). Through an elegant series of experiments, the authors found that the 24-hour rhythm in the toxicity of cyclophosphamide is not related to variation in the exposure to this drug, but rather to the 24-hour rhythms in the sensitivity of B cells to cyclophosphamide, which is influenced by the activity of the clock genes CLOCK and BMAL1.

## CHRONOPHARMACOLOGY: APPROACHES & CHALLENGES

The previous section highlighted the ubiquitous nature of 24-hour rhythms in physiology and provided examples of its effect on the pharmacokinetics, pharmacodynamics and toxicity of drugs. Although the relevance of these rhythms to the optimisation of drug treatments has been recognized within the field of chronobiology, this body of knowledge has yet to reach clinical practice (Paschos et al., 2010). In this section, the current approaches that are used in chronopharmacology and the challenges pertaining to the translation of the findings to the clinic are discussed.

To study the effect of time of day on the pharmacokinetics, pharmacodynamics or toxicity of a drug, the most obvious approach is to administer the drug of interest at various times of the day and subsequently measure the exposure or effect of the drug at those time points. Although continuous infusions of more than 24 hours are occasionally used instead (Bienert et al., 2013; Elting et al., 1990; Fleming et al., 2015), most chronopharmacological research described in the previous section took this former approach. With such a study design, the ability to detect a significant time-of-day effect greatly depends on the choice and number of dosing times. As many studies only use two dosing times in the morning and the afternoon or evening (for instance: (Bethke et al., 2010; Bleyzac et al., 2000; Cao et al., 2010; Lee et al., 2014; Martin et al., 2002)), it is possible that the peak and trough of the variable of interest are outside the studied intervals. Hence, if no effect of dosing time is detected, this may either be due to absence of 24-hour variation on the pharmacokinetic or pharmacodynamic parameter(s) of interest, or due to an unfortunate choice of time-points, rendering the study inconclusive. This should be considered in the design of prospective chronopharmacological studies.

Another factor to take into consideration in chronopharmacological research in humans is the large degree of heterogeneity among the population. Individuals differ in their

amplitude and phase, introducing a source of variability to any chronopharmacological study. This interindividual variability is associated with chronotype (morningness/ eveningness), demographic variables, or circadian rhythm disturbance due to shift work or transmeridian travel (Kerkhof, 1985). Although these factors can be – at least partly – controlled for in order to minimize the degree of unexplained interindividual variability, this is usually not reported and/or included in chronopharmacological studies.

Another limitation of many chronopharmacological studies is that typically one drug is investigated without paying attention to the implications of the findings to other drugs. However, given the large number of drugs used in clinical practice, it is virtually impossible to investigate the effect of time of day on all available drugs. As the pharmacokinetic and pharmacodynamic properties are a function of the underlying physiological processes that are shared between many different types of drugs, as described in the previous section, this raises the possibility of studying 24-hour variation in physiological process(es) using a model compound that represents a group of drugs.

A relative recent development within the field of drug discovery and development is the use of statistical and mathematical methods to model the pharmacokinetics and pharmacodynamics of a drug and the associated sources of variability (Milligan et al., 2013). Many of the challenges in chronopharmacology that were discussed above, including the characterization of interindividual variability and quantification of the effect of time of day on pharmacokinetic of pharmacodynamic parameters, can be addressed by the field of pharmacometrics. The next section will highlight the potential benefits of applying this field to chronopharmacology.

## PHARMACOMETRICS AND CHRONOPHARMACOLOGY

Having evolved over the past four decades, pharmacometrics is a relatively new scientific discipline that is becoming an increasingly important tool in the development and optimisation of new and existing drug therapies (Milligan et al., 2013). Pharmacometrics is the science of developing and applying statistical and mathematical models to analyse the fate and effect of drugs in a biological system. Within the field of pharmacometrics, population pharmacokinetic-pharmacodynamic (PKPD) modelling is used to quantitatively describe the time course of drug exposure (pharmacokinetics), the relationship between exposure and effect (pharmacodynamics) and the associated sources of variability among the population (Mould and Upton, 2012). In this section, the application of PKPD modelling to the field of chronopharmacology is discussed.

### Effect of time of day in PKPD models

As discussed above, time of day may affect the pharmacokinetics and pharmacodynamics of a drug, thereby introducing a significant source of variation in the data. Although frequently overlooked in PKPD models, there are several examples available in the literature that show how the effect of time of day can be incorporated in such a model.

*Baseline variation in pharmacodynamic models*

In general, a pharmacodynamic model describes the link between the concentration or dose and the drug effect. Functions used to describe continuous pharmacodynamic effects can, for example, be linear or $E_{max}$ and can be either directly connected to the measured drug concentration or modelled as an indirect effect to account for a delay between the concentration and the effect (Mould and Upton, 2012). A pharmacodynamic model generally involves a function to describe the baseline of the measured response as well.

In pharmacodynamic models, the effect of time of day is most commonly incorporated when the baseline parameter of interest exhibits 24-hour variation. A well-known example is the 24-hour variation in the QT interval on an ECG recording. This variation can be accounted for by describing the baseline as a cosine function with one or multiple harmonics (Chain et al., 2011; Piotrovsky, 2005). Furthermore, 24-hour variation of endogenous cortisol levels have been described by an indirect response model with a synthesis rate that exhibits 24-hour variation (Krzyzanski et al., 2000). Other rhythmic baseline parameters that have been implemented in PKPD models include intraocular pressure (Luu et al., 2010), mevalonic acid concentration in plasma as a marker for cholesterol synthesis (Aoyama et al., 2010), gastric acid secretion (Puchalski et al., 2001), acetylcholinesterase activity (Han et al., 2012) and prolactin release (Friberg et al., 2009). Although informative, these studies did not regard the notion that the pharmacokinetics or the concentration-effect relationship may also exhibit 24-hour variation.

*Rhythmic variation in exposure or effect*

While characterisation of a rhythmic pharmacodynamic baseline can be performed by analysing off-drug data that are commonly collected in clinical trials, identification of rhythmic variation in the exposure or effect of a drug requires a more specialized study design that involves either the use of multiple dosing times (Krzyzanski et al., 2000) or prolonged exposure to a drug (i.e. sustained exposure for at least 24 hours). Therefore, potential 24-hour variation in the pharmacokinetics or in the response to a drug is investigated less frequently. However, several examples are available in the literature, among which two main approaches can be distinguished.

The first approach involves the use of covariates. In general, covariates are factors that influence pharmacokinetic of pharmacodynamic parameters, such as demographic variables, laboratory values or disease state (Mould and Upton, 2012). For example, inclusion of the effect of body weight in a model allows for dosing adjustments based on weight in order to reach a more consistent drug exposure or effect among the population (Mould and Upton, 2012). In (pre-)clinical studies that involve multiple time-points of drug administration, different dosing times can also be investigated as potential covariates on the pharmacokinetic (Bienert et al., 2014; Chen et al., 2013; Musuamba et al., 2009; Salem et al., 2014) and/or pharmacodynamic (Fisher et al., 1992) parameters. Although often employed, this approach is of limited use as it only provides information at the discrete time points that were investigated in the study and therefore lacks predictive value for other time points.

Moreover, the notion that the time-dependent parameter may continue to change after dosing is neglected.

A second approach to study the 24-hour variation in the pharmacokinetics or pharmacodynamics of a drug is the addition of a trigonometric function with a fundamental component of 24 hours and - if supported by the data - multiple harmonic components, to a model parameter. This approach has been used previously in both population pharmacokinetic models (Bressolle et al., 1999; Lee et al., 2014; Tomalik-Scharte et al., 2014) as well as in a population pharmacodynamic model studying the effect of dosing time on the analgesic effect of fentanyl (Boom et al., 2010). In general, this approach enhances the predictive value of a model by providing a continuous description of a model parameter over the 24-hour period. Using this approach, the exposure or effect of a drug can be predicted or simulated at any time of the day instead of only at the dosing times used in the study.

**Population PKPD model development in a chronopharmacological context**

Typically, the development of any PKPD model starts by fitting a relatively simple model to a data set. By evaluating the model, misspecifications or biases can be identified and the model can subsequently be updated in an attempt to find a model that provides a better fit of the data. Like any mathematical model, a PKPD model is by definition a simplification of a real system and therefore no "true" or "right" model exists (Bonate, 2011). Certainly, some models are better representations of the real system than others, raising the question how one is to judge which model is "better" than another.

The general steps that are taken during the development of a PKPD model and the criteria to evaluate and compare the fit of these models have been extensively described elsewhere (Bonate, 2011; Mould and Upton, 2013; Upton and Mould, 2014). In this section, it will be discussed how to determine if there is an effect of time of day in pharmacokinetic or pharmacodynamic parameters.

*Time of day as a source of variation*
In a PKPD model, different sources of variability in the data, including interindividual variability, interoccasion variability (in a crossover design) and residual unexplained variability, can be distinguished and quantified. The degree of interindividual variability (IIV) on a model parameter shows the extent to which this parameter varies from individual to individual in the study population, whereas the degree of interoccasion variability (IOV) shows to what extent the parameter varies within an individual from one occasion to the next occasion (Bonate, 2011). The quantification of these different sources of variation are an important advantage of a PKPD model compared to traditional statistical methods that are commonly used to analyse the results of a clinical trial.

Time of day can also be regarded as a source of variation. In PKPD models based on studies involving multiple times of drug administration, boxplots of each parameter's interindividual variability (in studies with a parallel design) or interoccasion variability

(in studies with a crossover design) over dosing time may be informative. In theory, any bias present in these plots provides a rationale for investigating the inclusion of 24-hour variation in a model parameter. However, in most PKPD models in which a time-of-day effect is studied, the use of these types of plots to facilitate the identification of 24-hour variation in the model parameters is generally not reported.

*Time-of-day dependent bias in diagnostic plots*
An important aspect of model evaluation is the graphical examination of its goodness of fit. This includes the assessment of scatter plots of observed data versus population and individual predicted data and of the distribution of conditional weighted residuals with interaction (CWRESI) versus concentration or time after dose (Byon et al., 2013; Karlsson and Savic, 2007). In a chronopharmacological context, model diagnostic plots can be used to identify biases or misspecifications with regard to the time of day. For example, if 24-hour variation in any model parameter is not accounted for, a scatter plot of CWRESI over the time of day may show a time-dependent bias, indicating that the observed values are over-predicted at some time points and under-predicted at other time points. Such a bias was observed in a study into the chronopharmacology of cilostazol (Lee et al., 2014), which could be resolved by modelling the absorption rate constant as a cosine function with a period of 24 hours.

*Model selection*
An important concept in the selection of one PKPD model over the other is statistical significance: a model is generally selected if it provides a significantly better fit of the data. In population PKPD models, non-linear mixed effect modelling is used to estimate the parameter values that best fit the data. This involves a maximum likelihood approach (an extension of the least squares minimization used in linear regression), which returns an objective function value (OFV), a single numeric value that represents the fit the model (Mould and Upton, 2012). Whether a model provides a significantly better fit than another model is typically assessed by comparing their respective OFVs with the likelihood ratio test (for nested models), the Akaike information criterion or the Bayesian information criterion (Mould and Upton, 2013). These tests take into account the number of additional parameters that are added, such that a simpler model that fits the data equally well is chosen over a model which is more complex (i.e. which requires the estimation of more parameters). In a chronopharmacological context, for example, a cosine function with a fixed period of 24 hours to describe a model parameter, which requires the estimation of two additional parameters (the amplitude and the phase), is only included in a model if it provides a significantly better fit.

Physiological plausibility is another criterion for the selection of a model. For example, since renal function shows 24-hour variation (Wuerzner et al., 2014), it is biologically plausible that the clearance of a renally eliminated drug shows 24-hour variation, while a mechanistic reason for a 24-hour rhythm in the volume of distribution may be more difficult

to conceive. In case both models fit the data equally well, the model with more biological plausibility should be selected.

The clinical relevance of a model is also important. Daily variation in pharmacokinetics and/or pharmacodynamics may impact dosing decisions, as has been shown for chemotherapeutic agents in the treatment of different types of cancer (Lévi et al., 2010). However, this is not always the case. In a study investigating the chronopharmacokinetics of midazolam, it was found that the hepatic clearance of this drug shows statistically significant 24-hour variation that could be described by a single cosine function (Tomalik-Scharte et al., 2014). However, the relative amplitude of this function was 10%, which was lower than the degree of residual unexplained variability in the data. The authors therefore concluded that the effect of dosing time is not clinically relevant and does not influence therapeutic decisions.

Lastly, the predictive value of a model should be considered. In a chronopharmacological context, a model in which the 24-hour variation in a parameter is described by a continuous (e.g. sinusoidal) function allows for the estimation and simulation of the parameter at any time of the day, whereas the inclusion of different covariates representing different dosing times can only be used to estimate and simulate the parameter at the dosing times that were used in the original study.

In brief, this section provided an overview of the application of population PKPD modelling to the field of chronopharmacology, revealing several advantages over the use of traditional statistical methods. This includes a more rigorous quantification of the effect of time of day, the possibility of performing simulations as well as characterization of interindividual and interoccasion variability in the data.

## CONCLUSION

This chapter provided an overview of the influence of 24-hour rhythmicity in physiological processes on the pharmacokinetics and pharmacodynamics of drugs. From the extensive body of chronopharmacological research discussed in this chapter, a rather reductionist picture emerges. There are many examples that reveal the potential relevance of the 24-hour rhythms in physiology for the optimization of drug treatments scattered throughout the literature. However, a systematic approach to analyze and integrate these findings is lacking, which limits both the extrapolation of these findings to other types of drugs and the translation to clinical practice. In this light, PKPD modelling is a promising approach that may be able to overcome some of these limitations.

# REFERENCES

Abbott, N.J. (2013). Blood-brain barrier structure and function and the challenges for CNS drug delivery. J. Inherit. Metab. Dis. 36, 437–449.

Ando, H., Yanagihara, H., Sugimoto, K., Hayashi, Y., Tsuruoka, S., Takamura, T., Kaneko, S., and Fujimura, A. (2005). Daily rhythms of P-glycoprotein expression in mice. Chronobiol. Int. *22*, 655–665.

Aoyama, T., Omori, T., Watabe, S., Shioya, A., Ueno, T., Fukuda, N., and Matsumoto, Y. (2010). Pharmacokinetic/Pharmacodynamic Modeling and Simulation of Rosuvastatin Using an Extension of the Indirect Response Model by Incorporating a Circadian Rhythm. Biol. Pharm. Bull. *33*, 1082–1087.

Ballesta, A., Dulong, S., Abbara, C., Cohen, B., Okyar, A., Clairambault, J., and Levi, F. (2011). A combined experimental and mathematical approach for molecular-based optimization of irinotecan circadian delivery. PLoS Comput. Biol. *7*, e1002143.

Balsalobre, A., Damiola, F., and Schibler, U. (1998). A Serum Shock Induces Circadian Gene Expression in Mammalian Tissue Culture Cells. Cell *93*, 929–937.

Baraldo, M. (2008). The influence of circadian rhythms on the kinetics of drugs in humans. Expert Opin. Drug Metab. Toxicol. *4*, 175–192.

Beauchamp, D., and Labrecque, G. (2007). Chronobiology and chronotoxicology of antibiotics and aminoglycosides. Adv. Drug Deliv. Rev. *59*, 896–903.

Benedetti, M.S., Whomsley, R., Poggesi, I., Cawello, W., Mathy, F.-X., Delporte, M.-L., Papeleu, P., and Watelet, J.-B. (2009). Drug metabolism and pharmacokinetics. Drug Metab. Rev. *41*, 344–390.

Bethke, T.D., Huennemeyer, A., Lahu, G., and Lemmer, B. (2010). Chronopharmacology of roflumilast: a comparative pharmacokinetic study of morning versus evening administration in healthy adults. Chronobiol. Int. *27*, 1843–1853.

Bienert, A., Bartkowska-Sniatkowska, A., Wiczling, P., Rosada-Kurasińska, J., Grześkowiak, M., Zaba, C., Teżyk, A., Sokołowska, A., Kaliszan, R., and Grześkowiak, E. (2013). Assessing circadian rhythms during prolonged midazolam infusion in the pediatric intensive care unit (PICU) children. Pharmacol. Rep. *65*, 107–121.

Bienert, A., Płotek, W., Wiczling, P., Kostrzewski, B., Kamińska, A., Billert, H., Szczesny, D., Zaba, C., Teżyk, A., Buda, K., et al. (2014). The influence of the time of day on midazolam pharmacokinetics and pharmacodynamics in rabbits. Pharmacol. Rep. *66*, 143–152.

Bleyzac, N., Allard-Latour, B., Laffont, A., Mouret, J., Jelliffe, R., and Maire, P. (2000). Diurnal changes in the pharmacokinetic behavior of amikacin. Ther. Drug Monit. *22*, 307–312.

Bonate, P.L. (2011). Pharmacokinetic-Pharmacodynamic Modeling and Simulation (New York: Springer Science & Business Media).

Boom, M., Grefkens, J., van Dorp, E., Olofsen, E., Lourenssen, G., Aarts, L., Dahan, A., and Sarton, E. (2010). Opioid chronopharmacology: influence of timing of infusion on fentanyl's analgesic efficacy in healthy human volunteers. J. Pain Res. *3*, 183–190.

Bressolle, F., Joulia, J.M., Pinguet, F., Ychou, M., Astre, C., Duffour, J., and Gomeni, R. (1999). Circadian rhythm of 5-fluorouracil population pharmacokinetics in patients with metastatic colorectal cancer. Cancer Chemother. Pharmacol. *44*, 295–302.

Buijsen, J.G., van Acker, B.A., Koomen, G.C., Koopman, M.G., and Arisz, L. (1994). Circadian rhythm of glomerular filtration rate in patients after kidney transplantation. Nephrol.Dial.Transplant. *9*, 1330–1333.

Byon, W., Smith, M.K., Chan, P., Tortorici, M.A., Riley, S., Dai, H., Dong, J., Ruiz-Garcia, A., Sweeney, K., and Cronenberger, C. (2013). Establishing best practices and guidance in population modeling: an experience with an internal population pharmacokinetic analysis guidance. CPT Pharmacometrics Syst. Pharmacol. *2*, e51.

Cao, Q.-R., Cui, J.-H., Park, J.B., Han, H.-K., Lee, J., Oh, K.T., Park, I., and Lee, B.-J. (2010). Effect of food components and dosing times on the oral pharmacokinetics of nifedipine in rats. Int. J. Pharm. *396*, 39–44.

Chain, A.S.Y., Krudys, K.M., Danhof, M., and Della Pasqua, O. (2011). Assessing the probability of drug-induced QTc-interval prolongation during clinical drug development. Clin. Pharmacol. Ther. *90*, 867–

875.

Chen, R., Li, J., Hu, W., Wang, M., Zou, S., and Miao, L. (2013). Circadian variability of pharmacokinetics of cisplatin in patients with non-small-cell lung carcinoma: analysis with the NONMEM program. Cancer Chemother. Pharmacol. *72*, 1111–1123.

Conroy, D.A., Spielman, A.J., and Scott, R.Q. (2005). Daily rhythm of cerebral blood flow velocity. J. Circadian Rhythms *3*, 3.

Dallmann, R., Brown, S.A., and Gachon, F. (2014). Chronopharmacology: new insights and therapeutic implications. Annu. Rev. Pharmacol. Toxicol. *54*, 339–361.

Danhof, M., de Jongh, J., De Lange, E.C.M., Della Pasqua, O., Ploeger, B.A., and Voskuyl, R.A. (2007). Mechanism-based pharmacokinetic-pharmacodynamic modeling: biophase distribution, receptor theory, and dynamical systems analysis. Annu. Rev. Pharmacol. Toxicol. *47*, 357–400.

DeBruyne, J.P., Weaver, D.R., and Dallmann, R. (2014). The hepatic circadian clock modulates xenobiotic metabolism in mice. J. Biol. Rhythms *29*, 277–287.

Dibner, C., Schibler, U., and Albrecht, U. (2010). The mammalian circadian timing system: organization and coordination of central and peripheral clocks. Annu. Rev. Physiol. *72*, 517–549.

Drusano, G.L. (2004). Antimicrobial pharmacodynamics: critical interactions of "bug and drug". Nat. Rev. Microbiol. *2*, 289–300.

Duguay, D., and Cermakian, N. (2009). The crosstalk between physiology and circadian clock proteins. Chronobiol. Int. *26*, 1479–1513.

Elting, L., Bodey, G.P., Rosenbaum, B., and Fainstein, V. (1990). Circadian variation in serum amikacin levels. J. Clin. Pharmacol. *30*, 798–801.

Endo, Y., Jinnai, K., Endo, M., Fujita, K., and Kimura, F. (1990). Diurnal variation of cerebral blood flow in rat hippocampus. Stroke *21*, 1464–1469.

Fisher, L.E., Ludwig, E.A., Wald, J.A., Sloan, R.R., Middleton, E., and Jusko, W.J. (1992). Pharmacokinetics and pharmacodynamics of methylprednisolone when administered at 8 AM versus 4 PM. Clin. Pharmacol. Ther. *51*, 677–688.

Fleming, G.F., Schumm, P., Friberg, G., Ratain, M.J., Njiaju, U.O., and Schilsky, R.L. (2015). Circadian variation in plasma 5-fluorouracil concentrations during a 24 hour constant-rate infusion. BMC Cancer *15*, 1075.

Friberg, L.E., Vermeulen, A.M., Petersson, K.J.F., and Karlsson, M.O. (2009). An agonist-antagonist interaction model for prolactin release following risperidone and paliperidone treatment. Clin. Pharmacol. Ther. *85*, 409–417.

Gachon, F., Olela, F.F., Schaad, O., Descombes, P., and Schibler, U. (2006). The circadian PAR-domain basic leucine zipper transcription factors DBP, TEF, and HLF modulate basal and inducible xenobiotic detoxification. Cell Metab. *4*, 25–36.

Goo, R.H., Moore, J.G., Greenberg, E., and Alazraki, N.P. (1987). Circadian variation in gastric emptying of meals in humans. Gastroenterology *93*, 515–518.

Gorbacheva, V.Y., Kondratov, R. V, Zhang, R., Cherukuri, S., Gudkov, A. V, Takahashi, J.S., and Antoch, M.P. (2005). Circadian sensitivity to the chemotherapeutic agent cyclophosphamide depends on the functional status of the CLOCK/BMAL1 transactivation complex. Proc. Natl. Acad. Sci. U. S. A. *102*, 3407–3412.

Han, S., Lee, J., Jeon, S., Hong, T., and Yim, D.-S. (2012). Mixed-effect circadian rhythm model for human erythrocyte acetylcholinesterase activity--application to the proof of concept of cholinesterase inhibition by acorn extract in healthy subjects with galantamine as positive control. Eur. J. Clin. Pharmacol. *68*, 599–605.

Hayashi, Y., Ushijima, K., Ando, H., Yanagihara, H., Ishikawa, E., Tsuruoka, S.-I., Sugimoto, K.-I., and Fujimura, A. (2010). Influence of a time-restricted feeding schedule on the daily rhythm of abcb1a gene expression and its function in rat intestine. J. Pharmacol. Exp. Ther. *335*, 418–423.

Hermida, R.C., Ayala, D.E., Fernández, J.R., and Calvo, C. (2008). Chronotherapy improves blood pressure control and reverts the nondipper pattern in patients with resistant hypertension. Hypertension *51*, 69–76.

Hermida, R.C., Ayala, D.E., Mojón, A., and Fernández, J.R. (2010). Influence of circadian time of hypertension treatment on cardiovascular risk: results of the MAPEC study. Chronobiol. Int. *27*, 1629–1651.

Johnson, B.P., Walisser, J.A., Liu, Y., Shen, A.L., McDearmon, E.L., Moran, S.M., McIntosh, B.E., Vollrath, A.L., Schook, A.C., Takahashi, J.S., et al. (2014). Hepatocyte circadian clock controls acetaminophen bioactivation through NADPH-cytochrome P450 oxidoreductase. PNAS *111*, 18757 - 18762.

Junker, U., and Wirz, S. (2010). Review article: chronobiology: influence of circadian rhythms on the therapy of severe pain. J. Oncol. Pharm. Pract. *16*, 81–87.

Kamali, F., Fry, J.R., and Bell, G.D. (1987). Temporal variations in paracetamol absorption and metabolism in man. Xenobiotica; *17*, 635–641.

Karlsson, M.O., and Savic, R.M. (2007). Diagnosing model diagnostics. Clin. Pharmacol. Ther. *82*, 17–20.

Keaney, J., and Campbell, M. (2015). The dynamic blood-brain barrier. FEBS J. *282*, 4067–4079.

Keller, J., Groger, G., Cherian, L., Gunther, B., and Layer, P. (2001). Circadian coupling between pancreatic secretion and intestinal motility in humans. Am J Physiol Gastrointest Liver Physiol *280*, G273–G278.

Kerkhof, G.A. (1985). Inter-individual differences in the human circadian system: A review. Biol. Psychol. *20*, 83–112.

Klerman, E.B. (2005). Clinical aspects of human circadian rhythms. J. Biol. Rhythms *20*, 375–386.

Koopman, M.G., Koomen, G.C., Krediet, R.T., de Moor, E.A., Hoek, F.J., and Arisz, L. (1989). Circadian rhythm of glomerular filtration rate in normal individuals. Clin. Sci. (Lond). *77*, 105–111.

Krzyzanski, W., Chakraborty, A., and Jusko, W.J. (2000). Algorithm for application of Fourier analysis for biorhythmic baselines of pharmacodynamic indirect response models. Chronobiol. Int. *17*, 77–93.

Kumar, D., Wingate, D., and Ruckebusch, Y. (1986). Circadian variation in the propagation velocity of the migrating motor complex. Gastroenterology *91*, 926–930.

de Lange, E.C.M. (2013). The mastermind approach to CNS drug therapy: translational prediction of human brain distribution, target site kinetics, and therapeutic effects. Fluids Barriers CNS *10*, 12.

de Lange, E., and Hammarlund-Udenaes, M. (2015). Translational aspects of blood-brain barrier transport and central nervous system effects of drugs: From discovery to patients. Clin. Pharmacol. Ther. *97*, 380–394.

de Lange, E.C., Hesselink, M.B., Danhof, M., de Boer, A.G., and Breimer, D.D. (1995). The use of intracerebral microdialysis to determine changes in blood-brain barrier transport characteristics. Pharm. Res. *12*, 129–133.

Lee, D., Son, H., Lim, L.A., and Park, K. (2014). Population pharmacokinetic analysis of diurnal and seasonal variations of plasma concentrations of cilostazol in healthy volunteers. Ther. Drug Monit. *36*, 771–780.

Lemmer, B., and Nold, G. (1991). Circadian changes in estimated hepatic blood flow in healthy subjects. Br. J. Clin. Pharmacol. *32*, 627–629.

Lemmer, B., Nold, G., Behne, S., and Kaiser, R. (1991). Chronopharmacokinetics and Cardiovascular Effects of Nifedipine. Chronobiol. Int. *8*, 485–494.

Lévi, F., Okyar, A., Dulong, S., Innominato, P.F., and Clairambault, J. (2010). Circadian timing in cancer treatments. Annu. Rev. Pharmacol. Toxicol. *50*, 377–421.

Luu, K.T., Raber, S.R., Nickens, D.J., and Vicini, P. (2010). A model-based meta-analysis of the effect of latanoprost chronotherapy on the circadian intraocular pressure of patients with glaucoma or ocular hypertension. Clin. Pharmacol. Ther. *87*, 421–425.

Martin, P.D., Mitchell, P.D., and Schneck, D.W. (2002). Pharmacodynamic effects and pharmacokinetics of a new HMG-CoA reductase inhibitor, rosuvastatin, after morning or evening administration in healthy volunteers. Br. J. Clin. Pharmacol. *54*, 472–477.

Martinez, M.N., and Amidon, G.L. (2002). A mechanistic approach to understanding the factors affecting drug absorption: a review of fundamentals. J. Clin. Pharmacol. *42*, 620–643.

Miller, D.S. (2010). Regulation of P-glycoprotein and other ABC drug transporters at the blood-brain barrier. Trends Pharmacol. Sci. *31*, 246–254.

Milligan, P.A., Brown, M.J., Marchant, B., Martin, S.W., van der Graaf, P.H., Benson, N., Nucci, G., Nichols,

D.J., Boyd, R.A., Mandema, J.W., et al. (2013). Model-based drug development: a rational approach to efficiently accelerate drug development. Clin. Pharmacol. Ther. *93*, 502–514.

Mohawk, J.A., Green, C.B., and Takahashi, J.S. (2012). Central and peripheral circadian clocks in mammals. Annu. Rev. Neurosci. *35*, 445–462.

Mould, D.R., and Upton, R.N. (2012). Basic concepts in population modeling, simulation, and model-based drug development. CPT Pharmacometrics Syst. Pharmacol. *1*, e6.

Mould, D.R., and Upton, R.N. (2013). Basic concepts in population modeling, simulation, and model-based drug development-part 2: introduction to pharmacokinetic modeling methods. CPT Pharmacometrics Syst. Pharmacol. *2*, e38.

Murakami, Y., Higashi, Y., Matsunaga, N., Koyanagi, S., and Ohdo, S. (2008). Circadian clock-controlled intestinal expression of the multidrug-resistance gene mdr1a in mice. Gastroenterology *135*, 1636–1644.e3.

Musuamba, F.T., Mourad, M., Haufroid, V., Delattre, I.K., Verbeeck, R.K., and Wallemacq, P. (2009). Time of drug administration, CYP3A5 and ABCB1 genotypes, and analytical method influence tacrolimus pharmacokinetics: a population pharmacokinetic study. Ther. Drug Monit. *31*, 734–742.

Nagoshi, E., Saini, C., Bauer, C., Laroche, T., Naef, F., and Schibler, U. (2004). Circadian gene expression in individual fibroblasts: cell-autonomous and self-sustained oscillators pass time to daughter cells. Cell *119*, 693–705.

Nilsson, C., Ståhlberg, F., Thomsen, C., Henriksen, O., Herning, M., and Owman, C. (1992). Circadian variation in human cerebrospinal fluid production measured by magnetic resonance imaging. Am. J. Physiol. *262*, R20–R24.

Nilsson, C., Stahlberg, F., Gideon, P., Thomsen, C., and Henriksen, O. (1994). The nocturnal increase in human cerebrospinal fluid production is inhibited by a beta 1-receptor antagonist. Am J Physiol Regul. Integr. Comp Physiol *267*, R1445–R1448.

Ohkubo, T., Hozawa, A., Yamaguchi, J., Kikuya, M., Ohmori, K., Michimata, M., Matsubara, M., Hashimoto, J., Hoshi, H., Araki, T., et al. (2002). Prognostic significance of the nocturnal decline in blood pressure in individuals with and without high 24-h blood pressure: the Ohasama study. J. Hypertens. *20*, 2183–2189.

Ohno, M., Yamaguchi, I., Ito, T., Saiki, K., Yamamoto, I., and Azuma, J. (2000). Circadian variation of the urinary 6β-hydroxycortisol to cortisol ratio that would reflect hepatic CYP3A activity. Eur. J. Clin. Pharmacol. *55*, 861–865.

Okyar, A., Dressler, C., Hanafy, A., Baktir, G., Lemmer, B., and Spahn-Langguth, H. (2012). Circadian variations in exsorptive transport: in situ intestinal perfusion data and in vivo relevance. Chronobiol. Int. *29*, 443–453.

Panda, S., Antoch, M.P., Miller, B.H., Su, A.I., Schook, A.B., Straume, M., Schultz, P.G., Kay, S.A., Takahashi, J.S., and Hogenesch, J.B. (2002). Coordinated Transcription of Key Pathways in the Mouse by the Circadian Clock. Cell *109*, 307–320.

Paschos, G.K., Baggs, J.E., Hogenesch, J.B., and FitzGerald, G.A. (2010). The role of clock genes in pharmacology. Annu. Pharmacol Toxicol. *50:187-214*, 187–214.

Piotrovsky, V. (2005). Pharmacokinetic-pharmacodynamic modeling in the data analysis and interpretation of drug-induced QT/QTc prolongation. AAPS J. *7*, E609–E624.

Potts, A.L., Cheeseman, J.F., and Warman, G.R. (2011). Circadian rhythms and their development in children: implications for pharmacokinetics and pharmacodynamics in anesthesia. Paediatr. Anaesth. *21*, 238–246.

Puchalski, T.A., Krzyzanski, W., Blum, R.A., and Jusko, W.J. (2001). Pharmacodynamic modeling of lansoprazole using an indirect irreversible response model. J. Clin. Pharmacol. *41*, 251–258.

Rao, S.S.C., Sadeghi, P., Beaty, J., Kavlock, R., and Ackerson, K. (2001). Ambulatory 24-h colonic manometry in healthy humans. Am J Physiol Gastrointest Liver Physiol *280*, G629–G639.

Salem, A.H., Koenig, D., and Carlson, D. (2014). Pooled population pharmacokinetic analysis of phase I, II and III studies of linifanib in cancer patients. Clin. Pharmacokinet. *53*, 347–359.

Schibler, U., and Sassone-Corsi, P. (2002). A Web of Circadian Pacemakers. Cell *111*, 919–922.

Staessen, J.A. (1999). Predicting Cardiovascular Risk Using Conventional vs Ambulatory Blood Pressure in Older Patients With Systolic Hypertension. JAMA *282*, 539.

Stieger, B., and Gao, B. (2015). Drug Transporters in the Central Nervous System. Clin. Pharmacokinet. *54*, 225–242.

Stow, L.R., and Gumz, M.L. (2011). The Circadian Clock in the Kidney. J. Am. Soc. Nephrol. *22*, 598–604.

Takiguchi, T., Tomita, M., Matsunaga, N., Nakagawa, H., Koyanagi, S., and Ohdo, S. (2007). Molecular basis for rhythmic expression of CYP3A4 in serum-shocked HepG2 cells. Pharmacogenet. Genomics *17*, 1047–1056.

Tomalik-Scharte, D., Suleiman, A.A., Frechen, S., Kraus, D., Kerkweg, U., Rokitta, D., Di Gion, P., Queckenberg, C., and Fuhr, U. (2014). Population pharmacokinetic analysis of circadian rhythms in hepatic CYP3A activity using midazolam. J. Clin. Pharmacol. *54*, 1162–1169.

Upton, R.N., and Mould, D.R. (2014). Basic concepts in population modeling, simulation, and model-based drug development: part 3-introduction to pharmacodynamic modeling methods. CPT Pharmacometrics Syst. Pharmacol. *3*, e88.

Verdecchia, P., Porcellati, C., Schillaci, G., Borgioni, C., Ciucci, A., Battistelli, M., Guerrieri, M., Gatteschi, C., Zampi, I., Santucci, A., et al. (1994). Ambulatory blood pressure. An independent predictor of prognosis in essential hypertension. Hypertension *24*, 793–801.

Voogel, A.J., Koopman, M.G., Hart, A.A., van Montfrans, G.A., and Arisz, L. (2001). Circadian rhythms in systemic hemodynamics and renal function in healthy subjects and patients with nephrotic syndrome. Kidney Int. *59*, 1873–1880.

Welsh, D.K., Yoo, S.-H., Liu, A.C., Takahashi, J.S., and Kay, S.A. (2004). Bioluminescence imaging of individual fibroblasts reveals persistent, independently phased circadian rhythms of clock gene expression. Curr. Biol. *14*, 2289–2295.

Welsh, D.K., Takahashi, J.S., and Kay, S.A. (2010). Suprachiasmatic nucleus: cell autonomy and network properties. Annu. Rev. Physiol. *72*, 551–577.

Wuerzner, G., Firsov, D., and Bonny, O. (2014). Circadian glomerular function: from physiology to molecular and therapeutical aspects. Nephrol. Dial. Transplant *29*, 1475–1480.

Xu, C., Li, C.Y.-T., and Kong, A.-N.T. (2005). Induction of phase I, II and III drug metabolism/transport by xenobiotics. Arch. Pharm. Res. *28*, 249–268.

Zhang, R., Lahens, N.F., Ballance, H.I., Hughes, M.E., and Hogenesch, J.B. (2014). A circadian gene expression atlas in mammals: Implications for biology and medicine. Proc. Natl. Acad. Sci. *111*, 16219–16224.

Zylka, M.J., Shearman, L.P., Weaver, D.R., and Reppert, S.M. (1998). Three period Homologs in Mammals: Differential Light Responses in the Suprachiasmatic Circadian Clock and Oscillating Transcripts Outside of Brain. Neuron *20*, 1103–1110.

# CHAPTER

## Scope and intent of investigation

# 2

The aim of this thesis is to provide a structured framework for chronopharmacological studies, while concurrently touching upon several critical issues encountered during the development and optimization of new and existing drug treatments.

The general approach taken in this thesis to study the effect of the time of day on the pharmacokinetics, pharmacodynamics and/or side-effects of a drug involves the following three elements:

- The use of model compounds that can be used to study a physiological process;
- A strict study design that is optimally suited to evaluate the chronopharmacology of a drug, consisting of a sufficient number of dosing times distributed throughout the day and night;
- The use of PKPD modelling to characterize and quantify the extent of 24-hour variation in the time, concentration and effect relationships of a drug.

**Chapter 3** exemplifies the methodological framework on which the research described in this thesis is based. In this chapter, the 24-hour variation in the pharmacokinetics of the benzodiazepine midazolam is studied. Midazolam was used as a model compound to study CYP3A-mediated metabolism (Lee et al., 2002). A large proportion of the clinically used drugs are metabolized by the two CYP3A isozymes involved in xenobiotic metabolism (CYP3A4 and CYP3A5) (Benedetti et al., 2009). Therefore, evaluation of the 24-hour variation in midazolam pharmacokinetics provides insight into the pharmacokinetics of the numerous other CYP3A substrates as well.

In contrast to many examples available in the literature (as described in the introduction), the clinical trial described in **Chapter 3** was prospectively designed to study the 24-hour variation in the pharmacokinetics of midazolam, using six dosing times, appropriate control for stable diurnal rhythmicity before and during the study as well as a semi-simultaneous oral and intravenous administration. This yields detailed information about the effect of time of administration on the resulting concentration-time profile of the drug, which were subsequently analyzed by population pharmacokinetic (pop-PK) modelling. Hereby, the research described in **Chapter 3** demonstrates how pop-PK modelling can be used to study the effect of time of drug administration as an additional source of variation.

A similar strategy was used to study the 24-hour variation in the pharmacokinetics of the antibiotic levofloxacin in the clinical trial described in **Chapter 4**. Levofloxacin, being subject to minimal metabolism and active transport processes, was selected as a model compound for solubility and permeability independent absorption as well as passive renal elimination (Fish and Chow, 1997). These are two of the main pathways by which drugs are taken up and excreted by the body. Again combining a strict design that controls for the influences of food and fluid intake, posture and daily patterns in behavior with population pharmacokinetic modelling, the effect of dosing time on each of the pharmacokinetic parameters is precisely determined.

Delayed ventricular repolarization, manifested as a prolonged QT interval on an

electrocardiogram (ECG) recording, is one of the side-effects associated with the use of levofloxacin (Taubel et al., 2010). QT prolongation is a common side effect of a wide variety of cardiac and non-cardiac drugs that has potentially serious consequences, such as Torsade de Pointes and cardiac arrest (Kannankeril et al., 2010). For the proper evaluation of its safety profile, it is crucial to understand the factors that influence the relationship between the concentration of a drug and the QT interval. At present, it is unknown whether the effect of a drug on the length of the QT interval is influenced by the time of day. Building upon the pharmacokinetic model presented in **Chapter 4**, the effect of time of drug administration on the extent of levofloxacin-induced QT prolongation is investigated in **Chapter 5**.

Another important aspect of the development and optimization of drug treatments is to determine the concentration of a drug at its target site. As described in Chapter 1, this holds especially true for drugs targeted at the central nervous system, which is protected from the entry of exogenous compounds by a series of barriers, such as the blood brain barrier and the blood CSF barrier. Efflux transporters that drive their substrates from the brain back into the circulation, such as P-glycoprotein (P-gp), serve as an additional protective mechanism (Abbott et al., 2010). Twenty-four hour variation in the activity of P-gp may result in differences in brain concentrations depending on the time of drug administration, which could be exploited to either enhance or reduce the distribution of a P-gp substrate to the brain. Being a potent and specific substrate for P-gp (Kusuhara et al., 1997; Sziráki et al., 2011), quinidine was used in **Chapter 6** as a model drug to investigate whether P-gp mediated brain distribution shows 24-hour variation. **Chapter 6** also provides an example of the use of semi-physiologically based pharmacokinetic modelling in a chronobiological framework.

The objective of the study presented in **Chapter 7** was to apply the findings presented in Chapter 6 to a more clinically relevant drug. To this end, we investigated the brain distribution of morphine, a substrate of P-gp as well as of probenecid-sensitive transporters such as multidrug resistance-associated protein (Mrp) transporters, after administration at different dosing times.

In **Chapter 8**, the results of the work presented in Chapter 3-7 are summarized and placed in a broader perspective. The relevance of the findings will be discussed, as well as the possibilities for future research.

# REFERENCES

Abbott, N.J., Patabendige, A.A.K., Dolman, D.E.M., Yusof, S.R., and Begley, D.J. (2010). Structure and function of the blood-brain barrier. Neurobiol. Dis. 37, 13–25.

Benedetti, M.S., Whomsley, R., Poggesi, I., Cawello, W., Mathy, F.-X., Delporte, M.-L., Papeleu, P., and Watelet, J.-B. (2009). Drug metabolism and pharmacokinetics. Drug Metab. Rev. 41, 344–390.

Fish, D.N., and Chow, A.T. (1997). The clinical pharmacokinetics of levofloxacin. Clin. Pharmacokinet. 32, 101–119.

Kannankeril, P., Roden, D.M., and Darbar, D. (2010). Drug-induced long QT syndrome. Pharmacol. Rev. 62, 760–781.

Kusuhara, H., Suzuki, H., Terasaki, T., Kakee, A., Lemaire, M., and Sugiyama, Y. (1997). P-Glycoprotein mediates the efflux of quinidine across the blood-brain barrier. J. Pharmacol. Exp. Ther. 283, 574–580.

Lee, J.-I., Chaves-Gnecco, D., Amico, J.A., Kroboth, P.D., Wilson, J.W., and Frye, R.F. (2002). Application of semisimultaneous midazolam administration for hepatic and intestinal cytochrome P450 3A phenotyping. Clin. Pharmacol. Ther. 72, 718–728.

Sziráki, I., Erdo, F., Beéry, E., Molnár, P.M., Fazakas, C., Wilhelm, I., Makai, I., Kis, E., Herédi-Szabó, K., Abonyi, T., et al. (2011). Quinidine as an ABCB1 probe for testing drug interactions at the blood-brain barrier: an in vitro in vivo correlation study. J. Biomol. Screen. 16, 886–894.

Taubel, J., Naseem, A., Harada, T., Wang, D., Arezina, R., Lorch, U., and Camm, A.J. (2010). Levofloxacin can be used effectively as a positive control in thorough QT/QTc studies in healthy volunteers. Br. J. Clin. Pharmacol. 69, 391–400.

# CHAPTER

**Population pharmacokinetic model characterizing 24-hour variation in the pharmacokinetics of oral and intravenous midazolam in healthy volunteers**

## 3

Anne van Rongen[1,2,*]; Laura Kervezee[2,3,4,*]; Margreke J.E. Brill[1,2]; Helene van Meir[4]; Jan den Hartigh[5]; Henk-Jan Guchelaar[5]; Johanna H. Meijer[3]; Jacobus Burggraaf[2,4]; Floor van Oosterhout[3,4]

[1]Department of Clinical Pharmacy, St. Antonius Hospital, Nieuwegein
[2]Division of Pharmacology, Leiden Academic Centre for Drug Research, Leiden University, Leiden
[3]Department of Molecular Cell Biology, Leiden University Medical Center, Leiden
[4]Centre for Human Drug Research, Leiden
[5]Department of Clinical Pharmacy and Toxicology, Leiden University Medical Center, Leiden, The Netherlands
[*]These authors contributed equally to this work

## ABSTRACT

Daily rhythms in physiology may affect the pharmacokinetics of a drug. The aim of this study was to evaluate 24-hour variation in the pharmacokinetics of the CYP3A substrate midazolam. Oral (2mg) and intravenous (1mg) midazolam was administered at six time points throughout the 24-hour period in twelve healthy volunteers. Oral bioavailability (population mean value (RSE%) of 0.28 (7.1%)) showed 24-hour variation that was best parameterized as a cosine function with an amplitude of 0.04 (17.3%) and a peak at 12:14 in the afternoon. Absorption rate constant was 1.41 (4.7%) times increased after drug administration at 14:00. Clearance (0.38L/min (4.8%)) showed a minor 24-hour variation with an amplitude of 0.03 (14.8%) L/min and a peak at 18:50. Simulations show that dosing time minimally affects the concentration time profiles after intravenous administration, while concentrations are higher during the day compared to the night after oral dosing, reflecting considerable variation in intestinal processes.

## STUDY HIGHLIGHTS

What is the current knowledge on this topic?
- The pharmacokinetics of the CYP3A4 substrate midazolam may be subject to 24-hour variation, but previous studies did not assess all pharmacokinetic parameters simultaneously and yielded conflicting results.

What question did this study address?
- How do the pharmacokinetics of oral and intravenous midazolam depend on time of administration?

What this study adds to our knowledge?
- Oral bioavailability and absorption rate constant of midazolam show considerable 24-hour variation, while clearance shows minor fluctuations.
- Concentration-time profiles of midazolam are affected by dosing time after oral administration, but not after intravenous administration.

How might this change clinical pharmacology and therapeutics?
- Our design, with appropriate control for unperturbed circadian rhythmicity and semi-simultaneous oral and intravenous administration, combined with population pharmacokinetic modelling can be applied to study 24-hour variation in the pharmacokinetics of other model compounds, yielding detailed information on the effect of time of administration on the concentration profile.

## INTRODUCTION

Many physiological processes including gene expression, metabolism and organ function exhibit 24-hour variation (Meijer et al., 2012). As a result of these rhythms, the pharmacokinetics of drugs may vary over the day (Dallmann et al., 2014). Although different chronopharmacological studies have shown that the pharmacokinetics of several drugs depend on the time of administration (Baraldo, 2008; Bruguerolle et al., 2008; Kaur et al., 2013), this source of variability has not been evaluated systematically. A possible approach to methodically assess 24-hour variation in pharmacokinetic parameters is to study a model drug representing a group of drugs that are absorbed, distributed, metabolized and/or eliminated in a similar way. Such an approach requires a strict standardized study protocol with external validators to ensure that the research is performed with minimal or no disturbance of the physiological rhythms.

Midazolam is extensively metabolized by both hepatic and intestinal cytochrome P450 3A (CYP3A) and is considered a probe of CYP3A enzyme activity (Fuhr et al., 2007; Gorski et al., 1998; Lee et al., 2002; Thummel et al., 1996; Tsunoda et al., 1999). CYP3A is an important drug metabolizing enzyme, metabolizing 30% of clinically used drugs (Zanger and Schwab, 2013). In vitro research shows that hepatic CYP3A activity fluctuates during the 24-hour period (Froy, 2009; Takiguchi et al., 2007). Moreover, in vivo CYP3A activity in humans measured by urinary 6βhydroxy-cortisol to cortisol ratio showed diurnal variation by an average of 2.8 fold (Ohno et al., 2000).

Several chronopharmacokinetic studies on midazolam have been published (Bienert et al., 2013; Klotz and Reimann, 1984; Klotz and Ziegler, 1982; Koopmans et al., 1991; Tomalik-Scharte et al., 2014). In most of these studies, however, midazolam was administered either orally (Koopmans et al., 1991) or as an intravenous infusion (Bienert et al., 2013; Klotz and Reimann, 1984; Tomalik-Scharte et al., 2014), and therefore not all pharmacokinetic parameters (absorption rate constant, bioavailability and clearance) could be assessed separately. To distinguish between bioavailability, systemic clearance and volume of distribution, oral and intravenous administration should be combined in one single study. In the current study, we aimed to evaluate 24-hour variation in the pharmacokinetic parameters of midazolam after semi-simultaneous oral and intravenous administration in healthy volunteers.

## METHODS

### Study design and data

Healthy, non-smoking Caucasian male subjects, aged between 18 and 50 and a body mass index (BMI) between 18 and 30 kg/m$^2$ were recruited for this study, which took place at the Centre for Human Drug Research in Leiden, the Netherlands. Subjects were excluded from participation if any clinically significant abnormality was found in medical history, routine laboratory tests or 12-lead ECG recordings or if they used any medication, could be characterized as an extreme morning- or evening-type as determined by the Horne-

Ostberg Chronotype Questionnaire (Horne and Ostberg, 1976), made transmeridian flights or did shift work from a month prior to the start of the study. The study was approved by the Medical Ethics Committee of the Leiden University Medical Center and was carried out according to the ICH guidelines for good clinical practice(ICH).

From one week prior to each study visit, subjects were instructed to maintain a stable sleep-wake schedule (waking times between 07:00-08:00, bedtimes between 23:00-00:00). Subjects kept a sleep diary and wore an Actiwatch (CamNtech Actiwatch Light®, UK) to monitor their daily activity profiles. Subjects refrained from heavy exercise for 24 hours prior to a scheduled study visit and were not allowed to use products that interfere with CYP3A metabolism (such as grapefruit, banpeiyu, pomegranate, star fruit, black berry, and wild grape) for two weeks prior to the study, and no caffeinated drinks, alcoholic drinks, honey and cruciferous vegetables for 72 hours prior to the drug administration until 48 hours thereafter.

The study consisted of three study visits at which the subjects received a 2 mg oral midazolam solution and 1 mg intravenous midazolam (separated by 150 min) twice a day at a 12 hour interval. The clock times of midazolam administration differed for each study visit, so that data were collected at six different time points throughout the 24-hour period (oral administration at 10:00, 14:00, 18:00, 22:00, 02:00 and 06:00) in each of the 12 volunteers (Fig. 1a), with a washout period of at least two weeks between the study visits. Throughout the study visits, subjects remained in a semi-recumbent position. At night (23:30 until 07:30), lights were dimmed and subjects wore an eye mask. From two hours prior to drug administration, subjects fasted. A light meal was served at t=395min and a snack at t=540min after oral administration. Water was allowed as required.

Samples (2.7mL) to determine midazolam concentrations in serum were collected at t= 0, 15, 30, 45, 58, 65, 70, 75, 80, 90, 120, 148, 155, 165, 180, 210, 240, 270, 330 and 390 minutes after oral administration, as well as at t= 715 minutes in case it involved the first 12 hours of a study visit. Midazolam concentrations were measured using a validated liquid chromatographic tandem mass spectrometric (LC-MS/MS) assay (van Erp et al., 2011). Within-day and between-day inaccuracy and imprecision were less than 5% and the lower limit of quantitation (LLQ) was 0.3 μg/L (van Erp et al., 2011).

Samples to determine thyroid stimulating hormone (TSH) concentrations in serum (1.2 mL) were collected hourly during the study visits. TSH concentrations (μIU/mL) were measured by an electrochemiluminescence immunoassay (ECLIA, Cobas, Roche Diagnostics GmbH, Mannheim, Germany) on an Elecsys immunoassay analyser (Roche Diagnostics GmbH, Mannheim, Germany), calibrated against the World Health Organization Second Standard International Reference Preparation (80/558). The LLQ was 0.005μIU/mL. Blood pressure and heart rate were measured every two hours during the study visits.

Single component cosinor analysis was performed to evaluate the presence of a 24-hour rhythm in blood pressure, heart rate and endogenous TSH levels using R software (v2.15; R Foundation for Statistical Computing, Vienna, Austria). Cosinor analysis is a statistical method to fit a cosine function to longitudinal data. If the period assumed to be known
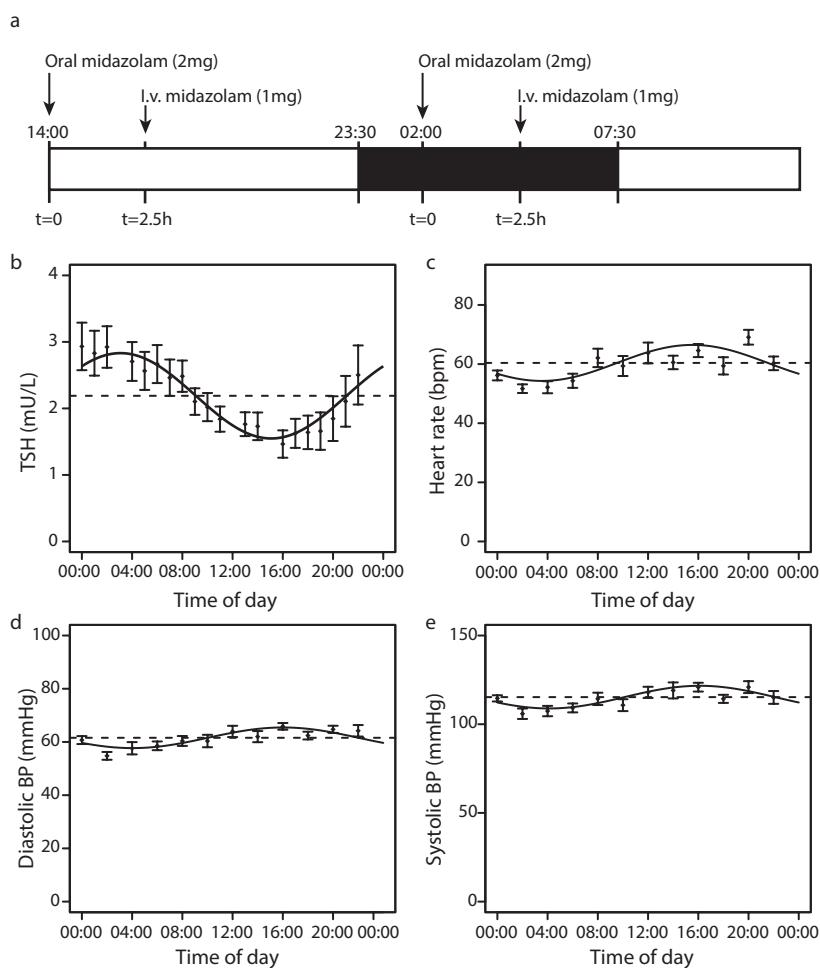
**Figure 1 (a)** Schematic representation of the drug administration protocol per study visit. Subjects completed two occasions, separated by 12 hours. At t=0, subjects received 2mg midazolam (MDZ) orally. At t=2.5h, subjects received 1mg midazolam intravenously. After 12 hours, the procedure was repeated. In each of the three study visit, drug administration took place at two different clock times (t=0 at 14:00 and 02:00 in this example), so drug administration occurred at six different clock times throughout the 24-hour period. The order of time of drug administration was randomized. The dark box indicates the clock times during which the subjects were instructed to sleep. **(b-e)** Mean values of TSH levels (b), heart rate (c), diastolic (d) and systolic blood pressure (e) obtained during the study visits across the 24-hour period (n=12 subjects). The solid lines show the cosine curve with a period of 24-hour that best fits the data, obtained through cosinor analysis.

(in this case 24 hours), a cosine function can be rewritten as a linear function and the data can be fitted via least squares regression (Cornelissen, 2014). The mesor, amplitude and acrophase can be calculated from the estimated intercept and coefficients.

**Population pharmacokinetic modeling**

The pharmacokinetic data were analyzed using non-linear mixed effects modeling

(NONMEM v7.2; ICON Development Solutions, Hanover, MD, USA)(Beal et al., 2009) and R (v2.15) (R Development Core Team, 2008), Pirana (v2.7.1), Xpose (4.5.0) and PsN (3.6.2) (Keizer et al., 2013) were used to visualize the data. The first-order conditional estimation method with interaction was used throughout model development.

*Structural and statistical model*
Pharmacokinetic models incorporating either two or three compartments with first order, zero order or combined first- and zero order oral absorption were investigated. Furthermore, the addition of one or more transit compartments or an oral absorption lag time was evaluated (Savic et al., 2007). Interindividual variability (IIV) in pharmacokinetic parameters was assumed to be log-normally distributed. Residual variability was investigated using proportional, additive or combined proportional and additive error models.

*Twenty-four hour variation*
Twenty-four hour variation in the different structural pharmacokinetic parameters was first explored by incorporating interoccasion variability (IOV), representing the variability between the six different times of administration, on each of these parameters of interest using the following equation (Karlsson and Sheiner, 1993):

$$\theta_{ij} = \theta_{mean} * e^{\eta i} + k_{ij} \qquad \text{(Equation 1)}$$

where is the individual parameter estimate at the $j^{th}$ occasion, is the population mean, $\eta_i$ is a random variable for the ith individual (IIV) and $k_{ij}$ is a random variable for the $i^{th}$ individual at the $j^{th}$ occasion (IOV). Both $\eta_i$ and $k_{ij}$ were assumed to be independently normally distributed with mean of zero and variances $\omega^2$ and $\pi^2$, respectively. The k values used in IOV plots are empirical Bayes estimates (EBEs) of the interoccasional random effect (NONMEM ETA) of the parameter involved.

   If a 24-hour rhythm was visually identified in IOV plots, a cosine function with a period of 24 hours (1440 minutes) was implemented in the model as follows:

$$P = \theta_i + \theta_{AMP} * \cos(2\pi * (t - \theta_{ACROPHASE}) / 1440 ) \qquad \text{(Equation 2)}$$

where P represents the studied pharmacokinetic parameter, $\theta_i$ the mesor (individual value of the pharmacokinetic parameter around which it oscillates), $\theta_{AMP}$ the amplitude and $\theta_{ACROPHASE}$ the acrophase (time of the peak of the cosine function). t represents the time in minutes starting at midnight of the first study visit and continuing until the end of the third study visit. It was assumed that the cosine function described the data accurately when no residual trend of diurnal variation was left in the IOV plots upon inclusion of the function and it resulted in a reduced IOV value. Twenty-four hour variation was also evaluated by estimation of different multiplication factors on the pharmacokinetic parameters for the six time-points of administration (10:00, 14:00, 18:00, 22:00, 02:00 and 06:00).

   If no full 24-hour variation could be identified for a pharmacokinetic parameter, but only an increase at a certain time interval of the day, this was parameterized as half a cycle of a

sine function:

$$INC = \theta_{AMP} * \sin(2\pi * (TSIN - \theta_{ON}) / \theta_{FR})$$ (Equation 3)

where INC represents the increase in a parameter, $\theta_{AMP}$ the amplitude, $\theta_{FR}$ the frequency of the oscillations (minutes), TSIN the clock time in minutes after 12:00 (noon) and $\theta_{ON}$ represents the onset of the increase in the parameter. The end of the increase in the pharmacokinetic parameter was calculated as follows:

$$END = 0.5 * \theta_{FR} + \theta_{ON}$$ (Equation 4)

*Model selection and internal model evaluation*
Model development and selection was guided by comparison of the objective function value (OFV, i.e. -2 log likelihood (-2LL)) between nested models, precision of parameter estimates and visual improvement in goodness-of-fit plots split by the six times of administration (observed versus individual-predicted concentrations, observed versus population-predicted concentrations, conditional weighted residuals versus time after dose and conditional weighted residuals versus population-predicted concentrations plots and individual plots). A p-value of <0.05 ($\Delta$OFV=-3.84 for one degree of freedom) was considered statistically significant. For internal model evaluation, a bootstrap analysis was performed using 250 replicates and visual predictive checks (VPCs), stratified by the six times of administration, were created using 1000 simulated datasets.

**Simulations**

The final population pharmacokinetic model was used to simulate the concentration-time curves of a subject dosed at 6 different administration times of a 7.5 mg oral dose or a 2 mg intravenous bolus dose.

# RESULTS

**Study participants**

Twelve healthy Caucasian male volunteers participated in the study. Their demographics are summarized in Table 1. One subject withdrew consent during the study due to personal reasons and was replaced by another study subject who was dosed according the same randomization order.

**Physiological parameters**

Several physiological variables, used to verify that the approach of our study is suited to assess diurnal rhythmicity in physiological processes, fluctuated over the 24-hour period (Fig. 1b-e). TSH levels showed significant 24-hour variation with a relative amplitude of 29% and peak levels around 03:05 at night ($r^2$=0.13, p<0.0001). Heart rate and diastolic and systolic blood pressure also exhibited a significant 24-hour rhythm ($r^2$=0.14, p<0.0001 for all three parameters) with relative amplitudes of 10%, 6.3% and 5.6%, respectively, and peaks

**Table 1:** Subject demographics

|  | N | Mean | SD | CV (%) | Median | Range |
|---|---|---|---|---|---|---|
| Age (years) | 12 | 21.8 | 3.19 | 14.6 | 22 | 18-27 |
| Weight (kg) | 12 | 76.0 | 8.65 | 11.4 | 75.4 | 63.4-92.9 |
| Body mass index (kg/m$^2$) | 12 | 22.3 | 2.37 | 10.6 | 21.9 | 18.8-25.8 |

N: number of subjects; SD: standard deviation; CV: coefficient of variation
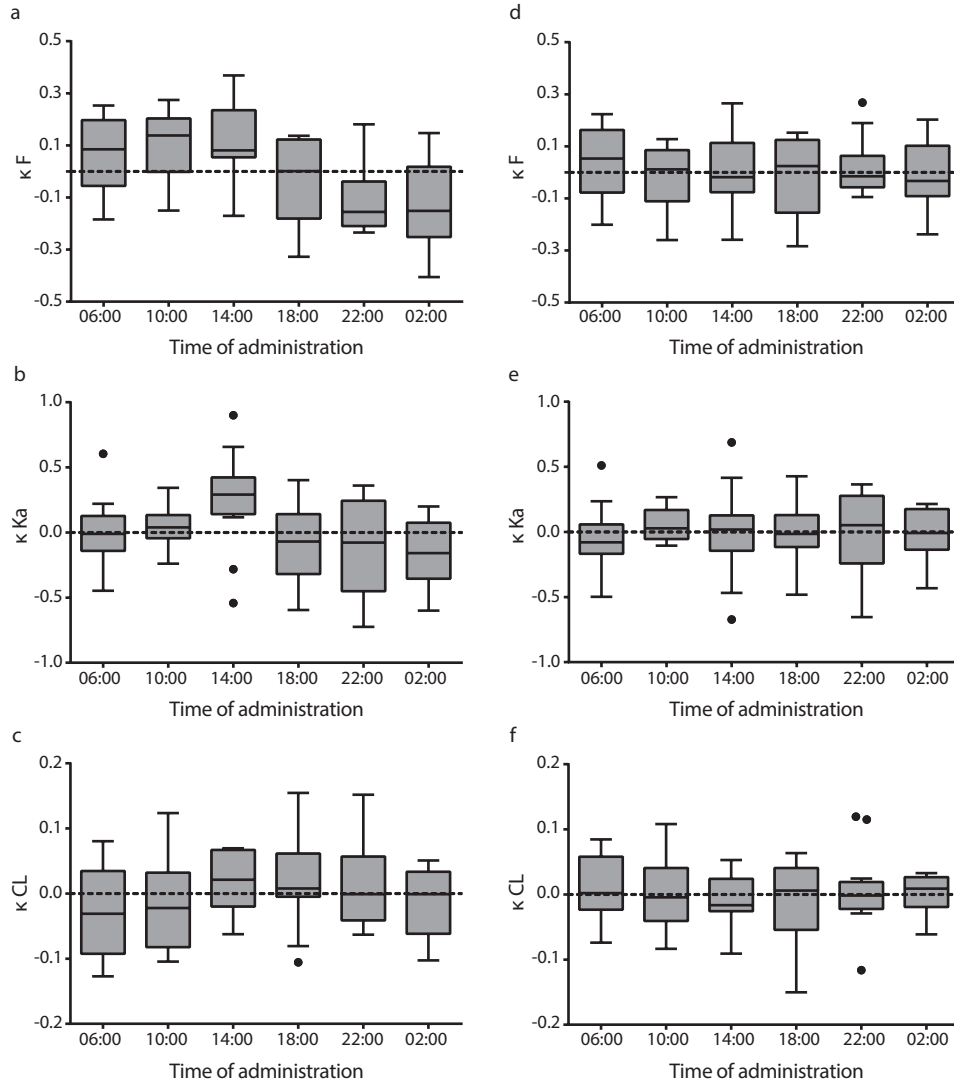


**Figure 2** Interoccasion variability (κ, kappa) versus time of administration of midazolam for oral bioavailability (F) **(a, d)**, absorption rate constant (Ka) **(b, e)** and clearance (CL) **(c, f)**. Left column represents IOV (κ) versus time plots of the simple model in which no cosine function was incorporated (a,b,c) and right column represents IOV (κ) versus time plots of the models after implementation of a cosine function for oral bioavailability (d), a multiplication factor at the 14:00 hour administration time for absorption rate constant (e) and a cosine function for clearance (f). The k values used in these IOV plots are empirical Bayes estimates (EBEs) of the interoccasional random effect (NONMEM ETA) in the parameter involved (oral bioavailability, absorption rate constant or clearance).

around 16:00.

**Population pharmacokinetic model and internal model evaluation**

The mean concentration time-profiles of midazolam after oral and intravenous administration at the six time points is shown in Supplementary Fig. 1. A three compartment PK model with equalized peripheral volumes of distribution best described the data. The peripheral volumes were equalized, as these values were almost equal and the model resulted in a similar objective function (p>0.05). Oral absorption of midazolam was best described by a one transit compartment absorption model, where oral absorption rate constant and transit compartment rate constant were equalized. Residual variability was best described by using a proportional error model for both oral and intravenous data.

To explore 24-hour variation in the different pharmacokinetic parameters, IOV was sequentially incorporated on oral bioavailability, absorption rate constant and systemic clearance (Supplementary Table 1). The presence of a 24-hour rhythm was most evident for oral bioavailability (Fig. 2a, p<0.001, ΔOFV -349). After implementation of IOV on absorption rate constant an increase in this parameter was identified after administration at 14:00 (Fig. 2b, p<0.001 ΔOFV -258). The magnitude of a possible 24-hour rhythm in clearance of midazolam seemed lower compared to oral bioavailability and absorption rate constant (Fig. 2c, p<0.001, ΔOFV -93). The η-shrinkage for the EBEs of the interoccasional random effect was higher than 30% for oral bioavailability and absorption rate constant (33% and 55%, respectively, Supplementary Table 1), resulting in potentially unreliable EBEs (Karlsson and Savic, 2007). Therefore, these observations necessitated further analysis by implementation of a cosine function on each of these parameters evaluated by objective function.

The 24-hour variation in bioavailability was accurately described by a cosine function (Equation 2), resulting in a significant improvement in OFV compared to the IOV on bioavailability model (p<0.001, ΔOFV -28) and in a reduced IOV value (from 20 to 15.4%, Supplementary Table 1). Alternatively, 24-hour variation in bioavailability was estimated by implementing different multiplication factors on this parameter for each of the six time points of administration. This multiplication factor model showed a similar fluctuation over the 24-hour period compared to the cosine model (Supplementary Fig. 2a) and had a similar OFV (2431 for the cosine model with 2 additional parameters versus 2430 for the multiplication factor model with 5 additional parameters, p>0.05 for 3 degrees of freedom). The cosine model was preferred over the multiplication factor model, because both the IOV model (Fig. 2a) and multiplication factor model (Supplementary Fig. 2a) revealed a cosine function in bioavailability and the cosine model required less parameters to be estimated, while having larger predictive value. After implementation of the cosine function for bioavailability, there was no remaining trend in IOV confirming the appropriateness of the cosine model for this parameter (Fig. 2d).

After implementation of the cosine function for bioavailability, the variation in absorption rate constant was modeled, which was best described by the estimation of a multiplication factor at 14:00 (p<0.01, ΔOFV -9, Supplementary Table 1). After
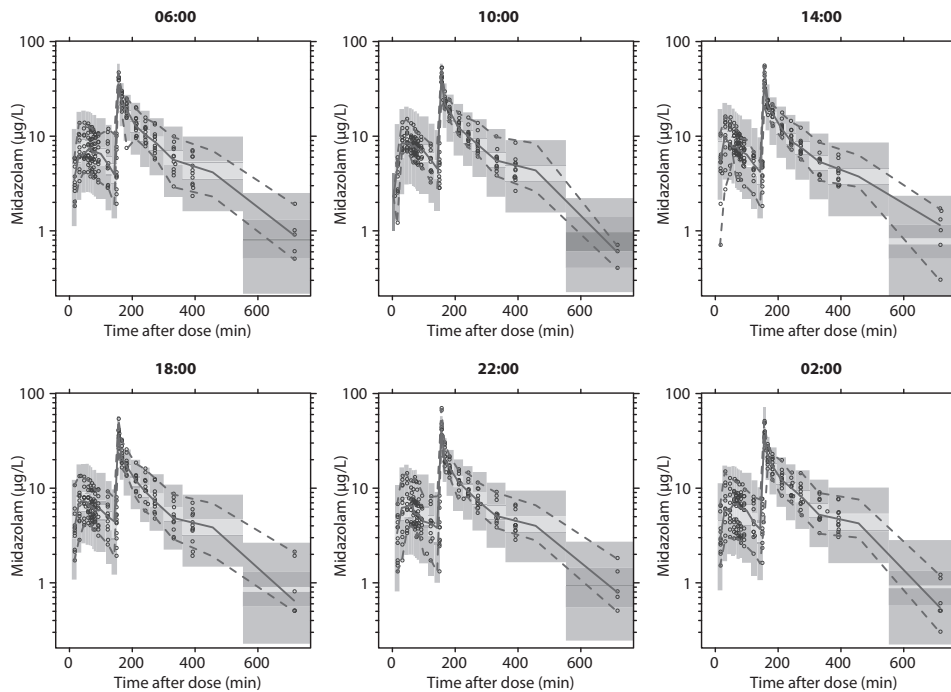
**Figure 3** Visual predictive checks of the final model stratified by time of midazolam administration (06:00, 10:00, 14:00, 18:00, 22:00 and 02:00). Observed concentrations are shown as half open circles with solid and lower and upper dashed lines showing the median, 2.5th and 97.5th percentiles of the observed data, respectively. The shaded areas represent 95% confidence intervals for the model predicted median, 2.5th, 97.5th percentiles constructed from 1000 simulated datasets of individuals from the original dataset.

implementation of this multiplication factor, IOV on absorption rate constant was removed from the model, because of the high η-shrinkage of the EBE of the interoccasional random effect (55%, Supplementary Table 1). Addition of multiplication factors on absorption rate constant at other time-points of administration did not further improve the model (p>0.05, Supplementary Fig. 2b). Alternatively, a cosine function was tested, but this model did not result in adequate prediction of the increased absorption rate constant at 14:00. Furthermore, inclusion of half a cycle of a sine function to describe the peak in absorption rate constant (Equation 3 and 4) resulted in a peak at 14:59 and an amplitude of 0.056min-1 (increase of 106%) and an onset and offset of the peak at 14:12 and 15:45, respectively. However, this model was very sensitive to initial parameter estimates and did not result in a significant improvement in OFV compared to the model with a multiplication factor at 14:00 (p>0.05, ΔOFV -3.7, 2 degrees of freedom). Therefore, the model with a multiplication factor at 14:00 was selected. No rhythm remained in the IOV plot after implementation of this factor (Fig. 2e). However, this plot should be viewed with caution because of the high ETA shrinkage and IOV on the absorption rate constant was therefore removed from the model, as described above. The multiplication factor estimated by this model was 1.46 (resulting in an absorption rate constant of 0.08 min-1), indicating a strong increase in absorption rate
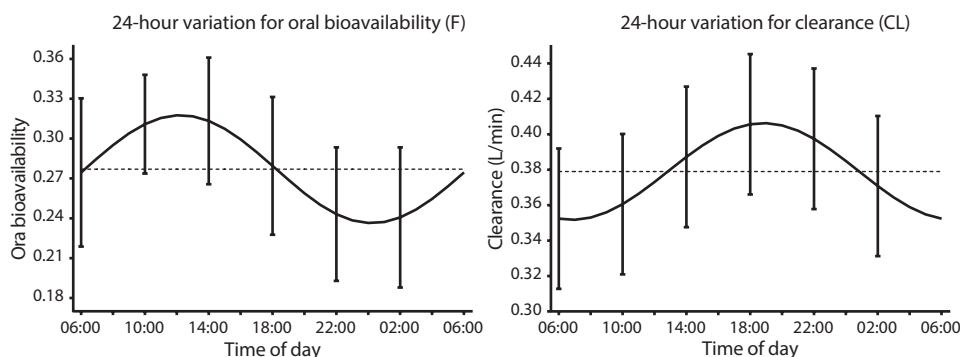
**Figure 4** Twenty-four hour fluctuation for oral bioavailability (F) and clearance (CL) according to the final model with the 95% confidence interval of the empirical Bayes estimates (EBEs) for F (IIV+IOV) and CL (IIV) at each administration time. For oral bioavailability, the time of the peak was estimated at 12:14 with an estimated amplitude of 0.041 (14.7% increase) (**left panel**). For clearance, the time of the peak was estimated at 18:50 with an estimated amplitude of 0.027 L/min (7.2% increase) (**right panel**).

constant after administration at 14:00.

After implementation of a cosine function for bioavailability and a multiplication factor for absorption rate constant, 24-hour related changes in clearance were modelled. For this parameter, 24-hour variation was best described by a cosine function (Equation 2), resulting in a significant decrease in OFV compared to the IOV model for clearance (p<0.001, ΔOFV -26, Supplementary Table 1). Since the IOV value was substantially smaller than the IIV on clearance, IOV on clearance was removed from the model. Clearance could also be described by estimation of different multiplication factors for each of the six times of drug administration (Supplementary Fig. 2c), resulting in similar variation over the 24-hour period as the cosine model. After implementation of the cosine function for clearance, there was no remaining trend in IOV on this parameter (Fig. 2f) (η shrinkage of 20%), confirming the appropriateness of the cosine model for clearance.

Hence, the final model selected to describe 24-hour variation in midazolam concentration profiles included a cosine function for bioavailability and clearance and a multiplication factor to describe the increase in absorption rate constant at 14:00. The model parameter values are summarized in Table 2. Observed versus individual predicted concentrations and observed versus population predicted midazolam concentrations of the final pharmacokinetic model for all six time-points of administration are shown in Supplementary Fig. 3. The final model was evaluated using bootstrap analysis, confirming that the model parameters could be estimated with good precision (Table 2). Furthermore, VPCs stratified by time of administration indicated good predictive performance for both oral and intravenous data with good agreement between observed data and model simulated confidence intervals for the median, 2.5th and 97.5th percentiles (Fig. 3). Fig. 4 shows the 24-hour variation in bioavailability and in clearance of the final model.The cosine function on bioavailability has a relative amplitude of 14.7% with a peak at 12:14, while the cosine function on clearance has a relative amplitude of 7.2% and a peak at 18:50.
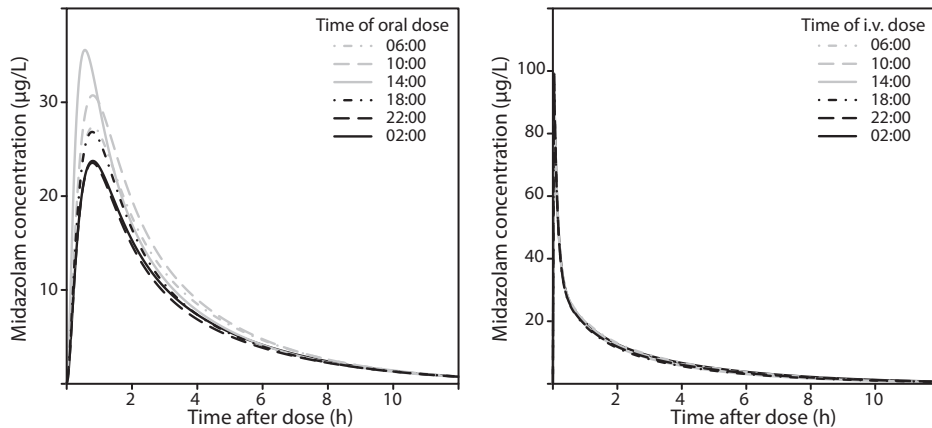
**Figure 5** Population predicted midazolam concentrations over time after 7.5 mg oral administration (**left panel**) and a 2 mg intravenous bolus (**right panel**) at 06:00, 10:00, 14:00, 18:00, 22:00 and 02:00.

**Simulations**

Population predicted midazolam concentrations after a 7.5 mg oral dose and 2 mg intravenous bolus dose in a typical subject dosed at six different times during the day (10:00, 14:00, 18:00, 22:00, 02:00 and 06:00) were simulated using the final model (Fig. 5). The oral midazolam dose simulations show that the concentrations after administration in the late morning and early afternoon (10:00 and 14:00) are higher compared to the concentrations after administration in the late evening and early night (22:00 and 02:00). In addition, the time to maximum concentration (Tmax) is shorter when midazolam is administered at 14:00. In contrast to the oral dose simulations, the intravenous dose simulations show almost no variation during the 24-hour period.

# DISCUSSION

This study aimed to evaluate the 24-hour variation in the pharmacokinetics of the CYP3A substrate midazolam after semi-simultaneous oral and intravenous administration at six different time points during the day (06:00, 10:00, 14:00, 18:00, 22:00 and 02:00). It was found that oral bioavailability and clearance are subject to 24-hour variation that could both be described by a cosine function. The peak of oral bioavailability was found at 12:14, with a relative difference between peak and trough values of 29.4%. The effect for clearance was found to be small with a peak at 18:50 and a relative difference between peak and trough levels of 14.4%. Furthermore, we found that absorption rate constant was increased 1.41 times after administration at 14:00.

Previous studies that investigated the diurnal variation of midazolam clearance in healthy volunteers did not yield consistent results (Bienert et al., 2013; Klotz and Reimann, 1984; Klotz and Ziegler, 1982; Koopmans et al., 1991; Tomalik-Scharte et al., 2014). In agreement with our results, Klotz and Ziegler found a higher clearance value in the evening compared

**Table 2** Population pharmacokinetic parameters of the final model for midazolam and results of the bootstrap analysis (250/250 resamples successful).

| Parameter | Model Estimates (RSE%) | Bootstrap Estimates (95% confidence interval) |
|---|---|---|
| CL= $CL_{mesor}$+Amp * cos((2π/1440)*(Time-Acrophase)) | | |
| $CL_{mesor}$ (L/min) | 0.379 (4.8) | 0.380 (0.344-0.417) |
| Amp (L/min) | 0.027 (14.8) | 0.028 (0.017-0.039) |
| Acrophase (min) | 1130 (2.9) | 1130.2 (1005.3-1204.7) |
| $V_{central}$ (L) | 18.2 (5.4) | 18.4 (15.3-20.9) |
| $V_{peripheral1}$ = $V_{peripheral2}$ (L) | 22.5 (2.5) | 22.4 (20.2-26.2) |
| Q (L/min) | 0.27 (6.8) | 0.269 (0.209-0.334) |
| $Q_2$ (L/min) | 1.31 (8.5) | 1.29 (1.08-1.56) |
| Ka = Ktr ($min^{-1}$) | 0.053 (5.8) | 0.053 (0.048-0.061) |
| Fraction Ka at 14:00 | 1.41 (4.7) | 1.41 (1.07-1.78) |
| F= $F_{mesor}$+Amp * cos((2π /1440)*(Time-Acrophase)) | | |
| F | 0.277 (7.1) | 0.275 (0.244-0.313) |
| Amp | 0.041 (17.3) | 0.041 (0.026-0.055) |
| Acrophase (min) | 734 (5.3) | 739.7 (667.0-821.0 ) |
| *Interindividual variability* | | |
| CL (%) | 16.2 (21) | 15.2 (9.7-19.6) |
| Ka (%) | 19.1 (21.9) | 18.7 (10.7-24.2) |
| F (%) | 23.3 (22.2) | 22.7 (15.8-28.8) |
| *Interoccasion variability* | | |
| F (%) | 14.8 (10.5) | 14.5 (11.5-17.9) |
| *Residual proportional error* | | |
| $\sigma_{oral}$ (%) | 18.0 (5.6) | 17.8 (15.8-19.8) |
| $\sigma_{intravenous}$ (%) | 15.4 (6.1) | 15.1 (13.2-17.3) |
| OFV (-2LL) | 2299 | 2242 (1723-2730) |

RSE = relative standard error (%); CL = systemic clearance of midazolam; Amp = amplitude; Acrophase = peak time of the cosine function in minutes after midnight; V = volume of distribution; Q = inter-compartmental clearance of midazolam between central and first peripheral compartment; Q2 = inter-compartmental clearance of midazolam between central and second peripheral compartment; Ka = oral absorption rate constant; Ktr= transit compartment rate constant; F = oral bioavailability; OFV = Objective Function Value

to the morning after intravenous administration (Klotz and Ziegler, 1982). More recently, Tomalik-Scharte et al. reported a cosine function in midazolam clearance over the day with a 10% increase at 15:00 (Tomalik-Scharte et al., 2014). This is consistent with our results, as we found a 7.2% maximum increase in clearance at 18:50. The small difference in peak time may be explained by the nature of the study; where Tomalik-Scharte et al. evaluated midazolam concentrations during the day upon a continuous intravenous infusion, we

studied an oral and intravenous bolus dose at 6 different times of administration. The fact that others found no influence of the time of administration on clearance may be explained by the low number of subjects in the study (Klotz and Reimann, 1984) and the fact that intensive care patients were studied, showing a disrupted circadian rhythm (Bienert et al., 2013). Hence, most chronopharmacokinetic studies about intravenous midazolam are in line with our findings of a relatively small 24-hour variation in midazolam clearance.

Our results about absorption processes of midazolam (24-hour variation in oral bioavailability and increase in absorption rate constant at 14:00) are not consistent with earlier chronopharmacokinetic studies on oral midazolam, finding no influence on Cmax, Tmax or oral bioavailability (Klotz and Ziegler, 1982; Koopmans et al., 1991). These discrepancies may be due to methodological differences. Klotz and Ziegler administered midazolam only at two different time points during the day (Klotz and Ziegler, 1982), and therefore the peak and trough may easily be missed. In the study of Koopmans et al., subjects were not allowed to lie down or sleep from 1 hour before to 8 hours after dosage (Koopmans et al., 1991), which could have disrupted the circadian rhythms in physiological processes of the subjects (Mullington et al., 2009). However, our finding of 24-hour variation in oral bioavailability of midazolam is supported by chronopharmacokinetic studies of other CYP3A substrates, such as nifedipine, tacrolimus and ciclosporin (Baraldo and Furlanut, 2006; Lemmer et al., 1991). Lemmer et al. showed an increased $C_{max}$ and 35% increase in oral bioavailability after a morning dose of immediate release nifedipine compared to an evening dose (Lemmer et al., 1991). Furthermore, studies with oral tacrolimus and ciclosporin showed in general an increased $C_{max}$ and AUC after morning dose compared to evening dosing (Baraldo and Furlanut, 2006; Iwahori et al., 2005; Min et al., 1996, 1997; Tada et al., 2003). Therefore, it seems that our findings on 24-hour variation in absorption processes are strengthened by the advanced study design that we used in comparison to previous oral midazolam studies that did not report these changes, and are supported by chronopharmacological studies of other CYP3A substrates.

Twenty-four hour variation in clearance and oral bioavailability as well as the increase in absorption rate constant can be explained by several physiological factors. Since midazolam is a typical probe for CYP3A activity (Gorski et al., 1998; Lee et al., 2002; Tsunoda et al., 1999), the rhythm in systemic clearance of midazolam may be explained by minor 24-hour variation in CYP3A activity. Multiple lines of evidence show that hepatic CYP3A activity fluctuates during the 24-hour period (Froy, 2009; Lu et al., 2013; Ohno et al., 2000; Takiguchi et al., 2007; Tomalik-Scharte et al., 2014). Like systemic clearance, 24-hour variation in oral bioavailability of midazolam may also be explained by variation in intestinal CYP3A activity, since CYP3A is present both in the gut wall and liver (Thummel et al., 1996). Another explanation for the variation in oral bioavailability may be the variation in splanchnic blood flow during the 24-hour period, which is supported by the findings of Lemmer et al., who demonstrated a 24-hour rhythm in hepatic blood flow (as a proxy for splanchnic blood flow) with a peak at 08:00 (Lemmer and Nold, 1991). This supports our finding that oral bioavailability is increased from the early morning until the end of the afternoon (Fig. 4).

An increased splanchnic blood flow will decrease the intestinal first pass effect, as it will carry the drug away from the enterocyte and the CYP3A enzyme (Patel et al., 2013; Yang et al., 2007). In contrast to oral bioavailability, the clearance of midazolam is not expected to be influenced by hepatic blood flow to such an extent, because midazolam is a low to intermediate extraction drug (extraction rate of 35%), making it relatively independent of hepatic blood flow (Tsunoda et al., 1999). The increase in absorption rate constant after oral administration at 14:00 may be explained by 24-hour variation in gastric emptying, gastrointestinal mobility and splanchnic blood flow (Dallmann et al., 2014; Hoogerwerf, 2010; Kumar et al., 1986; Lemmer and Nold, 1991), even though we could not identify a cosine function for absorption rate constant.

In this study, we utilized a semi-simultaneous design in which midazolam was administered as an oral and intravenous dose separated by 150 minutes (Lee et al., 2002). An advantage of this crossover approach is that intra-individual variability is limited, since the oral and intravenous dose are administered to the same individual at a relatively short time frame (Karlsson and Bredberg, 1989). By using six different time points of oral and intravenous midazolam administration, 24-hour variation in absorption parameters as well as clearance could be accurately identified. Moreover, we ensured that subjects had stable rest/activity patterns between the study days and controlled for the influence of eating and physical activity, both of which are known to have an impact on physiological rhythms (Froy, 2010). Another strength of our study design is that several endogenous markers, with known diurnal variation (heart rate, systolic/diastolic blood pressure and serum TSH levels) were used as external validators to verify that our approach, including the low dose of midazolam, did not interfere with normal circadian physiology of the subjects. We found that these endogenous markers show clear diurnal variation with peak and trough times that are comparable to values reported in the literature (Andersen et al., 2003; Guo and Stein, 2003). These findings indicate that the study population and design were well-suited to study diurnal variation of midazolam exposure.

As the pharmacokinetics of midazolam have been shown to be linear over a wide dose range (Halama et al., 2013; Misaka et al., 2010), we performed simulations on the basis of the final pharmacokinetic model using therapeutic doses. These simulations illustrate the findings of the current study by showing a substantial effect of time of administration on midazolam concentration-time profiles after oral administration, whereas this effect is minimal after intravenous administration. Midazolam concentrations after oral administration are higher in the morning and afternoon compared to concentrations after administration in the evening and night. In addition, the time to maximum concentration (Tmax) is shorter after oral administration at 14:00. In the clinic, midazolam is mainly given as an intravenous dose, for example as pre-medication or for induction of anesthesia, upon which the time of administration will have no clinical impact. However, midazolam is also prescribed as a hypnotic to patients with insomnia. For these patients, who take an oral dose in the evening, lower serum concentrations should be anticipated.

In conclusion, this study shows that oral bioavailability of midazolam is subject to 24-

hour variation and that absorption rate constant is increased at 14:00 in the afternoon. The clearance of midazolam is also subject to 24-hour variation, although its magnitude is small and without clinical significance. As a result, the 24-hour variation in oral bioavailability results in higher serum concentrations during the day compared to the night upon oral midazolam dosing, while the concentration-time profiles are hardly affected by time of administration after intravenous dosing. Future research should elucidate the specific processes that contribute to the 24-hour variation in the pharmacokinetics of midazolam, and of other drugs with similar physicochemical properties, for example by using markers for intestinal motility or blood flow.

## ACKNOWLEDGEMENTS

## CONFLICT OF INTEREST

The authors declare no conflict of interest.

# REFERENCES

Andersen, S., Bruun, N.H., Pedersen, K.M., and Laurberg, P. (2003). Biologic variation is important for interpretation of thyroid function tests. Thyroid 13, 1069–1078.

Baraldo, M. (2008). The influence of circadian rhythms on the kinetics of drugs in humans. Expert Opin. Drug Metab. Toxicol. 4, 175–192.

Baraldo, M., and Furlanut, M. (2006). Chronopharmacokinetics of ciclosporin and tacrolimus. Clin. Pharmacokinet. 45, 775–788.

Beal, S., Sheiner, L.B., Boeckmann, A., and Bauer, R.J. (2009). NONMEM User's Guides (1989-2009), Icon Development Solutions, Ellicott City, MD, USA.

Bienert, A., Bartkowska-Sniatkowska, A., Wiczling, P., Rosada-Kurasińska, J., Grześkowiak, M., Zaba, C., Teżyk, A., Sokołowska, A., Kaliszan, R., and Grześkowiak, E. (2013). Assessing circadian rhythms during prolonged midazolam infusion in the pediatric intensive care unit (PICU) children. Pharmacol. Rep. 65, 107–121.

Bruguerolle, B., Boulamery, A., and Simon, N. (2008). Biological rhythms: a neglected factor of variability in pharmacokinetic studies. J. Pharm. Sci. 97, 1099–1108.

Cornelissen, G. (2014). Cosinor-based rhythmometry. Theor. Biol. Med. Model. 11, 16.

Dallmann, R., Brown, S.A., and Gachon, F. (2014). Chronopharmacology: new insights and therapeutic implications. Annu. Rev. Pharmacol. Toxicol. 54, 339–361.

van Erp, N.P., Guchelaar, H.-J., Ploeger, B.A., Romijn, J.A., Hartigh, J. den, and Gelderblom, H. (2011). Mitotane has a strong and a durable inducing effect on CYP3A4 activity. Eur. J. Endocrinol. 164, 621–626.

Froy, O. (2009). Cytochrome P450 and the biological clock in mammals. Curr. Drug Metab. 10, 104–115.

Froy, O. (2010). Metabolism and circadian rhythms--implications for obesity. Endocr. Rev. 31, 1–24.

Fuhr, U., Jetter, A., and Kirchheiner, J. (2007). Appropriate phenotyping procedures for drug metabolizing enzymes and transporters in humans and their simultaneous use in the "cocktail" approach. Clin. Pharmacol. Ther. 81, 270–283.

Gorski, J.C., Jones, D.R., Haehner-Daniels, B.D., Hamman, M.A., O'Mara, E.M., and Hall, S.D. (1998). The contribution of intestinal and hepatic CYP3A to the interaction between midazolam and clarithromycin. Clin. Pharmacol. Ther. 64, 133–143.

Guo, Y.-F., and Stein, P.K. (2003). Circadian rhythm in the cardiovascular system: chronocardiology. Am. Heart J. 145, 779–786.

Halama, B., Hohmann, N., Burhenne, J., Weiss, J., Mikus, G., and Haefeli, W.E. (2013). A nanogram dose of the CYP3A probe substrate midazolam to evaluate drug interactions. Clin. Pharmacol. Ther. 93, 564–571.

Hoogerwerf, W.A. (2010). Role of clock genes in gastrointestinal motility. Am. J. Physiol. Gastrointest. Liver Physiol. 299, G549–G555.

Horne, J.A., and Ostberg, O. (1976). A self-assessment questionnaire to determine morningness-eveningness in human circadian rhythms. Int. J. Chronobiol. 4, 97–110.

ICH The International Conference on Harmonisation of Technical Requirements for Registration of Pharmaceuticals for Human Use.

Iwahori, T., Takeuchi, H., Matsuno, N., Johjima, Y., Konno, O., Nakamura, Y., Hama, K., Uchiyama, M., Ashizawa, T., Okuyama, K., et al. (2005). Pharmacokinetic differences between morning and evening administration of cyclosporine and tacrolimus therapy. Transplant. Proc. 37, 1739–1740.

Karlsson, M.O., and Bredberg, U. (1989). Estimation of Bioavailability on a Single Occasion After Semisimultaneous Drug Administration. Pharm. Res. 6, 817–821.

Karlsson, M.O., and Savic, R.M. (2007). Diagnosing model diagnostics. Clin. Pharmacol. Ther. 82, 17–20.

Karlsson, M.O., and Sheiner, L.B. (1993). The importance of modeling interoccasion variability in population pharmacokinetic analyses. J. Pharmacokinet. Biopharm. 21, 735–750.

Kaur, G., Phillips, C., Wong, K., and Saini, B. (2013). Timing is important in medication administration: a timely review of chronotherapy research. Int. J. Clin. Pharm. 35, 344–358.

Keizer, R.J., Karlsson, M.O., and Hooker, A. (2013). Modeling and Simulation Workbench for NONMEM: Tutorial on Pirana, PsN, and Xpose. CPT Pharmacometrics Syst. Pharmacol. 2, e50.

Klotz, U., and Reimann, I.W. (1984). Chronopharmacokinetic study with prolonged infusion of midazolam. Clin. Pharmacokinet. 9, 469–474.

Klotz, U., and Ziegler, G. (1982). Physiologic and temporal variation in hepatic elimination of midazolam. Clin. Pharmacol. Ther. 32, 107–112.

Koopmans, R., Dingemanse, J., Danhof, M., Horsten, G.P., and van Boxtel, C.J. (1991). The influence of dosage time of midazolam on its pharmacokinetics and effects in humans. Clin. Pharmacol. Ther. 50, 16–24.

Kumar, D., Wingate, D., and Ruckebusch, Y. (1986). Circadian variation in the propagation velocity of the migrating motor complex. Gastroenterology 91, 926–930.

Lee, J.-I., Chaves-Gnecco, D., Amico, J.A., Kroboth, P.D., Wilson, J.W., and Frye, R.F. (2002). Application of semisimultaneous midazolam administration for hepatic and intestinal cytochrome P450 3A phenotyping. Clin. Pharmacol. Ther. 72, 718–728.

Lemmer, B., and Nold, G. (1991). Circadian changes in estimated hepatic blood flow in healthy subjects. Br. J. Clin. Pharmacol. 32, 627–629.

Lemmer, B., Nold, G., Behne, S., and Kaiser, R. (1991). Chronopharmacokinetics and Cardiovascular Effects of Nifedipine. Chronobiol. Int. 8, 485–494.

Lu, Y.-F., Jin, T., Xu, Y., Zhang, D., Wu, Q., Zhang, Y.-K.J., and Liu, J. (2013). Sex differences in the circadian variation of cytochrome p450 genes and corresponding nuclear receptors in mouse liver. Chronobiol. Int. 30, 1135–1143.

Meijer, J.H., Colwell, C.S., Rohling, J.H.T., Houben, T., and Michel, S. (2012). Dynamic neuronal network organization of the circadian clock and possible deterioration in disease. Prog. Brain Res. 199, 143–162.

Min, D.I., Chen, H.Y., Fabrega, A., Ukah, F.O., Wu, Y.M., Corwin, C., Ashton, M.K., and Martin, M. (1996). Circadian variation of tacrolimus disposition in liver allograft recipients. Transplantation 62, 1190–1192.

Min, D.I., Chen, H.Y., Lee, M.K., Ashton, K., and Martin, M.F. (1997). Time-dependent disposition of tacrolimus and its effect on endothelin-1 in liver allograft recipients. Pharmacotherapy 17, 457–463.

Misaka, S., Uchida, S., Imai, H., Inui, N., Nishio, S., Ohashi, K., Watanabe, H., and Yamada, S. (2010). Pharmacokinetics and pharmacodynamics of low doses of midazolam administered intravenously and orally to healthy volunteers. Clin. Exp. Pharmacol. Physiol. 37, 290–295.

Mullington, J.M., Haack, M., Toth, M., Serrador, J.M., and Meier-Ewert, H.K. (2009). Cardiovascular, inflammatory, and metabolic consequences of sleep deprivation. Prog. Cardiovasc. Dis. 51, 294–302.

Ohno, M., Yamaguchi, I., Ito, T., Saiki, K., Yamamoto, I., and Azuma, J. (2000). Circadian variation of the urinary 6β-hydroxycortisol to cortisol ratio that would reflect hepatic CYP3A activity. Eur. J. Clin. Pharmacol. 55, 861–865.

Patel, N., Polak, S., Jamei, M., and Rostami Hodjegan, A. (2013). Quantitative prediction of circadian variation in pharmacokinetics based on in vitro data: dependence on route of administration in the case of BCS/BDDCS Class II and CYP3A4 substrate drug nifedipine. In 5th WCDATD/OrBiTo Meeting,.

R Development Core Team (2008). R: A language and environment for statistical computing. R Foundation for Statistical Computing (Vienna, Austria).

Savic, R.M., Jonker, D.M., Kerbusch, T., and Karlsson, M.O. (2007). Implementation of a transit compartment model for describing drug absorption in pharmacokinetic studies. J. Pharmacokinet. Pharmacodyn. 34, 711–726.

Tada, H., Satoh, S., Iinuma, M., Shimoda, N., Murakami, M., Hayase, Y., Kato, T., and Suzuki, T. (2003). Chronopharmacokinetics of tacrolimus in kidney transplant recipients: occurrence of acute rejection. J. Clin. Pharmacol. 43, 859–865.

Takiguchi, T., Tomita, M., Matsunaga, N., Nakagawa, H., Koyanagi, S., and Ohdo, S. (2007). Molecular basis for rhythmic expression of CYP3A4 in serum-shocked HepG2 cells. Pharmacogenet. Genomics 17, 1047–1056.

Thummel, K.E., O'Shea, D., Paine, M.F., Shen, D.D., Kunze, K.L., Perkins, J.D., and Wilkinson, G.R. (1996). Oral first-pass elimination of midazolam involves both gastrointestinal and hepatic CYP3A-mediated

metabolism. Clin. Pharmacol. Ther. 59, 491–502.

Tomalik-Scharte, D., Suleiman, A.A., Frechen, S., Kraus, D., Kerkweg, U., Rokitta, D., Di Gion, P., Queckenberg, C., and Fuhr, U. (2014). Population pharmacokinetic analysis of circadian rhythms in hepatic CYP3A activity using midazolam. J. Clin. Pharmacol. 54, 1162–1169.

Tsunoda, S.M., Velez, R.L., von Moltke, L.L., and Greenblatt, D.J. (1999). Differentiation of intestinal and hepatic cytochrome P450 3A activity with use of midazolam as an in vivo probe: effect of ketoconazole. Clin. Pharmacol. Ther. 66, 461–471.

Yang, J., Jamei, M., Yeo, K.R., Tucker, G.T., and Rostami-Hodjegan, A. (2007). Prediction of intestinal first-pass drug metabolism. Curr. Drug Metab. 8, 676–684.

Zanger, U.M., and Schwab, M. (2013). Cytochrome P450 enzymes in drug metabolism: regulation of gene expression, enzyme activities, and impact of genetic variation. Pharmacol. Ther. 138, 103–141.
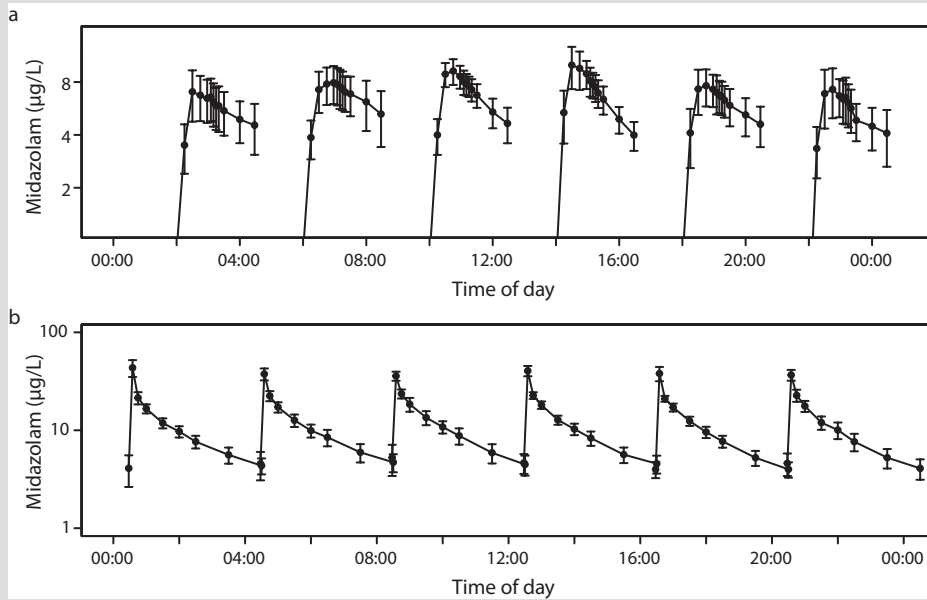
**Supplementary Figure 1** Concentration time profiles of midazolam after **(a)** oral and **(b)** intravenous administration at six different clock times. Data are presented as mean ± 95% confidence intervals
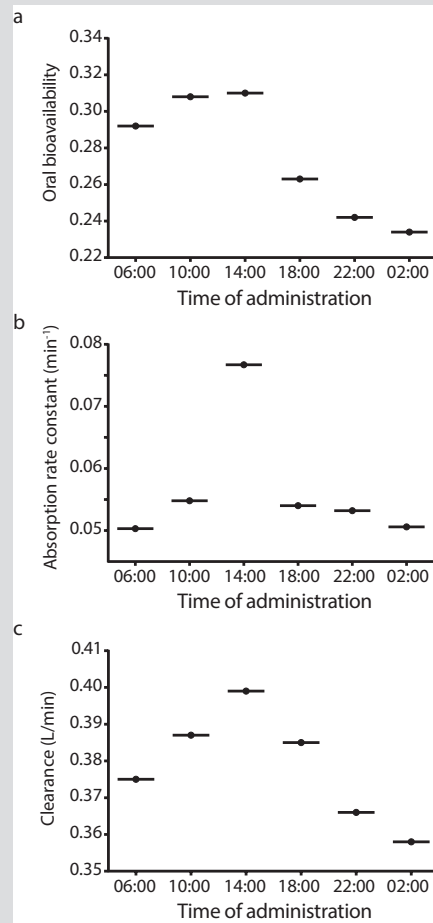
**Supplementary Figure 2** Oral bioavailability **(a)**, absorption rate constant **(b)** and clearance **(c)** versus time from models in which variation in parameters were estimated with different multiplication factors for each of the different administration times
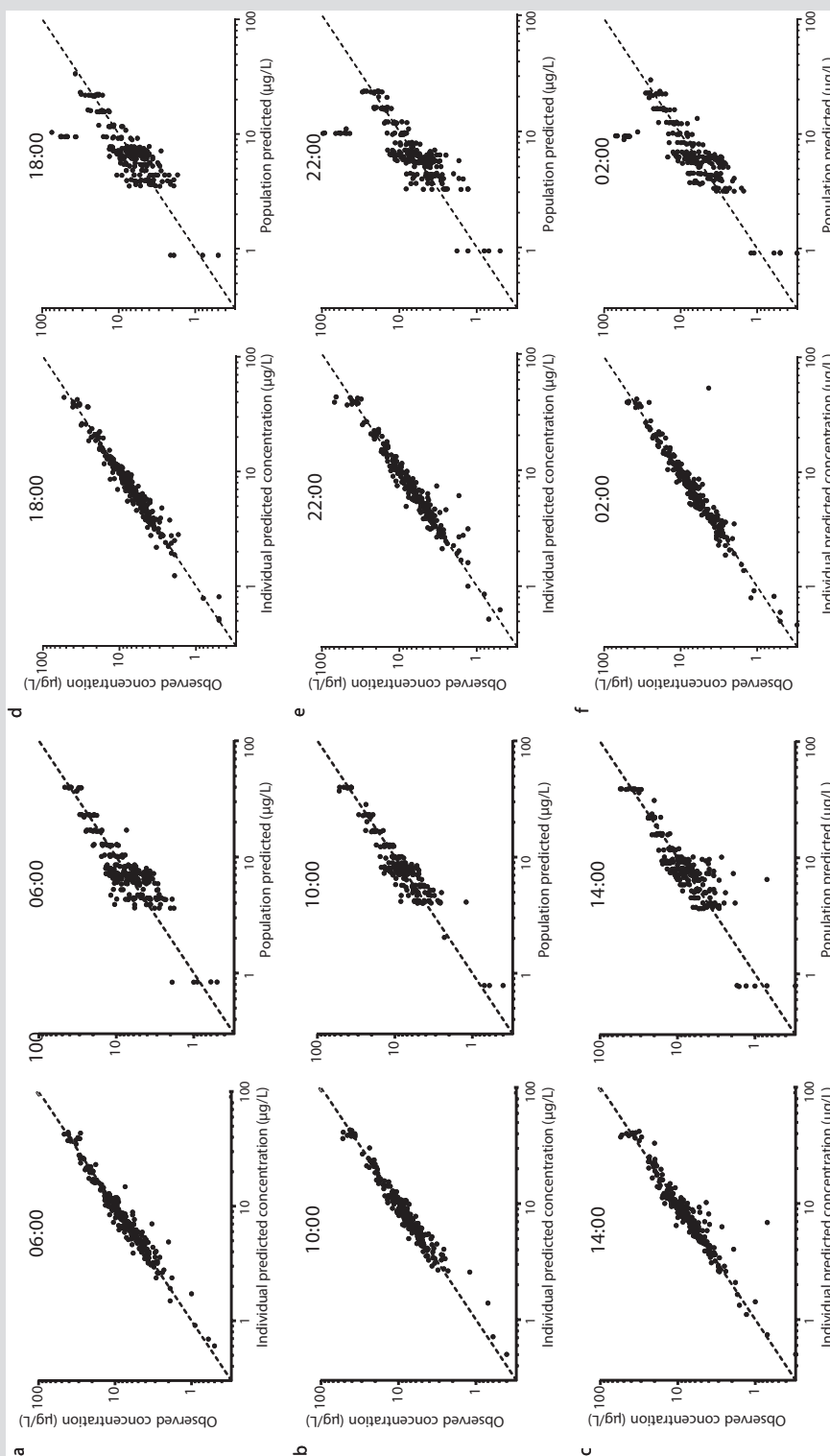
**Supplementary Figure 3** Observed versus individual-predicted concentrations (left panel) and observed versus population-predicted concentrations (right panel) of all 6 administration times (occasions) of the final model.

**Supplementary Table 1:** Summary of key model building steps and associated changes in objective function, interindividual variability, interoccasion variability, η-shrinkage and residual error

| Model | | OFV | # | | IIV (%) | η-shrink. IIV (%)[a] | IOV (%) | η-shrink. IOV (%)[a] | Residual error (%) | |
|---|---|---|---|---|---|---|---|---|---|---|
| | | | | | | | | | Oral | IV |
| Simple model | | 2807 | 12 | F | 23.6 | | | | 25.9 | 16.1 |
| | | | | Ka | 18.7 | | | | | |
| | | | | CL | 16 | | | | | |
| IOV F | | 2459 | 13 | F | 23.1 | | 20 | 33 | 19 | 16 |
| | | | | Ka | 21.4 | | | | | |
| | | | | CL | 16 | | | | | |
| IOV Ka | | 2548 | 13 | F | 25 | | | | 20.1 | 16.2 |
| | | | | Ka | 15.8 | 26 | 36 | 55 | | |
| | | | | CL | 15.4 | | | | | |
| IOV CL | | 2714 | 13 | F | 23.7 | | | | 24.9 | 14.7 |
| | | | | Ka | 19.2 | | | | | |
| | | | | CL | 15.8 | | 8.2 | 14 | | |
| IOV F + COS F | | 2431 | 15 | F | 23.1 | | 15.4 | 18 | 19 | 16.1 |
| | | | | Ka | 21 | | | | | |
| | | | | CL | 16 | | | | | |
| | + IOV Ka | 2087 | 16 | F | 24.7 | | 14.8 | 10 | 13.6 | 16 |
| | | | | Ka | 14.5 | 22 | 30.8 | 60 | | |
| | | | | CL | 15.8 | | | | | |
| IOV F + COS F | + IOV Ka + MF Ka 14:00 | 2078 | 17 | F | 24.6 | | 14.9 | 11 | 13.6 | 15.9 |
| | | | | Ka | 15.3 | 18 | 28.3 | 55 | | |
| | | | | CL | 15.5 | | | | | |
| | + MF Ka 14:00 (IOV Ka closed) | 2345 | 16 | F | 23.7 | | 15.0 | 14 | 18.1 | 16.0 |
| | | | | Ka | 19.4 | | | | | |
| | | | | CL | 15.9 | | | | | |
| | + IOV CL | 2284 | 17 | F | 24.4 | | 15.0 | 20 | 17.7 | 14.6 |
| | | | | Ka | 19.2 | | | | | |
| | | | | CL | 23.4 | | 8.0 | 25 | | |
| IOV F + COS F + MF Ka 14:00 | + IOV CL + COS CL | 2258 | 19 | F | 23.4 | | 14.1 | 18 | 17.7 | 14.4 |
| | | | | Ka | 18.9 | | | | | |
| | | | | CL | 15.9 | | 6.9 | 20 | | |
| | + COS CL (IOV CL closed) (Final model) | 2299 | 18 | F | 23.3 | | 14.8 | 12 | 18.0 | 15.4 |
| | | | | Ka | 19.1 | | | | | |
| | | | | CL | 16.2 | | | | | |

a. Only shrinkage values of ≥ 10% are reported.

# = number of parameters; shrink. = shrinkage; CL= clearance; COS= cosine function; F= oral bioavailability; IIV= interindividual variability; IOV= interoccasion variability; IV= intravenous; Ka= oral absorption rate; MF= multiplication factor

# CHAPTER

## Identifying 24-hour variation in the pharmacokinetics of levofloxacin: a population pharmacokinetic approach

# 4

Laura Kervezee[1,2]; Jasper Stevens[2]; Willem Birkhoff[2]; Ingrid M. C. Kamerling[2]; Theo de Boer[3]; Melloney Dröge[3]; Johanna H. Meijer[1,*]; Jacobus Burggraaf[2,*]

[1]Laboratory for Neurophysiology, Department of Molecular Cell Biology, Leiden University Medical Center, Leiden, the Netherlands
[2]Centre for Human Drug Research, Leiden, the Netherlands
[3]ABL Laboratories, Assen, the Netherlands
* These authors share senior authorship

# SUMMARY

**Aim:** The objective of this study was to investigate whether the pharmacokinetics of orally administered levofloxacin show 24-hour variation. Levofloxacin was used as a model compound for solubility- and permeability-independent absorption and passive renal elimination.

**Methods:** In this single centre, cross-over, open label study, twelve healthy subjects received an oral dose of 1000mg levofloxacin at six different time-points equally divided over the 24-hour period. Population pharmacokinetic modelling was used to identify potential 24-hour variation in the pharmacokinetic parameters of this drug.

**Results:** The pharmacokinetics of levofloxacin could be described by a one-compartment model with first-order clearance and a transit compartment to describe drug absorption. The fit of the model was significantly improved when the absorption rate constant was described as a cosine function with a fixed period of 24 hours, a relative amplitude of 47% and a peak around 8:00 in the morning. Despite this variation in absorption rate constant, simulations of a once-daily dosing regimen show that $T_{max}$, $C_{max}$ and the area under the curve at steady state are not affected by the time of drug administration.

**Conclusion:** The finding that the absorption rate constant shows considerable 24-hour variation may be relevant for drugs with similar physicochemical properties as levofloxacin that have a narrower therapeutic index. Levofloxacin, however, can be dosed without taking into account the time of day, at least in terms of its pharmacokinetics.

**What is already known about this subject:**

- The pharmacokinetics of drugs may show 24-hour variation, but this has rarely been systematically evaluated.
- Levofloxacin is an antibiotic whose oral absorption is limited by gastric emptying time and whose elimination occurs primarily via passive renal clearance, and can as such be used as a model compound to study 24-hour variation in these processes.

**What this study adds:**

- The absorption rate constant of levofloxacin shows considerable 24-hour variation, while other pharmacokinetic parameters seem constant throughout the day and night.
- This is relevant for drugs with similar physicochemical properties as levofloxacin that have a narrower therapeutic index, as the rhythm in absorption rate constant may be clinically relevant.

# INTRODUCTION

Understanding the variables that influence the therapeutic effect of drugs is essential to optimize dosing strategies. One potential source of variation is introduced by the 24-hour rhythms in physiology, which are generated by an endogenous clock mechanism that is entrained to the 24-hour light-dark cycle and that allows us to anticipate to daily environmental changes (Mohawk et al., 2012). These rhythms are known to affect the pharmacokinetics, pharmacodynamics and toxicity of drugs (Dallmann et al., 2014).

Many physiological processes in the human body are subject to 24-hour fluctuations (Baraldo, 2008), such as gastric emptying time (Goo et al., 1987), hepatic enzyme activity (Takiguchi et al., 2007) and kidney function (Koopman et al., 1989). The complex interplay between these rhythms may lead to substantial variation in the pharmacokinetic parameters of a drug over the day and the night. With an increased understanding of the effect of these rhythms on the pharmacokinetics of a drug, the design of new and existing drug therapies can be improved by taking into account the optimal time of drug administration.

Scattered throughout the literature are a large number of studies that investigate the chronopharmacology of a wide variety of drugs, such as antibiotics (Beauchamp and Labrecque, 2007). These studies often employ a design that limits the interpretation and application of their results, thereby hampering implementation of the findings in the clinic. For example, as many chronopharmacological studies compare the pharmacokinetics following drug administration at two time points separated by twelve hours (Bleyzac et al., 2000; Choi et al., 1999; Fauvelle et al., 1994; Hishikawa et al., 2001; Rao et al., 1997), it is likely that the peak and trough are outside the studied intervals. Furthermore, most studies use an isolated approach in which the chronopharmacokinetics of one particular drug is investigated, without considering the relevance of their findings to other drugs with similar characteristics.

To overcome these limitations, a more systematic approach is required. For example, by investigating the chronopharmacokinetics of a model drug that represents a class of drugs that are absorbed, metabolized and/or eliminated in a similar manner, the findings can be extrapolated beyond the drug under investigation. Secondly, the use of multiple time points of drug administration is crucial in order to fully capture potential fluctuations over the 24-hour period. Thirdly, employing population pharmacokinetic modelling facilitates the identification of sources of variability related not only to the time of drug administration, but also to inter-individual and intra-individual differences, as utilized previously with midazolam (van Rongen et al., 2015).

The aim of this study was to investigate the chronopharmacokinetics of levofloxacin, an antibiotic characterized by solubility- and permeability independent absorption, minimal metabolism and passive renal elimination (Fish and Chow, 1997; Frick et al., 1998). Additionally, levofloxacin does not act primarily on the central nervous system, unlike many other drugs with similar physicochemical properties, so its influence on the central circadian clock in the hypothalamus is likely minimal. As such, levofloxacin was used as a model

compound to study the possible influence of 24-hour rhythms in physiological processes that determine the pharmacokinetics of many other drugs with similar properties. We developed a population pharmacokinetic model describing data from a clinical trial in which twelve healthy male subjects received an oral dose of 1000mg levofloxacin at six different time-points equally distributed over the 24-hour period. Simulations were performed to evaluate the effect of time of administration on several pharmacokinetic markers.

## METHODS

### Subjects

Healthy male subjects, aged between 18-50 years and with a body mass index (BMI) between 18-30 kg/m$^2$, were considered for inclusion. Eligibility was based upon results of medical history, physical examination, vital signs and laboratory profiles of blood and urine. Exclusion criteria included the use of concomitant medication two weeks prior to first drug administration until the end of the study, smoking and consumption of more than 21 units of alcohol per week or more than 8 units of caffeine per day. Subjects were also excluded if they were classified as extreme morning or evening types by the Horne-Ostberg morningness/eveningness questionnaire (Horne and Ostberg, 1976), if they were involved in transmeridian flights or shift work within a month prior to the start of the study until the end of the study or if they were otherwise unable to maintain a normal diurnal rhythm. All subjects provided written informed consent prior to the study. The study was approved by the Medical Ethics Committee of the Leiden University Medical Center and registered in the European Clinical Trials Database (EudraCT Number: 2013-001976-39).

### Study design

This single centre, cross-over, open label study was carried out at the Centre of Human Drug Research in Leiden, the Netherlands. Subjects were randomly assigned to a treatment schedule consisting of six study visits separated by at least one week. A week prior to each study visit, subjects had to maintain a stable diurnal rhythm (waking times between 07:00 and 08:00, sleeping times between 23:00 and 00:00), which was verified by a sleep diary and a wrist-worn activity tracker (Daqtometer v2.4, Daqtix GmbH, Ötzen, Germany). Dietary restrictions included no caffeine or alcohol from 24 hours prior to drug administration and no dairy products or mineral fortified food supplements from 72 hours prior to drug administration.

Each study visit, subjects received an oral dose of 1000mg levofloxacin (Aurobindo Pharma B.V., Zwijndrecht, the Netherlands) with 200mL water at either 02:00, 06:00, 10:00, 14:00, 18:00 or 22:00 (Figure 1). Three hours after levofloxacin administration, subjects received an intravenous bolus of 5g inulin (250mg/mL; Inutest® from Fresenius Kabi, Zeist, the Netherlands). Subjects were fasted from t=-2h until t=6h. Subjects ate a maximum of four slices of bread at t=6h and a small snack at t=10h and drank at least 150mL water every 2 hours in order to keep fluid intake constant throughout the day and night. Between 23:30
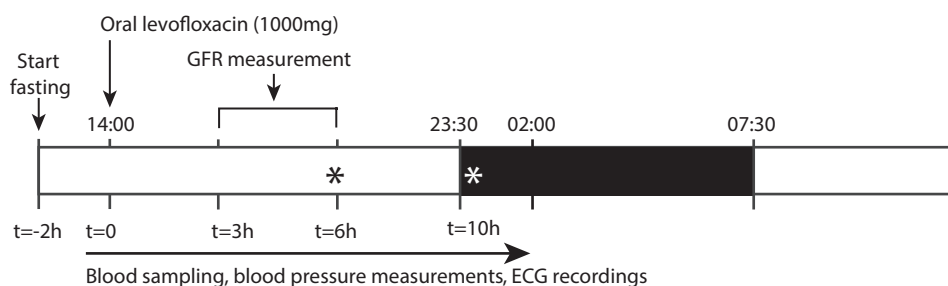
**Figure 1** Schematic representation of a study occasion with drug administration at 14:00. Asterisks indicate the time-points the subjects were instructed to eat a standardized meal. In other occasions, the time of drug administration, measurements and meals occurred at a different time point (t=0 at 02:00, 06:00, 10:00, 14:00, 18:00 or 22:00), while the time the lights were dimmed and subjects wore an eye-mask were similar in all occasions (represented by the dark box from 23:30 until 07:30).

and 07:30, the lights were dimmed, subjects wore eye masks and sleep disturbance was kept to a minimum. Subjects remained in a semi-recumbent position from 30 minutes prior to dosing until the end of the study visit (except occasional toilet visits).

Blood samples (2mL) from an indwelling intravenous catheter and twelve-lead electrocardiograms (ECGs) were taken at predetermined time points (Table 1). Levofloxacin samples were collected in heparinised tubes, placed on ice and centrifuged at 2000g for 10 minutes at 4°C. Inulin and thyroid stimulating hormone (TSH) samples were collected in non-additive tubes. After coagulation for at least 45 minutes at room temperature, the samples were centrifuged at 2000g for 10 minutes at 4°C. All samples were stored at -80°C until further analysis. ECG recordings were stored using the MUSE Cardiology Information System. Because levofloxacin is known to prolong the QT interval, changes in QT interval were closely monitored during the study visits.

## Levofloxacin

Acetonitrile protein-precipitation was used to isolate levofloxacin from plasma. Levofloxacin-d8 was added as internal standard. Chromatographic separation was performed on an XBridge C18 column using gradient elution. An API 4000 tandem mass spectrometer equipped with a Turbo Ion Spray probe operated in the multiple reaction monitoring (MRM) in positive mode was used for quantification. The lower limit of quantification (LLOQ) of this assay was 0.100 μg/mL. The inter-assay accuracy was between 101.1-111.0% and the inter-

**Table 1 Sampling times**

| Analyte | Sampling times[a] |
|---|---|
| Levofloxacin | 0, 0.5, 1, 1.5, 2, 2.5, 3, 4, 5, 6, 8, 10, 12h |
| Inulin[b] | 180, 185, 190, 195, 210, 240, 270 and 300 min |
| Thyroid stimulating hormone (TSH) | 0, 1, 2, 3, 4, 5, 6, 7, 8, 9, 10, 11h |
| ECG recordings | 0, 0.5, 1, 1.5, 2, 2.5, 3, 4, 6, 8, 12h |

a. t=0 defined as the time of levofloxacin administration

b. Inulin was administered at t=180min

assay variability was within 5.2%.

For non-compartmental analysis of the observed data, the maximal concentration (Cmax) and the time to Cmax (Tmax) were obtained directly from the individual data points. The area under the concentration-time curve from 0-12 hours after administration (AUC0-12) was calculated by the trapezoidal rule.

**Glomerular filtration rate**

Inulin concentrations in serum samples were determined by spectrophotometry. The determination was based on hydrolysis of inulin to fructose and formation of a purple-violet colour by fructose with ß-indolylacetic acid in concentrated hydrochloric acid. The LLOQ was 10.0 µg/mL. The inter-assay accuracy was between 103.3-110.2% and the inter-assay variability was within 8.0%. Systemic inulin clearance was calculated as the ratio of the dose to the baseline-corrected area under the curve from 0 to infinity using non-compartmental methods. To determine glomerular filtration rate (GFR), systemic inulin clearance was normalized by body surface area, calculated by the du Bois formula (Du Bois and Du Bois, 1916). Linear mixed effects modelling with the Nlme package in R (version 3.1.2, http://r-project.org) was used with GFR as the dependent variable, time of inulin administration as a fixed (categorical) effect and subject as a random effect. A likelihood ratio test of this model against the null model that included no fixed effect parameter was used to determine the effect of time of administration on GFR. $P < 0.05$ was considered significant. Coefficients and 95% confidence limits of the full model were determined using the Effects package in R.

**Thyroid stimulating hormone**

Endogenous TSH concentrations in serum were measured by an electrochemiluminescence immunoassay (ECLIA, Cobas, Roche Diagnostics GmbH, Mannheim, Germany) according to the manufacturer's protocol. The LLOQ of this assay was 0.3mU/L. The inter-assay variability was lower than 0.6% and the intra-assay variability was lower than 1.6%. The relative TSH level per hour was calculated as follows:

$$\text{Relative TSH (\%)} = TSH(t)_i / TSH_i * 100\% \qquad \text{Equation 1}$$

where $TSH(t)_i$ is the mean concentration of TSH of the $i^{th}$ subject at time t (sampling times were rounded to the nearest hour) and $TSH_i$ is the mean of all $TSH(t)_i$ values of the $i^{th}$ subject. The mean and 95% confidence intervals of the relative TSH levels per hour of all subjects combined was calculated and plotted against clock time.

**Pharmacokinetic model development**

A population PK model was developed to describe the concentration-time profiles of levofloxacin and to investigate the effect of time of administration on these profiles using nonlinear mixed effect modelling (NONMEM 7.3 (Beal et al., 2009)) in combination with Pirana (v2.8.2), PsN (version 3.7.6), Xpose (v4) and R (v3.1.2) to facilitate evaluation and graphical representation of the models (Keizer et al., 2013). Samples below LLOQ and

that were taken before Tmax were set to 0; samples that were below LLOQ and that were taken after the Tmax were omitted. The first-order method with conditional estimation and interaction (FOCEI) and the ADVAN6 subroutine was used throughout model development.

A stepwise approach was used to develop the population pharmacokinetic model. Different structural models (one- and two-compartment models) and the implementation of inter-individual variability (IIV) on the structural parameters were investigated. IIV was included according to equation 2:

$$P_i = \theta * e^{n_i} \qquad \text{Equation 2}$$

where $P_i$ is the pharmacokinetic parameter for the $i^{th}$ individual, $\theta$ is the population pharmacokinetic parameter and $\eta_i$ represents the IIV for the $i^{th}$ individual. Different models to describe residual error were tested (proportional, additive and combined). Various methods were used to characterize the absorption phase: zero-order absorption, sequential and parallel first- and zero-order absorption and first-order absorption with a lag-time and models with a fixed number of transit compartments or with an estimated number of transit compartments (Savic et al., 2007).

Next, several approaches to describe potential 24-hour variation in the pharmacokinetic parameters were assessed. Firstly, the 24-hour period was arbitrarily subdivided in equal sampling windows (e.g. for six equal sampling windows: window 1: 0:00-4:00, window 2: 4:00-8:00, etc.) and this was implemented as a covariate as follows:

$$\theta = \theta_{base} + \theta_{window} \qquad \text{Equation 3}$$

where $\theta$ is the population pharmacokinetic parameter, $\theta_{base}$ represents the base value of the pharmacokinetic parameter (fixed to the value obtained in the model that did not contain this covariate) and $\theta_{window}$ represents the additive change in the pharmacokinetic parameter during that window. Secondly, IOV was included on the pharmacokinetic parameters as described previously (Karlsson and Sheiner, 1993), with each occasion representing a different dosing time. Thirdly, 24-hour variation in each of the pharmacokinetic parameters was evaluated by describing it as a cosine function with a fixed period of 24 hours as follows:

$$\theta(t) = \theta_{Mesor} + \theta_{Amp} * \cos(2\pi * (t - \theta_{\varphi}) / 24 ) \qquad \text{Equation 4}$$

where $\theta(t)$ is the population pharmacokinetic parameter at time t (in hours after midnight), $\theta_{Mesor}$ represents the mesor (rhythm-adjusted mean), $\theta_{Amp}$ is the amplitude and $\theta_{\varphi}$ is the phase of the rhythm (corresponding to the time of peak in hours after midnight). If necessary, $\theta_{Mesor}$ was reparametrized to ensure the pharmacokinetic parameter remained positive during simulations (see below) as follows:

$$\theta_{Mesor} = e^{\theta_{trough}} + \theta_{Amp} \qquad \text{Equation 5}$$

where $\theta_{trough}$ is the value of the parameter at the trough of the cosine.

Covariate analysis was performed using a forward selection/backward elimination procedure. Continuous covariates (weight, height, lean body mass, body mass index, GFR and age) that showed a significant correlation (p<0.01, Pearson's correlation coefficient)
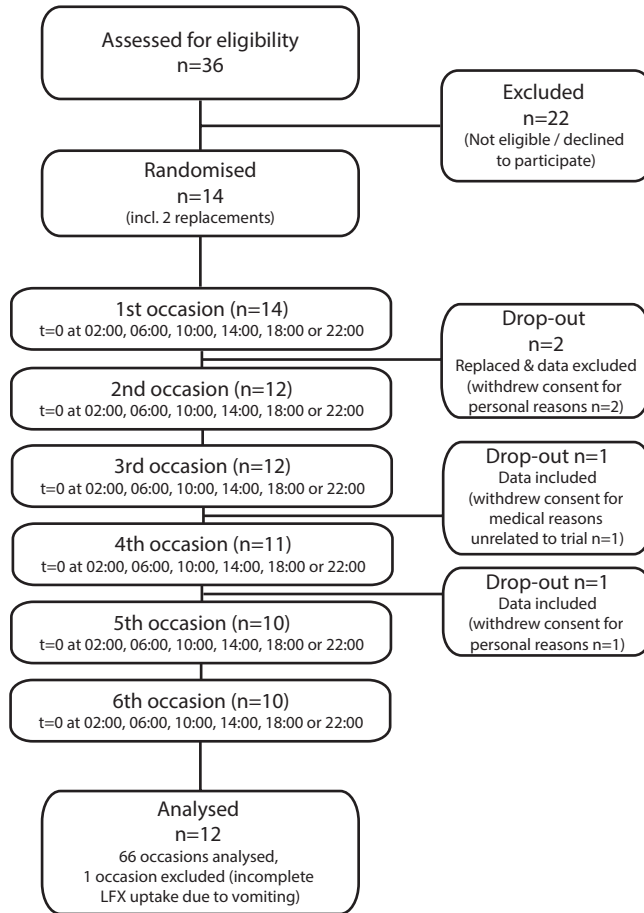
**Figure 2** Clinical trial flow diagram. Twelve subjects were enrolled and randomly allocated to one of the treatment sequences in which drug administration occurred at a different time point in each occasion. Two of the twelve subjects withdrew consent after the first study visit. Their data was excluded and they were replaced. One subject withdrew consent after three occasions; another subject withdrew consent after four occasions. These subjects were not replaced and their data was included in further analysis. Data from one occasion had to be excluded due to incomplete levofloxacin (LFX) uptake after vomiting.

with a pharmacokinetic parameter were considered for inclusion in the model. Potential covariates were included as follows:

$$\theta_i = \theta_{pop} * (COV_i / COV_m)^{\theta COV} \qquad \text{Equation 6}$$

where $\theta_i$ is the covariate-adjusted pharmacokinetic parameter for the ith individual, $\theta_{pop}$ the population predicted pharmacokinetic parameter, $COV_i$ the individual value of the covariate, $COV_m$ the median value of the covariate in the population and $\theta_{COV}$ represents the covariate effect.

Model selection was based on objective function value (OFV), precision and plausibility of the parameter estimates (compared to previously published values of levofloxacin pharmacokinetics (Peloquin et al., 2008; Tanigawara et al., 1995; Zhang et al., 2009)), degree of shrinkage and graphical evaluation of the fit of the models (Mould and Upton, 2013). The

likelihood ratio test was used to compare the fit of nested models, under the assumption that the difference in -2 times log likelihood is chi-square distributed with degrees of freedom (df) determined by the number of additional parameters. Hence, a model in which the OFV decreased at least 6.63 points (p<0.01) upon inclusion of one additional parameter was considered to provide a significantly better fit of the data than the parent model. A visual predictive check (VPC) based on 1000 simulated individuals and stratified on the time of administration was performed to determine how well the observed data is captured by the final model.

### Simulations

Simulations were performed using the package deSolve (v1.11) in R. To obtain the Cmax, Tmax and $AUC_{0-12}$ of the observed data (see above) to the model predicted data, the individual predicted parameter estimates were used to simulate the concentration-time profiles of the 12 subjects (sampling every minute from t=0 until t=12h). Concentration profiles of a once-daily 1000mg dose administered at different dosing times for seven days in 500 subjects were simulated using the fixed and random parameter estimates of the final model and the uncertainty around the fixed parameter estimates and the $C_{max}$, $T_{max}$ and the AUC during the dosing interval at steady state (referred to as $C_{max,ss}$, $T_{max,ss}$ and $AUC_{ss}$) were computed.

## RESULTS

### Subjects

A total of 66 occasions from 12 subjects were available for analysis (Figure 2). The demographics of the study population are summarized in Table 2. The treatment was generally well tolerated, although several adverse events (AEs) were reported, including headache (10% of the occasions), nausea (5.8%) and dizziness (5.8%). On several instances, the QT interval slightly increased after levofloxacin administration, but no QT-related AEs were reported.

**Table 2** Overview of subject demographics

|  | N | Mean | Range |
|---|---|---|---|
| Age (years) | 12 | 28.0 | 21.0-48.0 |
| Body mass index (kg/m2) | 12 | 24.0 | 19.4-29.2 |
| Height (cm) | 12 | 186 | 179-192 |
| Weight (kg) | 12 | 83.5 | 66.7-105 |
| Lean body mass (kg) | 12 | 61.1 | 55.2-69.3 |
| Glomerular filtration rate (mL/min/1.73m²) | 64[a] | 114 | 86.2-174 |

a. Two GFR values were missing due to problems with the administration of inulin. These values were replaced with the median value of GFR values from other occasions of this subject for covariate analysis.
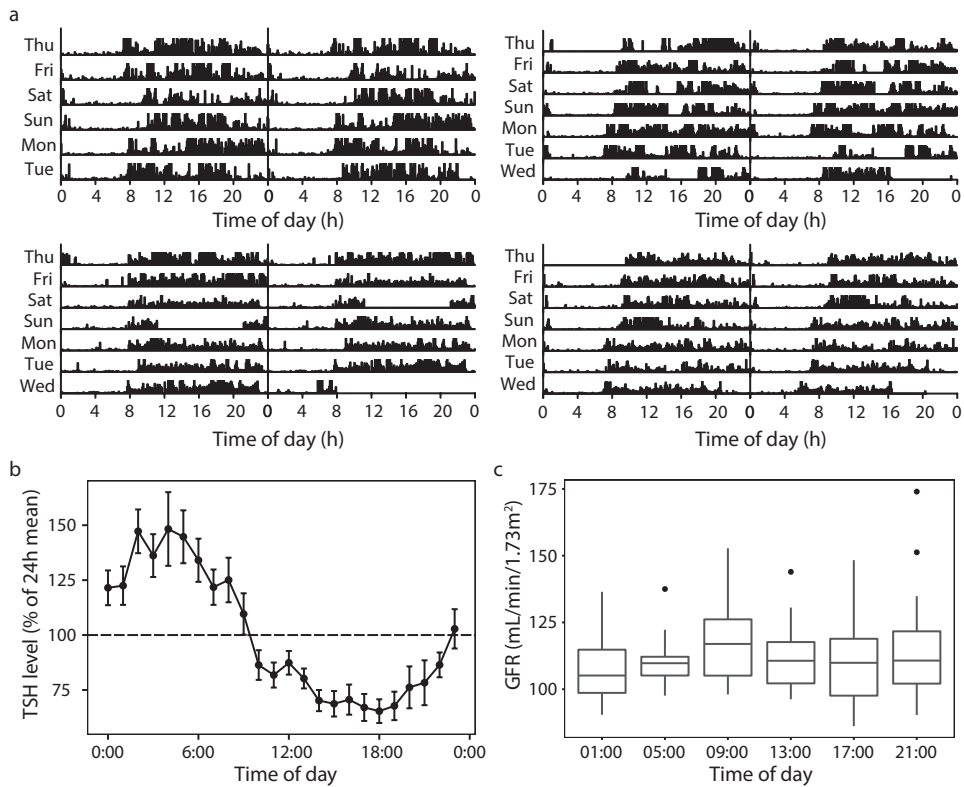
a



b



c



**Figure 3** Rhythms in physiological parameters. **(A)** Four representative actograms from different subjects collected one week before a study visit. Days are double-plotted for clarity. **(B)** Mean relative change in thyroid stimulation hormone (TSH) levels over the course of the 24-hour period in all subjects combined (error bars: 95% confidence intervals). Time of sample was rounded to the nearest hour. **(C)** Boxplots showing the distribution of glomerular filtration rate (GFR) at six time-points during the 24-hour period. Upper and lower hinges encompass the inter-quartile range (IQR); upper and lower whiskers extend to the highest and lowest value within the 1.5*IQR; points represent data beyond the whiskers.

**Physiological parameters**

Actigraphy data was collected a week prior to each study visit. Seventy percent of the actograms could be generated successfully and indicate that the subjects maintained a constant behavioural rhythm as instructed (Figure 3A). Furthermore, thyroid stimulating hormone (TSH) levels, a rhythmic marker that was collected hourly during the study visits, exhibited clear 24-hour rhythmicity with peak serum levels occurring between 02:00 and 05:00 at night in the population (Figure 3B) as well as on an individual level (Supplemental Figure 1). GFR showed small time of day variation (Figure 3C). Linear mixed effects modelling indicated that time of day significantly affected GFR ($\chi^2(5)$=11.8, p=0.038). The highest GFR was observed when inulin was administered at 09:00 in the morning (estimate [95% CI]: 118 [108-129] mL/min/1.73m$^2$) and lowest at 01:00 at night (108 [97-119] mL/min/1.73m$^2$), amounting to a maximal difference of 9%.
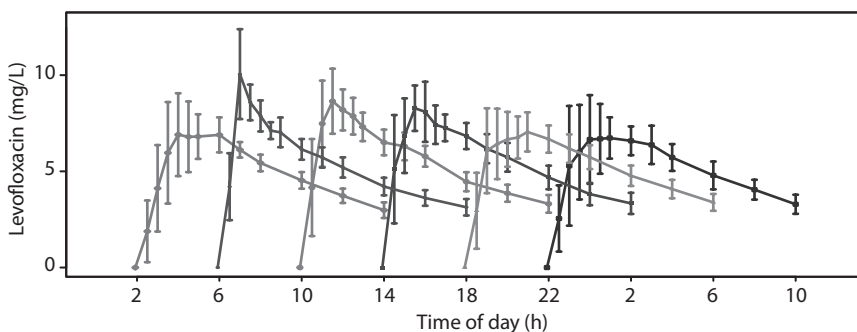
**Figure 4** Concentration time profiles of levofloxacin in plasma per time points of administration. Raw data is presented as mean ± 95% CI.

## Model development

Seven hundred ninety-two post-dose concentrations of levofloxacin were available for pharmacometric analysis. Nineteen samples (2.4%) were BLOQ. Mean concentration-time profiles are shown in Figure 4. When comparing different structural models, it was found that a one-compartment model with first-order absorption and elimination described the data well. Adding a second compartment did not improve the fit compared to the one-compartment model (ΔOFV -0.362). Inter-individual variability (IIV) could be identified on the absorption rate constant (Ka), apparent clearance (Cl/F) and central volume of distribution (V/F). A proportional error structure was used to describe the residual random variability. The absorption phase could be best described by adding a transit compartment with the transit rate constant (Ktr) equal to Ka. Covariance between IIV on Cl/F and V/F was included in this model.

Subsequently, it was investigated whether any of the pharmacokinetic parameters exhibited 24-hour variation. Firstly, we used six parameters (Eq. 3) to describe the effect of the time window during which a sample was taken on the pharmacokinetics of levofloxacin. This allowed us to explore the presence and shape of the 24-hour variation in the parameters, despite the relatively long half-life of the drug. Applying this approach to Cl/F, V/F or Ka resulted in a change in OFV of respectively -3.39 (p>0.01), -14.9 (p>0.01) and -52.4 (p<0.01, 5df). Hence, the fit of the model significantly improved when the effect of sampling window is included on Ka. Although the precision of these estimates of $\theta_{window}$ was low (RSE: 45-253%), a pattern was revealed that resembles a sinusoidal curve with higher Ka values during the early morning and afternoon and lower values during the evening and night (Figure 5A). A similar pattern was found when IOV was included on Ka (Figure 5B).

Because of the sinusoidal profile that was identified in Ka, it was attempted to describe this parameter as a cosine function (Eq. 4), with the mesor parametrized using Equation 5 and IIV included on $\theta_{trough}$. Inclusion of the cosine on Ka reduced OFV by -84.8 points (p<0.01, 2df) and has similar goodness of fit (Supplemental Figure 2) compared to the parent model (without variation in Ka). Of note, the shape of the cosine on Ka resembles the pattern that was found when IOV or the effect of sampling window was included on Ka (Figure 5C).
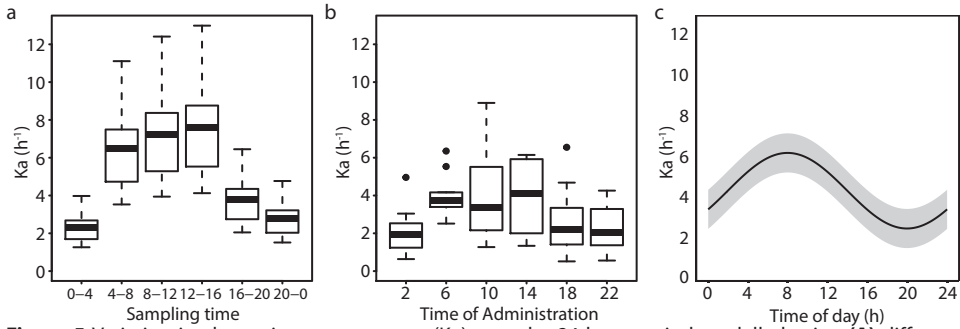
**Figure 5** Variation in absorption rate constant (Ka) over the 24-hour period modelled using **(A)** different additive terms depending on the time winding during which the sampling was performed, **(B)** interoccasion variability on the different times of administration and **(C)** the estimated cosine function with a fixed period of 24 hours. Grey area: 95% confidence interval of the individual predicted curves (including interindividual variability on $\theta_{trough}$).
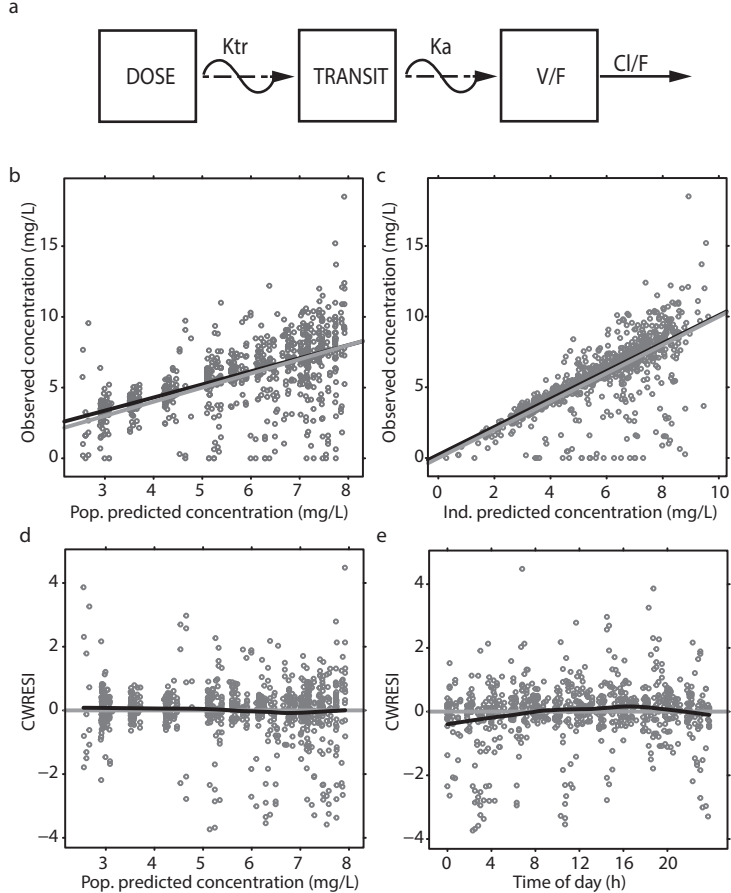


**Figure 6** Structure and fit of the final model. **(A)** Final model structure: a one-compartment model with linear absorption and clearance (Cl/F), one transit compartment and a cosine function to describe the absorption rate constant (Ka). V/F: volume of distribution; Ktr: transit rate constant. **(B-C)** Observed versus population predicted concentrations (B) and individual predicted concentrations (C). Light green lines: line of unity, black line: linear regression line. **(D-E)** Conditional weighted residuals with interaction (CWRESI) versus population predicted concentrations (D) and time of day (E). Light green lines: horizontal line through y=0; black line: LOESS curve with span=0.6

Therefore, this one-compartment model with one transit compartment (with Ktr=Ka) in which Ka was described as a cosine function with a period of 24 hours (referred to as the "cosine Ka model") was used for further model development (Figure 6A). Covariate analysis showed that none of the covariates that were tested (LBM on Cl/F, V/F and the mesor of Ka, age on the mesor of Ka and GFR on V/F and Cl/F) significantly improved the fit of the model.

The parameter estimates of the cosine Ka model are shown in Table 3. The population and individual predicted concentrations of the cosine Ka model describe the observed concentrations accurately (Figure 6B and C) and the conditional weighted residuals (CWRESI) are symmetrically distributed around zero, without substantial concentration- or time-dependent bias (Figure 6D and E). η and ε shrinkage were below 3%. A visual
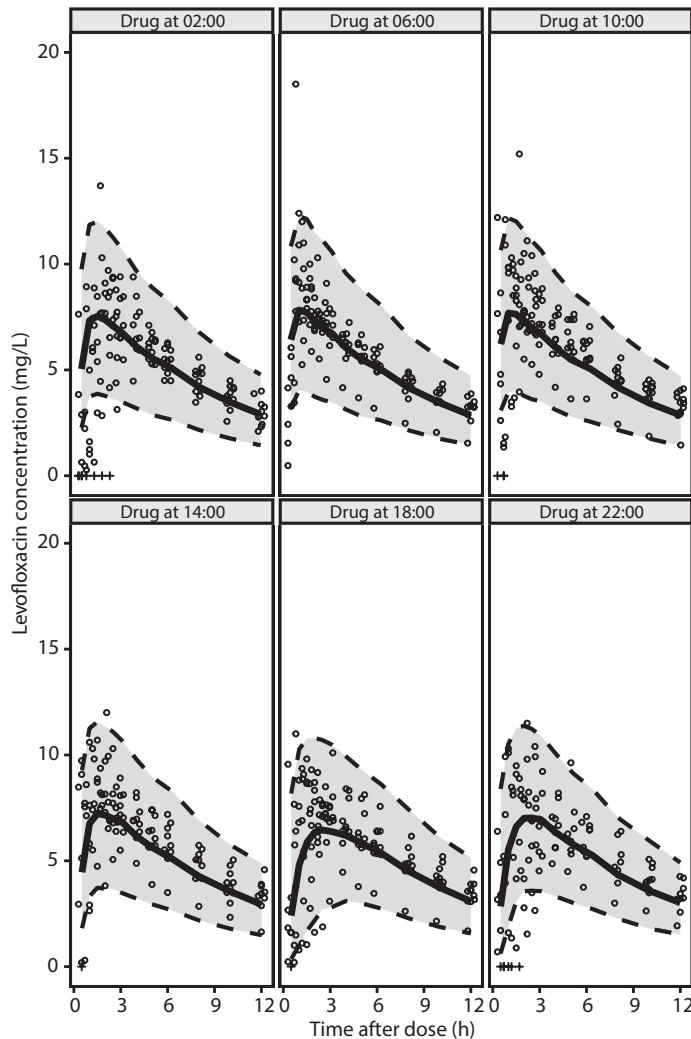


**Figure 7** Visual Predictive Check (VPC) stratified by time of administration. Solid line: Median of predicted concentrations, grey area enclosed by dashed lines: 90% prediction intervals of the simulated data. Circles: observed data. Crosses: data points below lower limit of quantification and before Cmax that were included in the data set used for model development.

**Table 3** Population parameter estimates of the final PK model.

| Parameter estimate | | Estimate (RSE %) | IIV %CV |
|---|---|---|---|
| Cl/F (L/h) | | 10.8 (6%) | 18.3% |
| V/F (L) | | 116 (4%) | 14.1% |
| Ka=Ktr | Trough (h⁻¹) | 2.10 (30%) | 91.6% |
| | Amplitude (h⁻¹) | 1.85 (18%) | ND |
| | Acrophase (h after midnight) | 7.97 (6%) | ND |
| Residual proportional error (%CV) | | 29.0% | |
| Covariance between Cl/F and V/F (%CV) | | 72.9% | |

RSE = relative standard error; CV = coefficient of variation; IIV = inter-individual variability; ND = not determined.

**Table 4 Steady-state values of a dosing regimen of once-daily 1000mg oral levofloxacin at 08:00, 18:00 and 23:00 simulated in 500 subjects.**

| | Time of drug administration | | |
|---|---|---|---|
| | **08:00** | **18:00** | **23:00** |
| $C_{max,ss}$ (mg/L) | 8.93 (6.51-12.1) | 8.13 (5.51-11.4) | 8.53 (6.09-11.7) |
| $T_{max,ss}$ (h) | 1.00 (0.50-1.50) | 2.30 (0.70-6.05) | 1.75 (0.70-3.25) |
| $AUC_{ss}$ (h*mg/L) | 92.6 (61.4-134) | 92.7 (61.3-134) | 92.7 (61.4-134) |

Median ± 95% confidence intervals. AUC: area under the curve; ss: steady-state

predictive check (VPC) shows that the model describes the observed variability well (Figure 7). Furthermore, non-compartmental analysis (NCA) of the observed profiles and of the model predicted profiles yielded comparable results and largely similar 24-hour fluctuations in Cmax and Tmax (Supplemental Table 1). The median Cmax of the observed data tended to be slightly higher than the median Cmax of the model predicted profiles. One reason for this discrepancy is that the $C_{max}$ (and $T_{max}$) of the observed data is inherently sensitive to the discrete sampling times employed in a study, while this is less so for a population pharmacokinetic approach. Secondly, the population PK model takes into account residual error in the data, while analysis of the observed data relies on the data points as they are measured.

### Simulations

A once-daily dosing regimen of 1000mg oral levofloxacin for seven days was simulated in 500 subjects with dosing times at 08:00, 18:00 and 23:00, representing three typically used dosing times (around breakfast, dinner or bedtime). These simulations show that $T_{max,ss}$, $C_{max,ss}$ and $AUC_{ss}$ are not significantly affected by dosing time (Table 4).

## DISCUSSION

In this study, we developed a population pharmacokinetic model based on data from a clinical trial in which levofloxacin was administered to twelve healthy subjects at six different time points throughout the 24-hour period. Levofloxacin pharmacokinetics could

be described by a one-compartment model with first-order clearance and one transit compartment to describe the absorption phase. Ka varied considerably throughout the day and night, which could be parametrized by a cosine function with a fixed period of 24 hours, a mesor of 3.95h$^{-1}$, a peak around 8:00 in the morning and a relative amplitude of 47%. This study shows how a chronopharmacological study design can be combined with population pharmacokinetics to quantitate the impact of time of administration on the concentration profiles of a drug.

The parameter estimates reported in the present study are comparable to those from previously published population pharmacokinetic models of oral levofloxacin (Peloquin et al., 2008; Tanigawara et al., 1995; Zhang et al., 2009). In these studies, the population parameter estimates for Ka range from 1.44 to 5.96h$^{-1}$. A potential explanation for this wide range of values is that the effect of time of administration was overlooked. We extend the previous findings by showing that the Ka varies over the 24 hour period with population parameter estimates ranging from 2.10h$^{-1}$ at 20:00 in the evening to 5.80h$^{-1}$ at 08:00 in the morning.

Several mechanisms could underlie the observed 24-hour rhythm in Ka. The rate of absorption of levofloxacin is mainly determined by gastric emptying as levofloxacin has a high solubility and permeability (Chen et al., 2011; Frick et al., 1998; Maezawa et al., 2013). Since gastric emptying time of a solid meal in human subjects shows significant 24-hour variation, being faster at 8:00 (half-time: 64.8±6.4 min) compared to 20:00 (97.1±11.5min) (Goo et al., 1987), the most likely explanation for the finding that the Ka of levofloxacin shows a 24-hour rhythm is variation in gastric emptying. However, we cannot exclude that variation in intestinal blood flow may also play a role (Dallmann et al., 2014).The involvement of other rhythmic processes in the absorption of levofloxacin is likely to be limited. For example, the absorption of levofloxacin is minimally affected by intestinal metabolism(Fish and Chow, 1997). Additionally, rhythmic activity of the efflux transporter p-glycoprotein in the intestine could affect drug absorption (Iwasaki et al., 2015; Okyar et al., 2012). However, the evidence that levofloxacin is a substrate for p-glycoprotein is conflicting (Naruhashi et al., 2001; Yamaguchi et al., 2000, 2001, 2002). Although it has been shown that the intestinal clearance of levofloxacin is reduced in the presence of a p-glycoprotein inhibitor in vivo, plasma concentrations of levofloxacin during the absorption phase were not affected (Yamaguchi et al., 2002).

During all study visits, GFR was measured three hours after levofloxacin administration. It was found that the effect of time of day on GFR was slight but statistically significant, being 9% higher at 09:00 in the morning compared to 01:00 at night. Since levofloxacin is mainly eliminated through passive renal elimination (Chien et al., 1997a, 1997b, 1998; Lubasch et al., 2000; Sprandel et al., 2004) and is only slightly affected by tubular secretion (Chien et al., 1997b; Lubasch et al., 2000; Okazaki et al., 1991; Sprandel et al., 2004), we hypothesized that GFR influences levofloxacin clearance and that the 24-hour variation in GFR is reflected in this parameter. However, including GFR as a covariate on clearance did not significantly improve the fit of the model. Although this observation is in line with some

studies (Peloquin et al., 2008; Tanigawara et al., 1995), other studies did find a correlation between total body clearance of levofloxacin and GFR, as measured by creatinine clearance (Chien et al., 1997b; Chow et al., 2001; Zhang et al., 2009). Possible explanations for this discrepancy are that our homogenous study population had a relatively narrow range of GFR values or that the minimal differences in GFR observed at different time points of administration do not affect the pharmacokinetics of levofloxacin.

Despite the relatively large amplitude of the rhythm in Ka (47%) that has a peak in the morning, the simulations we performed show that the AUC and Cmax, two parameters related to the bactericidal action of levofloxacin (Drusano et al., 2004; Preston et al., 1998; Shams and Evans, 2005), were not significantly influenced by time of administration. Therefore, our results suggest that oral levofloxacin can be dosed without taking into account the dosing time, at least in terms of parameters related to bacterial eradication. However, the rhythm in Ka may be relevant to other drugs that share the same drug disposition characteristics as levofloxacin (high solubility, high permeability and little metabolism) such as chloroquine (malaria prophylaxis and treatment), doxycycline (antimicrobial) and ethambutol (tuberculosis treatment) (Wu and Benet, 2005). Our findings may also apply to drugs with high solubility and high permeability but that are more extensively metabolized and/or have a shorter half-life. This group of drugs contains many drugs with a relative narrow therapeutic index, including CNS-active drugs such as antidepressants, anti-epileptics, and sedatives as well as antivirals and cardiovascular compounds (Wu and Benet, 2005). How different absorption profiles translate to differences in (first-pass) metabolism for these compounds is unknown, but it is conceivable that an increase in the rate or extent of absorption results in higher systemic concentrations.

This prospective study was specifically designed to detect 24-hour variation in pharmacokinetic parameters of levofloxacin. In addition to the use of six time points of administration, our subjects adhered to a stable sleep/wake rhythm with bedtimes between 23:00 and 0:00 and waking times between 07:00 and 08:00 prior to the study visits to ensure that the diurnal variation in physiological processes was not affected by an irregular lifestyle. Because TSH levels in serum show a robust 24-hour rhythm with a peak during the night (Russell et al., 2008; Weeke, 1973), we measured TSH levels hourly during the study visits as a positive control for rhythmic processes. The TSH levels in all our subjects show clear 24-hour variation with the peak at night, indicating that the study design did not interfere with this rhythmic process. Furthermore, the effect of food and fluid was minimized by timing the meals relative to dosing times and by ensuring a constant water intake throughout the day and night. On the one hand, this is a somewhat artificial situation that limits the direct translation of our findings to the clinic. On the other hand, this study increases our understanding of the 24-hour variation in levofloxacin pharmacokinetics in the absence of food effects and can be combined with studies that did investigate these effects (Lee et al., 1997; Tanigawara et al., 1995).

Population pharmacokinetic modelling is a powerful method to identify different sources of variability in pharmacokinetic parameters, such as interindividual variation and the effect

of subject-specific covariates, but it can also be used to explore variation induced by the rhythmic nature of physiological processes (Bienert et al., 2011; Bressolle et al., 1999; Chen et al., 2013; Lee et al., 2014; Musuamba et al., 2009; Salem et al., 2014). Several population pharmacokinetic studies on daily variations in the pharmacokinetics of drugs used the time of drug administration as a covariate (Bienert et al., 2011; Chen et al., 2013; Musuamba et al., 2009; Salem et al., 2014). This approach may be useful when sample collection takes place over a short time-window or when the drug is administered at a few clock times only. However, because levofloxacin has a relatively long half-life (6-8 hours) (Fish and Chow, 1997), we sampled for 12 hours after administration and the different occasions overlap considerably on the 24-hour time scale. In this case, the use of time of administration as a covariate may obscure the 24-hour variation in parameters such as Cl/F and V/F. We circumvented this issue by using the time window during which the samples were taken as a covariate. Applying this approach to Ka, we found that the model fit improved significantly and that the 24-hour variation of this parameter resembled a sinusoidal pattern that could be described instead as a cosine function with a period of 24 hours. The advantage of implementing a cosine function is that it better reflects the continuous nature of the 24-hour variation in physiological processes. Moreover, it enhances the predictive value of the model by providing an estimate of the parameter at all time-points of the 24-hour period.

In conclusion, we show that the Ka of levofloxacin depends on the time of day that can be described by a cosine function with a period of 24 hours, a relative amplitude of 47% and a peak around 8:00 in the morning, while clearance and volume of distribution are not affected by time of day. Our simulations indicate that the 24-hour variation in absorption rate constant does not affect variables related to bacterial eradication such as AUC or Cmax. Therefore, in terms of pharmacokinetics, levofloxacin can be dosed regardless of the time of day. More importantly, these results can be applied to drugs with similar physicochemical properties as levofloxacin. For drugs with a narrower therapeutic index, the rhythm in absorption rate constant may be clinically relevant.

## CONFLICT OF INTEREST

# REFERENCES

Baraldo, M. (2008). The influence of circadian rhythms on the kinetics of drugs in humans. Expert Opin. Drug Metab. Toxicol. 4, 175–192.

Beal, S., Sheiner, L.B., Boeckmann, A., and Bauer, R.J. (2009). NONMEM User's Guides (1989-2009), Icon Development Solutions, Ellicott City, MD, USA.

Beauchamp, D., and Labrecque, G. (2007). Chronobiology and chronotoxicology of antibiotics and aminoglycosides. Adv. Drug Deliv. Rev. 59, 896–903.

Bienert, A., Płotek, W., Zawidzka, I., Ratajczak, N., Szczesny, D., Wiczling, P., Kokot, Z.J., Matysiak, J., and Grześkowiak, E. (2011). Influence of time of day on propofol pharmacokinetics and pharmacodynamics in rabbits. Chronobiol. Int. 28, 318–329.

Bleyzac, N., Allard-Latour, B., Laffont, A., Mouret, J., Jelliffe, R., and Maire, P. (2000). Diurnal changes in the pharmacokinetic behavior of amikacin. Ther. Drug Monit. 22, 307–312.

Du Bois, D., and Du Bois, E.F. (1916). A formula to estimate the approximate surface area if height and weight be known. Arch. Intern. Med. 17, 863–871.

Bressolle, F., Joulia, J.M., Pinguet, F., Ychou, M., Astre, C., Duffour, J., and Gomeni, R. (1999). Circadian rhythm of 5-fluorouracil population pharmacokinetics in patients with metastatic colorectal cancer. Cancer Chemother. Pharmacol. 44, 295–302.

Chen, M.-L., Amidon, G.L., Benet, L.Z., Lennernas, H., and Yu, L.X. (2011). The BCS, BDDCS, and regulatory guidances. Pharm. Res. 28, 1774–1778.

Chen, R., Li, J., Hu, W., Wang, M., Zou, S., and Miao, L. (2013). Circadian variability of pharmacokinetics of cisplatin in patients with non-small-cell lung carcinoma: analysis with the NONMEM program. Cancer Chemother. Pharmacol. 72, 1111–1123.

Chien, S., Rogge, M., Gisclon, L., Curtin, C., Wong, F., Natarajan, J., Williams, R., Fowler, C., Cheung, W., and Chow, A. (1997a). Pharmacokinetic profile of levofloxacin following once-daily 500- milligram oral or intravenous doses. Antimicrob. Agents Chemother. 41, 2256–2260.

Chien, S.C., Chow, A.T., Natarajan, J., Williams, R.R., Wong, F.A., Rogge, M.C., and Nayak, R.K. (1997b). Absence of age and gender effects on the pharmacokinetics of a single 500-milligram oral dose of levofloxacin in healthy subjects. Antimicrob. Agents Chemother. 41, 1562–1565.

Chien, S.C., Wong, F.A., Fowler, C.L., Callery-D'Amico, S. V, Williams, R.R., Nayak, R., and Chow, A.T. (1998). Double-blind evaluation of the safety and pharmacokinetics of multiple oral once-daily 750-milligram and 1-gram doses of levofloxacin in healthy volunteers. Antimicrob. Agents Chemother. 42, 885–888.

Choi, J.S., Kim, C.K., and Lee, B.J. (1999). Administration-time differences in the pharmacokinetics of gentamicin intravenously delivered to human beings. Chronobiol. Int. 16, 821–829.

Chow, A.T., Fowler, C., Williams, R.R., Morgan, N., Kaminski, S., and Natarajan, J. (2001). Safety and pharmacokinetics of multiple 750-milligram doses of intravenous levofloxacin in healthy volunteers. Antimicrob.Agents Chemother. 45, 2122–2125.

Dallmann, R., Brown, S.A., and Gachon, F. (2014). Chronopharmacology: new insights and therapeutic implications. Annu. Rev. Pharmacol. Toxicol. 54, 339–361.

Drusano, G.L., Preston, S.L., Fowler, C., Corrado, M., Weisinger, B., and Kahn, J. (2004). Relationship between fluoroquinolone area under the curve: minimum inhibitory concentration ratio and the probability of eradication of the infecting pathogen, in patients with nosocomial pneumonia. J. Infect. Dis. 189, 1590–1597.

Fauvelle, F., Perrin, P., Belfayol, L., Boukari, M., Cherrier, P., Bosio, A.M., Tod, M., Coulaud, J.M., and Petitjean, O. (1994). Fever and associated changes in glomerular filtration rate erase anticipated diurnal variations in aminoglycoside pharmacokinetics. Antimicrob. Agents Chemother. 38, 620–623.

Fish, D.N., and Chow, A.T. (1997). The clinical pharmacokinetics of levofloxacin. Clin. Pharmacokinet. 32, 101–119.

Frick, A., Möller, H., and Wirbitzki, E. (1998). Biopharmaceutical characterization of oral immediate release drug products. In vitro/in vivo comparison of phenoxymethylpenicillin potassium, glimepiride and levofloxacin. Eur. J. Pharm. Biopharm. 46, 305–311.

Goo, R.H., Moore, J.G., Greenberg, E., and Alazraki, N.P. (1987). Circadian variation in gastric emptying of

meals in humans. Gastroenterology 93, 515–518.

Hishikawa, S., Kobayashi, E., Sugimoto, K., Miyata, M., and Fujimura, A. (2001). Diurnal variation in the biliary excretion of flomoxef in patients with percutaneous transhepatic biliary drainage. Br. J. Clin. Pharmacol. 52, 65–68.

Horne, J.A., and Ostberg, O. (1976). A self-assessment questionnaire to determine morningness-eveningness in human circadian rhythms. Int. J. Chronobiol. 4, 97–110.

Iwasaki, M., Koyanagi, S., Suzuki, N., Katamune, C., Matsunaga, N., Watanabe, N., Takahashi, M., Izumi, T., and Ohdo, S. (2015). Circadian Modulation in the Intestinal Absorption of P-glycoprotein Substrates in Monkeys. Mol. Pharmacol. 88, 29-37

Karlsson, M.O., and Sheiner, L.B. (1993). The importance of modeling interoccasion variability in population pharmacokinetic analyses. J. Pharmacokinet. Biopharm. 21, 735–750.

Keizer, R.J., Karlsson, M.O., and Hooker, A. (2013). Modeling and Simulation Workbench for NONMEM: Tutorial on Pirana, PsN, and Xpose. CPT Pharmacometrics Syst. Pharmacol. 2, e50.

Koopman, M.G., Koomen, G.C., Krediet, R.T., de Moor, E.A., Hoek, F.J., and Arisz, L. (1989). Circadian rhythm of glomerular filtration rate in normal individuals. Clin. Sci. (Lond). 77, 105–111.

Lee, D., Son, H., Lim, L.A., and Park, K. (2014). Population pharmacokinetic analysis of diurnal and seasonal variations of plasma concentrations of cilostazol in healthy volunteers. Ther. Drug Monit. 36, 771–780.

Lee, L., Hafkin, B., Lee, I., Hoh, J., and Dix, R. (1997). Effects of food and sucralfate on a single oral dose of 500 milligrams of levofloxacin in healthy subjects. Antimicrob. Agents Chemother. 41, 2196–2200.

Lubasch, A., Keller, I., Borner, K., Koeppe, P., and Lode, H. (2000). Comparative pharmacokinetics of ciprofloxacin, gatifloxacin, grepafloxacin, levofloxacin, trovafloxacin, and moxifloxacin after single oral administration in healthy volunteers. Antimicrob. Agents Chemother. 44, 2600–2603.

Maezawa, K., Yajima, R., Terajima, T., Kizu, J., and Hori, S. (2013). Dissolution profile of 24 levofloxacin (100 mg) tablets. J. Infect. Chemother. 19, 996–998.

Mohawk, J.A., Green, C.B., and Takahashi, J.S. (2012). Central and peripheral circadian clocks in mammals. Annu. Rev. Neurosci. 35, 445–462.

Mould, D.R., and Upton, R.N. (2013). Basic concepts in population modeling, simulation, and model-based drug development-part 2: introduction to pharmacokinetic modeling methods. CPT Pharmacometrics Syst. Pharmacol. 2, e38.

Musuamba, F.T., Mourad, M., Haufroid, V., Delattre, I.K., Verbeeck, R.K., and Wallemacq, P. (2009). Time of drug administration, CYP3A5 and ABCB1 genotypes, and analytical method influence tacrolimus pharmacokinetics: a population pharmacokinetic study. Ther. Drug Monit. 31, 734–742.

Naruhashi, K., Tamai, I., Inoue, N., Muraoka, H., Sai, Y., Suzuki, N., and Tsuji, A. (2001). Active intestinal secretion of new quinolone antimicrobials and the partial contribution of P-glycoprotein. J. Pharm. Pharmacol. 53, 699–709.

Okazaki, O., Kojima, C., Hakusui, H., and Nakashima, M. (1991). Enantioselective disposition of ofloxacin in humans. Antimicrob. Agents Chemother. 35, 2106–2109.

Okyar, A., Dressler, C., Hanafy, A., Baktir, G., Lemmer, B., and Spahn-Langguth, H. (2012). Circadian variations in exsorptive transport: in situ intestinal perfusion data and in vivo relevance. Chronobiol. Int. 29, 443–453.

Peloquin, C.A., Hadad, D.J., Molino, L.P.D., Palaci, M., Boom, W.H., Dietze, R., and Johnson, J.L. (2008). Population pharmacokinetics of levofloxacin, gatifloxacin, and moxifloxacin in adults with pulmonary tuberculosis. Antimicrob. Agents Chemother. 52, 852–857.

Preston, S.L., Drusano, G.L., Berman, A.L., Fowler, C.L., Chow, A.T., Dornseif, B., Reichl, V., Natarajan, J., and Corrado, M. (1998). Pharmacodynamics of Levofloxacin. JAMA 279, 125–129.

Rao, V. V, Rambhau, D., Rao, B.R., and Srinivasu, P. (1997). Circadian variation in urinary excretion of ciprofloxacin after a single-dose oral administration at 1000 and 2200 hours in human subjects. Antimicrob. Agents Chemother. 41, 1802–1804.

van Rongen, A., Kervezee, L., Brill, M., van Meir, H., den Hartigh, J., Guchelaar, H.-J., Meijer, J., Burggraaf, J., and van Oosterhout, F. (2015). Population Pharmacokinetic Model Characterizing 24-Hour Variation in

the Pharmacokinetics of Oral and Intravenous Midazolam in Healthy Volunteers. CPT Pharmacometrics Syst. Pharmacol. 4, 454–464.

Russell, W., Harrison, R.F., Smith, N., Darzy, K., Shalet, S., Weetman, A.P., and Ross, R.J. (2008). Free Triiodothyronine Has a Distinct Circadian Rhythm That Is Delayed but Parallels Thyrotropin Levels. J. Clin. Endocrinol. Metab. 93, 2300–2306.

Salem, A.H., Koenig, D., and Carlson, D. (2014). Pooled population pharmacokinetic analysis of phase I, II and III studies of linifanib in cancer patients. Clin. Pharmacokinet. 53, 347–359.

Savic, R.M., Jonker, D.M., Kerbusch, T., and Karlsson, M.O. (2007). Implementation of a transit compartment model for describing drug absorption in pharmacokinetic studies. J. Pharmacokinet. Pharmacodyn. 34, 711–726.

Shams, W.E., and Evans, M.E. (2005). Guide to Selection of Fluoroquinolones in Patients with Lower Respiratory Tract Infections. Drugs 65, 949–991.

Sprandel, K.A., Schriever, C.A., Pendland, S.L., Quinn, J.P., Gotfried, M.H., Hackett, S., Graham, M.B., Danziger, L.H., and Rodvold, K.A. (2004). Pharmacokinetics and pharmacodynamics of intravenous levofloxacin at 750 milligrams and various doses of metronidazole in healthy adult subjects. Antimicrob. Agents Chemother. 48, 4597–4605.

Takiguchi, T., Tomita, M., Matsunaga, N., Nakagawa, H., Koyanagi, S., and Ohdo, S. (2007). Molecular basis for rhythmic expression of CYP3A4 in serum-shocked HepG2 cells. Pharmacogenet. Genomics 17, 1047–1056.

Tanigawara, Y., Nomura, H., Kagimoto, N., Okumura, K., and Hori, R. (1995). Premarketing population pharmacokinetic study of levofloxacin in normal subjects and patients with infectious diseases. Biol. Pharm. Bull. 18, 315–320.

Weeke, J. (1973). Circadian variation of the serum thyrotropin level in normal subjects. Scand. J. Clin. Lab. Invest. 31, 337–342.

Wu, C.-Y., and Benet, L.Z. (2005). Predicting Drug Disposition via Application of BCS: Transport/ Absorption/ Elimination Interplay and Development of a Biopharmaceutics Drug Disposition Classification System. Pharm. Res. 22, 11–23.

Yamaguchi, H., Yano, I., Hashimoto, Y., and Inui, K.I. (2000). Secretory mechanisms of grepafloxacin and levofloxacin in the human intestinal cell line caco-2. J. Pharmacol. Exp. Ther. 295, 360–366.

Yamaguchi, H., Yano, I., Saito, H., and Inui, K. (2001). Transport characteristics of grepafloxacin and levofloxacin in the human intestinal cell line Caco-2. Eur. J. Pharmacol. 431, 297–303.

Yamaguchi, H., Yano, I., Saito, H., and Inui, K. (2002). Pharmacokinetic Role of P-Glycoprotein in Oral Bioavailability and Intestinal Secretion of Grepafloxacin in Vivo. J. Pharmacol. Exp. Ther. 300, 1063–1069.

Zhang, J., Xu, J.F., Liu, Y. Bin, Xiao, Z.K., Huang, J.A., Si, B., Sun, S.H., Xia, Q.M., Wu, X.J., Cao, G.Y., et al. (2009). Population pharmacokinetics of oral levofloxacin 500 mg once-daily dosage in community-acquired lower respiratory tract infections: results of a prospective multicenter study in China. J. Infect. Chemother. 15, 293–300.
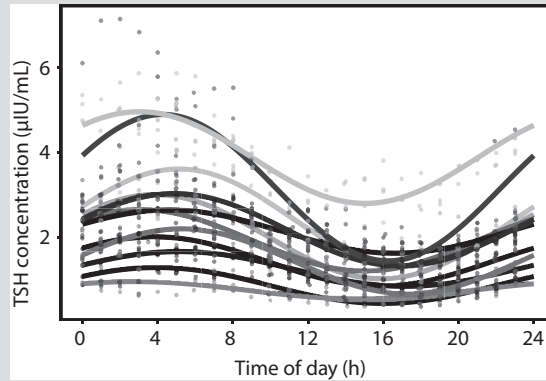
**Supplementary Figure 1** Variation in thyroid stimulating hormone (TSH) levels over the course of the 24-hour period in the twelve subjects. Dots: observed data; lines: cosine fitted through the data per subject by cosinor analysis. Different colours represent the 12 different subjects. Data from the six separate occasions were combined.
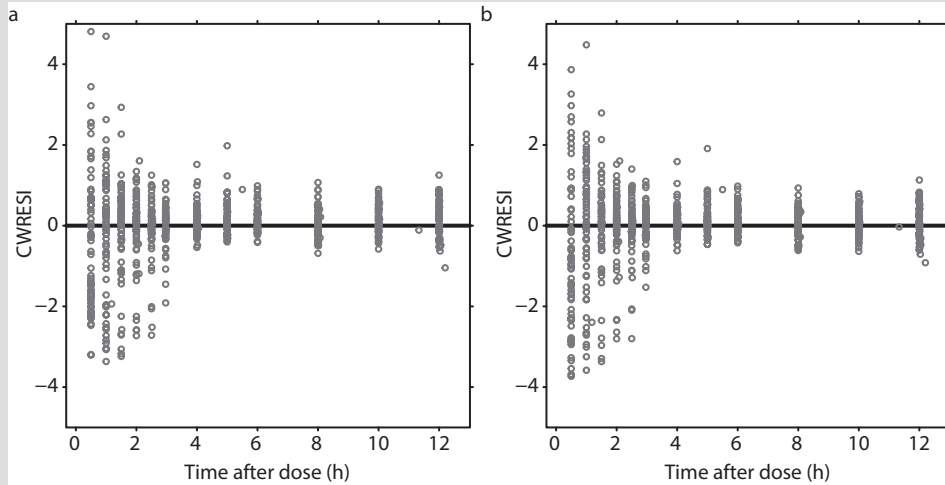


**Supplementary Figure 2** Comparison of conditional weighted residuals (CWRESI) versus time after dose of the model without a cosine implemented on Ka **(A)** and of the model with a cosine implemented on Ka **(B)**.

**Supplementary Table 1** Comparison of $C_{max}$, $T_{max}$ and $AUC_{0-12}$ of the observed and individual predicted concentration profiles. Data is shown as median (range).

| Time of administration | $C_{max}$ (mg/L) | | $T_{max}$ (h) | | $AUC_{0-12}$ (h*mg/L) | |
|---|---|---|---|---|---|---|
| | Observed profiles | Individual model predictions[a] | Observed profiles | Individual model predictions[a] | Observed profiles | Individual model predictions[a] |
| 02:00 | 9.1 (5.5-14) | 8.1 (5.6-9.4) | 2.0 (1.0-5.0) | 1.2 (0.8-1.9) | 59.9 (33.3-79.3) | 63.3 (40.9-72.9) |
| 06:00 | 9.3 (7.8-19) | 8.3 (5.8-9.7) | 1.0 (1.0-2.0) | 0.9 (0.7-1.4) | 64.2 (39.6-75.0) | 63.8 (41.1-73.8) |
| 10:00 | 10 (6.9-15) | 8.3 (5.7-9.6) | 1.0 (0.5-2.5) | 1.0 (0.7-1.5) | 66.5 (42.6-74.7) | 63.7 (41.1-73.7) |
| 14:00 | 9.2 (5.5-12) | 7.8 (5.5-8.8) | 1.3 (0.5-3.0) | 1.3 (0.9-2.4) | 64.7 (38.4-79.3) | 62.6 (40.7-72.2) |
| 18:00 | 8.7 (6.7-11) | 7.4 (5.1-8.5) | 1.8 (1.0-4.0) | 1.9 (1.1-6.5) | 63.2 (41.0-76.7) | 61.3 (39.9-68.4) |
| 22:00 | 9.8 (5.7-12) | 8.0 (5.3-8.7) | 2.3 (1.0-5.5) | 1.6 (1.0-3.7) | 63.7 (42.2-74.9) | 63.8 (40.2-69.9) |

$C_{max}$: maximal concentration; $T_{max}$: time to reach $C_{max}$; $AUC_{0-12}$: area under the concentration-time curve from 0 to 12h after administration.

# CHAPTER

## Levofloxacin-induced QTc prolongation depends on the time of drug administration

# 5

Laura Kervezee[1,2,3]; Verena Gotta[3,*]; Jasper Stevens[2,*]; Willem Birkhoff[2]; Ingrid M.C. Kamerling[2]; Meindert Danhof[3]; Johanna H. Meijer[1,**]; Jacobus Burggraaf[2,**]

[1]Laboratory for Neurophysiology, Department of Molecular Cell Biology, Leiden University Medical Center, Leiden, the Netherlands
[2]Centre for Human Drug Research, Leiden, the Netherlands
[3]Division of Pharmacology, Leiden Academic Center for Drug Research, Leiden University, Leiden, the Netherlands
[*]These authors contributed equally
[**]These authors share senior authorship

## ABSTRACT

Understanding the factors influencing a drug's potential to prolong the QTc interval on an electrocardiogram is essential for the correct evaluation of its safety profile. To explore the effect of dosing time on drug-induced QTc prolongation, a randomized, cross-over, clinical trial was conducted in which 12 healthy male subjects received levofloxacin at 02:00, 06:00, 10:00, 14:00, 18:00 and 22:00. Using a pharmacokinetic-pharmacodynamic modelling approach to account for variations in pharmacokinetics, heart rate and daily variation in baseline QT, we find that the concentration-QT relationship shows a 24-hour sinusoidal rhythm. Simulations show that the extent of levofloxacin-induced QT prolongation depends on dosing time, with the largest effect at 14:00 (1.73 [95% prediction interval: 1.56-1.90] ms per mg/L) and the smallest effect at 06:00 (-0.04 [-0.19-0.12] ms per mg/L). These results suggest that 24-hour variation in the concentration-QT relationship could be a potentially confounding factor in the assessment of drug-induced QTc prolongation.

## STUDY HIGHLIGHTS

**What is the current knowledge on the topic?**
- The propensity of new drugs to prolong the QTc interval is typically assessed in a clinical trial in which drug administration occurs at a fixed time of the day
- Many factors, including time of day, may influence the relationship between the concentration of a drug and the extent of QTc prolongation

**What question this study addressed?**
- The objective of this study was to investigate the effect of dosing time on the extent of levofloxacin-induced QTc prolongation.

**What this study adds to our knowledge?**
- The relationship between the levofloxacin concentration and the extent of QTc prolongation varies systematically over the course of the day
- Dosing time is a potentially confounding factor in the assessment of drug-induced QTc prolongation.

**How this might change drug discovery, development and/or clinical therapeutics?**
- To accurately assess a drug's effect on the QTc interval, an approach is required that takes into account the time of drug administration

# INTRODUCTION

Over the past decades, several non-cardiac drugs have been withdrawn from the market or their use has been restricted due to their propensity to delay ventricular repolarization (Roden, 2004). This potentially serious side-effect is manifested as a prolonged heart rate-corrected QT (QTc) interval on the electrocardiogram (ECG). The most common mechanism by which drugs cause QTc prolongation is through blockade of the hERG channel, a potassium channel that underlies the rapid component of the delayed rectifier potassium current (IKr) in cardiomyocytes(Sanguinetti and Tristani-Firouzi, 2006). Reduced IKr delays cardiac repolarization and, often in combination with other predisposing factors such as genetic polymorphisms or hypokalemia, may lead to the occurrence of early afterdepolarizations and Torsades de Pointes (Kannankeril et al., 2010).

Much effort has been put into the identification of the different sources of variability that affect the extent of drug-induced QTc prolongation, including gender, age, ethnicity, co-morbidity and co-medication (Malik and Camm, 2001). Moreover, it is well known that the baseline QTc interval shows 24-hour variation (Bonnemeier et al., 2003; Browne et al., 1983a). Based on the 24-hour variations in various physiological processes, such as serum potassium levels (Schmidt et al., 2015) and cardiac ion channel expression (Jeyaraj et al., 2012; Schroder et al., 2013, 2015; Yamashita et al., 2003), it has also been suggested that the magnitude of the effect of a drug on the QTc interval may depend on the time of day (Dallmann et al., 2014; Watanabe et al., 2012). However, this hypothesis has not been investigated directly. In fact, current approaches to evaluate drug-induced QT prolongation during drug development include one time-point of drug administration and exclude night-time recordings (Malik et al., 2008), thereby relying on the implicit assumption that delayed ventricular repolarization does not depend on dosing time.

To test this assumption, we investigated whether the sensitivity to drug-induced QTc prolongation varies during the 24-hour period, using levofloxacin as a model compound. Levofloxacin is a fluoroquinolone antibiotic that blocks hERG channels (Alexandrou et al., 2006; Kang et al., 2001). Causing a slight but significant prolongation of the QTc interval l(Noel et al., 2003; Sugiyama et al., 2012; Taubel et al., 2010), it was shown previously that levofloxacin can be used as a positive comparator in thorough-QT (TQT) studies (Taubel et al., 2010). In this study, we used pharmacokinetic-pharmacodynamic modelling to characterize the relationship between levofloxacin concentration and the extent of QTc prolongation after oral administration to twelve healthy male subjects at six different time-points during the day and night.

# METHODS

### Study design

Data used for model development were obtained from a clinical trial that was described previously (Kervezee et al., 2016). Briefly, 67 occasions were completed by twelve healthy subjects (10 subjects completed 6 occasions, 1 subject completed 3 occasions, 1 subject

completed 4 occasions). In each occasion, the subjects received an oral dose of 1000mg levofloxacin (Aurobindo Pharma B.V., Zwijndrecht, the Netherlands) at a different time of day (t=0 at 02:00, 06:00, 10:00, 14:00, 18:00 and 22:00). The occasions were separated by at least one week and each subject was randomly allocated to a sequence of dosing times. Subjects fasted from t=-2h until t=6h. At t=6h and t=10h, subjects were allowed to eat a maximum of four slices of bread and a small snack, respectively. Twelve-lead ECGs were recorded at t=0, 0.5, 1, 1.5, 2, 2.5, 3, 4, 6, 8, 12h after dosing using a Marquette MAC 5500 (GE Healthcare, Milwaukee, Wisconsin, USA) and stored using the MUSE Cardiology Information System (GE Healthcare). The ECG parameters (RR and QT intervals) were calculated automatically and each ECG recording was manually reviewed by a physician. Blood samples to measure levofloxacin and potassium concentrations were drawn via an indwelling intravenous catheter immediately after each ECG recording and at t=5 and 10h. The concentration of levofloxacin in these samples was analyzed by an LCMS method (Kervezee et al., 2016). The study was approved by the Medical Ethics Committee of the Leiden University Medical Centre and registered in the European Clinical Trials Database (EudraCT Number: 2013-001976-39). All subjects gave written informed consent prior to the study.

**Data exploration**

For data exploration, drug concentrations and the change from the pre-dose QT interval, corrected for heart rate by the Fridericia formula (ΔQTcF), was stratified by time of drug administration and plotted over time as mean and 95% confidence intervals. The relationship between observed levofloxacin concentrations in plasma and ΔQTcF was also stratified by dosing time. Linear mixed effects modelling to assess this relationship was performed with the nlme package (v3.1.118) in R (v3.1.2 R Development Core Team, 2008), using ΔQTcF as the dependent variable, drug concentration and dosing time as fixed effects (including interaction) and subject as random effect.

**Pharmacodynamic modeling**

Population modelling was performed using NONMEM (v7.3 Icon plc, Dublin, Ireland(Beal et al., 2009)). R, Pirana (v2.8.2), PsN (v3.7.6) and Xpose (v4) were used for evaluation and graphical representation of the models (Keizer et al., 2013). First-order conditional estimation with interaction (FOCEI) was used throughout the analysis and interindividual variability (IIV) and interoccasion variability (IOV) in model parameters were assumed to be log-normally distributed. Additive and proportional error structures were considered to describe the residual error. A sequential modelling approach was used: firstly, a baseline model was developed based on the pre-dose QT data; secondly, the concentration-effect relationship was modelled using pre- and post-dose QT data.

**Baseline model**

To describe the relationship between the QT and RR interval as well as potential 24-hour variation in the QT interval in the absence of levofloxacin, a baseline model was developed

as described previously (Chain et al., 2011) using Equation 1.

$$QT_{baseline}(t) = QT_0 * RR^\alpha + \Sigma^N_{(n=1)}[A_n * \cos(2\pi * n * (t-\varphi_n) / 24) \qquad \text{Equation 1}$$

where $QT_0$ represents the intercept of the QT-RR relationship in ms, RR is the observed RR interval in s, $\alpha$ is the correction factor for RR, N is the total number of harmonics included in the model, $A_n$ is the amplitude of the 24-hour variation of the $n^{th}$ harmonic in ms, $\varphi_n$ is the acrophase (time of peak) of the $n^{th}$ harmonic in hours after midnight and t is the time of the observation in hours after midnight. The number of harmonic terms was determined by the criteria for statistical significance explained below. Because sleep may affect the QT-RR relationship(Browne et al., 1983b; Extramiana et al., 1999), the use of a separate value of $\alpha$ during sleep (between 23:30 and 07:30) was investigated. A linear mixed effects model (as described above) was used to investigate whether the $\alpha$ estimated by the final baseline model adequately removed the dependency of the QTc interval on RR, using QTc as the dependent variable, RR as fixed effect and interaction between dosing time and RR, and subject as random effect.

**Drug effect model**

The concentration-dependency of QTc (PD) and temporal relationship between PK and PD effects (PK-PD) was modeled using the pre- and post-dose ECG recordings. Individual pharmacokinetic parameters were fixed to their estimates from a previously reported population pharmacokinetic model (Kervezee et al., 2016) and used to predict individual concentration-time profiles for PK-PD modeling. Briefly, the PK model was a one compartment model with one transit compartment to describe the absorption phase. The transit rate constant (Ktr) was equalized to the absorption rate constant (Ka), which both showed 24-hour variation that was modeled as a cosine function with a fixed period of 24 hours.

Throughout development of the drug-effect model, the fixed-effect estimates of $QT_0$, $\alpha$, A and $\varphi$ were fixed to the values obtained in the baseline model, while the concentration-effect parameters as well as IIV and IOV were estimated. Initially, a linear model was appended to the baseline model shown in Equation 1 to describe the concentration-effect relationship as follows:

$$QT(t) = QT_{baseline}(t) + Slope * C \qquad \text{Equation 2}$$

where $QT_{baseline}(t)$ is the model described in equation 1, Slope is a linear term to describe the concentration-QT relationship (in ms per mg/L) and C is the levofloxacin concentration in plasma (in mg/L). Because it has been reported that a 1000mg oral dose of levofloxacin may transiently increase heart rate (Noel et al., 2004; Taubel et al., 2010), which could affect the relationship between the QT and RR interval, inclusion of a separate $\alpha$ for off- and on-drug data was considered as recommended previously (Garnett et al., 2012).

A sequential modeling strategy was applied to investigate whether the effect of levofloxacin on the QT interval is influenced by time of day. Firstly, IOV was included on

the slope parameter, with the different dosing times representing the different occasions. Secondly, it was investigated whether any bias in the distribution of the occasion-specific random effects could be reduced by estimating separate values for slope for each of the 24 hours or by describing slope as a cosine function with one or more harmonic terms and a principal period of 24 hours (Equation 3).

$$\text{Slope} = \text{Slope\_Mesor} + \Sigma_{(n=1)}^{N} [ \text{Slope\_A}_n * \cos( 2\pi * n * (t\text{-Slope\_}\varphi_n)/24)] \qquad \text{Equation 3}$$

The use of these approaches was possible because the data were collected evenly across the 24-hour period with an average of 30 ECG recordings per hour (range: 24-36 observations).

Potassium levels in plasma were considered as a covariate on $QT_0$ or Slope as follows:

$$P_{i,j,t} = \theta_P + \theta_{POT} * (\text{Potassium}_{i,j,t} - \text{Potassium}_{Median}) \qquad \text{Equation 4}$$

With parameter $P_{i,j,t}$ as a function of $\theta_P$ (typical parameter value), $\theta_{POT}$ (linear change in P per unit of potassium) and the difference between the potassium concentration in the ith individual on the jth occasion at sampling time t and the median concentration of potassium in the population (4 mmol/L).

**Model evaluation**

Model selection was based on objective function value (OFV), plausibility and precision of the parameter estimates, and goodness-of-fit plots. The fit of nested models was compared using the likelihood ratio test with the significance level set at p=0.01, corresponding to a drop in OFV of at least 6.63 points upon inclusion of one additional parameter, assuming that the difference in OFV is $\chi^2$ distributed. The fit of non-nested models was compared using the Akaike information criterion (AIC) (Mould and Upton, 2013).

Because the baseline parameters were fixed to the values obtained with a limited pre-dose data set during development of the drug-effect model, we determined whether misspecification of the baseline model affects the estimated concentration-QT relationship in the final model by fixing the 24-hour variation in the baseline QTc to values reported literature (Chain et al., 2011; Dubois et al., 2016; Green et al., 2014; Smetana et al., 2002, 2003). Additionally, the bias and precision of the parameter estimates of the final model, with all (baseline and drug-effect) parameters estimated, were evaluated using a bootstrap analysis with 500 resampled datasets. The parameter estimates returned by the bootstrap were summarized as medians and 95% prediction intervals of the parameters.

**Clinical trial simulation**

The fixed and random parameter estimates of the PK-PD model were used to simulate clinical trials in which concentration and QTc profiles were obtained in 24 subjects receiving a placebo, therapeutic dose (500 mg) and supratherapeutic dose (1500mg) in a crossover design. Five hundred clinical trials with PK and PD sampling at t=0, 0.5, 1, 1.5, 2, 2.5, 3, 3.5, 4, 8, 12, 16, 20, 24h post-dose and additional PD sampling at t=-2 and -1h were simulated
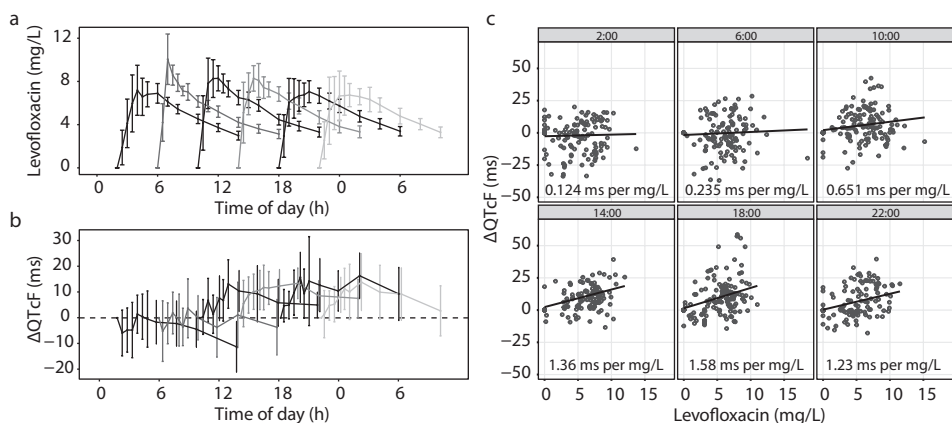
**Figure 1** Concentration time profiles of levofloxacin in plasma **(a)** and the change from pre-dose QT interval corrected for heart rate by the Fridericia formula (ΔQTcF) over time **(b)** after dosing at six different clock times. Data are presented as mean ± 95% confidence intervals. Concentration time profiles were published previously(Kervezee et al., 2016). **(c)** The relationship between levofloxacin concentration and ΔQTcF after dosing at six different clock times. Dots in c represent observed data points; lines and numbers show the estimated regression coefficients from a linear mixed effect model.

per dosing time (02:00, 06:00, 10:00, 14:00, 18:00 and 22:00) and were re-estimated with two alternative PK-PD models: (1) a model that did not include a concentration-effect relationship and (2) a model that did include a linear concentration-effect relationship. The pharmacokinetic component of the alternative models were simplified versions of the final pharmacokinetic model (no covariance between CL and V, no cosine and IIV on Ka, no transit compartment) to accommodate the simpler study design. A significant drug effect was observed if the OFV returned by alternative model 2 was more than 3.84 points (significance level α=0.05) lower than the OFV in alternative model 1. These simulations and re-estimations were performed using the stochastic simulation and estimation (SSE) tool in PsN. The output was used to compute 1) the slope of the drug effect; 2) the percentage of studies in which a significant drug effect was observed and 3) the percentage of studies in which the upper limit of the two sided 90% confidence interval of the ΔQTc at the population predicted $C_{max}$ exceeded 10ms in alternative model 2.

## RESULTS

### Data exploration

The concentration-time profiles of levofloxacin in plasma and the change from pre-dose QT interval corrected for heart rate by the Fridericia formula (ΔQTcF) after administration of a 1000mg oral dose at six different time-points are shown in Figure 1A and B. There was a significant interaction between the effect of levofloxacin concentration and the effect of dosing time (p=0.0319; linear mixed effects model), indicating that dosing time influences the relationship between levofloxacin concentration and ΔQTcF (Figure 1C).
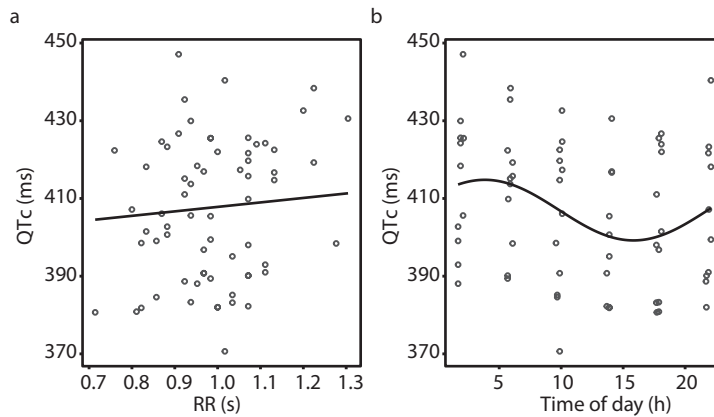
**Figure 2 (a)** The relationship between the RR interval and the QTc interval in pre-dose ECG recordings after correction for heart-rate with the coefficient estimated by the baseline model (α=0.216). The line shows the regression coefficient estimated by a linear mixed effect model **(b)** Variation in pre-dose QTc interval over the time of day. The line shows the shape of the cosine function estimated by the baseline model. The dots in (a and b) show observed data.

## Baseline QT model

To correct for potential 24-hour variation in the baseline QT interval and for study-specific dependency of the QT interval on heart rate, a baseline model was developed. The parameter estimates of this model are shown in Supplemental Table 1. A proportional error structure was used to describe the residual error. Interindividual and interoccasion variability were included on the intercept of the QT-RR relationship ($QT_0$). A one harmonic cosine function with a period of 24 hours best described the variation in the baseline QT interval over the course of the day (ΔOFV -15; p<0.01; 2df). Inclusion of an additional harmonic with a period of 12 hours did not further improve the fit of the model (ΔOFV -3.1; p>0.05; 2df vs model with 24-h cosine). Accounting for this 24-hour variation in the baseline QT interval decreased the interoccasion variability on $QT_0$ from 3% to 2.3% and removed a bias observed in the conditional weighted residuals (CWRESI) over time of day (Supplemental Figure 1). Estimation of a separate value of α during sleep did not significantly improve the fit of the model (ΔOFV -6.2, p>0.01, 1df). This baseline model adequately removed the dependency of the QTc interval on the RR, as evidenced by the non-significant effect of RR on QTc (p=0.49; linear mixed effects model), and described the 24-hour variation in the QTc intervals of the baseline data (Figure 2).There was no indication that the relationship between the QT and RR interval depends on time of day (Supplemental Figure 2).

## Drug effect model

The development process of the drug-effect model and corresponding changes in OFV are shown in Table 1. A linear function best described the relationship between drug concentration and the QT interval, but a bias was observed in CWRESI versus the time of day (Figure 3A). Additionally, the distribution of the interoccasion variability on the
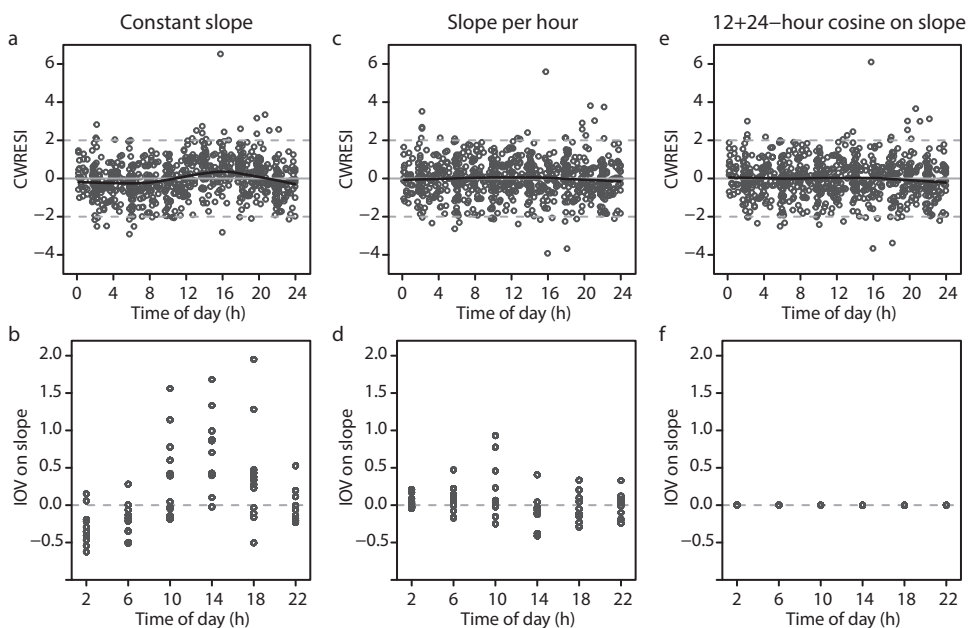
**Figure 3** Distribution of the conditional weighted residuals with interaction (CWRESI) and of interoccasion variability (IOV) on slope versus time of day in a model in which the linear concentration-effect relationship is constant over the 24 hours **(a-b)**, includes 24 estimates of slope depending on the time of the ECG recording **(c-d)**, and is described by a cosine function with two harmonics with periods of 24 and 12 hours **(e-f)**. Black line in panels a, c and e: non-parametric regression line (loess curve with span 0.6).

concentration-QT relationship depended on the time of drug administration (Figure 3B). These biases could be corrected by estimating a separate value for the concentration-QT relationship for each of the 24 hours (Figure 3C and D). Alternatively, describing the concentration-QT relationship by a cosine function with two harmonic terms with periods of 24 and 12 hours significantly improved the fit of the model and also corrected the bias in CWRESI over time of day and interoccasion variability (Figure 3E and F). Interoccasion variability was reduced to 0.3% and no longer affected the fit of the model.

Inclusion of potassium as a covariate on $QT_0$ significantly improved the model fit (see Table 1). It was found that for a 1mmol/L increase in potassium levels, $QT_0$ decreased by 5.7ms. However, the uncertainty in the parameter estimate was large (65%), while other parameter estimates were minimally affected. Potassium levels varied over the 24-hour period within a narrow physiological range (Supplemental Figure 3), so the observed effect of potassium on the QT interval is of limited clinical relevance in this study. Therefore, this parameter was not further included in the model.

**Model evaluation**

The values of the concentration-QT relationship from the model in which this relationship was estimated independently for each of the 24 hours had a low level of precision, but followed a sinusoidal-like pattern over time, with higher values in the afternoon and lower

**Table 1** Changes in objective function values during model development. Models shown in bold were selected for subsequent modelling steps.

| Model no.[a] | Reference model | Description | d.f.[b] | OFV | ΔOFV |
|---|---|---|---|---|---|
| **01** | | Baseline model with linear C-QT | | 3910 | |
| 02 | 01 | C-QT as $E_{max}$ function | 1 | 3904 | -6 |
| 03 | 01 | Separate α for on-drug measurements | 1 | 3909 | -1 |
| 04 | 01 | IIV on C-QT | 1 | 3903 | -7 |
| **05** | **01** | **IOV on C-QT** | **1** | **3898** | **-12** |
| 06 | 05 | IIV and IOV on C-QT | 2 | 3898 | 0 |
| 07 | 05 | Estimation of C-QT per hour | 24 | 3754 | -144 |
| **08** | **05** | **C-QT as cosine with 24-hour period** | **3** | **3860** | **-38** |
| **09** | **08** | **C-QT with additional 12-hour cosine** | **5** | **3786** | **-74** |
| **10** | **09** | **No IOV on C-QT** | **4** | **3786** | **0** |
| 11 | 10 | Potassium as covariate on $QT_0$ | 5 | 3773 | -13 |
| 12 | 10 | Potassium as covariate on C-QT | 5 | 3779 | -6 |
| 13 | 11 | Potassium as covariate on $QT_0$ and C-QT | 6 | 3773 | 0 |
| **Final model** | **10** | **All parameters estimated** | **-** | **3783** | **-** |

OFV: objective function value; ΔOFV: change in OFV compared to reference model; d.f.: degrees of freedom; IOV: inter-occasion variability; IIV: inter-individual variability; C-QT: concentration-QT relationship

a. $QT_0$, α, $\varphi_{baseline}$ and amplitude$_{baseline}$ were fixed to the values of the baseline model; pre- and post-dose data included

b. Compared to Model01
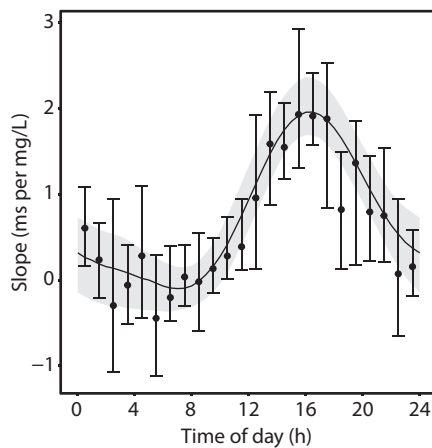


**Figure 4** 24-hour variation in slope. Dots: median ± 95 prediction intervals derived from 500 bootstrap runs of the model in which a separate value for slope was estimated for each of the 24 hours. Solid black line: estimated cosine function from the model with fixed baseline parameters, with the light grey area representing the 95% prediction interval derived from 500 bootstrap runs.

values in the early morning (Figure 4, dots). This pattern was closely matched by the model in which the concentration-QT relationship was described by a two harmonic cosine function (Figure 4, line). The cosine model was selected over the model with 24 separate estimates because of a lower AIC ($\Delta$AIC = -6), indicating a better trade-off between model complexity (number of model parameters) and fit of the data. Additionally, providing a continuous description of the variation in the concentration-QT relationship over the 24-hour period, the cosine model has more predictive value than the other model.

Of note, comparable parameter estimates and a similar shape of the cosine function were obtained when $QT_0$, α, A and φ were estimated with the full (on- and off- drug) data set instead of fixed to the values of the baseline model (Table 2 and Supplemental Figure 4). Additionally, we found that, regardless of the baseline model used, the shape of the estimated 24-hour variation in the concentration-QT relationship was characterized by a peak in the late afternoon and a trough in the early morning (Supplemental Figure 4).

**Table 2** Parameter estimates of the final QT model with fixed baseline parameters and estimated baseline parameters.

| Parameter | | Value (RSE) (fixed baseline parameters) | Value (RSE)[b] (estimated baseline parameters) | Bootstrap median (95% CI) |
|---|---|---|---|---|
| OFV | | 3786 | 3783 | |
| $QT_0$ (ms) | | 407[a] | 409 (1%) | 409 (399-419) |
| α | | 0.216[a] | 0.211 (6%) | 0.210 (0.190-0.243) |
| A (ms) | | 7.8[a] | 6.27 (24%) | 6.28 (3.54-9.28) |
| φ (h from midnight) | | 3.84[a] | 4.11 (11%) | 4.05 (3.16-4.93) |
| Slope | Mesor (ms per mg/L) | 0.73 (19%) | 0.73 (18%) | 0.73 (0.49-1.04) |
| | $A_1$ (ms per mg/L) | 0.977 (10%) | 0.763 (25%) | 0.772 (0.409-1.12) |
| | $φ_1$ (h from midnight) | 16.7 (1%) | 17.3 (3%) | 17.3 (16.3-19.0) |
| | $A_2$ (ms per mg/L) | 0.274 (21%) | 0.269 (22%) | 0.285 (0.159-0.395) |
| | $φ_2$ (h from midnight) | 15.8 (3%) | 15.8 (4%) | 15.8 (14.7-16.9) |
| IIV $QT_0$ (CV%) | | 4.3% (23%) | 4.3% (22%) | 4.1% (2.3-5.9) |
| IOV $QT_0$ (CV%) | | 1.4% (10%) | 1.4% (10%) | 1.3% (1.1-1.6) |
| Proportional residual error (CV%) | | 1.8% (5.8%) | 1.8% (6%) | 1.8% (1.6-2.0) |

a. Values fixed to parameter estimates from the baseline QT model

b. All parameters were estimated simultaneously using the full pre- and post-dose dataset

OFV: Objective Function Value; $QT_0$: intercept of QT-RR relationship; α correction term for RR interval, A: amplitude of the 24-hour variation in QT; φ: acrophase (time of peak) of the 24-hour variation in QT; Slope: C-QT relationship; Slope_Mesor: rhythm-adjusted mean of the slope; Slope_$A_1$ and Slope_$A_2$: amplitude of the first and second harmonic of slope, respectively; Slope_ $φ_1$ and Slope_ $φ_2$: phase of the first and second harmonic of slope, respectively, IIV: interindividual variability; IOV interoccasion variability; RSE: relative standard error.

**Table 3** Results of clinical trial simulations in which oral doses of 0, 500 and 1500mg levofloxacin were administered to 24 subjects in a crossover design. 500 clinical trials were simulated per dosing time.

| Dosing time | Slope (ms per mg/L) (median [95% PI]) | Trials with significant drug effect (%) [95% CI][a] | Trials with upper limit 90% CI of ΔQTc > 10ms (%) [95% CI] |
|---|---|---|---|
| 02:00 | 0.27 [0.11-0.44] | 85 [82-88] | 0 [0-0.8] |
| 06:00 | -0.04 [-0.19-0.12] | 5.2 [3.6-7.5] | 0 [0-0.8] |
| 10:00 | 0.71 [0.55-0.88] | 100 [99-100] | 44 [40-49] |
| 14:00 | 1.73 [1.56-1.90] | 100 [99-100] | 100 [99-100] |
| 18:00 | 1.08 [0.88-1.29] | 99 [98-100] | 96 [94-97] |
| 22:00 | 0.50 [0.33-0.69] | 99 [98-100] | 0 [0-0.8] |

CI: Wilson confidence interval; PI: prediction interval; ΔQTc: change from the baseline QT interval corrected for heart rate

The parameter estimates of the final model, in which the baseline and concentration-effect parameters were simultaneously estimated, showed good precision (RSE values between 1 and 25%; Table 2) and the population and individual predicted data were in agreement with the observed data (Supplemental Figure 5). The parameter estimates returned by bootstrap analysis were similar to the parameter estimates of the final model, indicating the robustness of the model (Table 2).

**Clinical trial simulations**

Our findings suggest that the concentration-QT relationship changes over time during a study occasion, while in a typical clinical trial this relationship is characterized by a single, linear, slope estimate. The predicted effect of dosing time on levofloxacin-induced QT prolongation is illustrated by clinical trial simulations (Table 3). We found that dosing time affects the linear concentration-QT relationship, the proportion of trials in which a significant drug effect was detected, and the proportion of trials in which the upper two-sided 90% confidence bound of ΔQTc at Cmax exceeded 10ms.

# DISCUSSION

In this study, we explored the implicit assumption that drug-induced QTc prolongation is not influenced by dosing time. Our results show that the relationship between the concentration of levofloxacin and the extent of QTc prolongation systematically varies over the course of the day. Using the developed PK-PD model to simulate clinical trials in which a therapeutic and a supratherapeutic dose of levofloxacin are administered, we show that dosing time would consequently influence the probability that a significant drug effect is detected. Likewise, the probability that the upper 90% confidence limit of the ΔQTc exceeds 10ms would depend on dosing time. Hence, if the developed model from this study on levofloxacin also applies to other drugs, dosing time influences the probability to detect drug-induced QT prolongation.

Our pharmacokinetic-pharmacodynamic model predicts that the largest drug effect occurs at 16:15, when the QTc interval increases by 1.7 ms per mg/L of levofloxacin, while the drug effect is virtually absent at 7:00. In a typical clinical trial, a linear slope is calculated to determine the concentration-QT relationship. Our model suggests that this slope estimate depends on the range of slope estimates that is present over time across the study period, but is most heavily influenced by the slope around the $C_{max}$. For a clinical trial starting in the morning at 6:00 or 10:00, our simulations predict that the estimated concentration-QT relationship is -0.04 ms per mg/L and 0.71 ms per mg/L, respectively. This range of drug effects encompasses the value of 0.36 ms per mg/L that was found in a previous study that investigated the relationship between levofloxacin concentration and QTc interval in healthy subjects that was presumably started in the morning (Taubel et al., 2010).

Variation in pharmacodynamics can only be correctly analyzed if the variation in pharmacokinetics is properly accounted for. The concentration-time profiles of levofloxacin used in this study were derived from a pharmacokinetic model in which 24-hour variation in the pharmacokinetic parameters was implemented (Kervezee et al., 2016). Because this pharmacokinetic model was built using the same dataset as the current study, we used the individual post-hoc parameter estimates from this model as input for our PK-PD model. Therefore, the variation in the relationship between levofloxacin concentration and the QT interval can be attributed to variation in the sensitivity to levofloxacin, rather than to an artifact introduced by incorrect description of its pharmacokinetics.

Various physiological mechanisms may underlie the 24-hour variation in the extent of levofloxacin-induced QTc prolongation. We investigated whether variation in potassium levels may provide an explanation for our findings. Potassium levels showed 24-hour variation with higher levels during the day and lowest levels during the night, which is in line with previously published potassium profiles (Moore Ede et al., 1975; Schmidt et al., 2015; Sennels et al., 2012). However, we found that the variation in potassium cannot account for the 24-hour variation in the concentration-QT parameter. Another explanation may be 24-hour variation in the expression of ion channels in cardiomyocytes, which has been reported in experimental animal models (Jeyaraj et al., 2012; Schroder et al., 2013, 2015; Yamashita et al., 2003). It remains to be elucidated if rhythmic expression of cardiac ion channels affects the QT-prolonging potential of a drug and to what extent this applies to humans.

By showing that the sensitivity to the QTc prolonging effects of a drug varies systematically over the day and night, our study calls into question the implicit - but untested - assumption that the relationship between a drug and the QTc interval is independent of the time of day. This assumption is the basis of most clinical research on drug-induced QTc prolongation. For example, the current ICH E14 guidelines require the conduct of a thorough QT (TQT) study for every new drug under development (ICH, 2005). In a TQT study, dosing typically occurs at the same clock time in every occasion in order to perform time-matched baseline subtraction. This approach assumes a constant concentration-effect relationship over time, while our findings indicate that this relationship varies considerably over the course of the

24-hour period. Using clinical trial simulations, we show that the extent of drug induced QT prolongation may thus depend on the time of day that it is investigated. This finding is relevant in the current debate on the utility of the TQT study, in which it has been proposed that data from early phase clinical trials, combined with integrated PK-PD analysis, is a more informative approach to evaluate the QT prolonging potential of new drugs (Chain et al., 2011; Darpo et al., 2015; France and Della Pasqua, 2015; Rohatagi et al., 2009). By showing that potentially clinically relevant effects on the QT interval cannot be detected within the strict design of a TQT study, which is commonly limited to dosing in the morning, our study offers a strong argument in favor of assessing these effects by a more sophisticated design in which the dosing time is taken into account.

 As this study was exploratory in nature, several limitations need to be considered. Firstly, the study population was relatively small and homogenous, consisting of healthy males between the age of 21 and 48 years, and factors such as food intake and sleep/wake rhythms were strictly standardized (Kervezee et al., 2016). Hence, to what extent our findings can be extrapolated to other populations and to real-life conditions remains to be investigated (Chain et al., 2013). Secondly, the use of continuous ECG recordings or triplicate recordings may have resulted in a richer dataset. Nevertheless, the high precision of the parameter estimates and the results of the bootstrap analysis suggest that the parameters could be precisely estimated with our dataset. Lastly, we did not include a placebo arm in our study, because the aim of the study was to investigate the effect of time of day on drug-induced QTc prolongation, and, as such, the subjects served as their own controls. Notwithstanding, we obtained sufficient pre-dose data in order to build a baseline model with precise parameter estimates that are comparable to previously published baseline models (Chain et al., 2011). Additionally, applying previously published baseline models to our data set results in a similar shape of the 24-hour variation in the concentration-QT relationship, further reducing the likelihood that our baseline model is misspecified.

An important question is to what extent our results are applicable to other drugs with QTc-prolonging potential. As the mechanism by which levofloxacin prolongs the QTc interval, namely blockade of the hERG channel is shared by most other QTc-prolonging drugs (Kannankeril et al., 2010), it is unlikely that the observed time-of-day dependency is a drug-specific property. Nevertheless, future research is warranted to extend our findings to other drugs that prolong the QTc interval. In this light, it will be useful to retrospectively and prospectively assess the effect of dosing time on the extent of drug-induced QTc prolongation in clinical studies with multiple daily dosing.

In conclusion, the tacit assumption that a drug's effect on the QTc interval is constant over the course of the day should not be taken for granted, as we show that the probability of detecting a significant drug effect depends on the time that a clinical trial is carried out, at least within the constraints of our study design. Future research into the relevance of our findings for other types of drugs as well as for other (patient) populations is crucial from both a regulatory as well as clinical perspective.

## ACKNOWLEDGEMENTS

## CONFLICT OF INTEREST

# REFERENCES

Alexandrou, A.J., Duncan, R.S., Sullivan, A., Hancox, J.C., Leishman, D.J., Witchel, H.J., and Leaney, J.L. (2006). Mechanism of hERG K+ channel blockade by the fluoroquinolone antibiotic moxifloxacin. Br. J. Pharmacol. 147, 905–916.

Beal, S., Sheiner, L.B., Boeckmann, A., and Bauer, R.J. (2009). NONMEM User's Guides (1989-2009), Icon Development Solutions, Ellicott City, MD, USA.

Bonnemeier, H., Wiegand, U.K., Braasch, W., Brandes, A., Richardt, G., and Potratz, J. (2003). Circadian profile of QT interval and QT interval variability in 172 healthy volunteers. Pacing Clin. Electrophysiol. PACE 26, 377–382.

Browne, K.F., Prystowsky, E., Heger, J.J., Chilson, D.A., and Zipes, D.P. (1983a). Prolongation of the Q-T interval in man during sleep. Am. J. Cardiol. 52, 55–59.

Browne, K.F., Prystowsky, E., Heger, J.J., Chilson, D.A., and Zipes, D.P. (1983b). Prolongation of the Q-T interval in man during sleep. Am. J. Cardiol. 52, 55–59.

Chain, A.S.Y., Krudys, K.M., Danhof, M., and Della Pasqua, O. (2011). Assessing the probability of drug-induced QTc-interval prolongation during clinical drug development. CPT 90, 867–875

Chain, A.S.Y., Dieleman, J.P., van Noord, C., Hofman, A., Stricker, B.H.C., Danhof, M., Sturkenboom, M.C.J.M., and Della Pasqua, O. (2013). Not-in-trial simulation I: Bridging cardiovascular risk from clinical trials to real-life conditions. Br. J. Clin. Pharmacol. 76, 964–972.

Dallmann, R., Brown, S.A., and Gachon, F. (2014). Chronopharmacology: new insights and therapeutic implications. Annu. Rev. Pharmacol. Toxicol. 54, 339–361.

Darpo, B., Benson, C., Dota, C., Ferber, G., Garnett, C., Green, C.L., Jarugula, V., Johannesen, L., Keirns, J., Krudys, K., et al. (2015). Results from the IQ-CSRC prospective study support replacement of the thorough QT study by QT assessment in the early clinical phase. Clin. Pharmacol. Ther. 97, 326–335.

Dubois, V.F.S., de Witte, W.E.A., Visser, S.A.G., Danhof, M., and Della Pasqua, O. (2016). Assessment of Interspecies Differences in Drug-Induced QTc Interval Prolongation in Cynomolgus Monkeys, Dogs and Humans. Pharm. Res. 33, 40–51.

Extramiana, F., Maison-Blanche, P., Badilini, F., Pinoteau, J., Deseo, T., and Coumel, P. (1999). Circadian modulation of QT rate dependence in healthy volunteers. J. Electrocardiol. 32, 33–43.

France, N.P., and Della Pasqua, O. (2015). The role of concentration-effect relationships in the assessment of QTc interval prolongation. Br. J. Clin. Pharmacol. 79, 117–131.

Garnett, C.E., Zhu, H., Malik, M., Fossa, A.A., Zhang, J., Badilini, F., Li, J., Darpö, B., Sager, P., and Rodriguez, I. (2012). Methodologies to characterize the QT/corrected QT interval in the presence of drug-induced heart rate changes or other autonomic effects. Am. Heart J. 163, 912–930.

Green, J.A., Patel, A.K., Patel, B.R., Hussaini, A., Harrell, E.J., McDonald, M.J., Carter, N., Mohamed, K., Duparc, S., and Miller, A.K. (2014). Tafenoquine at therapeutic concentrations does not prolong Fridericia-corrected QT interval in healthy subjects. J. Clin. Pharmacol. 54, 995–1005.

ICH (2005). E14 Clinical evaluation of QT/QTc interval prolongation and proarrhythmic potential for non-antiarrhythmic drugs. Guidance to industry. Fed. Regist. 70, 61134–61135.

Jeyaraj, D., Haldar, S.M., Wan, X., McCauley, M.D., Ripperger, J.A., Hu, K., Lu, Y., Eapen, B.L., Sharma, N., Ficker, E., et al. (2012). Circadian rhythms govern cardiac repolarization and arrhythmogenesis. Nature 483, 96–99.

Kang, J., Wang, L., Chen, X.-L., Triggle, D.J., and Rampe, D. (2001). Interactions of a Series of Fluoroquinolone Antibacterial Drugs with the Human Cardiac K+ Channel HERG. Mol. Pharmacol. 59, 122–126.

Kannankeril, P., Roden, D.M., and Darbar, D. (2010). Drug-induced long QT syndrome. Pharmacol. Rev. 62, 760–781.

Keizer, R.J., Karlsson, M.O., and Hooker, A. (2013). Modeling and Simulation Workbench for NONMEM: Tutorial on Pirana, PsN, and Xpose. CPT Pharmacometrics Syst. Pharmacol. 2, e50.

Kervezee, L., Stevens, J., Birkhoff, W., Kamerling, I.M.C., de Boer, T., Dröge, M., Meijer, J.H., and Burggraaf, J. (2016). Identifying 24-hour variation in the pharmacokinetics of levofloxacin: a population pharmacokinetic approach. Br. J. Clin. Pharmacol. 81, 256–268.

Malik, M., and Camm, A.J. (2001). Evaluation of Drug-Induced QT Interval Prolongation. Drug Saf. 24, 323–351.

Malik, M., Hnatkova, K., Schmidt, A., and Smetana, P. (2008). Accurately measured and properly heart-rate corrected QTc intervals show little daytime variability. Heart Rhythm 5, 1424–1431.

Moore Ede, M.C., Brennan, M.F., and Ball, M.R. (1975). Circadian variation of intercompartmental potassium fluxes in man. J Appl Physiol 38, 163–170.

Mould, D.R., and Upton, R.N. (2013). Basic concepts in population modeling, simulation, and model-based drug development-part 2: introduction to pharmacokinetic modeling methods. CPT Pharmacometrics Syst. Pharmacol. 2, e38.

Noel, G.J., Natarajan, J., Chien, S., Hunt, T.L., Goodman, D.B., and Abels, R. (2003). Effects of three fluoroquinolones on QT interval in healthy adults after single doses. Clin.Pharmacol.Ther. 73, 292–303.

Noel, G.J., Goodman, D.B., Chien, S., Solanki, B., Padmanabhan, M., and Natarajan, J. (2004). Measuring the effects of supratherapeutic doses of levofloxacin on healthy volunteers using four methods of QT correction and periodic and continuous ECG recordings. J. Clin. Pharmacol. 44, 464–473.

R Development Core Team (2008). R: A language and environment for statistical computing. R Foundation for Statistical Computing (Vienna, Austria).

Roden, D.M. (2004). Drug-induced prolongation of the QT interval. N. Engl. J. Med. 350, 1013–1022.

Rohatagi, S., Carrothers, T.J., Kuwabara-Wagg, J., and Khariton, T. (2009). Is a thorough QTc study necessary? The role of modeling and simulation in evaluating the QTc prolongation potential of drugs. J. Clin. Pharmacol. 49, 1284–1296.

Sanguinetti, M.C., and Tristani-Firouzi, M. (2006). hERG potassium channels and cardiac arrhythmia. Nature 440, 463–469.

Schmidt, S.T., Ditting, T., Deutsch, B., Schutte, R., Friedrich, S., Kistner, I., Ott, C., Raff, U., Veelken, R., and Schmieder, R.E. (2015). Circadian rhythm and day to day variability of serum potassium concentration: a pilot study. J. Nephrol. 28, 165–172.

Schroder, E.A., Lefta, M., Zhang, X., Bartos, D.C., Feng, H.-Z., Zhao, Y., Patwardhan, A., Jin, J.-P., Esser, K.A., and Delisle, B.P. (2013). The cardiomyocyte molecular clock, regulation of Scn5a, and arrhythmia susceptibility. Am. J. Physiol. Cell Physiol. 304, C954–C965.

Schroder, E.A., Burgess, D.E., Zhang, X., Lefta, M., Smith, J.L., Patwardhan, A., Bartos, D.C., Elayi, C.S., Esser, K.A., and Delisle, B.P. (2015). The Cardiomyocyte Molecular Clock Regulates the Circadian Expression of Kcnh2 and Contributes to Ventricular Repolarization. Hear. Rhythm.

Sennels, H.P., Jørgensen, H.L., Goetze, J.P., and Fahrenkrug, J. (2012). Rhythmic 24-hour variations of frequently used clinical biochemical parameters in healthy young males--the Bispebjerg study of diurnal variations. Scand. J. Clin. Lab. Invest. 72, 287–295.

Smetana, P., Batchvarov, V.N., Hnatkova, K., Camm, A.J., and Malik, M. (2002). Sex differences in repolarization homogeneity and its circadian pattern. Am. J. Physiol. Heart Circ. Physiol. 282, H1889–H1897.

Smetana, P., Batchvarov, V., Hnatkova, K., Camm, A.J., and Malik, M. (2003). Circadian rhythm of the corrected QT interval: impact of different heart rate correction models. Pacing Clin. Electrophysiol. 26, 383–386.

Sugiyama, A., Nakamura, Y., Nishimura, S., Adachi-Akahane, S., Kumagai, Y., Gayed, J., Naseem, A., Ferber, G., Taubel, J., and Camm, J. (2012). Comparison of the effects of levofloxacin on QT/QTc interval assessed in both healthy Japanese and Caucasian subjects. Br. J. Clin. Pharmacol. 73, 455–459.

Taubel, J., Naseem, A., Harada, T., Wang, D., Arezina, R., Lorch, U., and Camm, A.J. (2010). Levofloxacin can be used effectively as a positive control in thorough QT/QTc studies in healthy volunteers. Br. J. Clin. Pharmacol. 69, 391–400.

Watanabe, J., Suzuki, Y., Fukui, N., Ono, S., Sugai, T., Tsuneyama, N., and Someya, T. (2012). Increased risk of antipsychotic-related QT prolongation during nighttime: a 24-hour holter electrocardiogram recording study. J. Clin. Psychopharmacol. 32, 18–22.

Yamashita, T., Sekiguchi, A., Iwasaki, Y., Sagara, K., Iinuma, H., Hatano, S., Fu, L.-T., and Watanabe, H. (2003). Circadian variation of cardiac K+ channel gene expression. Circulation 107, 1917–1922.
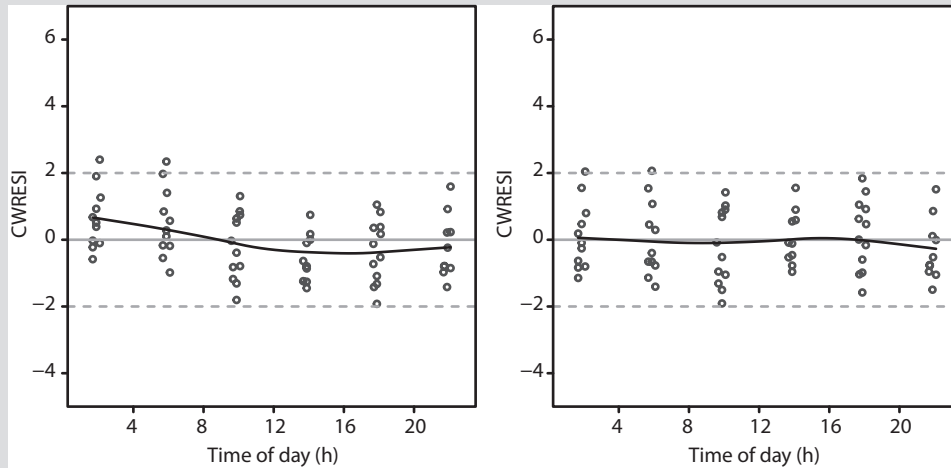
**Supplementary Figure 1** Conditional weighted residuals with interaction (CWRESI) of baseline model without **(left)** and with **(right)** correction for 24-hour rhythm in the QT interval.
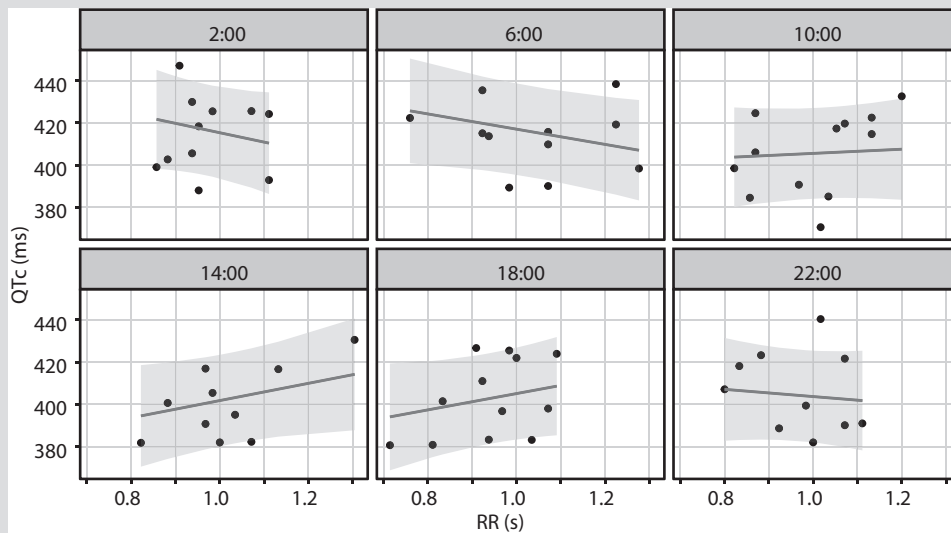


**Supplementary Figure 2** The relationship between the RR interval and the QTc interval in the baseline recordings split by time of day. The QT interval was corrected by the study-specific α obtained from the baseline model (α=0.216). A linear mixed effect with QTc as the dependent variable, RR as the fixed effect, dosing time as a categorical variable, interaction between RR and dosing time and subject as a random effect shows that the interaction between RR and dosing time (p=0.1617) and the effect of RR on QTc (p=0.5706) are not significant. Solid lines: predicted slopes of the model. Shaded areas: 95% prediction intervals.
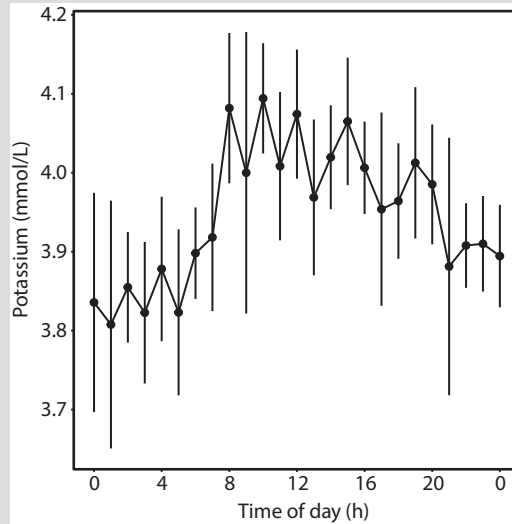
**Supplementary Figure 3** Mean concentrations of potassium in plasma. Sampling times were rounded to the nearest hour. Error bars represent 95% confidence intervals.
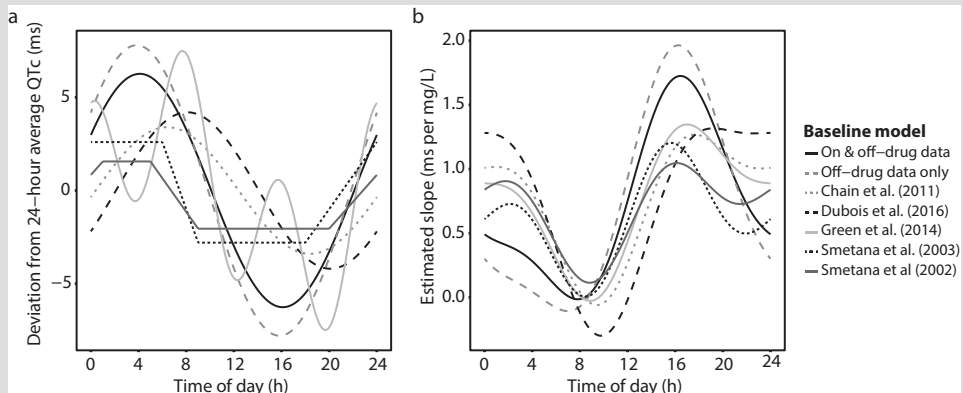


**Supplementary Figure 4 (a)** 24-hour variation in baseline QT interval estimated with the full (on- and off-drug) data set (dark red line), with the pre-dose (off-drug) data set only (light red line) and reported in various publications (blue, green and orange lines). **(b)** Estimated 24-hour variation in concentration-QT relationship using the baseline models shown in panel a.
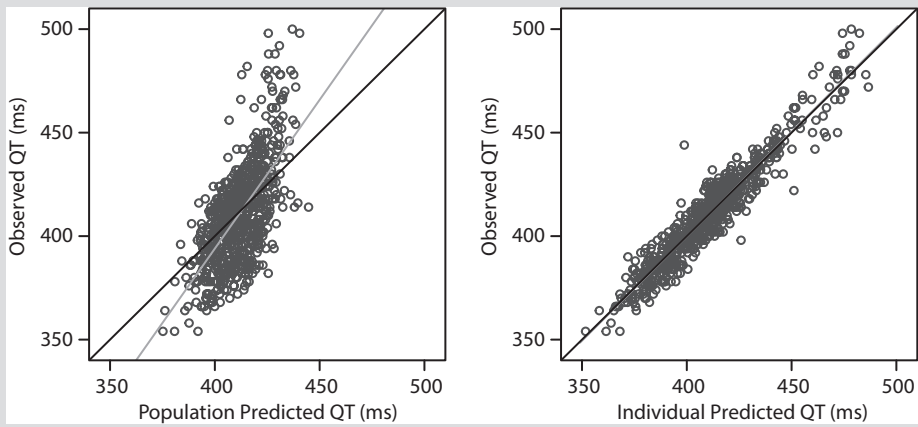
**Supplementary Figure 5** Goodness of fit plots of the final model. Observed versus population **(left)** and individual **(right)** predicted QT intervals.

**Supplemental Table 1** Parameter estimates of the baseline QT model

| Parameter | Estimate (RSE) |
|---|---|
| $QT_0$ (ms) | 407 (1.1%) |
| α | 0.216 (18%) |
| A (ms) | 7.8 (28%) |
| φ (h from midnight) | 3.84 (22%) |
| IIV $QT_0$ (%) | 3.5% (16%) |
| IOV $QT_0$ (%) | 2.3% (13%) |
| Proportional residual error (%) | 1.2% (45.2%) |

$QT_0$: intercept of QT-RR relationship; α correction term for RR interval, A: amplitude of the 24-hour variation in QT; φ: acrophase (time of peak) of the 24-hour variation in QT; IIV: interindividual variability; IOV: interoccasion variability; RSE: relative standard error.

**Supplemenatary Code 1** Model code of the final model used in NONMEM v7.3

```
$PROBLEM
$DATA 4_NONMEMDataFiles/CHDR1227_NMdataset_QT_LFX_v11.0.csv IGNORE=I;

$INPUT ID OCC TALD DV HR AMT MDV CMT EVID ADMINTIME TIME TSHPEAK TSHPEAK2 RR QTCF QTCR BMI
HGT WGT LBM AGE CLI VI MESORI AMPI PHASEI OBSCONC TINTERVAL

$SUB ADVAN6 TOL=5
$MODEL
COMP(DEPOT)
COMP(CENTRAL)
COMP(TRANSIT)

$PK
;Interocc var
OC1=0
IF(ADMINTIME.EQ.2)OC1=1
OC2=0
IF(ADMINTIME.EQ.6)OC2=1
OC3=0
IF(ADMINTIME.EQ.10)OC3=1
OC4=0
IF(ADMINTIME.EQ.14)OC4=1
OC5=0
IF(ADMINTIME.EQ.18)OC5=1
OC6=0
IF(ADMINTIME.EQ.22)OC6=1

BOV = ETA(10)*OC1+ETA(11)*OC2+ETA(12)*OC3+ETA(13)*OC4+ETA(14)*OC5+ETA(15)*OC6

; Baseline model
TVBSL = THETA(1)
BSL = TVBSL*EXP(ETA(1)+BOV)
ALPH = THETA(2)*EXP(ETA(2))
AMP24 = THETA(3)*EXP(ETA(3))
PHASE24 = THETA(4)*EXP(ETA(4))
CIRC = AMP24*COS(6.283185*(TIME-PHASE24)/24)

; Drug effect model
SLPMESOR = THETA(5)*EXP(ETA(5))
SLPAMP = THETA(6)*EXP(ETA(6))
SLPPHASE = THETA(7)*EXP(ETA(7))

SLPAMP12 = THETA(8)*EXP(ETA(8))
SLPPHASE12 = THETA(9)*EXP(ETA(9))

SLOPE    =    SLPMESOR+SLPAMP*COS(6.283185*(TIME-SLPPHASE)/24)+SLPAMP12*COS(6.283185*(TIME-
SLPPHASE12)/12)

;PK model
KA=MESORI+AMPI*COS(6.283185*(TIME-PHASEI)/24)
CL=CLI
V=VI
KTR=KA

K13 = KA
```

```
K32 = KTR
K20 = CL/V

$DES
DADT(1) = -K13*A(1)
DADT(2) = K32*A(3)-K20*A(2)
DADT(3) = K13*A(1)-K32*A(3)

$ERROR
CPPR = A(2)/V
IPRED=BSL*RR**ALPH+CIRC+SLOPE*CPPR
Y=IPRED*(1+EPS(1))

$THETA
407                     ; BSL
0.216                   ; ALPHA
7.8                     ; AMP24
3.84                    ; PHASE24
0.1                     ; SLPMESOR
(0,1,10)                ; SLPAMP24
(0.1,12,23.9)           ; SLPPHASE24
(0,1,10)                ; SLPAMP12
(0.1,12,23.9)           ; SLPPHASE12

$OMEGA
0.1                     ; BSL
0 FIX                   ; ALPH
0 FIX                   ; AMP24
0 FIX                   ; PHASE24
0 FIX                   ; SLOPE MESOR
0 FIX                   ; SLPAMP
0 FIX                   ; SLPPHASE
0 FIX                   ; SLPAMP12
0 FIX                   ; SLPPHASE12
$OMEGA BLOCK(1) 0.1                      ; IOV on BSL
$OMEGA BLOCK(1) SAME                     ; IOV on BSL
$OMEGA BLOCK(1) SAME                     ; IOV on BSL
$OMEGA BLOCK(1) SAME                     ; IOV on BSL
$OMEGA BLOCK(1) SAME                     ; IOV on BSL
$OMEGA BLOCK(1) SAME                     ; IOV on BSL

$SIGMA
0.05

$EST PRINT=5 MAX=9999 METHOD=1 INTERACTION POSTHOC NOABORT

$COV COMP PRINT=E

$TABLE ID OCC ADMINTIME TIME TALD IPRED PRED CWRESI RES WRES CWRES MDV SLOPE SLPMESOR SLPAMP
SLPPHASE SLPAMP12 SLPPHASE12 RR DV BSL ALPH AMP24 PHASE24 CPPR ETA1 BOV CLI VI KA MESORI AMPI
PHASEI OBSCONC NOPRINT ONEHEADER FILE=sdtabRun1101b_FINAL
```
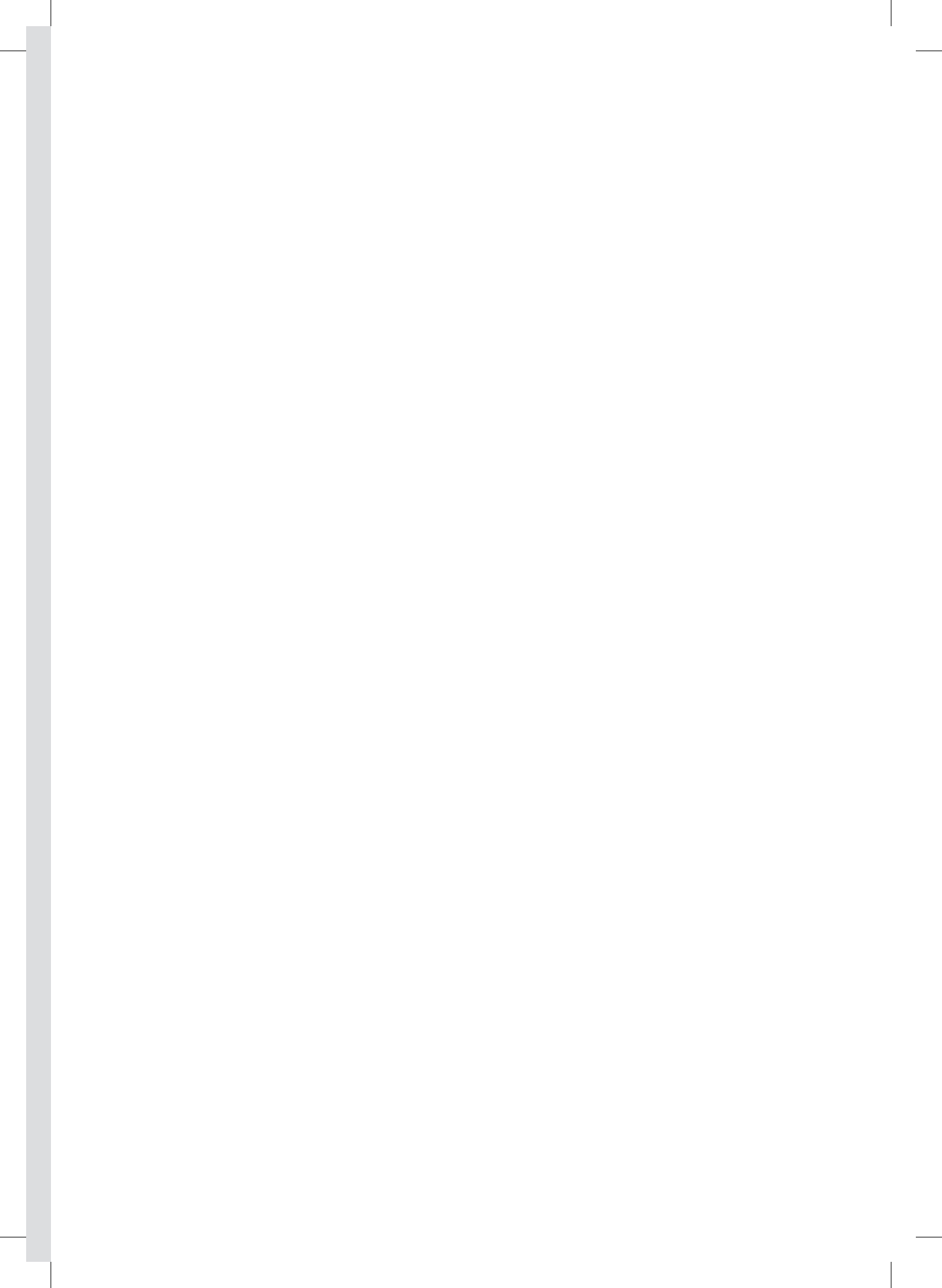
# CHAPTER

## Diurnal Variation in P-glycoprotein-Mediated Transport and Cerebrospinal Fluid Turnover in the Brain

# 6

Laura Kervezee[1,2]; Robin Hartman[2]; Dirk-Jan van den Berg[2]; Shinji Shimizu[2]; Yumi Emoto-Yamamoto[2]; Johanna H. Meijer[1,*]; Elizabeth C.M. de Lange[2,*]

[1]Laboratory for Neurophysiology, Department of Molecular Cell Biology, Leiden University Medical Center, Leiden, the Netherlands;
[2]Division of Pharmacology, Leiden Academic Center for Drug Research, Leiden University, Leiden, the Netherlands
[*]These authors contributed equally to this work

## ABSTRACT

Nearly all bodily processes exhibit circadian rhythmicity. As a consequence, the pharmacokinetic and pharmacodynamic properties of a drug may also vary with time of day. The objective of this study was to investigate diurnal variation in processes that regulate drug concentrations in the brain, focusing on P-glycoprotein (P-gp). This efflux transporter limits the distribution of many drugs in the brain. To this end, the exposure to the P-gp substrate quinidine was determined in the plasma and brain tissue after intravenous administration in rats at six different time points over the 24-h period. Our results indicate that time of administration significantly affects the exposure to quinidine in the brain. Upon inhibition of P-gp, exposure to quinidine in brain tissue is constant over the 24-h period. To gain more insight into processes regulating brain concentrations, we used intracerebral microdialysis to determine the concentration of quinidine in brain extracellular fluid (ECF) and cerebrospinal fluid (CSF) after intravenous administration at two different time points. The data were analyzed by physiologically based pharmacokinetic modeling using NONMEM. The model shows that the variation is due to higher activity of P-gp-mediated transport from the deep brain compartment to the plasma compartment during the active period. Furthermore, the analysis reveals that CSF flux is higher in the resting period compared to the active period. In conclusion, we show that the exposure to a P-gp substrate in the brain depends on time of administration, thereby providing a new strategy for drug targeting to the brain.

## INTRODUCTION

The treatment of brain tumors, infectious diseases, and various neurological disorders is often unsuccessful because the entry of most clinically available drugs into the brain is restricted (Abbott et al., 2010). This is due to a number of protective mechanisms that prevent the distribution of potentially toxic compounds in the brain but, at the same time, impede drugs from reaching their target site in the central nervous system (CNS). For example, several types of efflux transporters are expressed in the brain, which expel a wide variety of exogenous substances from the brain back into the circulation (Abbott et al., 2010; Ohtsuki and Terasaki, 2007).

A well-known efflux transporter in the CNS is P-glycoprotein (P-gp). At the level of the blood–brain barrier (BBB), it restricts the entry of many, mainly hydrophobic, drugs to the brain(Schinkel et al., 1994). Although P-gp is mostly known for its role in the efflux of its substrates at the BBB, it is also expressed in blood–cerebrospinal fluid (CSF) barrier (BCSFB) as well as in parenchymal cells types, such as astrocytes and pericytes (Bendayan et al., 2006). Several strategies have been proposed to diminish P-gp-mediated efflux, but it has been difficult to implement these strategies in the clinic and, especially, to apply them to chronic diseases (Potschka, 2010).

The pharmacokinetic and pharmacodynamic properties of a wide variety of drugs show diurnal variation, which is a result of 24-h rhythms in, for example, gastrointestinal function, activity of xenobiotic-metabolizing enzymes, blood flow, and glomerular filtration rate (Dallmann et al., 2014). Consequently, therapeutic efficiency as well as the severity of side effects of drugs may vary with time of day (Buttgereit et al., 2010; Hermida et al., 2008; Watanabe et al., 2012). Regarding P-gp, it has been shown that its expression and activity show a diurnal rhythm in the intestines of rodents, leading to different plasma concentrations of orally administered P-gp substrates depending on the time of administration (Ando et al., 2005; Ballesta et al., 2011; Hayashi et al., 2010; Murakami et al., 2008; Okyar et al., 2012; Stearns et al., 2008).

The objective of this study was to examine whether the distribution of P-gp substrates in the CNS depends on time of administration. Diurnal variation in P-gp activity could be exploited to either increase or reduce the effect of P-gp on CNS target site distribution, depending on whether the aim is to limit or enhance CNS distribution of the drug. Other processes that govern CNS target site concentrations (de Lange, 2013), such as CSF turnover, may also vary over the course of the day. Understanding the effect of time of administration on CNS target site distribution may be useful to improve the efficiency of therapies involving P-gp substrates.

In this study, the concentration of the P-gp substrate quinidine was determined in plasma and brain tissue after intravenous administration at six different time points over the 24-h period in rats. As we observed a significant 24-h variation in P-gp-mediated drug transport in brain tissue, we next used intracerebral microdialysis to obtain quinidine concentration–time profiles in brain extracellular fluid (ECF) and in CSF at two different

times of the day. Using physiologically based pharmacokinetic (PBPK) modeling to describe quinidine brain distribution (Westerhout et al., 2013), we were able to explore differences in P-gp-mediated transport and CSF flux between the active and resting period of the animals. The results show that time is an important consideration in the design of drug treatments targeted at the CNS.

## MATERIALS AND METHODS

### Animals

Male Wistar rats (Charles River, The Netherlands) were housed in groups under standard environmental conditions (12:12LD cycle) with free access to water and food (SDS, Technilab-BMI, Someren, the Netherlands). After surgery, the rats were kept individually. All animal procedures were performed in accordance with the Dutch law on animal experimentation and were approved by the Animal Ethics Committee of the Leiden University (protocol number DEC12088).

### Chemicals and solutions

Quinidine, quinidine sulfate dehydrate, and quinine were obtained from Sigma-Aldrich (Zwijndrecht, the Netherlands); tariquidar from Xenova Group PLC (Cambridge, UK); saline and 5% glucose in saline from the Leiden University Medical Centre (Leiden, the Netherlands); Heparin from LEO Pharma BV (Breda, the Netherlands); nembutal and isoflurane from AUV (Cuijk, the Netherlands); phosphoric acid and boric acid from Merck (Darmstadt, Germany), sodium hydroxide and triethyl amine (TEA) from Baker (Enschede, the Netherlands); and methanol, methyl tert-butyl ether (TBME), and acetonitrile from Biosolve (Valkenswaard, the Netherlands). Perfusion fluid (PF) for microdialysis experiments was prepared as described previously (Moghaddam and Bunney, 1989).

### Surgery

Animals were anesthetized by isoflurane during surgical procedures (induction, 5%; maintenance, 1–2%). A cannula was inserted in the femoral artery and femoral vein 7 days prior to the experiment as described previously (Westerhout et al., 2013). Animals used for microdialysis experiments also received microdialysis guides with dummy probes (CMA, Solna, Sweden) in the caudate putamen (CP; coordinates from bregma, AP-1.0 mm L+3.0 mm V-3.4 mm) and in the cisterna magna (CM; coordinates from lambda, AP-2.51 mm L+2.04 mm V-8.34 mm, at an angle of 25° anterior from the dorsoventral axis and 11° lateral from the anteroposterior axis) (Westerhout et al., 2013). Twenty-four hours before the experiment, the dummy probes in CP and CM were replaced by 4 and 1 mm microdialysis probes (CMA), respectively.

### Drug administration, serial blood sampling, and collection of brain tissue

Brain distribution experiments were performed at six different time points across the 24-h

period; t =0 (start of quinidine administration) was at Zeitgeber Time (ZT) 0, ZT4, ZT8, ZT12, ZT16, or ZT20 (±10 min), with ZT12 defined as the moment of lights off. Microdialysis and in vivo recovery experiments were performed with t=0 at ZT8 or ZT20. The number of animals per group is shown in Supplemental Table 1. Between ZT12 and ZT0 experiments were conducted in dim red light.

Animals were pretreated with an intravenous infusion of vehicle (5% glucose in saline) or 15 mg/kg tariquidar in 5% glucose at t =−25 min for 10 min at a rate of 500 µL/min/kg with a syringe pump (Pump 22 Multiple Syringe Pump, Harvard Apparatus, Holliston, MA, USA). In brain distribution and microdialysis experiments, quinidine (10 mg/kg) was administered intravenously at t=0 in 10 min at a rate of 250 µL/min/kg. Blood samples (100 µL) were collected at t =−10, 10, 30, 60, 90, 120, 150, 180, 210, and 240 min in heparinized Eppendorf tubes and centrifuged for 10 min at 5,000 rpm (Eppendorf Microcentrifuge Model 5415D) to obtain plasma. Plasma was stored at −20°C until analysis. At t=240 min, the rats were sacrificed with an intravenous injection of Nembutal and transcardially perfused with PBS until the organs were free of blood. Brain tissue was removed and stored at −80°C.

### Intracerebral microdialysis

Microdialysis probe inlets were connected to a syringe filled with PF, and the outlets were connected to a fraction collector (Univentor microsampler 820, Univentor Ltd, Zejtun, Malta) with FEP tubing. Perfusion of the microdialysis probes with a syringe pump (Bioanalytical Systems Inc., West Lafayette, USA) started 2 h prior to quinidine administration. Perfusion rate was set to 1 µL/min. Samples were collected every 20 min until t=240 min and stored at −80°C.

### In vivo retrodialysis

The recovery of quinidine into the microdialysis probe was determined by in vivo retrodialysis. Probes were perfused with blank PF for 2 hours, after which the concentration of quinidine in PF was changed every 2 h from 20 to 50 ng/mL and to 200 ng/mL. Samples were collected every 20 min at a perfusion rate of 1 µL/min. The probe recovery (extraction fraction) was calculated as described by Westerhout et al. (2013). The extraction fractions from the probes located in CP and CM were used to convert the measured microdialysate concentrations to ECF and CSF concentrations, respectively.

### Plasma protein binding

To determine the degree of plasma protein binding of quinidine, 50 µL aliquots of each plasma sample taken at t=30 min and t =90 min were pooled per experimental time point (ZT) and pre-treatment (vehicle or TQD). The samples were equilibrated at 37°C for 30 min, and 200 µL was added to a pre-heated Centrifree 30 K ultrafiltration device (Millipore BV, Etten-Leur, the Netherlands). The samples were centrifuged for 20 min at 5,000 rpm at 37°C according to the manufacturer's protocol. The unbound fraction of quinidine in plasma (funbound) was calculated by dividing the concentration of the ultrafiltrate by the

concentration in the unfiltered sample.

## Measurement of quinidine concentration in microdialysate, plasma, and brain homogenates

Quinidine concentrations in plasma, microdialysates, and brain homogenates were measured using high-performance liquid chromatography (HPLC) with fluorescence detection as described earlier (Syvänen et al., 2012). Microdialysates (10 μL) were directly injected into the HPLC system using a mobile phase with an acetonitrile/buffer ratio of 17:83 (v/v). Brain tissue was homogenized in 50 mM phosphate buffer (pH7.4) using the Bullet Blender 5 (Next Advance Inc., NY, USA) according to the manufacturer's protocol. Brain homogenates were diluted 6× (w/v) in 50 mM phosphate buffer (pH7.4). Extraction of quinidine from plasma and brain homogenate was performed as described earlier (Syvänen et al., 2012). The injection volume was 2–20 μL depending on the type of sample. The mobile phase consisted of acetonitrile and buffer in a ratio of 14:86 (v/v).

## Data analysis

Areas under the curve (AUC in ng/mL*min) of unbound quinidine in plasma from 0 to 240 min after administration (AUCPLu,0–240) were calculated using the trapezoidal rule. Ratios between parameters were determined for each animal individually before calculating the mean per group. The means of two groups were compared by an unpaired Student's t test (normally distributed data) or a Mann–Whitney U test (not normally distributed data). To compare the means of more than two groups, an ANOVA (normally distributed data) or Kruskal–Wallis test (not normally distributed data) was used. Normal distribution was assessed by the Sharipo–Wilk test. p values below 0.05 were considered significant. Statistical analyses and graphical visualization were performed with R version 2.14.1 or version 3.0.1 (R Foundation for Statistical Computing, Vienna, Austria).

## Physiologically based pharmacokinetic modeling

PBPK brain distribution modeling was performed to investigate the effect of time of administration on the pharmacokinetics of quinidine in plasma, total brain, ECF, and CSF quantitatively using a nonlinear mixed effect model approach with NONMEM software version VII (GloboMax LLC, Hanover, MD, USA). The PBPK model describing brain distribution of quinidine that was previously published (Westerhout et al., 2013) was applied to the data (Supplemental Figure 1). Data obtained during the microdialysis experiments in this study were added to the previously obtained data produced with the same experimental method during the resting period of the animals (Westerhout et al., 2013). Using covariate analysis, the effect of time of administration was tested on parameters describing P-gp-mediated transport and CSF flux. Statistical significance was based on changes in the objective function value (OFV; $p < 0.05$). The difference in the OFV obtained by comparing each model was assumed to be asymptotically chi-squared distributed with degrees of freedom (df) equal to the difference in the number of parameters between the two models. Goodness-

**Figure 1** Quinidine exposure in plasma and brain in vehicle-treated animals. **(a)** Time–concentration profiles of unbound quinidine in plasma. Different symbols represent the different experimental time points (ZT0, 4, 8, 12, 16, and 20). Asterisks indicate significant effect of ZT on plasma concentration at the designated sampling times (n = 6–8 animals per group). **(b)** Area under the curve for unbound quinidine in plasma from 0 to 240 min after administration ($AUC_{PLu,0-240}$) at different experimental time points (n = 5–8 animals per group). No significant time of day effect on $AUC_{PLu,0-240}$ was found (p > 0.05, ANOVA). **(c)** Quinidine concentration at t = 240 min in brain homogenate relative to plasma AUC ($C_{BR}:AUC_{PLu,0-240}$) at different experimental time points (n = 4–8 animals per group). Time of administration significantly affects this ratio (p < 0.05, Kruskal–Wallis rank sum test). Mean ± SEM in all graphs. n.s. not significant; *p < 0.05

of-fit plots (model predicted vs. observed data values) were evaluated by diagnostic scatter plots. The stability and performance of the final model were confirmed by a visual predictive check on the simulated distribution of the concentration data to cover over 90% of the observed data.

# RESULTS

**Time of administration has no effect on plasma pharmacokinetics of quinidine**

We first determined the mean concentration–time profiles of unbound quinidine in plasma

after intravenous administration at six experimental time points (ZT0-20) (Fig. 1a). Unbound plasma concentrations were derived from total plasma concentrations corrected for by the unbound fraction in plasma ($0.286 \pm 0.006$). Total and unbound concentrations of quinidine in plasma showed a highly significant linear correlation ($r2 = 0.953$, $N = 24$, $p = 0.000$, Pearson's correlation; Supplemental Figure 2A). The unbound fraction did not depend on time of administration ($F_{(5,17)} = 2.52$, $p = 0.07$, two-way ANOVA; Supplemental Figure 2B) and pre-treatment with TQD ($F_{(1,17)} = 1.70$, $p = 0.21$, two-way ANOVA; Supplemental Figure 2C)

The unbound quinidine concentration in plasma in vehicle-treated animals at $t = 30$, 90, 120, 150, 210, and 240 min was influenced by time of administration ($p < 0.05$, one-way ANOVA or Kruskal–Wallis, as appropriate; Fig. 1a). Time of administration had no significant effect on the area under the time concentration curve of unbound quinidine in plasma from 0 to 240 min after administration ($AUC_{PLu(0–240)}$) (Fig. 1b; $F_{(5,34)} = 1.49$, $p = 0.220$, one-way ANOVA). These results indicate that the total exposure to quinidine in plasma is not affected by time of administration.

**Quinidine brain tissue concentration shows significant diurnal variation**

The concentration of quinidine in brain tissue at $t = 240$ ($C_{BR}$) relative to $AUC_{PLu(0–240)}$ was found to be significantly affected by time of administration (Fig. 1c $H(5) = 14.9$, $p = 0.011$, Kruskal–Wallis test). In experiments conducted in the resting period of the animals (i.e., animals treated at ZT0, ZT4, and ZT8), the $C_{BR}$: $AUC_{PLu(0–240)}$ was on average twice as high compared to the ratio in the active period (at ZT12, ZT16, or ZT20). These results indicate that the exposure to the P-gp substrate quinidine in the brain, relative to plasma exposure, exhibits diurnal variation.

**Diurnal variation of total brain quinidine concentrations is due to the variation in P-gp-mediated transport**

To determine whether the effect of time of administration on the exposure to quinidine in brain tissue is due to variation in P-gp-mediated transport over the 24-h period, we administered the selective P-gp inhibitor tariquidar intravenously 30 min prior to quinidine administration at ZT0, 4, 8, 12, 16, or 20. Time of administration did not significantly affect unbound plasma concentrations of quinidine at any of the sampling points (Fig. 2a) and had no effect on $AUC_{PLu(0–240)}$ (Fig. 2b; $F_{(5,33)} = 0.635$, $p = 0.675$, one-way ANOVA) in tariquidar-treated animals, indicating that also in this group of animals, time of administration does not affect exposure to quinidine in plasma. Importantly, time of administration also did not significantly affect $C_{BR}$: $AUC_{PLu(0–240)}$ of quinidine after tariquidar treatment (Fig. 2c $F_{(5,31)} = 1.28$, $p = 0.297$, one-way ANOVA). Hence, tariquidar pre-treatment abolished the diurnal variation in $C_{BR}$: $AUC_{PLu(0–240)}$ that was observed in vehicle-treated animals. These results indicate that the exposure to quinidine in the brain relative to plasma levels exhibits diurnal variation unless P-gp is inhibited.
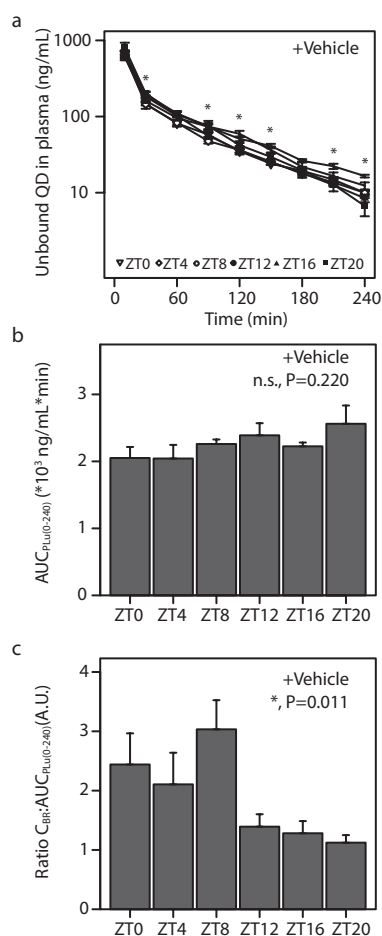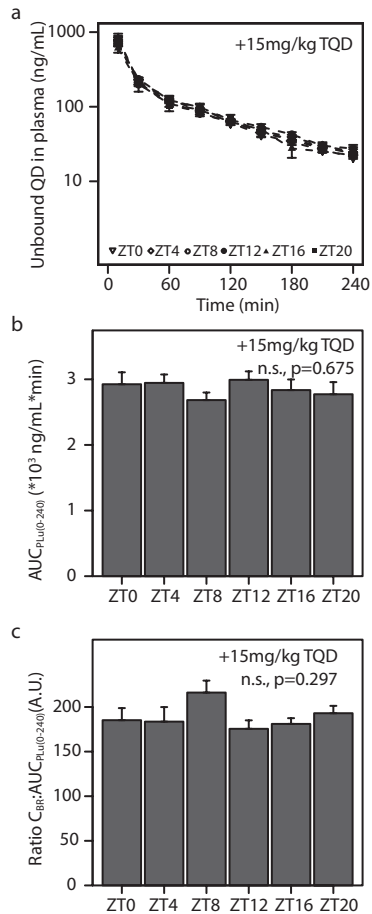
**Figure 2** Quinidine exposure in plasma and brain in tariquidar-treated animals. **(a)** Time– concentration profiles of unbound quinidine in plasma. Different symbols represent the different experimental time points (ZT0, 4, 8, 12, 16, or 20). No significant effect of ZT was found between plasma concentrations at different sampling times (n = 6–8 animals per group). **(b)** Area under the curve for unbound quinidine in plasma from 0 to 240 min after administration (AUC$_{PLu,0-240}$) at different experimental time points (n = 5–8 animals per group). No significant time of day effect on AUC$_{PLu,0-240}$ was found (p > 0.05, ANOVA). **(c)** Quinidine concentration at t = 240 min in brain homogenate relative to plasma AUC (C$_{BR}$:AUC$_{PLu,0-240}$) at different experimental time points (n = 4–8 animals per group). No significant time of day effect was found on this ratio in tariquidar-treated animals (p > 0.05, ANOVA). Mean ± SEM in all graphs. n.s. not significant

## Exposure to quinidine in CNS is influenced by diurnal variation in P-gp activity and CSF flux

Next, we used intracerebral microdialysis to determine unbound concentrations of quinidine in brain extracellular fluid (ECF) and cerebrospinal fluid (CSF) from 0 to 240 min after intravenous quinidine administration at ZT8 (resting period) and ZT20 (active period of the animals). The extraction fractions (4 mm probe, 13 ± 1.4%; 1 mm probe, 8.4 ± 2.6%) were used to calculate unbound concentrations in ECF and CSF from microdialysate concentrations.
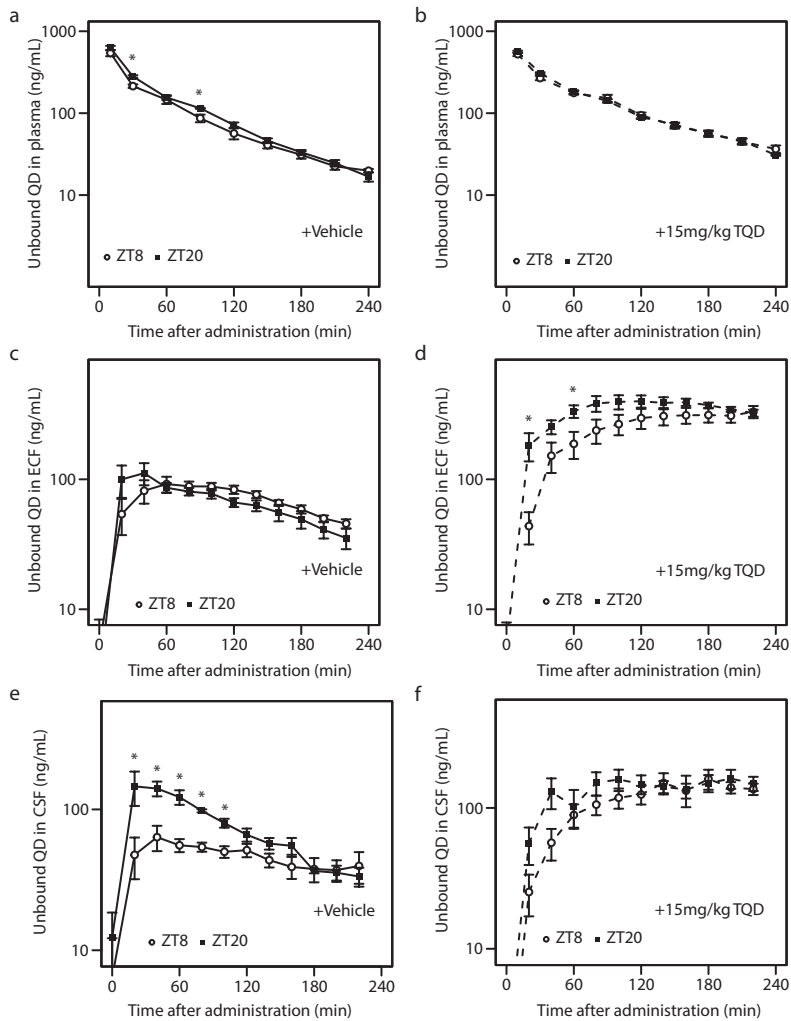
**Figure 3** Microdialysis experiments in vehicle- and TQD-treated animals. Time–concentration profiles of unbound quinidine in plasma (**A-B**, n = 7–8 animals/group), ECF (**C-D**, n = 7–8 animals/group), and CSF (**E-F**, n = 6–8 animals/group) at ZT8 (open symbols) and ZT20 (closed symbols) in vehicle-treated animals (a, c, e) and TQD-treated animals (b, d, f). Asterisks indicate significant effect of ZT on quinidine concentration at the designated sampling times (p < 0.05, two-sided t test or Mann–Whitney U test). Mean ± SEM in all graphs. *p < 0.05

We calculated the mean concentration–time profiles of unbound quinidine in plasma, ECF, and CSF (Fig. 3) as well as $C_{BR}$: $AUC_{PLu(0-240)}$ (Supplemental Figure 3B-C) at ZT8 and ZT20 in vehicle- and TQD-treated animals. The fraction unbound of quinidine in plasma (0.276 ± 0.015) was not significantly different in these experiments compared to that observed in the brain distribution experiments (t(29) = 0.747, p = 0.461, two-sided t-test, Supplemental Figure 2D). Also, $AUC_{PLu(0-240)}$ and $C_{BR}$: $AUC_{PLu(0-240)}$ measured in these experiments were comparable to those obtained in brain distribution experiments (Supplemental Figure 3). In vehicle-treated animals, ECF concentrations were not significantly affected by time of administration at any of the sampling times (Fig. 3c), while CSF concentrations were

**Table 1** Covariate analysis

| Covariate | Change in OFV[a] | P-value |
|---|---|---|
| Time of administration (P-gp) | -155.6 | <0.05 |
| Time of administration ($Q_{CSF}$) | -37.7 | <0.05 |
| Time of administration (P-gp and $Q_{CSF}$) | -190.5 | <0.05 |

a. Change in Objective Function Value (OFV) after addition of the covariate on various parameters, compared to the model that does not take into account time of administration on any of the parameters.

higher in the first 100 min after administration in the active period compared to the values obtained after administration in the resting period (Fig. 3e). In tariquidar-treated animals, time of administration significantly affected ECF concentrations at two sampling times (Fig. 3d), but had no effect on CSF concentrations (Fig. 3f).

The data from the microdialysis experiments were fitted to a PBPK model that was previously used to describe quinidine pharmacokinetics in plasma, ECF, CSF, and deep brain tissue (Westerhout et al., 2013). We investigated the effect of time of administration on the parameters describing P-gp-mediated transport from the plasma compartment to and from deep brain tissue, ECF and CSF, and on CSF flux. Using covariate analysis, we found that the model that takes into account the effect of time of administration on both P-gp-mediated transport and CSF flux best described the data (Table 1), indicating that time of administration significantly influences P-gp-mediated transport and CSF flux. The parameter estimates of the model (Table 2) show that the estimated P-gp-mediated transport of quinidine from the deep brain compartment to plasma is almost 2.9× higher during the active period of the animals compared to the resting period (659 vs 228 μL/ min, Table 2). Furthermore, CSF flux is almost twice as high during the resting period of the animals compared to the active period (0.522 vs 0.227 μL/min, Table 2).

## DISCUSSION

In this study, we show that the exposure to the P-gp substrate quinidine in total brain tissue is subject to significant diurnal variation. This variation is abolished by pre-treatment with the selective P-gp inhibitor tariquidar, indicating a selective P-gp-mediated origin. The exposure to quinidine in brain tissue is lower during the active period compared to the resting period of the animals, which shows that the activity of P-gp is elevated during the active period. PBPK modeling based on plasma, ECF, CSF, and total brain concentrations of quinidine after intravenous administration in the active and resting period of the animals supports these findings by showing that time of administration significantly affects P-gp-mediated transport as well as CSF flux. Therefore, the findings presented in this study show that the exposure to a drug in the brain is affected by time of administration and provides a mechanism that involves 24-h variation in the activity of P-gp-mediated transport and CSF flux.

Circadian rhythms are present in many bodily processes and are controlled by a central clock located in the hypothalamus (Meijer et al., 2012). Rhythms in peripheral organs are

**Table 2** Parameter estimates of the PBPK model.

| Parameter | | | Value | Unit | RSE |
|---|---|---|---|---|---|
| *Estimates* | | | | | |
| $CL_E$ | passive | | 83.3 | mL/min | 10.3% |
| | +P-gp | | 52.7 | mL/min | 6.5% |
| $Q_{PL-PER1}$ | passive | | 831 | mL/min | 9.6% |
| $Q_{PL-PER2}$ | passive | | 93.5 | mL/min | 18.3% |
| $CL_{PL-Deep\ Brain}$ | passive | | 982 | µL/min | 14.7% |
| | +P-gp | | NA[a] | µL/min | |
| $CL_{Deep\ Brain-PL}$ | passive | | 12.3 | µL/min | 19.8% |
| | +P-gp | Resting period | 228 | µL/min | 17.7% |
| | +P-gp | Active period | 659 | µL/min | 15.6% |
| $CL_{PL-ECF}$ | passive | | 25.7 | µL/min | 12.5% |
| | +P-gp | Resting period | 17 | µL/min | 18.5% |
| | +P-gp | Active period | 18.3 | µL/min | 18.5% |
| $CL_{ECF-PL}$ | passive | | 4.63 | µL/min | 15.2% |
| | +P-gp | Resting period | 3.14 | µL/min | 36.3% |
| | +P-gp | Active period | 3.98 | µL/min | 48.0% |
| $CL_{PL-LV}$ | passive | | 3.23 | µL/min | 19.9% |
| | +P-gp | Resting period | 1.55 | µL/min | 30.1% |
| | +P-gp | Active period | 2.44 | µL/min | 17.5% |
| $CL_{LV-PL}$ | passive | | 0.513 | µL/min | 24.0% |
| | +P-gp | | NA[a] | µL/min | |
| $CL_{PL-CM}$ | passive | | 0.753 | µL/min | 23.5% |
| | +P-gp | | NA[a] | µL/min | |
| $CL_{CM-PL}$ | passive | | 1.02 | µL/min | 33.7% |
| | +P-gp | | NA[a] | µL/min | |
| $Q_{ECF}$[b] | | | 0.2 | µL/min | |
| $Q_{CSF}$ | | Resting period | 0.522 | µL/min | 28.5% |
| | | Active period | 0.227 | µL/min | 36.0% |
| $V_{PL}$[b] | | | 10.6 | mL | |
| $V_{PER1}$ | | | 7.42 | L | 5.7% |
| $V_{PER2}$ | | | 7.09 | L | 17.3% |
| $V_{Deep\ Brain}$[b] | | | 1440 | µL | |
| $V_{ECF}$[b] | | | 290 | µL | |
| $V_{LV}$[b] | | | 50 | µL | |
| $V_{TFV}$[b] | | | 50 | µL | |
| $V_{CM}$[b] | | | 17 | µL | |
| $V_{SAS}$[b] | | | 180 | µL | |

Table 2 *(cont.)*

| | | | |
|---|---|---|---|
| *Interindividual variability* | | | |
| $CL_E$ | 33.2 | % | 17.2% |
| *Residual error* | | | |
| PL | 42.8 | % | 13.9% |
| ECF | 33.0 | % | 13.9% |
| LV | 31.9 | % | 18.7% |
| CM | 36.2 | % | 13.8% |
| Deep Brain | 35.6 | % | 13.4% |

Abbreviations: PER1 and PER2: peripheral compartment 1 and 2; PL: plasma; ECF: brain extracellular fluid; LV: lateral ventricle; CM: cisterna magna; $Q_{ECF}$ and $Q_{CSF}$: ECF and CSF flow; V = volume of distribution of the compartments; TFV: third and fourth ventricle; SAS: subarachnoid space; +P-gp: effect of P-gp mediated transport on the parameter; IIV: inter-individual variability.

a. Parameter not available

b. Physiological values, derived from literature (Westerhout et al, 2013).

synchronized by the central clock, but are driven locally by an intracellular translational–transcriptional feedback loop with a period of approximately 24-h (Mohawk et al., 2012). This clock mechanism is responsible for the circadian rhythm that is found in the transcription, translation, and post-translational modification of many genes and their associated proteins (Mohawk et al., 2012). Our results show that the distribution of quinidine in the brain depends on time of administration due to variation in two processes. Firstly, we find that the estimated activity of P-gp-mediated transport is higher during the active period of the animals compared to the resting period. This is in line with several in vitro and in vivo studies that have shown 24-h variation in the expression and activity of P-gp in several different cell types (Ando et al., 2005; Ballesta et al., 2011; Hayashi et al., 2010; Murakami et al., 2008; Okyar et al., 2012; Stearns et al., 2008). For example, Okyar et al. (2012) found that the activity of P-gp in the intestine is higher during the active period of rats (Okyar et al., 2012). Future studies investigating the activity of P-gp in different cell types of the CNS across the 24-h cycle may provide further information on the molecular mechanisms underlying the findings presented in this study.

In addition to 24-h variation in P-gp activity, the PBPK model (Westerhout et al., 2013) that was used to describe the effect of time of administration on the pharmacokinetics of quinidine in the brain shows that CSF flow is larger during the resting period of the animals compared to the active period. In line with these findings, a recent study showed that sleep markedly increases CSF influx, thereby facilitating the removal of metabolic waste products from the CNS (Xie et al., 2013). This process may also affect the distribution of peripherally administered drugs in the brain. With the design used in this study, we cannot exclude the possibility that the sleep/wake state of the animal, rather than diurnal rhythmicity as such, is responsible for the variation in CSF flow or P-gp function over the 24-h period.

The variation in P-gp activity over the 24-h cycle had a much larger effect on quinidine concentrations in the brain tissue than in ECF. Total brain concentrations reflect the

concentration of quinidine in both ECF and intracellular fluid (ICF) of brain parenchymal cells. The relatively small difference in the effect of P-gp on the clearance of quinidine from ECF to plasma during the active and resting periods of the animals cannot account for the large difference in the effect of P-gp on the clearance of quinidine from brain tissue to plasma. Therefore, we propose that an additional P-gp-dependent barrier between the ECF or plasma and the ICF of brain parenchymal cells gives rise to the observed variation. The existence of an additional barrier that affects the distribution of drugs in parenchymal cells has previously been suggested by the observation that valproic acid, an anticonvulsant drug, is subject to active efflux at the parenchymal cell membrane (Scism et al., 2000). Although valproic acid is not a P-gp substrate (Baltes et al., 2007), Scism et al. (Scism et al., 2000) show that the parenchymal cell membrane can play an important role in the distribution of drugs in the brain. Furthermore, Syvänen et al. (2012) show that induction of status epilepticus in rats affects P-gp activity at the level of the parenchyma rather than at the BBB.

Several lines of evidence suggest that P-gp is present in brain parenchymal cells, such as in pericytes and astrocytes (Bendayan et al., 2006; Golden and Pardridge, 1999; Shimizu et al., 2008). P-gp does not seem to be present in neurons in the healthy mammalian brain, but its expression is rapidly induced when challenged, for example, by hypoxic stress or the induction of status epilepticus (Lazarowski et al., 2007; Volk et al., 2004). Importantly, it should be kept in mind that experiments are generally conducted during the resting period of the animals, which is the time window during which P-gp activity is lowest according to our findings. The existence of a barrier from the ECF to the ICF is of special interest for drugs that have an intracellular CNS target. Future studies should aim to elucidate this process more clearly.

A question that needs to be addressed is to what extent a twofold increase in total brain exposure is clinically relevant. Several strategies have been proposed to minimize the effect of P-gp on its substrates that are used as drugs to treat various CNS disorders. For example, pharmacological inhibition of P-gp by tariquidar in humans leads to a dose-dependent increase in brain uptake of a P-gp substrate (Kreisl et al., 2010; Wagner et al., 2009). At a dose of 6 mg/kg, there is a fourfold increase in brain uptake of radiolabeled loperamide (Kreisl et al., 2010). However, this dose requires intravenous infusion for more than 1 h due to a hemolytic effect of one the co-solvents (Bauer et al., 2013; Kreisl et al., 2010). Another limitation associated with P-gp inhibitors in humans is that the unbound plasma concentrations are relatively low, which limits the degree of P-gp inhibition (Kalvass et al., 2013). In light of these findings, the more than twofold increase in brain exposure that was observed in this study, by investigating a naturally occurring physiological process, could therefore well be of clinical relevance. This holds especially true for drugs with a narrow therapeutic index in which a slight increase in brain concentration leads to a large increase in effect size.

In summary, this study indicates that the exposure to a P-gp substrate in the brain is subject to diurnal variation. Using a selective and potent P-gp inhibitor, we are able to show that this is due to variation of P-gp-mediated transport which is markedly elevated during

the active period of the animals compared to the resting period. Furthermore, CSF flux is increased during the resting period, which may also cause variations in the exposure to a drug in the brain. Importantly, these findings emphasize the need to take into account the timing of drug administration, both in clinical and experimental situations. Dosing at the appropriate time of the day may be an effective strategy to modulate the delivery of P-gp substrates to the brain.

## CONFLICT OF INTEREST

The authors declare no conflict of interest.

## ACKNOWLEDGEMENTS

# REFERENCES

Abbott, N.J., Patabendige, A.A.K., Dolman, D.E.M., Yusof, S.R., and Begley, D.J. (2010). Structure and function of the blood-brain barrier. Neurobiol. Dis. 37, 13–25.

Ando, H., Yanagihara, H., Sugimoto, K., Hayashi, Y., Tsuruoka, S., Takamura, T., Kaneko, S., and Fujimura, A. (2005). Daily rhythms of P-glycoprotein expression in mice. Chronobiol. Int. 22, 655–665.

Ballesta, A., Dulong, S., Abbara, C., Cohen, B., Okyar, A., Clairambault, J., and Levi, F. (2011). A combined experimental and mathematical approach for molecular-based optimization of irinotecan circadian delivery. PLoS Comput. Biol. 7, e1002143.

Baltes, S., Fedrowitz, M., Tortós, C.L., Potschka, H., and Löscher, W. (2007). Valproic acid is not a substrate for P-glycoprotein or multidrug resistance proteins 1 and 2 in a number of in vitro and in vivo transport assays. J. Pharmacol. Exp. Ther. 320, 331–343.

Bauer, M., Zeitlinger, M., Todorut, D., Böhmdorfer, M., Müller, M., Langer, O., and Jäger, W. (2013). Pharmacokinetics of single ascending doses of the P-glycoprotein inhibitor tariquidar in healthy subjects. Pharmacology 91, 12–19.

Bendayan, R., Ronaldson, P.T., Gingras, D., and Bendayan, M. (2006). In situ localization of P-glycoprotein (ABCB1) in human and rat brain. J. Histochem. Cytochem. 54, 1159–1167.

Buttgereit, F., Doering, G., Schaeffler, A., Witte, S., Sierakowski, S., Gromnica-Ihle, E., Jeka, S., Krueger, K., Szechinski, J., and Alten, R. (2010). Targeting pathophysiological rhythms: prednisone chronotherapy shows sustained efficacy in rheumatoid arthritis. Ann. Rheum. Dis. 69, 1275–1280.

Dallmann, R., Brown, S.A., and Gachon, F. (2014). Chronopharmacology: new insights and therapeutic implications. Annu. Rev. Pharmacol. Toxicol. 54, 339–361.

Golden, P.L., and Pardridge, W.M. (1999). P-glycoprotein on astrocyte foot processes of unfixed isolated human brain capillaries. Brain Res. 819, 143–146.

Hayashi, Y., Ushijima, K., Ando, H., Yanagihara, H., Ishikawa, E., Tsuruoka, S.-I., Sugimoto, K.-I., and Fujimura, A. (2010). Influence of a time-restricted feeding schedule on the daily rhythm of abcb1a gene expression and its function in rat intestine. J. Pharmacol. Exp. Ther. 335, 418–423.

Hermida, R.C., Ayala, D.E., Fernández, J.R., and Calvo, C. (2008). Chronotherapy improves blood pressure control and reverts the nondipper pattern in patients with resistant hypertension. Hypertension 51, 69–76.

Kalvass, J.C., Polli, J.W., Bourdet, D.L., Feng, B., Huang, S.-M., Liu, X., Smith, Q.R., Zhang, L.K., and Zamek-Gliszczynski, M.J. (2013). Why clinical modulation of efflux transport at the human blood-brain barrier is unlikely: the ITC evidence-based position. Clin. Pharmacol. Ther. 94, 80–94.

Kreisl, W.C., Liow, J.-S., Kimura, N., Seneca, N., Zoghbi, S.S., Morse, C.L., Herscovitch, P., Pike, V.W., and Innis, R.B. (2010). P-glycoprotein function at the blood-brain barrier in humans can be quantified with the substrate radiotracer 11C-N-desmethyl-loperamide. J. Nucl. Med. 51, 559–566.

De Lange, E.C.M. (2013). The mastermind approach to CNS drug therapy: translational prediction of human brain distribution, target site kinetics, and therapeutic effects. Fluids Barriers CNS 10, 12.

Lazarowski, A., Caltana, L., Merelli, A., Rubio, M.D., Ramos, A.J., and Brusco, A. (2007). Neuronal mdr-1 gene expression after experimental focal hypoxia: a new obstacle for neuroprotection? J. Neurol. Sci. 258, 84–92.

Meijer, J.H., Colwell, C.S., Rohling, J.H.T., Houben, T., and Michel, S. (2012). Dynamic neuronal network organization of the circadian clock and possible deterioration in disease. Prog. Brain Res. 199, 143–162.

Moghaddam, B., and Bunney, B.S. (1989). Ionic Composition of Microdialysis Perfusing Solution Alters the Pharmacological Responsiveness and Basal Outflow of Striatal Dopamine. J. Neurochem. 53, 652–654.

Mohawk, J.A., Green, C.B., and Takahashi, J.S. (2012). Central and peripheral circadian clocks in mammals. Annu. Rev. Neurosci. 35, 445–462.

Murakami, Y., Higashi, Y., Matsunaga, N., Koyanagi, S., and Ohdo, S. (2008). Circadian clock-controlled intestinal expression of the multidrug-resistance gene mdr1a in mice. Gastroenterology 135, 1636–1644.e3.

Ohtsuki, S., and Terasaki, T. (2007). Contribution of carrier-mediated transport systems to the blood-

brain barrier as a supporting and protecting interface for the brain; importance for CNS drug discovery and development. Pharm. Res. 24, 1745–1758.

Okyar, A., Dressler, C., Hanafy, A., Baktir, G., Lemmer, B., and Spahn-Langguth, H. (2012). Circadian variations in exsorptive transport: in situ intestinal perfusion data and in vivo relevance. Chronobiol. Int. 29, 443–453.

Potschka, H. (2010). Targeting regulation of ABC efflux transporters in brain diseases: a novel therapeutic approach. Pharmacol. Ther. 125, 118–127.

Schinkel, A.H., Smit, J.J., van Tellingen, O., Beijnen, J.H., Wagenaar, E., van Deemter, L., Mol, C.A., van der Valk, M.A., Robanus-Maandag, E.C., and te Riele, H.P. (1994). Disruption of the mouse mdr1a P-glycoprotein gene leads to a deficiency in the blood-brain barrier and to increased sensitivity to drugs. Cell 77, 491–502.

Scism, J.L., Powers, K.M., Artru, A.A., Lewis, L., and Shen, D.D. (2000). Probenecid-inhibitable efflux transport of valproic acid in the brain parenchymal cells of rabbits: a microdialysis study. Brain Res. 884, 77–86.

Shimizu, F., Sano, Y., Maeda, T., Abe, M.-A., Nakayama, H., Takahashi, R.-I., Ueda, M., Ohtsuki, S., Terasaki, T., Obinata, M., et al. (2008). Peripheral nerve pericytes originating from the blood-nerve barrier expresses tight junctional molecules and transporters as barrier-forming cells. J. Cell. Physiol. 217, 388–399.

Stearns, A.T., Balakrishnan, A., Rhoads, D.B., Ashley, S.W., and Tavakkolizadeh, A. (2008). Diurnal rhythmicity in the transcription of jejunal drug transporters. J. Pharmacol. Sci. 108, 144–148.

Syvänen, S., Schenke, M., van den Berg, D.-J., Voskuyl, R.A., and de Lange, E.C. (2012). Alteration in P-glycoprotein functionality affects intrabrain distribution of quinidine more than brain entry-a study in rats subjected to status epilepticus by kainate. AAPS J. 14, 87–96.

Volk, H.., Burkhardt, K., Potschka, H., Chen, J., Becker, A., and Löscher, W. (2004). Neuronal expression of the drug efflux transporter P-glycoprotein in the rat hippocampus after limbic seizures. Neuroscience 123, 751–759.

Wagner, C.C., Bauer, M., Karch, R., Feurstein, T., Kopp, S., Chiba, P., Kletter, K., Löscher, W., Müller, M., Zeitlinger, M., et al. (2009). A pilot study to assess the efficacy of tariquidar to inhibit P-glycoprotein at the human blood-brain barrier with (R)-11C-verapamil and PET. J. Nucl. Med. 50, 1954–1961.

Watanabe, J., Suzuki, Y., Fukui, N., Ono, S., Sugai, T., Tsuneyama, N., and Someya, T. (2012). Increased risk of antipsychotic-related QT prolongation during nighttime: a 24-hour holter electrocardiogram recording study. J. Clin. Psychopharmacol. 32, 18–22.

Westerhout, J., Smeets, J., Danhof, M., and de Lange, E.C.M. (2013). The impact of P-gp functionality on non-steady state relationships between CSF and brain extracellular fluid. J. Pharmacokinet. Pharmacodyn. 40, 327–342.

Xie, L., Kang, H., Xu, Q., Chen, M.J., Liao, Y., Thiyagarajan, M., O'Donnell, J., Christensen, D.J., Nicholson, C., Iliff, J.J., et al. (2013). Sleep drives metabolite clearance from the adult brain. Science 342, 373–377.
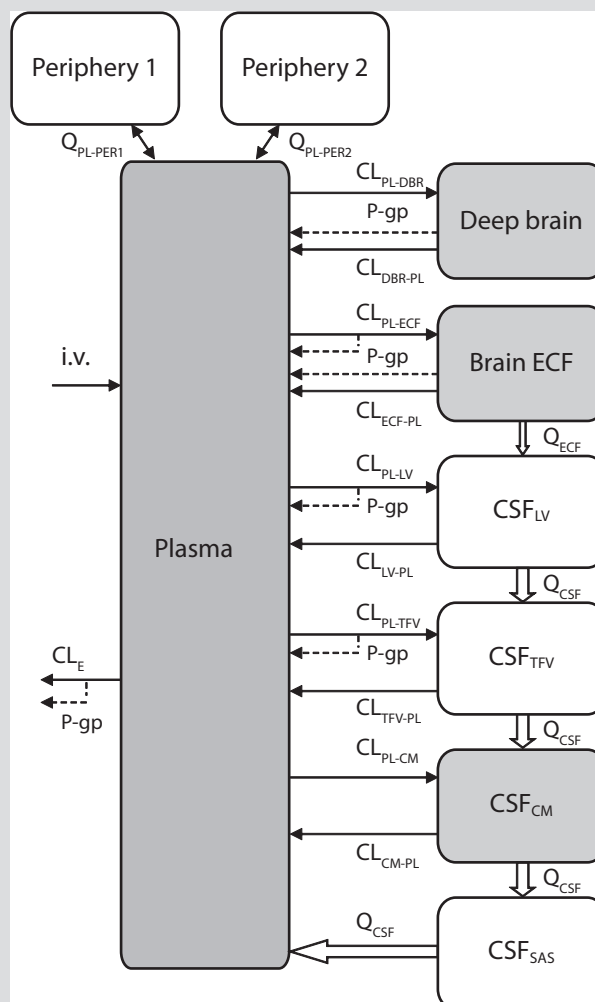
**Supplementary Figure 1** Diagram of the PBPK model used to describe quinidine brain distribution. I.v. denotes the intravenous dose that enters the plasma compartment. CLE is the elimination clearance from plasma. $Q_{PL-PER1}$ and $Q_{PL-PER2}$ are the clearances from the plasma compartment to the two peripheral compartments. Drug distribution from plasma to the brain is described by bi-directional clearance between the plasma compartment and the deep brain compartment ($CL_{PL-DBR}$ and $CL_{DBR-PL}$), brain ECF compartment ($CL_{PL-ECF}$ and $CL_{ECF-PL}$), and different CSF compartments (lateral ventricle: $CL_{PL-LV}$ and $CL_{LV-PL}$; third and fourth ventricle: $CL_{PL-TFV}$ and $CL_{TFV-PL}$ and cisterna magna: $CL_{PL-CM}$ and $CL_{CM-PL}$). QECF denotes the flow rate of brain ECF to CSF and $Q_{CSF}$ is the flow rate of CSF between the different CSF compartments ($CSF_{SAS}$ refers to CSF in the subarachnoid space). Dashed arrows with the subscript P-gp represent P-glycoprotein mediated transport, which can either hinder drug influx or enhance drug efflux. The effect of P-gp on $CL_{PL-CM}$, $CL_{CM-PL}$, $CL_{TFV-PL}$, $CL_{LV-PL}$ and $CL_{PL-DBR}$ was not estimated, so these arrows were not included in the diagram. The grey physiological compartments indicate the data specifically obtained in the current study. All analyses were performed by using the subroutine ADVAN 6 and first-order conditional estimation with interaction.
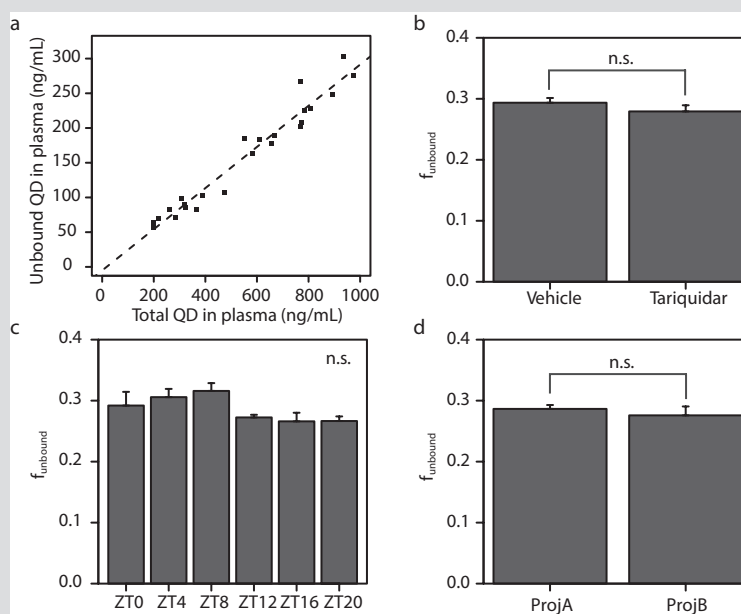
**Supplementary Figure 2.** Plasma protein binding. **(A)** Correlation between total and unbound quinidine concentrations in plasma from the brain distribution experiments. There is a strong linear correlation between total and unbound concentrations ($r^2$=0.953, N=24 samples, p=0.000). **(B-C)** Effect of tariquidar treatment (B, n=12 samples per group) and experimental time point (C, n=4 samples per group) on the unbound fraction of quinidine in plasma. A two-way ANOVA showed no significant effect of TQD treatment (TQD vs. vehicle: $F_{(1,17)}$=1.70, p=0.21) and of time of administration ($F_{(5,17)}$=2.52, p=0.07). **(D)** Effect of experimental set-up on the unbound fraction of quinidine in plasma. There is no significant difference in the unbound fraction between brain distribution (projA, n=24 samples) and microdialysis experiments (projB, n=7 samples) ($t_{(29)}$=0.747, p=0.46, t-test). Mean±SEM in all graphs. N.s.: not significant.
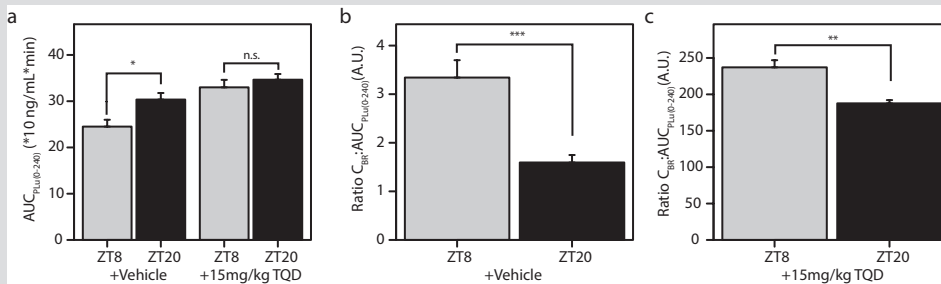
**Supplementary Figure 3** Quinidine exposure in plasma and brain in the microdialysis group. **(A)** Area under the curve for unbound quinidine in plasma from 0 to 240 minutes after administration ($AUC_{PLu,0-240}$) at different experimental time points in vehicle and TQD treated animals (n=7-8 animals/group). Time of administration had a significant on $AUC_{PLu,0-240}$ in vehicle treated animals (t(12)=-2.84, p=0.014, t-test), but not in TQD treated animals (t(13)=-0.79, p=0.44, t-test). **(B-C)** Quinidine concentration at t=240min in brain tissue relative to plasma AUC ($C_{BR}$:$AUC_{PLu,0-240}$) at different experimental time points in vehicle (B) and TQD (C) treated animals (n=6-7 animals per group). Time of administration significantly affects this ratio in vehicle treated animals (t(11)=4.74, p=0.0006, t-test) and to a lesser extent in TQD treated animals (W=41, p=0.002). Mean±SEM in all graphs. N.s.: not significant; *p<0.05; **p<0.01; ***p<001.

**Supplementary Table 1** Number of animals per treatment group

| Experiment | ZT0 | ZT4 | ZT8 | ZT12 | ZT16 | ZT20 |
|---|---|---|---|---|---|---|
| Brain distribution | | | | | | |
| Vehicle + 10mg/kg quinidine | 7 | 8 | 5 | 8 | 8 | 5 |
| 15mg/kg tariquidar + 10mg/kg quinidine | 7 | 7 | 6 | 7 | 6 | 5 |
| Microdialysis | | | | | | |
| Vehicle + 10mg/kg quinidine | ND | ND | 8 | ND | ND | 6 |
| 15mg/kg tariquidar + 10mg/kg quinidine | ND | ND | 8 | ND | ND | 7 |
| In vivo retrodialysis | | | | | | |
| Vehicle + 10mg/kg quinidine | ND | ND | 1 | ND | ND | 2 |
| 15mg/kg tariquidar + 10mg.kg quinidine | ND | ND | 1 | ND | ND | 1 |
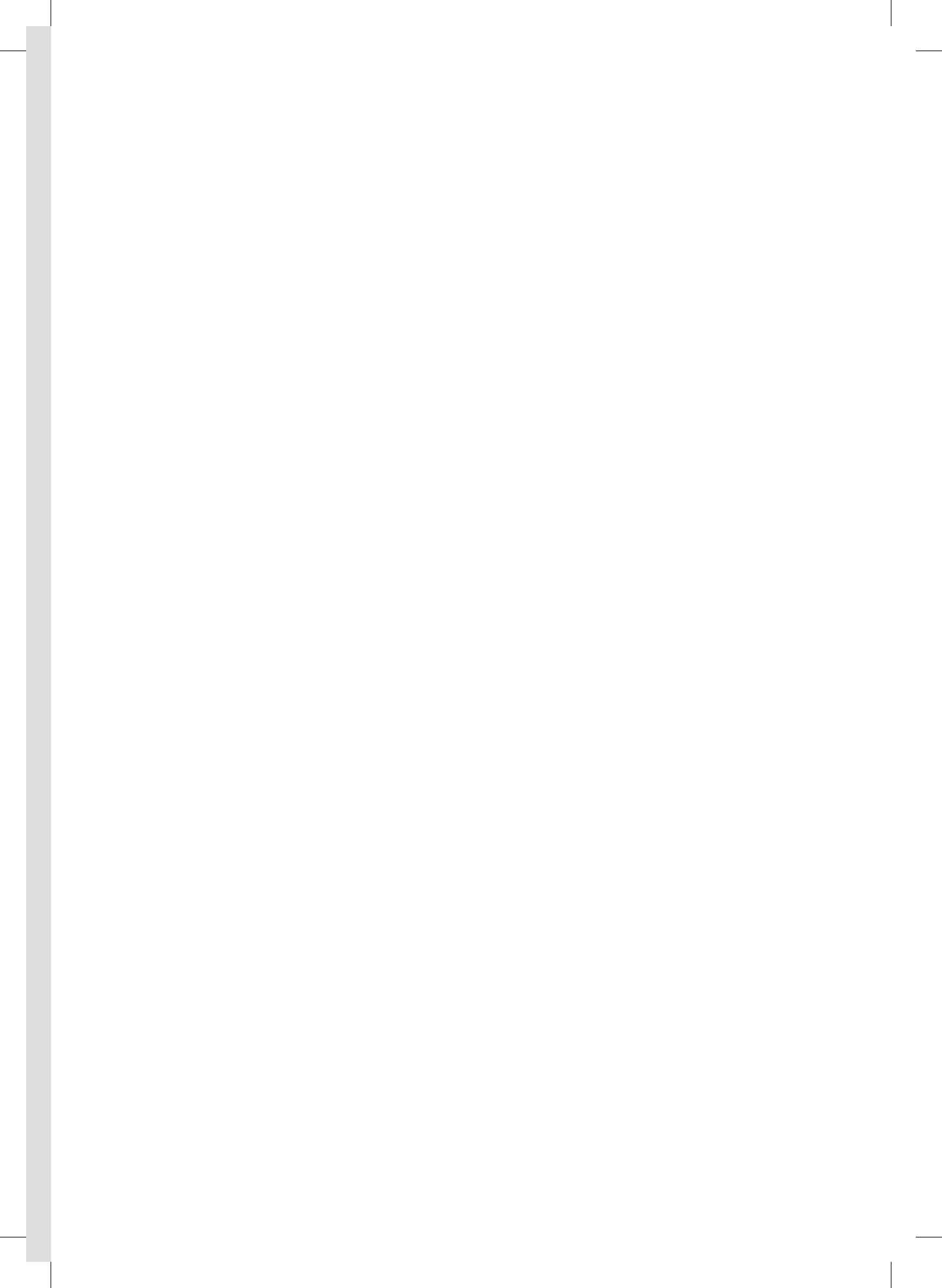
# CHAPTER

## Diurnal variation in the pharmacokinetics and brain distribution of morphine

# 7

Laura Kervezee[1,2]; Robin Hartman[2]; Dirk-Jan van den Berg[2]; Johanna H. Meijer[1,*]; Elizabeth C.M. de Lange[2,*]

[1]Laboratory for Neurophysiology, Department of Molecular Cell Biology, Leiden University Medical Center, Leiden, the Netherlands;
[2]Division of Pharmacology, Leiden Academic Center for Drug Research, Leiden University, Leiden, the Netherlands
*These authors share senior authorship

# ABSTRACT

The pharmacokinetics and pharmacodynamics of drugs are influenced by daily fluctuations in physiological processes. The aim of this study was to determine the effect of dosing time on the pharmacokinetics and brain distribution of morphine. To this end, 4 mg/kg morphine was administered intravenously to male Wistar rats that were either pre-treated with a vehicle solution or tariquidar and probenecid to inhibit processes involved in the active transport of morphine. Non-linear mixed effects modelling was used to describe the concentration-time profiles of morphine and its metabolite M3G in plasma and brain tissue. We find that the efflux of morphine from brain tissue back into the circulation is characterized by a 24-hour rhythm with the lowest efflux during the two light-dark phase transitions with a difference between peak and trough of 20%. The active processes involved in the clearance of morphine and its metabolite M3G from plasma also show 24-hour variation with the highest value in the middle of the dark phase being 54% higher than the lowest value at the start of the light phase. As a result of these fluctuations in pharmacokinetic parameters, the concentrations of morphine in the brain and of M3G in plasma depend on the time of day. Hence, time of day presents a considerable source of variation in the pharmacokinetics of morphine, which could be used to optimize the dosing strategy of morphine.

## INTRODUCTION

Morphine is the most widely used opioid for the treatment of moderate to severe pain, despite the many side-effects associated with its use. Therefore, establishing a dosing regimen that results in adequate analgesia and minimal adverse side-effects is crucial, but remains a challenge due to the high degree of intra- and interindividual variability associated with the pharmacokinetics and pharmacodynamics of this drug (Sverrisdóttir et al., 2015). Time of day presents a considerable source of variation in the pharmacokinetics and pharmacodynamics of a wide variety of drugs due to daily rhythms in physiological processes (Dallmann et al., 2014).

There are several indications that time of day influences morphine's effect. For example, it has been shown that the requirement of self-administered morphine fluctuates over the 24-hour period in patients with post-operative pain (Junker and Wirz, 2010; Potts et al., 2011). Additionally, in mice, the analgesic effect of morphine depends on the time of administration: while most studies found that the analgesic effect of morphine is highest during the dark period (Bornschein et al., 1977; Cui et al., 2005; Lutsch and Morris, 1971; Morris and Lutsch, 1967; Yoshida et al., 2003, 2005), some reports found that the analgesic effect of morphine either follows the 24-hour pattern in baseline pain sensitivity (Kavaliers and Hirst, 1983; Oliverio et al., 1982) or is highest during the light period (Güney et al., 1998; Rasmussen and Farr, 2003). However, the physiological mechanisms that underlie these variations in morphine-induced analgesia are unknown.

To gain a more structured overview of the effect of dosing time on the therapeutic effect of morphine, it is essential to first determine 24-hour variation in the pharmacokinetics and in the brain distribution of morphine. Although the effect of dosing time on the exposure to morphine has previously received some attention (Dohoo, 1997; Gourlay et al., 1995), these studies neither determined the 24-hour variation in the different pharmacokinetic parameters of morphine, nor did they address the 24-hour variation in its distribution to the brain, morphine's main site of action.

The concentration of morphine in blood and subsequently in the central nervous system depends on several processes. For example, morphine is primarily metabolized by UDP glucuronosyl transferase (UGT) 2B7 in the liver (De Gregori et al., 2011; Somogyi et al., 2007), the expression of which is regulated by the molecular clock and shows 24-hour variation (Dallmann et al., 2014; Zhang et al., 2009). Additionally, morphine brain distribution is affected by efflux transport proteins such as P-glycoprotein and probenecid-sensitive transporters such as multidrug-resistance proteins (mrps) (Sverrisdóttir et al., 2015; Thompson et al., 2000; Tunblad et al., 2003; Xie et al., 1999). P-glycoprotein mediated transport in the brain depends on the time of drug administration (Kervezee et al., 2014).

To determine 24-hour variation in the pharmacokinetic parameters of morphine, we used a study design in which morphine is intravenously administered to rats at six time-points during the 24-hour period combined with a pharmacokinetic modelling approach. Results from this study enhance our understanding of the processes that underlie the

observed time-of-day dependent analgesic effect of morphine.

## METHODS & MATERIALS

### Animals

Male Wister WU rats (Charles River, the Netherlands) were housed in groups for at least twelve days under standard environmental conditions (humidity 60%, ambient temperature 21oC) with food (Laboratory chow, Hope Farms, Woerden, The Netherlands) and water ad libitum. After surgery, animals were kept individually until the end of the experiment under otherwise similar conditions. Half of the animals were kept in a light-dark cycle with lights on at 8:00 and lights off at 20:00; the other half was kept under a reversed schedule (8:00 lights off, 20:00 lights on). The weight of the animals was monitored daily. The animal procedures were performed in accordance with the Dutch law on animal experimentation and were approved by the Animal Ethics Committee of the Leiden University (protocol number DEC14041).

### Study design

Cannulation of the femoral artery and vein was performed as described previously (Westerhout et al., 2012). Anesthesia was induced and maintained by respectively 5% and 1-2% isoflurane throughout the surgical procedures. Experiments were conducted seven days after surgery and started at one of six different time points (t =0 at either Zeitgeber time (ZT) 0, 4, 8, 12, 16 or 20, with ZT12 defined as the moment that lights are turned off). Experiments that took place during the dark phase were conducted under dim red light. At t= -25 min, tariquidar (15mg/kg; XR9576 from Avant pharmaceuticals, London, UK, in 5% glucose) or vehicle (5% glucose) was administered for 10 minutes, followed by administration of probenecid (150mg/kg; Sigma-Aldrich, Zwijndrecht, the Netherlands, in 5% NaHCO$_3$) or vehicle (5% NaHCO$_3$) for 10 minutes. Half of the animals received a combination of tariquidar and probenecid (inhibitor-treated group), the other half received the two vehicle solutions (vehicle-treated group). At t=0, morphine HCl (4mg/kg; Pharmachemie BV, Haarlem, the Netherlands in saline) was administered for 10 minutes. All drugs were administered intravenously using a syringe pump (Pump 22 Multiple Syringe Pump, Harvard Apparatus, Holliston, MA, USA). Blood samples (150 µL) were drawn at t=-5, 10, 20, 30, 45, 60, 90 and 120 min as well as at t = 180 and/or 240 min, depending on when the experiment was terminated. Blood was collected in heparinized Eppendorf cups and centrifuged for 10 min at 5000 rpm (Eppendorf Microcentrifuge Model 5415D) at 4°C to separate plasma from other blood constituents. Plasma samples were stored on ice until the end of the experiment and subsequently at -20°C until further analysis.

At either t=120, 180 or 240 min, animals were euthanized by an overdose of Nembutal, transcardially perfused and decapitated. Brain tissue was removed, immediately placed on ice and subsequently stored at -80°C until further analysis.

**SPE-LC-MS/MS analysis**

Morphine and morphine-3-glucoronide (M3G) were measured in plasma and brain tissue using liquid chromatography tandem mass spectrometry (LC-MS/MS). The SPE-LC-MS system consisted of a Finnigan Surveyor MS pump, a Finnigan TSQ Quantum Ultra triple quadrupole system (Thermo Fisher Scientific, Breda, The Netherlands), a SPE cartridge holder and a HySphere Resin GP Cartridge (Spark-Holland, Emmen, The Netherlands) and a Shimadzu Nexera UHPLC system. A Vision HT column 150×2.1mm, 5μm, Basic (Grace Altech, Breda, The Netherlands) with a column filter of 2μm (Phenomenex, Utrecht, The Netherlands) was used for all chromatographic separations. The sheath gas flow was set to 40 and the auxiliary gas flow was set to 55 (Arbitrary units). The capillary temperature was 275 0C and the spray voltage was 3500V.

For the analysis of plasma samples, 20μL of internal standard (1000ng/mL mix of deuterated morphine and M3G), 20μL milli-Q H2O were added to an aliquot of 20μL sample. Protein precipitation was done by adding 1mL of acetonitrile (Biosolve BV, Valkenswaard, the Netherlands) and centrifuging for 10 minutes at 20,000xg (Eppendorf Microcentrifuge Model 5415D, Eppendorf AG, Hamburg, Germany). The supernatant was evaporated by a CentriVap Vacuum Concentration System (Labconco, Kansas City, MO, USA).

Brain tissue samples were homogenized using a Bullet Blender 5 (Next Advance Inc, Averill Park, NY, USA) as described previously [23]. An aliquot of 600μL brain homogenate, 100μL internal standard (500ng/mL morphine-D3 and M3G-D3) and 100μL MQ H2O were mixed before addition of 5mL acetonitrile. After centrifugation at 3800xg, samples were evaporated by a vortex evaporator (Labconco, Kansas City, MO, USA).

Pellets from either plasma and brain tissue samples were subsequently dissolved by sonification after adding 40μL (to plasma samples) or 100μL (to brain samples) 10mM ammonium acetate pH10. After centrifugation for 10min at 20,000xg, samples were transferred to a glass HPLC vial. The calibration curve ranged from 5 to10000 ng/mL for plasma measurements, and from 5 to 2000 ng/mL for brain tissue measurements. 10μL was injected onto the LCMS system.

After injection of the sample, the SPE column was flushed with 1mL 10 mM ammonium acetate pH 10 (mobile phase A) for 1 minute to remove the salts and other interferences. After the loading step, the SPE was switched in line with the LC column and the compounds were eluted onto the LC column. Flushing of the SPE column was performed under acidic conditions by 3 mL of 90 % acetonitrile with 0.1 % formic acid at a flow rate of 1mL/min. The SPE column was re-equilibrated before the next injection with mobile phase A at a flow of 0.5mL/min for 4 min. Each SPE column was used for a maximum of 100 injections. The compounds were separated by the LC system with an increasing percentage of acetonitrile (from 3 to 97% in 4 min) with 0.1% formic acid at a flow of 200μL/min. The calibration curves of morphine and M3G were constructed by linear regression (weighing factor 1/Y) using LCQuan software.

The inter-assay accuracy for morphine and M3G in plasma and brain tissue was between 91 and 111%, and the intra-assay variability was below 15%. The lower limit of quantification

was 5ng/mL for both morphine and M3G in plasma and brain tissue. Concentrations of M3G in brain tissue were consistently below LLOQ and were therefore not included in further data processing.

**Data processing**

Samples below LLOQ (<1%) were marked in the data set but were retained, as described previously (Keizer et al., 2015). Concentrations (ng/mL) were converted to nanamol/mL using the molecular weight of morphine.HCl (321.8g/mol) and M3G (free base) (461.47g/mol). Based on protein binding values of morphine in rats that have been reported previously (Bickel et al., 1996; Boström et al., 2008; Letrent et al., 1999; Stain-Texier et al., 1999; Tunblad et al., 2004), an unbound fraction of 70% was used. The degree of plasma protein binding of M3G is very low (unbound fraction of 93% (Bickel et al., 1996)) and was not taken into account in further analysis.

**Population pharmacokinetic model development**

A population pharmacokinetic model was developed to describe the concentration-time profiles of morphine and M3G in plasma and in morphine brain tissue using nonlinear mixed effects modelling (NONMEM 7.3; Beal et al., 2009), in combination with Pirana (v2.8.2), PsN (v3.7.6), Xpose (v4) and R (v3.1.2) to facilitate evaluation and graphical representation of the models (Keizer et al., 2013).

To compare the fit of nested models, the likelihood ratio test was used, under the assumption that the difference in -2 log-likelihood is $\chi^2$ distributed with degrees of freedom (d.f.) determined by the number of additional parameters in the more complex model. Hence, a decrease in Objective Function Value (OFV) of at least 3.84 points (p-value <0.05) with one additional parameter was considered to provide a significantly better fit of the data compared to its parent model. The fit of non-nested models were compared using the Akaike Information Criterion (AIC) (Mould and Upton, 2013).The first-order method with conditional estimation and interaction (FOCEI) and the ADVAN6 subroutine with user-specified differential equations were used throughout model development. Model selection was based on OFV, precision and plausibility of parameter estimates, graphical evaluation of the goodness of fit and visual predictive checks (VPC).

Interanimal variability was described using Equation 1:

$$P_i = P * e^{\eta i} \hspace{4cm} \text{Equation 1}$$

Where $P_i$ is the individual parameter estimate of the $i^{th}$ animal, P is the typical parameter estimate in the population and $\eta_i$ is the interanimal variability for the $i^{th}$ animal. Additive, proportional and combined error models were considered to describe the residual variability (Mould and Upton, 2013).

Pre-treatment with probenecid and tariquidar was assumed to inhibit all active transport processes. Therefore, this effect was assessed on clearance parameters as follows:

$$P = \theta_{passive} + \theta_{active} * (1 - TRT) \hspace{3cm} \text{Equation 2}$$

where $\theta_{passive}$ is the passive component of the clearance parameter, $\theta_{active}$ is the active component of the clearance parameter and TRT is the treatment group (0 for vehicle-treated animals; 1 for inhibitor-treated animals). The effect of the inhibitors on other (non-clearance) parameters was assessed as follows:

$$P = \theta * \theta_{INH}^{TRT} \hspace{6cm} \text{Equation 3}$$

where $\theta_{INH}$ is the fractional change in parameter $\theta$ in the presence of inhibitor treatment.

A sequential approach was used to develop the population PK model. In the first step, a PK model was developed for morphine and M3G concentrations in plasma. Different structural models were considered (different number of peripheral compartments, linear or Michaelis-Menten clearance). Interanimal variability was assessed on the parameters and the effect of active transport inhibition treatment were considered using a forward inclusion approach. The volume of the M3G compartment was set equal to the volume of the central morphine compartment to yield a structurally identifiable model.

In the second step, the morphine concentrations in brain tissue were added to the data set and the PK model was extended to describe the concentration profile in brain tissue. Because one brain tissue concentration was available per animal, interanimal variability was not investigated on these parameters.

Lastly, the effect of time of day on the pharmacokinetic parameters was assessed. As an exploratory approach, the distribution of conditional weighted residuals with interaction (CWRESI) over time was investigated per treatment-group. Subsequently, it was investigated whether the model fit could be improved by describing one or more parameters by a sinusoidal function with a principal period of 24-hour and one or more harmonic terms (Equation 4).

$$P = \theta_{Mesor} + \Sigma_{(n=1)}^{N} [\theta_{Amplitude,n} * \cos(2\pi * n * (t - \theta_{\varphi,n}) / 24] \hspace{2cm} \text{Equation 4}$$

In this equation, $\theta_{Mesor}$ represents the rhythm-adjusted mean value of the parameter, N is the total number of harmonics included in the model, $\theta_{Amplitude,n}$ is the amplitude of the $n^{th}$ harmonic, $\theta_{\varphi,n}$ is the acrophase (time of peak in minutes after onset of light period) of the $n^{th}$ harmonic and t is the time with t=0 defined as the onset of the light period. The number of harmonic terms included in the model was determined by the criteria for statistical significance described above.

**Simulations**

Simulations to assess the effect of 24-hour variation in the pharmacokinetic parameters on the concentration-time profiles of morphine and M3G in plasma and brain were performed using the package deSolve (v1.11) in R. Two dosing regimens were simulated: 1) a single 10min. intravenous infusion of 4 mg/kg morphine to a rat of 250g with dosing at 0, 4, 8, 12, 16 and 20 hours after onset of the light period and 2) a continuous infusion of 0.5mg/kg/h to a rat of 250g for 24 hours starting at 4 and 16 hours after the onset of the light period.

# RESULTS

## Morphine and M3G pharmacokinetics in plasma

Data from three animals were missing due to complications during surgery and data from four animals were missing due to difficulties with the cannulas during the experiment, so data from 89 animals (mean weight ± standard deviation: 269 ± 29g) were available for pharmacometric analysis. Table 1 shows the number of animals per treatment group. Morphine and M3G concentrations in plasma in vehicle-treated animals and in inhibitor-treated animals at each of the six dosing times is shown in upper and middle panels of Figure 1.

**Table 1** Number of animals per treatment group

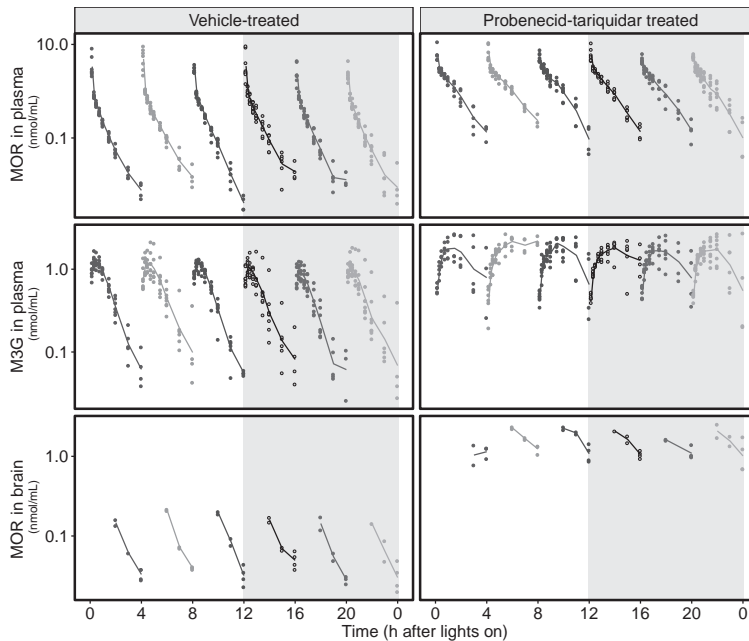| Dosing time | No. of vehicle-treated animals | No. of inhibitor-treated animals |
|---|---|---|
| 0 | 7 | 5 |
| 4 | 8 | 7 |
| 8 | 8 | 8 |
| 12 | 8 | 7 |
| 16 | 8 | 7 |
| 20 | 8 | 8 |
| **TOTAL** | 47 | 42 |



**Figure 1** Concentration profiles of morphine (MOR) in plasma (upper panels), M3G in plasma (middle panels) and MOR in brain tissue (lower panels) in vehicle-treated (left) and inhibitor-treated animals (right) after different dosing times.
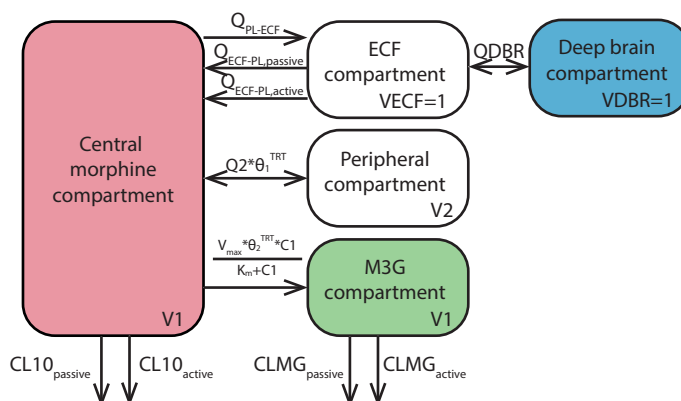
**Figure 2** Structure of the final combined plasma-brain model. Colored compartments indicated the site of sampling (red: morphine concentrations in plasma; green: M3G concentrations in plasma; blue: morphine concentrations in brain tissue).

The concentration-time profiles of morphine were initially described by a model consisting of a central compartment, one peripheral compartment and linear clearance from the body. It was attempted to include a second peripheral morphine compartment, but the parameter estimates were very sensitive to the initial values that were provided, so this was not included in the model. To account for the difference in morphine pharmacokinetics between vehicle-treated animals and inhibitor-treated animals, the clearance of morphine from the body ($CL_{10}$) was split into an active and a passive component as described in Equation 2, resulting in a significant improvement of the model fit ($\Delta$OFV -208, p<0.01, 1 d.f.) and reducing the interanimal variability on $CL_{10}$ from 123% to 23%.

The conversion of morphine to M3G was at first described as a linear process, but it was found that it showed concentration-dependent saturation that could be described by Michaelis-Menten kinetics ($\Delta$OFV -402, p<0.01, 1 d.f.). Subsequent incorporation of interanimal variability and the effect of inhibitor treatment resulted in a model with interanimal variability included on $CL_{10}$, the clearance of M3G from plasma ($CL_{M3G}$), intercompartmental clearance ($Q_2$) and the maximum conversion rate of morphine to M3G ($V_{max}$).

**Morphine pharmacokinetics in brain tissue**

Morphine concentrations in brain tissue in vehicle-treated animals and inhibitor-treated animals at each of the six dosing times are shown in the lower panels of Figure 1. The plasma model was extended to describe these concentration-time profiles. The base model, consisting of one brain compartment and inter-compartmental clearance ($Q_{BR}$) to describe the transport to and from plasma, described the brain concentrations poorly and showed high residual unexplained variability (128%). In subsequent modelling steps, it was found that a model that described the brain concentrations as deep brain concentrations that was indirectly linked to the central plasma compartment by a transit compartment referred to as the extra-cellular fluid (ECF) compartment, known as an important compartment
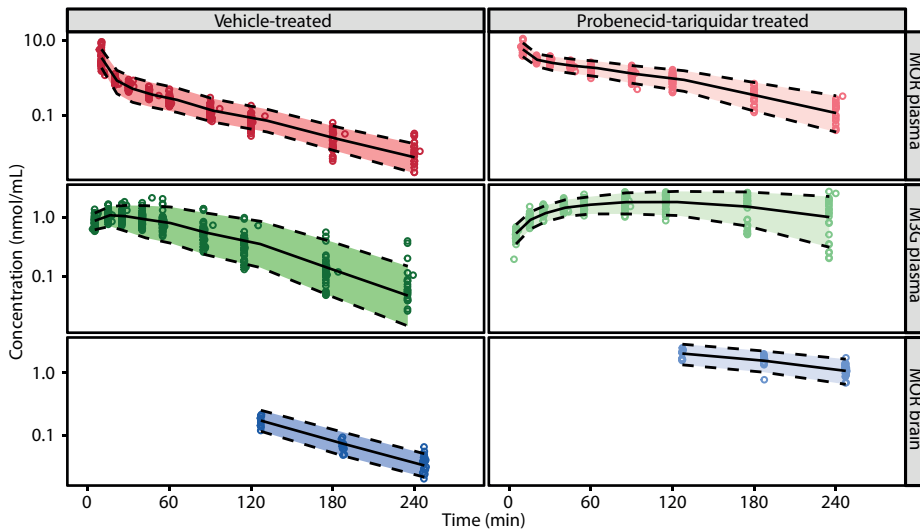
**Figure 3** Visual predictive check (VPC) stratified by treatment group. Dots: observed data; solid line: median of the predicted concentrations; shaded areas enclosed by dashed lines: 90% prediction intervals of the simulated data.
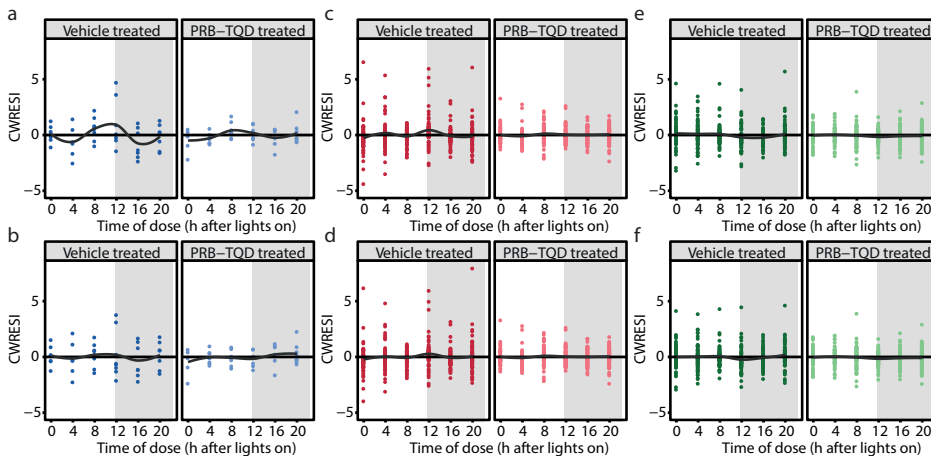


**Figure 4** Distribution of CWRESI vs time of dose in vehicle-treated (dark symbols) and probenecid (PRB) – tariquidar (TQD) treated (light symbols) animals. **(a, c, e)** CWRESI distribution in the model without cosine functions of morphine concentrations in brain (a) and in plasma (c) and of M3G concentrations in plasma (e). **(b)** CWRESI distribution in the model with a 24+12-hour cosine included on $Q_{ECF-PL}$ of morphine concentrations in brain. **(d, f)** CWRESI distribution in the model with a 24+12-hour cosine function included on $CL_{10,active}$ and $CL_{M3G, active}$ of morphine concentrations in plasma (d) and of M3G concentrations in plasma (f).

for morphine distribution into the brain (Bouw et al., 2000), could best describe the brain concentrations data. In the final brain model, drug transport between the deep brain compartment and the ECF compartment were described by a single clearance parameter and the flow between the ECF compartment and the plasma compartment by an influx parameter ($Q_{PL-ECF}$) and an efflux parameter that was split into a passive ($Q_{ECF-PL,passive}$) and an active ($Q_{ECF-PL,active}$) component (Figure 2).
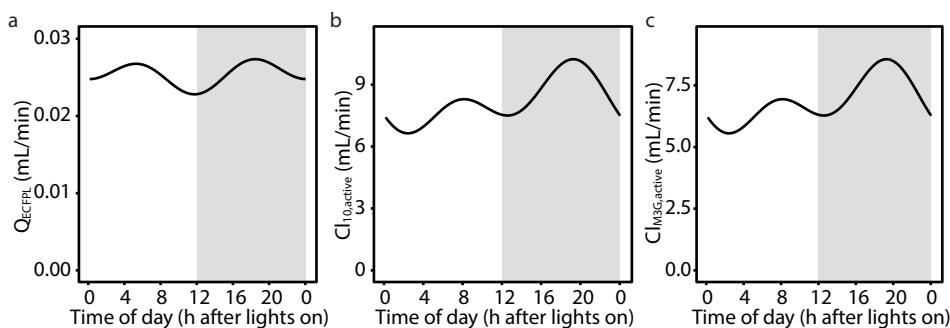
**Figure 5** Shape of the cosine functions included on $Q_{ECF-PL}$ (a), $CL_{10,active}$ (b) and $CL_{M3G,active}$ (c).
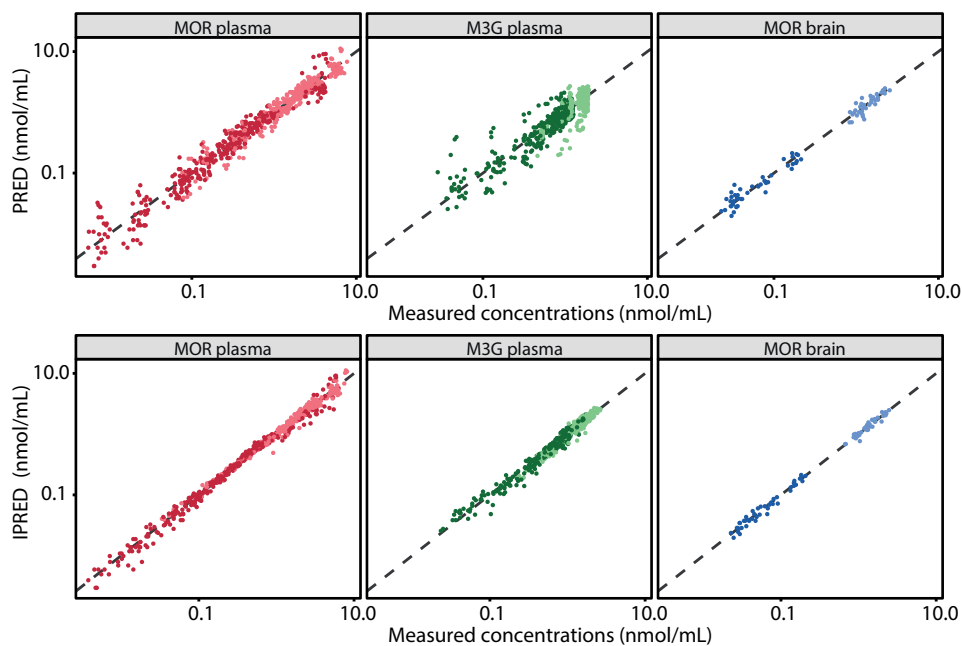


**Figure 6** Measured versus population predicted (PRED; upper panels) and individual predicted (IPRED; lower panels) concentrations of morphine (MOR) in plasma (left, red), M3G in plasma (middle, green) and MOR in brain tissue (right, blue) of the final model. Dark coloured symbols represent vehicle-treated animals; light coloured symbols represent inhibitor-treated animals. Dotted line: line of unity.

The volumes of the ECF and deep brain compartment were fixed to 1, because these values could not be estimated with sufficient precision. This model described the central trend and the variability in the brain concentrations well (Figure 3). The parameter estimates of the final combined plasma and brain model are shown in Supplemental Table 1. Of note, the residual unexplained variability of the brain concentrations was reduced from 128% to 13%.

**Twenty-four hour variation in morphine pharmacokinetics**

The distribution of CWRESI of the morphine concentrations in brain of both vehicle and inhibitor-treated animals showed clear time-of-day dependent bias with peaks around

the light-dark transitions (Figure 4A). Inclusion of a two-harmonic cosine function with a 24-hour and 12-hour component on the efflux of morphine from the ECF compartment to plasma ($Q_{ECF-PL}$) significantly improved the fit of the model (ΔOFV -16, p<0.005, 4 d.f.). This cosine function adequately removed this bias (Figure 4B) and provided a better fit compared to implementation of a two-harmonic cosine function on the influx parameter ($Q_{PL-ECF}$) (AIC = -2.7). Moreover, residual unexplained variability of the brain concentrations was reduced from 13.1% to 11.9%. The 24-hour and 12-hour components of this cosine function had a peak at 22.8 hours and 5.9 hours after lights on and relative amplitudes of 4.1% and 6.3%, respectively (Figure 5A).

The CWRESI of morphine and M3G in plasma did not reveal a time-of-day dependent bias (Figure 4C and E). Nevertheless, it was found that inclusion of the same two-harmonic cosine with a 24-hour and 12-hour component on $CL_{M3G,active}$ and $CL_{10,active}$ significantly improved the fit of the model (ΔOFV -28, p<0.005, 4 d.f.). Inclusion of this cosine minimally affected the distribution of CWRESI over time-of-day (Figure 4D and F). The 24-hour and 12-hour components of this cosine function had a peak at 18 hours and 7.6 hours after lights on and relative amplitudes of 13% and 12.5%, respectively (Figure 5B and C).

In the final model (Run8202), the cosine function on $Q_{ECF-PL}$ was combined with the cosine functions on $CL_{M3G,active}$ and $CL_{10,active}$. This model described the observed concentrations well (Figure 6). Parameter estimates from this model and from a bootstrap (500 runs) are shown in Table 2.



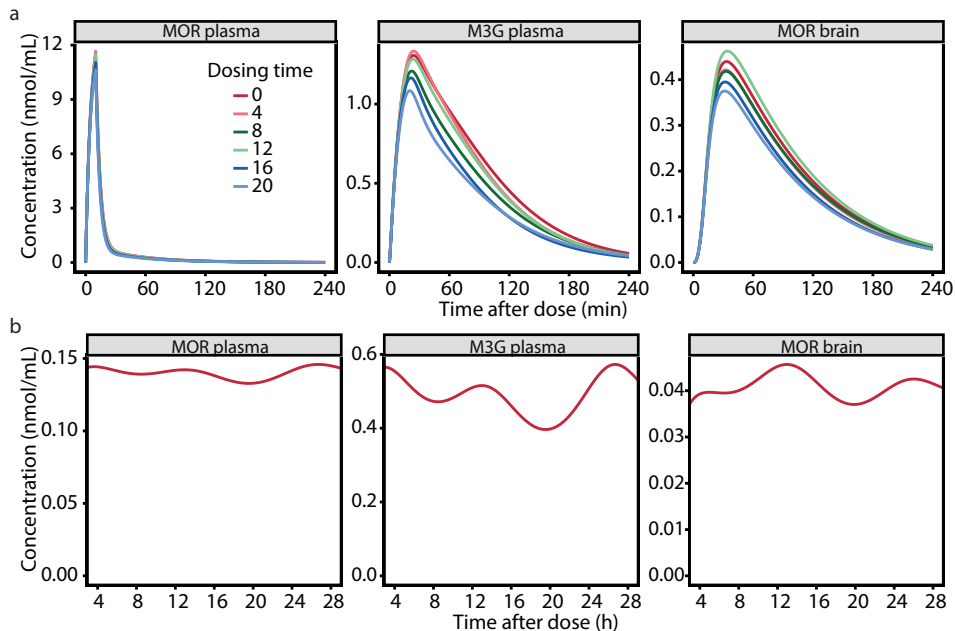**Figure 7** Simulations of morphine (MOR) concentration-time profiles in plasma (left), M3G concentrations in plasma (middle) and morphine concentrations in brain (right) after a 10 min. intravenous infusion of 4 mg/kg at six different dosing times (start of infusion at t=0, 4, 8, 12, 16, 20 hours after light onset) **(a)** and during a continuous infusion of 1mg/kg/h started at 0 hours after light onset **(b)**.

**Table 2** Parameter estimates of combined plasma and brain model (with 24-hour variation included on $CL_{10,active}$, $CL_{M3G,active}$ and $Q_{ECF-PL}$) and results from bootstrap analysis (444/500 resamples successful)

| Parameter | Units | Equation | θ | Estimate | RSE | Bootstrap median (90% P.I.) |
|---|---|---|---|---|---|---|
| *Morphine plasma* | | | | | | |
| $CL_{10}$ | mL/min | $CL_{10} = \theta_{CL10,passive} + CL_{10,active} * (1-TRT)$ | $\theta_{CL10,passive}$ | 4.97 | 4.4% | 4.98 (4.63 - 5.35) |
| | | | $\theta_{mesor}$ | 8.24 | 16.7% | 8.19 (6.12 – 10.7) |
| | | With $CL_{10,active} = \theta_{mesor} * (1+\theta_{amp,24} * \cos(2\pi * (t - \theta_{phase,24})/1440) + \theta_{amp,12} * \cos(2\pi * (t-\theta_{phase,12})/720))$ | $\theta_{amp,24}$ | 0.123 | 46.3% | 14.5 (5.61 – 25) |
| | | | $\theta_{phase,24}$ | 1070 | 11.8% | 1053 (839 - 1240) |
| | | | $\theta_{amp,12}$ | 0.126 | 42% | 13.3 (5.17 – 22.6) |
| | | | $\theta_{phase,12}$ | 461 | 8.6% | 463 (384 – 547) |
| V1 | mL | $V1 = \theta_{V1}$ | $\theta_{V1}$ | 109 | 16.3% | 109 (80.6 - 144) |
| Q2 | mL/min | $Q2 = \theta_{Q2} * \theta_{Q2,INH}^{TRT}$ | $\theta_{Q2}$ | 11.0 | 8.9% | 11.0 (9.25 – 12.4) |
| | | | $\theta_{Q2,INH}$ | 1.52 | 5% | 1.52 (1.40 – 1.67) |
| V2 | mL | $V2 = \theta_{V2}$ | $\theta_{V2}$ | 508 | 4.9% | 505 (454 – 537) |
| *M3G plasma* | | | | | | |
| $V_{m,MET}$ | mL/min | $V_{m,MET} = \theta_{VM} * \theta_{VM,INH}^{TRT}$ | $\theta_{VM}$ | 15.4 | 7.9% | 15.5 (13.7 – 17.7) |
| | | | $\theta_{VM,INH}$ | 0.443 | 11.7% | 0.440 (0.358 – 0.539) |
| $K_{m,MET}$ | nmol/mL | $K_{m,MET} = \theta_{KM}$ | $\theta_{KM}$ | 0.325 | 18.4% | 0.327 (0.250 – 0.490) |
| $CL_{M3G}$ | mL/min | $CL_{M3G} = \theta_{CLM3G,passive} + CL_{M3G,active} * (1-TRT)$ | $\theta_{CLM3G,passive}$ | 2.8 | 15.4% | 2.76 (2.14 – 3.51) |
| | | | $\theta_{Mesor}$ | 6.85 | 11.3% | 6.83 (5.39 – 8.04) |
| | | With $CL_{M3G,active} = \theta_{mesor} * (1+\theta_{amp,24} * \cos(2\pi * (t - \theta_{phase,24})/1440) + \theta_{amp,12} * \cos(2\pi * (t-\theta_{phase,12})/720))$ | $\theta_{amp,24}$ | See $CL_{10,active}$ | | |
| | | | $\theta_{phase,24}$ | See $CL_{10,active}$ | | |
| | | | $\theta_{amp,12}$ | See $CL_{10,active}$ | | |
| | | | $\theta_{phase,12}$ | See $CL_{10,active}$ | | |
| *Morphine brain* | | | | | | |
| $V_{DBR}$ | mL | $V_{DBR} = \theta V_{DBR}$ | $\theta_{VDBR}$ | 1 FIX | | |
| $Q_{DBR}$ | mL/min | $Q_{DBR} = \theta Q_{DBR}$ | $\theta_{QDBR}$ | 0.0184 | 6.0% | 0.0185 (0.0167 – 0.0209) |
| $V_{ECF}$ | mL | $V_{ECF} = \theta V_{ECF}$ | $\theta_{VECF}$ | 1 FIX | | |
| $Q_{ECF-PL}$ | mL/min | | $\theta_{QECFPL,passive}$ | 0.0256 | 9.5% | 0.0251 (0.0211 - 0.0301) |
| | | | $\theta_{QECFPL,active}$ | 0.0834 | 12.4% | 0.0824 (0.0659 – 0.103) |
| | | $Q_{ECF-PL} = (\theta_{QECFPL,passive} + Q_{ECFPL,active} * (1-TRT)) * (1 + \theta_{amp,24} * \cos(2\pi * (t - \theta_{phase,24})/1440) + \theta_{amp,12} * \cos(2\pi * (t-\theta_{phase,12})/720))$ | $\theta_{amp,24}$ | 0.376 | 42% | 4.33 (1.75 – 6.82) |
| | | | $\theta_{phase,24}$ | 1390 | 7.4% | 1390 (1150 – 1600) |
| | | | $\theta_{amp,12}$ | 0.633 | 32.2% | 6.76 (3.79 – 10.5) |
| | | | $\theta_{phase,12}$ | 1060 | 3.3% | 1060 (990 – 1120) |
| $Q_{PL-ECF}$ | mL/min | $Q_{PL-ECF} = \theta_{QPLECF}$ | $\theta_{QPLECF}$ | 0.0322 | 10.5% | 0.0316 (0.260 – 0.0386) |
| *Inter-animal variability (CV%)* | | | | | | |
| $\omega^2 CL_{10}$ | | | | 17.3 | | 16.8 |
| $\omega^2 V_{m,MET}$ | | | | 22.2 | | 21.9 |
| $\omega^2 CL_{M3G}$ | | | | 43.5 | | 42.6 |
| $\omega^2 Q2$ | | | | 18.7 | | 18.4 |
| $\omega^2 V_{m,MET} \sim \omega^2 CL_{M3G}$ (untransformed) | | | | 0.0761 | | 0.0742 |
| *Residual unexplained variability (%)* | | | | | | |
| $\sigma_{PL}$ | | | | 17.0 | | 16.8 |
| $\sigma_{M3G}$ | | | | 14.5 | | 14.4 |
| $\sigma_{DBR}$ | | | | 11.8 | | 11.3 |

**Simulations**

The final model was used to perform simulations to show the impact of dosing time on the concentration profiles of morphine and M3G. As shown in Figure 7A, morphine concentrations in plasma after a single intravenous infusion are minimally affected by dosing time. However, morphine concentrations in brain tissue are influenced by dosing time with the lowest concentrations attained after administration at 20 hours after the onset of the light period and the highest concentrations after 12 hours after the onset of the light period. M3G concentrations were lowest and highest after administration at 4 and 20 hours after the onset of the light period, respectively. During a continuous infusion at steady-state, simulations indicate that morphine and M3G concentrations in plasma and morphine concentrations in brain fluctuate during the 24-hour period (Figure 7B).

# DISCUSSION

In this study, we have been able to characterize the effect of dosing time on processes that are involved in the distribution, metabolism and excretion of morphine through the development of a population pharmacokinetic model. By inhibiting P-gp and probenecid-sensitive transporters, the active and passive processes involved in the distribution and clearance of morphine could be investigated separately (Bourasset and Scherrmann, 2006; Groenendaal et al., 2007; Letrent et al., 1999; Tunblad et al., 2003; Xie et al., 1999). We show that the transport of morphine from brain tissue back into the circulation shows a characteristic 24-hour rhythm with the lowest efflux during the light-dark phase transitions. The active processes involved in the clearance of morphine and its metabolite M3G from plasma also show 24-hour variation with the peak in the middle of the dark phase. Using simulations, we show that the concentrations profiles of morphine in brain tissue and of M3G in plasma are affected by time of day. These findings indicate that dosing time should be taken into account in the optimization of morphine's dosing regimen.

Our results show that inhibition of active transport processes by probenecid and tariquidar alters both the systemic pharmacokinetics and the brain distribution of morphine. With regard to systemic pharmacokinetics, inhibition of active transport reduced the systemic clearance of morphine, increased its intercompartmental clearance and lowered the maximal conversion rate of morphine to M3G. Because it was previously found that P-gp inhibition does not influence morphine concentrations in plasma (Groenendaal et al., 2007; Letrent et al., 1998, 1999; Xie et al., 1999), while probenecid treatment has been reported to reduce systemic morphine clearance and the formation of M3G in rats (Tunblad et al., 2003), we hypothesize that the systemic effects we observed are due to probenecid treatment. Probenecid inhibits multiple multidrug resistance proteins (mrps) (Dresser et al., 2001) that are expressed not only in the blood-brain barrier (Stieger and Gao, 2015), but also in the kidney and liver (Lee and Kim, 2004; Zelcer et al., 2001, 2005) and thereby affects the renal and hepatic elimination of drugs (Lee and Kim, 2004). Although we cannot exclude the contribution of other processes, we propose that the effect of probenecid on the systemic

pharmacokinetics of morphine is due to inhibition of mrp transporters in kidney and liver.

Active transport inhibition also altered the brain distribution of morphine. Brain concentrations could be best described by a model in which a "deep brain" compartment was linked to the central plasma compartment by an extra-cellular fluid (ECF) compartment. An additional transport component that was absent inhibitor-treated animals was identified on the transport of morphine from the ECF compartment to plasma. This confirms previous findings that morphine is subject to active efflux transport mediated by P-gp and probenecid-sensitive transporters (Bourasset and Scherrmann, 2006; Groenendaal et al., 2007; Letrent et al., 1999; Tunblad et al., 2003; Xie et al., 1999).

Our findings indicate that several processes involved in morphine pharmacokinetics show 24-hour variation. It was previously shown in cancer patients that the maximal concentration (Cmax) and the area under concentration-time profile (AUC) at steady state are higher at 18:00 than at 10:00 and 14:00 after oral administration (Gourlay et al., 1995). In dogs, the AUC and Cmax of oral sustained release morphine were significantly higher after dosing at 7:30 than after dosing at 19:30 (Dohoo, 1997). However, in the present study, we have been able to quantify the relative contribution of the processes involved in the distribution, metabolism and elimination of morphine more precisely through the use of six dosing times and the development of a population pharmacokinetic model. We find that the active component of the systemic clearance of morphine and M3G show 24-hour variation with a difference of 54% between the lowest value and the highest value. A physiological explanation of these findings could be the observation that the expression of various probenecid-sensitive transporters show 24-hour variation in the kidney (Gachon and Firsov, 2011). However, future research to elucidate the underlying mechanisms is warranted.

Furthermore, we find that the transport of morphine from the brain to the blood shows a 12-hour rhythm with the lowest values at the transitions of the light/dark phase. This rhythm could be described by a 24-hour and 12-hour sinusoidal function on this parameter with a difference between the highest and lowest efflux of 20%. Importantly, the inclusion of this function in the model resolved a time-of-day dependent bias observed in the conditionally weighted residuals. In a previous study we found that the efflux of the P-gp substrate quinidine from the brain to plasma is more than two-fold higher during the dark phase compared to the light phase in the presence of functional P-gp transport, but not when P-gp transport is blocked (Kervezee et al., 2014). In the present study, we do not find this P-gp dependent effect for morphine. While quinidine is a selective P-gp substrate, morphine has more complex transport mechanisms across the BBB, which is not only affected by P-gp but also by probenecid-sensitive transporters. The daily variation in P-gp activity may be (partly) counterbalanced by a differentially-phased variation in probenecid-sensitive transporters. Hence, multiple mechanisms likely give rise to the 12-hour rhythm in the transport of morphine from the brain to blood.

We performed simulations of a single intravenous dose and of a continuous infusion regimen to visualize the effect of the daily rhythmicity in morphine pharmacokinetics on the

concentration-time profiles in plasma and brain tissue. Although morphine concentrations in plasma are minimally affected by dosing time, metabolite concentrations in plasma and morphine concentrations in brain tissue do depend on the time of day. This finding has several important implications: it indicates that time of day can be a substantial source of variation in the pharmacokinetics and, possibly, the pharmacodynamics of morphine when it is not properly accounted for, but also that these systematic variations could be exploited to optimize morphine's dosing regimen.

## CONFLICT OF INTEREST

## ACKNOWLEDGEMENTS

# REFERENCES

Beal, S., Sheiner, L.B., Boeckmann, A., and Bauer, R.J. (2009). NONMEM User's Guides (1989-2009), Icon Development Solutions, Ellicott City, MD, USA.

Bickel, U., Schumacher, O.P., Kang, Y.S., and Voigt, K. (1996). Poor permeability of morphine 3-glucuronide and morphine 6-glucuronide through the blood-brain barrier in the rat. J. Pharmacol. Exp. Ther. 278, 107–113.

Bornschein, R.L., Crockett, R.S., and Smith, R.P. (1977). Diurnal variations in the analgesic effectiveness of morphine in mice. Pharmacol. Biochem. Behav. 6, 621–626.

Boström, E., Hammarlund-Udenaes, M., and Simonsson, U.S.H. (2008). Blood-brain barrier transport helps to explain discrepancies in in vivo potency between oxycodone and morphine. Anesthesiology 108, 495–505.

Bourasset, F., and Scherrmann, J.-M. (2006). Carrier-mediated processes at several rat brain interfaces determine the neuropharmacokinetics of morphine and morphine-6-beta-D-glucuronide. Life Sci. 78, 2302–2314.

Bouw, M.R., Gårdmark, M., and Hammarlund-Udenaes, M. (2000). Pharmacokinetic-Pharmacodynamic Modelling of Morphine Transport Across the Blood-Brain Barrier as a Cause of the Antinociceptive Effect Delay in Rats—A Microdialysis Study. Pharm. Res. 17, 1220–1227.

Cui, Y., Sugimoto, K., Araki, N., Sudoh, T., and Fujimura, A. (2005). Chronopharmacology of morphine in mice. Chronobiol. Int. 22, 515–522.

Dallmann, R., Brown, S.A., and Gachon, F. (2014). Chronopharmacology: new insights and therapeutic implications. Annu. Rev. Pharmacol. Toxicol. 54, 339–361.

Dohoo, S. (1997). Steady-state pharmacokinetics of oral sustained-release morphine sulphate in dogs. J. Vet. Pharmacol. Ther. 20, 129–133.

Dresser, M.J., Leabman, M.K., and Giacomini, K.M. (2001). Transporters involved in the elimination of drugs in the kidney: Organic anion transporters and organic cation transporters. J. Pharm. Sci. 90, 397–421.

Gachon, F., and Firsov, D. (2011). The role of circadian timing system on drug metabolism and detoxification. Expert Opin. Drug Metab. Toxicol. 7, 147–158.

Gourlay, G.K., Plummer, J.L., and Cherry, D.A. (1995). Chronopharmacokinetic variability in plasma morphine concentrations following oral doses of morphine solution. Pain 61, 375–381.

De Gregori, S., De Gregori, M., Ranzani, G.N., Allegri, M., Minella, C., and Regazzi, M. (2011). Morphine metabolism, transport and brain disposition. Metab. Brain Dis. 27, 1–5.

Groenendaal, D., Freijer, J., de Mik, D., Bouw, M.R., Danhof, M., and de Lange, E.C.M. (2007). Population pharmacokinetic modelling of non-linear brain distribution of morphine: influence of active saturable influx and P-glycoprotein mediated efflux. Br. J. Pharmacol. 151, 701–712.

Güney, H.Z., Görgün, C.Z., Tunçtan, B., Uludağ, O., Hodoğlugil, U., Abacioğlu, N., and Zengil, H. (1998). Circadian-rhythm-dependent effects of L-NG-nitroarginine methyl ester (L-NAME) on morphine-induced analgesia. Chronobiol. Int. 15, 283–289.

Junker, U., and Wirz, S. (2010). Review article: chronobiology: influence of circadian rhythms on the therapy of severe pain. J. Oncol. Pharm. Pract. 16, 81–87.

Kavaliers, M., and Hirst, M. (1983). Daily rhythms of analgesia in mice: effects of age and photoperiod. Brain Res. 279, 387–393.

Keizer, R.J., Karlsson, M.O., and Hooker, A. (2013). Modeling and Simulation Workbench for NONMEM: Tutorial on Pirana, PsN, and Xpose. CPT Pharmacometrics Syst. Pharmacol. 2, e50.

Keizer, R.J., Jansen, R.S., Rosing, H., Thijssen, B., Beijnen, J.H., Schellens, J.H.M., and Huitema, A.D.R. (2015). Incorporation of concentration data below the limit of quantification in population pharmacokinetic analyses. Pharmacol. Res. Perspect. 3, e00131.

Kervezee, L., Hartman, R., van den Berg, D.-J., Shimizu, S., Emoto-Yamamoto, Y., Meijer, J.H., and de Lange, E.C.M. (2014). Diurnal Variation in P-glycoprotein-Mediated Transport and Cerebrospinal Fluid Turnover in the Brain. AAPS J. 16, 1029–1037.

Lee, W., and Kim, R.B. (2004). Transporters and renal drug elimination. Annu. Rev. Pharmacol. Toxicol.

44, 137–166.

Letrent, S.P., Pollack, G.M., Brouwer, K.R., and Brouwer, K.L.R. (1998). Effect of GF120918, a Potent P-glycoprotein Inhibitor, on Morphine Pharmacokinetics and Pharmacodynamics in the Rat. Pharm. Res. 15, 599–605.

Letrent, S.P., Pollack, G.M., Brouwer, K.R., and Brouwer, K.L.R. (1999). Effects of a Potent and Specific P-Glycoprotein Inhibitor on the Blood-Brain Barrier Distribution and Antinociceptive Effect of Morphine in the Rat. Drug Metab. Dispos. 27, 827–834.

Lutsch, E.F., and Morris, R.W. (1971). Light reversal of a morphine-induced analgesia susceptibility rhythm in mice. Experientia 27, 420–421.

Morris, R.W., and Lutsch, E.F. (1967). Susceptibility to morphine-induced analgesia in mice. Nature 216, 494–495.

Mould, D.R., and Upton, R.N. (2013). Basic concepts in population modeling, simulation, and model-based drug development-part 2: introduction to pharmacokinetic modeling methods. CPT Pharmacometrics Syst. Pharmacol. 2, e38.

Oliverio, A., Castellano, C., and Puglisi-Allegra, S. (1982). Opiate analgesia: Evidence for circadian rhythms in mice. Brain Res. 249, 265–270.

Potts, A.L., Cheeseman, J.F., and Warman, G.R. (2011). Circadian rhythms and their development in children: implications for pharmacokinetics and pharmacodynamics in anesthesia. Paediatr. Anaesth. 21, 238–246.

Rasmussen, N.A., and Farr, L.A. (2003). Effects of Morphine and Time of Day on Pain and Beta-Endorphin. Biol. Res. Nurs. 5, 105–116.

Somogyi, A. a, Barratt, D.T., and Coller, J.K. (2007). Pharmacogenetics of opioids. Clin. Pharmacol. Ther. 81, 429–444.

Stain-Texier, F., Boschi, G., Sandouk, P., and Scherrmann, J.M. (1999). Elevated concentrations of morphine 6-beta-D-glucuronide in brain extracellular fluid despite low blood-brain barrier permeability. Br. J. Pharmacol. 128, 917–924.

Stieger, B., and Gao, B. (2015). Drug Transporters in the Central Nervous System. Clin. Pharmacokinet. 54, 225–242.

Sverrisdóttir, E., Lund, T.M., Olesen, A.E., Drewes, A.M., Christrup, L.L., and Kreilgaard, M. (2015). A review of morphine and morphine-6-glucuronide's pharmacokinetic-pharmacodynamic relationships in experimental and clinical pain. Eur. J. Pharm. Sci. 74, 45–62.

Thompson, S.J., Koszdin, K., and Bernards, C.M. (2000). Opiate-induced analgesia is increased and prolonged in mice lacking P-glycoprotein. Anesthesiology 92, 1392–1399.

Tunblad, K., Jonsson, E.N., and Hammarlund-Udenaes, M. (2003). Morphine Blood-Brain Barrier Transport Is Influenced by Probenecid Co-Administration. Pharm. Res. 20, 618–623.

Tunblad, K., Hammarlund-Udenaes, M., and Jonsson, E.N. (2004). An Integrated Model for the Analysis of Pharmacokinetic Data from Microdialysis Experiments. Pharm. Res. 21, 1698–1707.

Westerhout, J., Ploeger, B., Smeets, J., Danhof, M., and de Lange, E.C.M. (2012). Physiologically based pharmacokinetic modeling to investigate regional brain distribution kinetics in rats. AAPS J. 14, 543–553.

Xie, R., Hammarlund-Udenaes, M., de Boer, A.G., and de Lange, E.C. (1999). The role of P-glycoprotein in blood-brain barrier transport of morphine: transcortical microdialysis studies in mdr1a (-/-) and mdr1a (+/+) mice. Br. J. Pharmacol. 128, 563–568.

Yoshida, M., Ohdo, S., Takane, H., Tomiyoshi, Y., Matsuo, A., Yukawa, E., and Higuchi, S. (2003). Chronopharmacology of analgesic effect and its tolerance induced by morphine in mice. J. Pharmacol. Exp. Ther. 305, 1200–1205.

Yoshida, M., Koyanagi, S., Matsuo, A., Fujioka, T., To, H., Higuchi, S., and Ohdo, S. (2005). Glucocorticoid hormone regulates the circadian coordination of micro-opioid receptor expression in mouse brainstem. J. Pharmacol. Exp. Ther. 315, 1119–1124.

Zelcer, N., Saeki, T., Reid, G., Beijnen, J.H., and Borst, P. (2001). Characterization of drug transport by the human multidrug resistance protein 3 (ABCC3). J. Biol. Chem. 276, 46400–46407.

Zelcer, N., van de Wetering, K., Hillebrand, M., Sarton, E., Kuil, A., Wielinga, P.R., Tephly, T., Dahan, A., Beijnen, J.H., and Borst, P. (2005). Mice lacking multidrug resistance protein 3 show altered morphine pharmacokinetics and morphine-6-glucuronide antinociception. Proc. Natl. Acad. Sci. U. S. A. 102, 7274–7279.

Zhang, Y.-K.J., Yeager, R.L., and Klaassen, C.D. (2009). Circadian expression profiles of drug-processing genes and transcription factors in mouse liver. Drug Metab. Dispos. 37, 106–115.

**Supplementary Table 1** Parameter estimates of combined plasma and brain model (without 24-hour variation included on $CL_{10,active}$, $CL_{M3G,active}$ and $Q_{ECF-PL}$)

| Parameter | Units | Equation | θ | Estimate | RSE |
|---|---|---|---|---|---|
| *Morphine plasma* | | | | | |
| $CL_{10}$ | mL/min | $CL_{10} = \theta_{CL10,passive} + \theta_{CL10,active} * (1\text{-TRT})$ | $\theta_{CL10,passive}$ | 4.95 | 4.5% |
| | | | $\theta_{CL10,active}$ | 8.27 | 17% |
| V1 | mL | $V1 = \theta_{V1}$ | $\theta_{V1}$ | 110 | 16.6% |
| Q2 | mL/min | $Q2 = \theta_{Q2} * \theta_{Q2,INH}{}^{TRT}$ | $\theta_{Q2}$ | 11 | 8.7% |
| | | | $\theta_{Q2,INH}$ | 1.53 | 5% |
| V2 | mL | $V2 = \theta_{V2}$ | $\theta_{V2}$ | 511 | 4.8% |
| *M3G plasma* | | | | | |
| $V_{m,MET}$ | mL/min | $V_{m,MET} = \theta_{VM} * \theta_{VM,INH}{}^{TRT}$ | $\theta_{VM}$ | 15.6 | 7.8% |
| | | | $\theta_{VM,INH}$ | 0.443 | 11.9% |
| $K_{m,MET}$ | nmol/mL | $K_{m,MET} = \theta_{KM}$ | $\theta_{KM}$ | 0.329 | 19.1% |
| $CL_{M3G}$ | mL/min | $CL_{M3G} = \theta_{CLM3G,passive} + \theta_{CL3MG,active} * (1\text{-TRT})$ | $\theta_{CLM3G,passive}$ | 2.82 | 15.6% |
| | | | $\theta_{CLM3G,active}$ | 6.9 | 11.4% |
| *Morphine brain* | | | | | |
| $V_{DBR}$ | mL | $V_{DBR} = \theta_{VDBR}$ | $\theta_{VDBR}$ | 1 FIX | |
| $Q_{DBR}$ | mL/min | $Q_{DBR} = \theta_{QDBR}$ | $\theta_{QDBR}$ | 0.0183 | 6.7% |
| $V_{ECF}$ | mL | $V_{ECF} = \theta_{VECF}$ | $\theta_{VECF}$ | 1 FIX | |
| $Q_{ECF-PL}$ | mL/min | $Q_{ECF-PL} = \theta_{QECFPL,passive} + Q_{ECFPL,active} * (1\text{-TRT})$ | $\theta_{QECFPL,passive}$ | 0.0257 | 9.8% |
| | | | $\theta_{QECFPL,active}$ | 0.0839 | 13.2% |
| $Q_{PL-ECF}$ | mL/min | $Q_{PL-ECF} = \theta_{QPLECF}$ | $\theta_{QPLECF}$ | 0.0325 | 10.6% |
| *Inter-animal variability (CV%)* | | | | | |
| $\omega^2\, CL_{10}$ | | | | 18.3 | |
| $\omega^2 V_{m,MET}$ | | | | 21.7 | |
| $\omega^2\, CL_{M3G}$ | | | | 43.9 | |
| $\omega^2\, Q2$ | | | | 18.3 | |
| $\omega^2\, V_{m,MET} \sim \omega^2\, CL_{M3G}$ | | | | 84.0 | |
| *Residual unexplained variability (%)* | | | | | |
| $\sigma_{PL}$ | | | | 17.4 | |
| $\sigma_{M3G}$ | | | | 14.6 | |
| $\sigma_{DBR}$ | | | | 13.1 | |

RSE: relative standard error
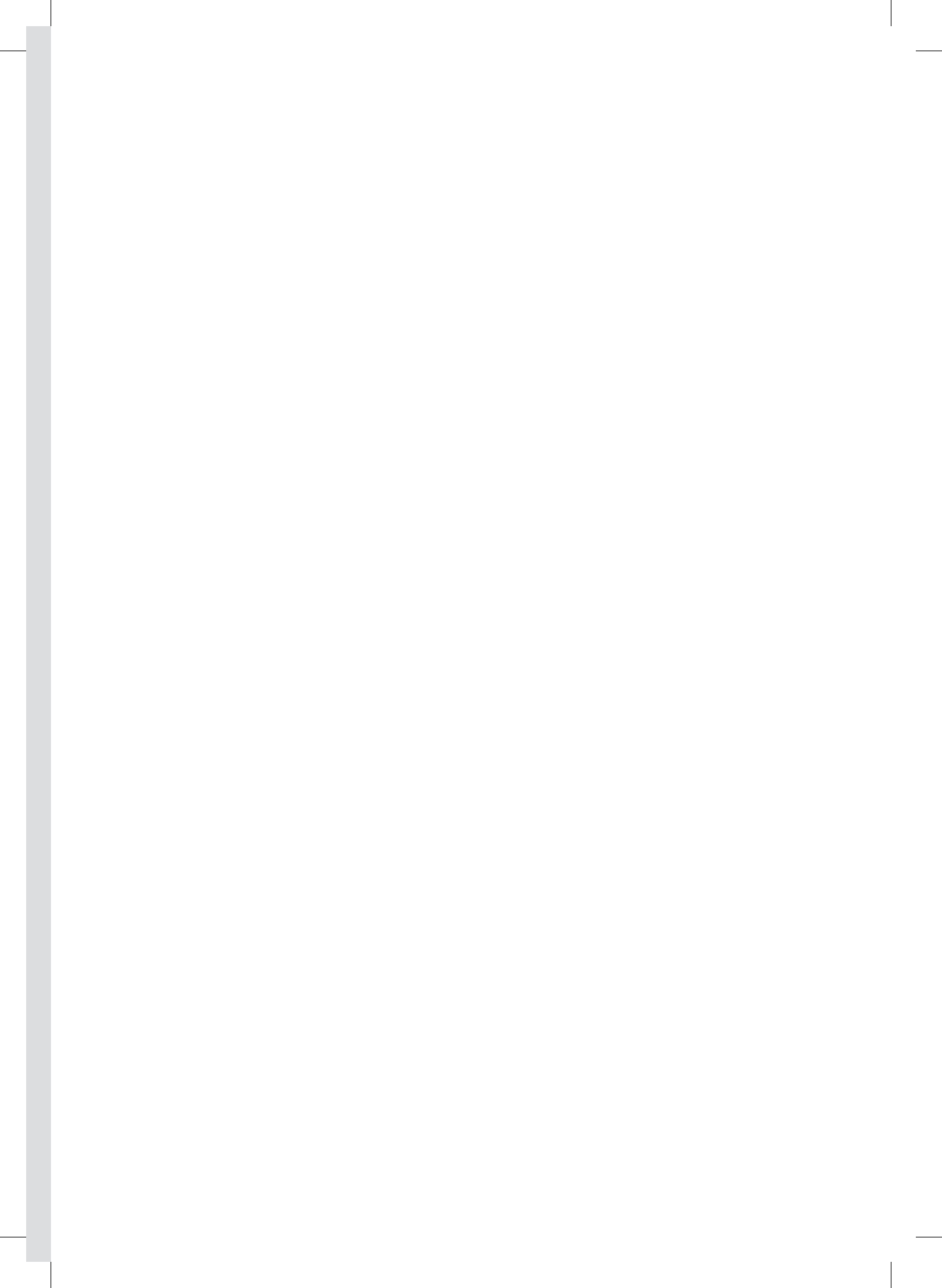
# CHAPTER

## General discussion

8

A thorough understanding of the physiological processes that determine a drug's exposure and effect is required to address the challenges encountered during the development or optimisation of new and existing drug therapies. Although rarely considered by the pharmaceutical industry or clinicians, 24-hour rhythms in physiology can potentially influence the pharmacokinetics and pharmacodynamics of drugs. In **Chapter 1**, the current state of the field of chronopharmacology, which aims to characterize the influence of daily physiological rhythms on drug treatments, was reviewed. Although this field has existed for decades, we identified several methodological issues in the current body of literature that often precludes implementation of chronopharmacological principles in clinical practice. In general, it was found that a systematic approach to analyse and integrate the data obtained within this field is currently lacking. Therefore, the aim of this thesis was to develop a more structured approach to study the effect of 24-hour variation on the exposure and effect of drugs.

As explained in **Chapter 2**, this approach involves (1) the use of probe drugs, (2) prospectively designed studies optimally suited to investigate chronopharmacology, and (3) the application of pharmacokinetic-pharmacodynamic modelling for data analysis. Here, this approach is discussed in the context of the results presented in **Chapter 3-7**. Subsequently, the clinical implications and future perspectives of this research are considered.

## THE USE OF PROBE DRUGS IN CHRONOPHARMACOLOGY

In theory, the exposure and effect of each drug could be influenced by daily rhythms in physiological processes in a unique manner. However, considering the vast amount of drugs currently used in clinical practice, it is neither feasible nor desirable to study the effect of dosing time on all of these drugs separately. Therefore, a key characteristic of the approach described in this thesis was the use of probe drugs to study the effect of 24-hour variation in specific physiological processes on their pharmacokinetics or pharmacodynamics. Midazolam was used as a CYP3A-substrate in the clinical trial described in **Chapter 3**. The rationale for using levofloxacin as a model compound in **Chapter 4** and **Chapter 5** was two-fold. Characterized by complete absorption and very limited metabolism, levofloxacin is an ideal compound to investigate solubility- and permeability-independent absorption and passive renal elimination. Additionally, as an inhibitor of cardiac hERG channels, it was used to study drug-induced QT prolongation. In **Chapter 6**, quinidine was chosen as a model compound to investigate P-glycoprotein mediated transport in the brain. Finally, in **Chapter 7**, we used morphine as a substrate of P-glycoprotein as well as of probenecid-sensitive transporters such as multidrug resistance-associated proteins (mrp). In addition to enhancing our understanding of morphine brain distribution, we gained insight into UGT2B7-mediated metabolism by the measurement of the plasma concentrations of morphine's metabolite M3G. This way, we acquired a substantial body of knowledge of the 24-hour variation in these physiological processes, which will be discussed here.

**Drug absorption**

Most drugs are administered orally and need to be absorbed before reaching the systemic circulation. In its most simple form, drug absorption involves the passive diffusion of drug molecules across the lipid bilayers of the intestinal epithelium, the extent of which is influenced by a drug's permeability and solubility. We studied 24-hour variation in the rate and extent of drug absorption in **Chapter 3** and **4**.

In **Chapter 3**, a randomized crossover study is described that involved the administration of an oral (2 mg) and intravenous (1 mg) dose of midazolam to 12 healthy volunteers at six different time-points using a semi-simultaneous dosing regimen. Previous clinical studies into the effect of dosing time on the pharmacokinetic parameters of midazolam did not yield consistent results. While two studies found significant diurnal variation in midazolam pharmacokinetics after intravenous infusion (Klotz and Ziegler, 1982; Tomalik-Scharte et al., 2014), another study did not observe these differences (Klotz and Reimann, 1984). Furthermore, two studies addressed the effect of time of administration on midazolam pharmacokinetics after an oral dose (Klotz and Ziegler, 1982; Koopmans et al., 1991), which both observed that the absorption of the drug is not affected by the dosing times employed in the studies. Taken together, these studies exemplify the issues that were raised in Chapter 1, including the use of a limited number dosing times and suboptimal statistical methods. By performing the trial described in **Chapter 3**, we could identify the absorption and clearance parameters separately and construct a detailed profile of the variation over the 24-hour period. Our findings indicate that oral bioavailability showed significant 24-hour variation that could be described by a sinusoidal function with a peak at 12:14 in the afternoon and a relative amplitude of 14.2%. In combination with a 1.41 increase in the absorption rate constant at 14:00, this results in a higher exposure to this drug after oral dosing in the morning and afternoon, compared to oral dosing in the evening and night.

Because we found in **Chapter 3** that dosing time has the largest effect on processes related to drug absorption, this was further investigated in **Chapter 4**. As discussed in Chapter 1, most processes that influence the rate of absorption are more active during the morning compared to the evening, suggesting enhanced absorption during this time period. Indeed, there are indications that the absorption of some lipophilic drugs is faster in the morning (Baraldo, 2008). In **Chapter 4**, the daily variation in the rate of absorption of levofloxacin, a drug characterized by high solubility, high permeability, and minimal metabolism, could be very accurately determined. Substantial variation was identified in the absorption rate of levofloxacin with an amplitude of 47% and a peak at 8:00 in the morning.

Levofloxacin is used in the clinic as an antibiotic to treat a variety of bacterial infections. As a concentration-dependent antibiotic, levofloxacin's exposure, measured by the area under the curve (AUC), or the maximal concentration ($C_{max}$) determine its clinical effectiveness (Drusano, 2004; Preston et al., 1998). The simulations performed in **Chapter 4** indicate that the AUC and $C_{max}$ are not significantly affected by dosing time despite the substantial variation in the absorption rate constant. Therefore, we concluded that, in clinical practice,

levofloxacin can be dosed without taking into account the time of day, at least in terms of its pharmacokinetic parameters.

**Drug distribution to the brain**

Although drug concentration-time profiles in plasma are typically used to assess the relationships between drug exposure and effect, it is the drug concentration at the target site that ultimately drives its effect (De Lange, 2013). Especially for drugs targeted at the brain, plasma concentrations are a poor predictor of target site concentrations because the blood brain barrier (BBB) restricts the entry of drugs to the brain. Understanding the mechanisms underlying the effect of drugs targeted to the brain therefore necessitates local measurement of drug concentrations. In **Chapter 6** and **7**, we investigated 24-hour variation in processes involved in the distribution of drugs in the brain using the rat as a pre-clinical animal model.

In the first part of **Chapter 6**, quinidine was administered intravenously at six different time-points across the 24-hour period to assess P-gp mediated distribution in the brain (Kusuhara et al., 1997; Sziráki et al., 2011). By measuring the quinidine concentration in plasma and brain tissue, it was found that the exposure to this drug in the brain is affected by time of drug administration. When the animals were pre-treated with the potent and selective P-gp inhibitor tariquidar (Mistry et al., 2001), this dosing time-dependent effect was abolished, suggesting that 24-hour variation in P-gp activity is responsible for the observed effect.

In the second part of **Chapter 6**, the microdialysis technique was used to obtain unbound quinidine concentrations in ECF and cerebral spinal fluid (CSF) after drug administration at the two time points that showed the largest difference in brain concentrations in the first part of the study. Microdialysis is currently the only available technique to measure unbound extracellular fluid (ECF) concentrations in the brain over time (De Lange, 2013). Subsequently, the systems-based pharmacokinetic model developed by Westerhout et al. (2013) was applied to the data to investigate the effect of dosing time on the pharmacokinetic parameters of quinidine in the presence and absence of functional P-gp activity. This analysis showed that the variation in brain concentrations could be described by higher activity of P-gp-mediated transport from the deep brain compartment to the plasma compartment during the active period. Furthermore, CSF flux was higher in the resting period compared to the active period. This study showed that dosing time is a considerable source of variation in the distribution of quinidine, and possibly other P-gp substrates, in the brain and suggests that taking into account time of day is a way to optimize drug treatments targeted at the brain.

Within the study design used in **Chapter 6**, we could not account for the effect of sleep on our results. Sleep, independent of circadian rhythmicity, was recently shown to have a profound influence on the clearance of potentially toxic molecules from the brain through an increase in interstitial fluid fluxes mediated by the glymphatic system (Jessen et al., 2015; Xie et al., 2013). Although the implications of this finding on the clearance of drugs from

the brain have yet to be determined, it may be an explanation for the increased CSF flow during sleep that we observed in **Chapter 6**. However, with regard to the 24-hour variation observed in P-gp activity, it was recently found using PET imaging that P-gp function in rats exhibits a 24-hour rhythm independent of sleep (Savolainen et al., 2015), suggesting that the observed 24-hour variation in P-gp mediated transport to brain tissue in **Chapter 6** is not affected by the sleep/wake state of the animal.

In **Chapter 7**, the effect of dosing time on the systemic pharmacokinetics and brain distribution of morphine was investigated. The possibility that daily variation in the analgesic effect of morphine is caused by fluctuations in the pharmacokinetics of morphine was already raised by Lutsch and Morris (1971), who suggested that the daily analgesia pattern produced by morphine could be due to rhythmic variation in the detoxification and/ or distribution of morphine, or could result from variable permeability of the blood-brain barrier during the 24-hour period. This would result in 24-hour variations in the quantity of morphine arriving at and reacting with its receptor (Lutsch and Morris, 1971). Although the absorption of morphine after oral administration is influenced by dosing time (Dohoo, 1997; Gourlay et al., 1995), the study described in **Chapter 7** was the first to directly test the hypothesis that the brain distribution of morphine displays 24-hour variation.

To quantify the effect of time of day on morphine brain distribution, a pharmacokinetic model was developed based on the experimental data. It was found that the efflux of morphine from the brain ECF compartment into the circulation can be best described by a sinusoidal function with 24-hour and 12-hour harmonic terms. The shape of this cosine function is characterized by troughs around the light/dark phase transitions. In combination with the rhythms found in the active clearance of morphine and its metabolite M3G from the system, this results in highest morphine concentrations in brain in the early dark phase. This finding is in line with previous research showing that the highest analgesic effect of morphine in the dark phase (Bornschein et al., 1977; Cui et al., 2005; Lutsch and Morris, 1971; Morris and Lutsch, 1967; Yoshida et al., 2003), although it should be noted that others reported the highest effect in the light phase (Güney et al., 1998; Rasmussen and Farr, 2003) or no effect of dosing time (Kavaliers and Hirst, 1983; Oliverio et al., 1982). Future research should focus on establishing the link between the rhythm in brain exposure to morphine and its analgesic effect through PK-PD modelling.

### Drug elimination

Important pathways in the elimination of drugs are renal excretion or metabolic conversion. In the clinical trial described in **Chapter 4**, glomerular filtration rate (GFR), measured by inulin clearance, was determined at six different time-points across the 24-hour period in twelve healthy subjects. Time of day significantly affected GFR, with the highest value at 9:00 in the morning and the lowest value at 01:00 at night, which is in line with previous research (Buijsen et al., 1994; Koopman et al., 1989; Voogel et al., 2001). However, the relative difference in GFR between these two time points was 9%, which is too small to be clinically relevant. Likewise, in **Chapter 4**, we could not identify significant 24-hour rhythmicity in

the clearance of levofloxacin, a drug mainly eliminated through passive renal elimination (Fish and Chow, 1997). Hence, 24-hour variation in kidney function minimally affects the pharmacokinetic profile of levofloxacin at different time-points throughout the day and night.

In contrast to levofloxacin, the contribution of renal elimination of midazolam is negligible, with the percentage of midazolam that is excreted unchanged in urine being around 0.02% (Smith et al., 1981). Instead, the primary pathway of midazolam elimination is hepatic metabolism by CYP3A enzymes (Thummel et al., 1996). In **Chapter 3**, a small but significant 24-hour rhythm was identified in the clearance of midazolam with a peak at 18:50 in the evening. As midazolam has an extraction rate of 35% (Tsunoda et al., 1999), this rhythm is probably not due to variation in hepatic blood flow (Lemmer and Nold, 1991), but rather to 24-hour variation in hepatic CYP3A activity (Ohno et al., 2000; Takiguchi et al., 2007). Of note, CYP3A4 transcript levels in serum-shocked cultured human hepatic cells vary over the 24-hour period by more than threefold, while we and others find a rhythm in midazolam clearance with a relative amplitude of 10-15% (Tomalik-Scharte et al., 2014). Additionally, simulations revealed that this rhythm has a limited effect on the concentration-time profiles of midazolam in plasma after intravenous dosing. This demonstrates the need for translational approaches that directly try to establish a mechanistic link between changes in gene expression with functional characterization of physiological processes.

**Daily variation in drug-effect relationships**

In addition to daily rhythms in pharmacokinetics, the relationship between drug concentration and the desired therapeutic effect and/or adverse side-effects may also show 24-hour variation. As discussed in **Chapter 1**, there is ample evidence that the effect or toxicity of many drugs varies over the 24-hour period. However, the quantification of these relationships through PK-PD modelling is not commonly performed. In **Chapter 5**, we investigated whether the extent of drug-induced QT prolongation depends on the time of day and show that PK-PD modelling is a powerful tool to assess 24-hour variation in drug-effect relationships.

Drug-induced QT prolongation, a sign of delayed ventricular repolarization manifested on the electrocardiogram (ECG), is a common side-effect of many different types of drugs that can result in potentially fatal ventricular arrhythmias (Kannankeril et al., 2010). The ICH E14 guidelines, formulated by the International Conference on Harmonisation (ICH) and subsequently adopted by the regulatory agencies in the US, Europe and Japan, stipulate the execution of a "thorough QT/QTc" (TQT) study for all new drugs prior to approval (ICH, 2005). This involves a dedicated clinical trial in which the effect of a placebo, a therapeutic and a supra-therapeutic dose on the QT interval is carefully evaluated. The potential of a drug to prolong the QT interval is determined by calculating the baseline-subtracted mean change in the QT interval at multiple time-points after dosing compared to placebo. If the upper bound of the 95% confidence interval exceeds 10ms, the TQT study is regarded positive, i.e. it confirms the null-hypothesis that the drug has an effect on the QT interval. The outcome

of a TQT study has large impact, as a positive trial requires substantial ECG monitoring during the subsequent phases of drug development (Darpo et al., 2015).

Levofloxacin prolongs the QT interval to a small extent (Taubel et al., 2010) through inhibition of hERG potassium channels (Kang et al., 2001). Since hERG channel blockade is the most common mechanism by which drugs prolong the QT interval, levofloxacin was used in Chapter 5 as a model compound to investigate whether drug-induced QT prolongation is influenced by time of day. Building upon the pharmacokinetic model developed in Chapter 4, we show that the sensitivity to levofloxacin varies considerably over the day. This variation was described by a two-harmonic sinusoidal function with a peak in the late afternoon and a trough in the early morning. In the context of studies that provided circumstantial evidence that drugs may alter the daily variation in the duration of the QT interval (Antimisiaris et al., 1994; Watanabe et al., 2012), **Chapter 5** is the first study to characterize and quantify this relationship.

The finding that the sensitivity to a QT-prolonging drug varies over the 24-hour period is relevant for the recent reports that provide a mechanistic link between circadian rhythmicity and the development of cardiac arrhythmias. In mice, circadian variation in QT interval duration is controlled by the transcription factor Klf15, which is rhythmically expressed in cardiomyocytes (Jeyaraj et al., 2012). This control is possibly exerted through the rhythmic induction of KChIP2 expression, a critical subunit involved in cardiac repolarisation. Aberrant expression of Klf15 results in a loss of rhythmic QT variation and enhances the susceptibility to ventricular arrhythmias (Jeyaraj et al., 2012). Furthermore, the clock gene Bmal1 regulates the expression of Scn5a, a cardiac voltage-gated sodium channel, and Kcnh2, the murine form of hERG potassium channel. In the absence of Bmal1, ventricular repolarization is altered (Schroder et al., 2013, 2015). These findings indicate that rhythmic transcription of cardiac ion channels may affect the electrophysiology of the heart. Future studies are warranted to investigate if and to what extent the rhythmic expression of ion channels provides an explanation for the time-of-day dependent changes in cardiac sensitivity to QT prolonging drugs.

In current practice, each occasion in a TQT study is conducted at the same time of day. In this way, the 24-hour variation in the baseline QT interval and the autonomic changes that occur during sleep can be controlled for (Browne et al., 1983; Extramiana et al., 1999). However, this approach relies on the implicit assumption that drug-induced QT prolongation is independent of time of day, potentially introducing a bias in TQT studies that might lead to an inaccurate assessment of the risk to patients who may take the drug at any time point (Dallmann et al., 2014). Our clinical trial simulation-based results presented in **Chapter 5** challenge this assumption by showing that the extent of levofloxacin-induced QT prolongation is heavily influenced by dosing time, with the largest effect of 1.73 [95% P.I. 1.56-1.90] ms per mg/L predicted after dosing at 14:00 and the smallest effect of -0.04 [-0.19-0.12] ms per mg/L after dosing at 06:00. Accordingly, we found that the predicted probability of a positive outcome of a dedicated QT trial varies considerably over the course of the day, with the highest probability observed after drug administration at 14:00 and

the lowest probability after drug administration at night (22:00, 02:00 and 06:00). Although future research is warranted to investigate whether these findings can be replicated with other QT-prolonging drugs under placebo-controlled conditions, it suggests that the time at which clinical trials are conducted may introduce bias in testing drug-induced QT prolongation. Hence, current drug safety evaluations may systematically misjudge the risk to patients by ignoring time of day.

## DESIGN OF CHRONOPHARMACOLOGICAL STUDIES

An overarching feature of the studies described in **Chapter 3-7** is that they were prospectively designed to evaluate the effect of time of day on the pharmacokinetic and/or pharmacodynamic properties of various probe drugs. Among the many chronopharmacological studies cited in **Chapter 1** that used a limited number of dosing times and therefore may have missed the peak and trough of the parameters of interest, a key asset of the studies described in this thesis is the use of six dosing times equally distributed over the 24-hour period. As described in more detail below, this allowed us to precisely characterize the variation in pharmacokinetic or pharmacodynamic parameters over the 24-hour period through the use of mathematical modelling and simulation.

The studies described in this thesis were conducted under tightly controlled laboratory conditions. For example, the studies described in **Chapter 3, 4** and **5** were conducted in healthy male volunteers with an intermediate chronotype and a stable diurnal activity rhythm. This was assessed through a chronotype questionnaire, sleep diaries and actigraphy recordings prior to the study. During the study days, sleep disturbance was kept to a minimum and subjects wore eye masks during the night to prevent any disruptive effect of light exposure or sleep deprivation on physiological rhythms (Mullington et al., 2009). Additionally, the timing of food and water intake was tightly controlled to limit their potential influence (Singh, 1999). This approach allowed determining 24-hour variations in the pharmacokinetics and pharmacodynamics of drugs with as little confounders as possible. These dedicated clinical trials provide a basis for further research under more realistic conditions. In this regard, population-wide studies such as the Rotterdam Study are valuable sources of data that can be used to assess drug exposure and effect in typical patient populations under real-life conditions (Chain et al., 2013).

## PK-PD MODELLING IN CHRONOPHARMACOLOGY

Pharmacokinetic-pharmacodynamic modelling is being increasingly used within the academia and pharmaceutical industry to guide decisions in drug discovery and development. In this thesis, PK-PD modelling was applied to the field of chronopharmacology, with special attention given to the means to identify 24-hour variation in pharmacokinetic and pharmacodynamic parameters.

In **Chapter 1**, it was put forward that diagnostic plots are an essential tool to facilitate the identification of 24-hour variation in the model parameters, although their use is rarely
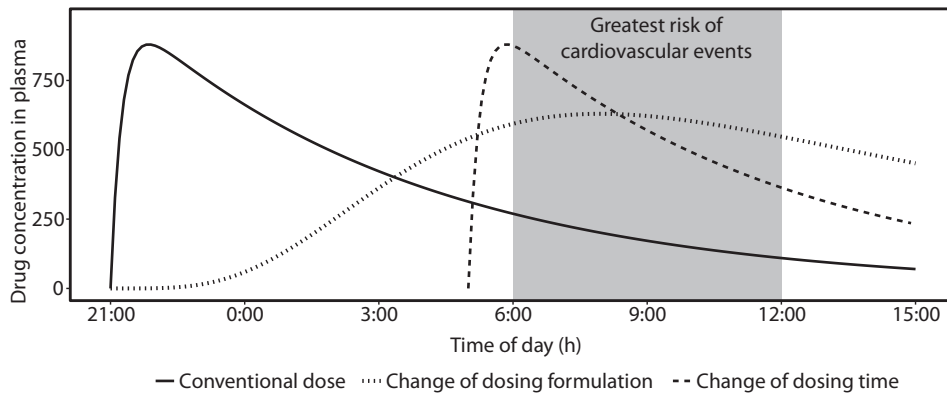
**Figure 1** Modification of dosing regimen to provide optimal exposure at the desired time window. Administration of a conventional hypertensive drug before bedtime results in low drug concentrations in plasma during the time window during which the risk of cardiovascular events is greatest (solid line). Adjusting dosing time (dashed line) results in higher concentrations during this period but requires administration at an unpractical point of time. Adjusting the dosing formulation to a delayed onset sustained-release form (dotted line) provides favourable concentrations during the entire critical time-window and allows for a more practical dosing time. Image adapted from Wertheimer et al., 2005.

reported. In the PK-PD models that were developed in the context of the research described in this thesis, graphical evaluation of the improvement of fit has been instrumental. In **Chapter 3**, describing the bioavailability and the clearance of midazolam by sinusoidal functions with a period of 24 hours resolved the time-of-day dependent bias observed in the interoccasion variability, in addition to improving the fit of the model as judged by the decrease in objective function value (OFV). Likewise, accounting for the increase in the absorption rate constant at 14:00 reduced the bias in interoccasion variability in this parameter. Similarly, in **Chapter 4**, it was found that the distribution of interoccasion variability on the absorption rate constant of levofloxacin varied over the 24-hour period, which could also be described by a sinusoidal function. In **Chapter 5**, a large degree of interoccasion variability was present on QT0, the parameter that describes the QT interval at baseline, which was reduced to 0 after accounting for the time-of-day dependent changes in the levofloxacin-QT relationship. The distribution of residuals over time of day can also be used to visualize an improvement of fit (Lee et al., 2014). In **Chapter 5**, the bias in the distribution of the conditional weighted residuals with interaction (CWRESI) over time of day was removed after inclusion of the sinusoidal function on the levofloxacin-QT relationship. In **Chapter 7**, similar improvements were noted in the CWRESI distribution over time by describing the efflux from morphine from the brain to plasma by a sinusoidal function. These approaches to identify systematic 24-hour variation during the development of a pharmacokinetic and pharmacodynamic model can be applied to future chronopharmacological research.

Throughout this thesis, sinusoidal functions have been used to describe variation in pharmacokinetic and pharmacodynamic parameters, while, as discussed in **Chapter 1,** previous studies typically used dosing time as a covariate. It could be argued that using dosing time as a covariate is a less biased approach as it does not make assumptions regarding the shape of the variation. However, sinusoidal functions have several advantages

as it provides a continuous description of parameters over time. This allows for the simulation of dosing times and regimens that were not investigated in the original study. In **Chapter 4, 5** and **7**, the advantage of this approach was shown through the use of simulations. For example, in **Chapter 5**, we were able to show that dosing time may introduce bias in the predicted outcome of thorough QT-like studies. Additionally, the use of sinusoidal functions is helpful in the case of drugs with a long half-life, as the physiological processes underlying the pharmacokinetic parameters will continue to change after dosing.

Together, these strategies can be used to support decisions during the development of chronopharmacological models.

# CLINICAL IMPLICATIONS

A key question that emerges from this thesis concerns the implications for drug development and clinical practice.

### Chronopharmacology in drug development

Collectively, the studies described in this thesis have shown that time of day is a considerable source of variation in the pharmacokinetic and pharmacodynamic parameters of a drug that can be identified and precisely quantified through modelling and simulation. If not taken into consideration, time-of-day dependent variation can be easily mistaken for inter- or intraindividual variation. However, characterizing time of day during drug development is not only required to account for and understand this source of variation, it is also essential in order to benefit from systematic fluctuations in physiology. For example, the finding that P-gp mediated transport differs by more than two-fold between the day and night (**Chapter 6**), can be employed to optimize the exposure of P-gp substrates to the brain. Therapeutic P-gp substrates that have their target in the brain, such as those used for the treatment of neurological disorders, should be dosed at the time at which the exposure is maximal. P-gp
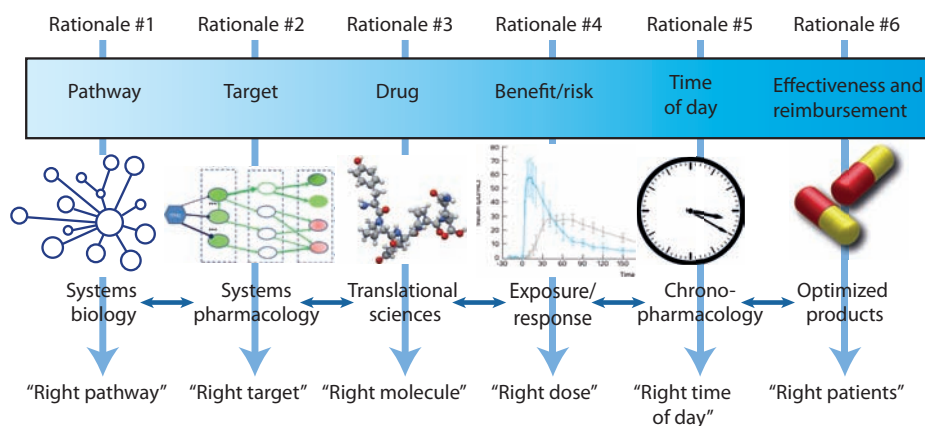


**Figure 2** The integrated view of model-based drug discovery and development, expanded to include chronopharmacology. This paradigm, without rationale #5, was originally presented by van der Graaf and Benson (2011). The research presented in this thesis shows that this paradigm should be extended to include chronopharmacological considerations. Figure adapted from Milligan et al. (2013).

substrates that act systemically and that inflict adverse neurological side effects, should be dosed at the time at which the exposure to the brain is minimal. Modulating transporter function at the human BBB through pharmacological means has proven difficult (Kalvass et al., 2013). In this light, the changes that might occur under normal physiological conditions might be of interest. Therefore, future research is warranted to investigate to what extent the results presented in **Chapter 6** apply to human patients.

Additionally, the results presented in **Chapter 5** ask for more attention on dosing time-dependent effects during drug development as a means of reducing the risk to patients once a drug is released on the market. If the findings presented in this chapter apply to other hERG inhibiting drugs in a placebo-controlled clinical trial, this calls for a circadian testing policy to be adopted by drug developers, at least in the context of drug-induced QT prolongation (Dallmann et al., 2014).

### Chronopharmacology in clinical practice

In a clinical setting, the aim of chronopharmacology is to time therapies such that the effect is maximal while the unwanted side-effects are minimal. This can be achieved in two ways: either by adjusting the administration time of conventional drug formulations and/or by altering the formulation (Figure 1) (Kaur et al., 2016). However, these strategies require accurate patient adherence, which may be an issue especially when drug are taken by patients at home (Smolensky and Peppas, 2007). Timing compliance has been reported to be particularly low. For example, the percentage of doses taken within an 8±1 h interval of a three times daily oral dose of an antibiotic was reported to be as low as 10.9% (Cals et al., 2008). In this light, worth noticing that morning compliance is generally higher than evening compliance (for example Kahook and Noecker, 2007; Kardas, 2004; Vrijens et al., 2008), although the opposite has been reported as well (Jonasson, 2000). Hence, the low degree of time-of-day dependent compliance should be taken into account when devising chronopharmacological dosing regimens.

One strategy to increase compliance would be proper training of the clinicians and pharmacists that instruct patients about optimal drug use (Kaur et al., 2016). However, another promising avenue for the field of chronotherapy is the development of programmable pumps and other advanced drug delivery systems that, for example, release drugs in response to circulating biomarker levels in the blood (Smolensky and Peppas, 2007).

## CONCLUDING REMARKS AND FUTURE PERSPECTIVES

In their seminal paper on systems pharmacology, van der Graaf and Benson (2011) stated that for modelling and simulation to achieve its full potential, the different stages of the R&D cycle should be integrated into an enhanced quantitative drug discovery and development paradigm that includes identification of the "right pathway, right target, right molecule, right dose and right patient". This thesis indicates that this paradigm should be extended to include the "right time of day" (Figure 2) and provides a framework for integrating of this

principle in the field of modelling and simulation.

As shown in Figure 2, full implementation of chronopharmacology during drug discovery and development requires integration of this field among the other disciplines employed in the field of pharmacology. Therefore, translational studies that aim to unravel the underlying mechanisms will be instrumental to the advancement of chronopharmacology in the clinic. Recently, it was reported that the majority of best-selling drugs directly target the product of a gene that is rhythmically expressed, suggesting that the effect of these drugs depend on the time of day (Zhang et al., 2014). Together with the systematic approach presented in this thesis, this opens up new avenues for further research into the effect of time on the exposure and effect of drugs that can bridge the gap from bench to bedside.

# REFERENCES

Antimisiaris, M., Sarma, J.S.M., Schoenbaum, M.P., Sharma, P.P., Venkataraman, K., Singh, B.N., and Christenson, P. (1994). Effects of amiodarone on the circadian rhythm and power spectral changes of heart rate and QT interval: Significance for the control of sudden cardiac death. Am. Heart J. 128, 884–891.

Baraldo, M. (2008). The influence of circadian rhythms on the kinetics of drugs in humans. Expert Opin. Drug Metab. Toxicol. 4, 175–192.

Bornschein, R.L., Crockett, R.S., and Smith, R.P. (1977). Diurnal variations in the analgesic effectiveness of morphine in mice. Pharmacol. Biochem. Behav. 6, 621–626.

Browne, K.F., Prystowsky, E., Heger, J.J., Chilson, D.A., and Zipes, D.P. (1983). Prolongation of the Q-T interval in man during sleep. Am. J. Cardiol. 52, 55–59.

Buijsen, J.G., van Acker, B.A., Koomen, G.C., Koopman, M.G., and Arisz, L. (1994). Circadian rhythm of glomerular filtration rate in patients after kidney transplantation. Nephrol.Dial.Transplant. 9, 1330–1333.

Cals, J.W.L., Hopstaken, R.M., Le Doux, P.H.A., Driessen, G.A., Nelemans, P.J., and Dinant, G.-J. (2008). Dose timing and patient compliance with two antibiotic treatment regimens for lower respiratory tract infections in primary care. Int. J. Antimicrob. Agents 31, 531–536.

Chain, A.S.Y., Dieleman, J.P., van Noord, C., Hofman, A., Stricker, B.H.C., Danhof, M., Sturkenboom, M.C.J.M., and Della Pasqua, O. (2013). Not-in-trial simulation I: Bridging cardiovascular risk from clinical trials to real-life conditions. Br. J. Clin. Pharmacol. 76, 964–972.

Cui, Y., Sugimoto, K., Araki, N., Sudoh, T., and Fujimura, A. (2005). Chronopharmacology of morphine in mice. Chronobiol. Int. 22, 515–522.

Dallmann, R., Brown, S.A., and Gachon, F. (2014). Chronopharmacology: new insights and therapeutic implications. Annu. Rev. Pharmacol. Toxicol. 54, 339–361.

Darpo, B., Benson, C., Dota, C., Ferber, G., Garnett, C., Green, C.L., Jarugula, V., Johannesen, L., Keirns, J., Krudys, K., et al. (2015). Results from the IQ-CSRC prospective study support replacement of the thorough QT study by QT assessment in the early clinical phase. Clin. Pharmacol. Ther. 97, 326–335.

Dohoo, S. (1997). Steady-state pharmacokinetics of oral sustained-release morphine sulphate in dogs. J. Vet. Pharmacol. Ther. 20, 129–133.

Drusano, G.L. (2004). Antimicrobial pharmacodynamics: critical interactions of "bug and drug". Nat. Rev. Microbiol. 2, 289–300.

Extramiana, F., Maison-Blanche, P., Badilini, F., Pinoteau, J., Deseo, T., and Coumel, P. (1999). Circadian modulation of QT rate dependence in healthy volunteers. J. Electrocardiol. 32, 33–43.

Fish, D.N., and Chow, A.T. (1997). The clinical pharmacokinetics of levofloxacin. Clin. Pharmacokinet. 32, 101–119.

Gourlay, G.K., Plummer, J.L., and Cherry, D.A. (1995). Chronopharmacokinetic variability in plasma morphine concentrations following oral doses of morphine solution. Pain 61, 375–381.

van der Graaf, P.H., and Benson, N. (2011). Systems pharmacology: bridging systems biology and pharmacokinetics-pharmacodynamics (PKPD) in drug discovery and development. Pharm. Res. 28, 1460–1464.

Güney, H.Z., Görgün, C.Z., Tunçtan, B., Uludağ, O., Hodoğlugil, U., Abacioğlu, N., and Zengil, H. (1998). Circadian-rhythm-dependent effects of L-NG-nitroarginine methyl ester (L-NAME) on morphine-induced analgesia. Chronobiol. Int. 15, 283–289.

ICH (2005). E14 Clinical evaluation of QT/QTc interval prolongation and proarrhythmic potential for non-antiarrhythmic drugs. Guidance to industry. Fed. Regist. 70, 61134–61135.

Jessen, N.A., Munk, A.S.F., Lundgaard, I., and Nedergaard, M. (2015). The Glymphatic System: A Beginner's Guide. Neurochem. Res. 40, 2583–2599.

Jeyaraj, D., Haldar, S.M., Wan, X., McCauley, M.D., Ripperger, J.A., Hu, K., Lu, Y., Eapen, B.L., Sharma, N., Ficker, E., et al. (2012). Circadian rhythms govern cardiac repolarization and arrhythmogenesis. Nature 483, 96–99.

Jonasson, G. (2000). Asthma drug adherence in a long term clinical trial. Arch. Dis. Child. 83, 330–333.

Kahook, M.Y., and Noecker, R.J. (2007). Evaluation of adherence to morning versus evening glaucoma medication dosing regimens. Clin. Ophthalmol. 1, 79–83.

Kalvass, J.C., Polli, J.W., Bourdet, D.L., Feng, B., Huang, S.-M., Liu, X., Smith, Q.R., Zhang, L.K., and Zamek-Gliszczynski, M.J. (2013). Why clinical modulation of efflux transport at the human blood-brain barrier is unlikely: the ITC evidence-based position. Clin. Pharmacol. Ther. 94, 80–94.

Kang, J., Wang, L., Chen, X.-L., Triggle, D.J., and Rampe, D. (2001). Interactions of a Series of Fluoroquinolone Antibacterial Drugs with the Human Cardiac K+ Channel HERG. Mol. Pharmacol. 59, 122–126.

Kannankeril, P., Roden, D.M., and Darbar, D. (2010). Drug-induced long QT syndrome. Pharmacol. Rev. 62, 760–781.

Kardas, P. (2004). Comparison of once daily versus twice daily oral nitrates in stable angina pectoris. Am. J. Cardiol. 94, 213–216.

Kaur, G., Gan, Y.-L., Phillips, C.L., Wong, K., and Saini, B. (2016). Chronotherapy in practice: the perspective of the community pharmacist. Int. J. Clin. Pharm. 38, 171–182.

Kavaliers, M., and Hirst, M. (1983). Daily rhythms of analgesia in mice: effects of age and photoperiod. Brain Res. 279, 387–393.

Klotz, U., and Reimann, I.W. (1984). Chronopharmacokinetic study with prolonged infusion of midazolam. Clin. Pharmacokinet. 9, 469–474.

Klotz, U., and Ziegler, G. (1982). Physiologic and temporal variation in hepatic elimination of midazolam. Clin. Pharmacol. Ther. 32, 107–112.

Koopman, M.G., Koomen, G.C., Krediet, R.T., de Moor, E.A., Hoek, F.J., and Arisz, L. (1989). Circadian rhythm of glomerular filtration rate in normal individuals. Clin. Sci. (Lond). 77, 105–111.

Koopmans, R., Dingemanse, J., Danhof, M., Horsten, G.P., and van Boxtel, C.J. (1991). The influence of dosage time of midazolam on its pharmacokinetics and effects in humans. Clin. Pharmacol. Ther. 50, 16–24.

Kusuhara, H., Suzuki, H., Terasaki, T., Kakee, A., Lemaire, M., and Sugiyama, Y. (1997). P-Glycoprotein mediates the efflux of quinidine across the blood-brain barrier. J. Pharmacol. Exp. Ther. 283, 574–580.

De Lange, E.C.M. (2013). The mastermind approach to CNS drug therapy: translational prediction of human brain distribution, target site kinetics, and therapeutic effects. Fluids Barriers CNS 10, 12.

Lee, D., Son, H., Lim, L.A., and Park, K. (2014). Population pharmacokinetic analysis of diurnal and seasonal variations of plasma concentrations of cilostazol in healthy volunteers. Ther. Drug Monit. 36, 771–780.

Lemmer, B., and Nold, G. (1991). Circadian changes in estimated hepatic blood flow in healthy subjects. Br. J. Clin. Pharmacol. 32, 627–629.

Lutsch, E.F., and Morris, R.W. (1971). Light reversal of a morphine-induced analgesia susceptibility rhythm in mice. Experientia 27, 420–421.

Milligan, P.A., Brown, M.J., Marchant, B., Martin, S.W., van der Graaf, P.H., Benson, N., Nucci, G., Nichols, D.J., Boyd, R.A., Mandema, J.W., et al. (2013). Model-based drug development: a rational approach to efficiently accelerate drug development. Clin. Pharmacol. Ther. 93, 502–514.

Mistry, P., Stewart, A.J., Dangerfield, W., Okiji, S., Liddle, C., Bootle, D., Plumb, J.A., Templeton, D., and Charlton, P. (2001). In vitro and in vivo reversal of P-glycoprotein-mediated multidrug resistance by a novel potent modulator, XR9576. Cancer Res. 61, 749–758.

Morris, R.W., and Lutsch, E.F. (1967). Susceptibility to morphine-induced analgesia in mice. Nature 216, 494–495.

Mullington, J.M., Haack, M., Toth, M., Serrador, J.M., and Meier-Ewert, H.K. (2009). Cardiovascular, inflammatory, and metabolic consequences of sleep deprivation. Prog. Cardiovasc. Dis. 51, 294–302.

Ohno, M., Yamaguchi, I., Ito, T., Saiki, K., Yamamoto, I., and Azuma, J. (2000). Circadian variation of the urinary 6β-hydroxycortisol to cortisol ratio that would reflect hepatic CYP3A activity. Eur. J. Clin. Pharmacol. 55, 861–865.

Oliverio, A., Castellano, C., and Puglisi-Allegra, S. (1982). Opiate analgesia: Evidence for circadian rhythms in mice. Brain Res. 249, 265–270.

Preston, S.L., Drusano, G.L., Berman, A.L., Fowler, C.L., Chow, A.T., Dornseif, B., Reichl, V., Natarajan, J., and Corrado, M. (1998). Pharmacodynamics of Levofloxacin. JAMA 279, 125–129.

Rasmussen, N.A., and Farr, L.A. (2003). Effects of Morphine and Time of Day on Pain and Beta-Endorphin. Biol. Res. Nurs. 5, 105–116.

Savolainen, H., Meerlo, P., van Waarde, A., Elsinga, P., Windhorst, A.D., Colabufo, N., and Luurtsema, G. (2015). PET imaging of P-glycoprotein function at the rodent BBB: Diurnal fluctuations and impact of sleep deprivation. In EANM Congress, p. OP286.

Schroder, E.A., Lefta, M., Zhang, X., Bartos, D.C., Feng, H.-Z., Zhao, Y., Patwardhan, A., Jin, J.-P., Esser, K.A., and Delisle, B.P. (2013). The cardiomyocyte molecular clock, regulation of Scn5a, and arrhythmia susceptibility. Am. J. Physiol. Cell Physiol. 304, C954–C965.

Schroder, E.A., Burgess, D.E., Zhang, X., Lefta, M., Smith, J.L., Patwardhan, A., Bartos, D.C., Elayi, C.S., Esser, K.A., and Delisle, B.P. (2015). The Cardiomyocyte Molecular Clock Regulates the Circadian Expression of Kcnh2 and Contributes to Ventricular Repolarization. Hear. Rhythm.

Singh, B.N. (1999). Effects of food on clinical pharmacokinetics. Clin. Pharmacokinet. 37, 213–255.

Smith, M.T., Eadie, M.J., and Brophy, T.O. (1981). The pharmacokinetics of midazolam in man. Eur. J. Clin. Pharmacol. 19, 271–278.

Smolensky, M.H., and Peppas, N.A. (2007). Chronobiology, drug delivery, and chronotherapeutics. Adv. Drug Deliv. Rev. 59, 828–851.

Sziráki, I., Erdo, F., Beéry, E., Molnár, P.M., Fazakas, C., Wilhelm, I., Makai, I., Kis, E., Herédi-Szabó, K., Abonyi, T., et al. (2011). Quinidine as an ABCB1 probe for testing drug interactions at the blood-brain barrier: an in vitro in vivo correlation study. J. Biomol. Screen. 16, 886–894.

Takiguchi, T., Tomita, M., Matsunaga, N., Nakagawa, H., Koyanagi, S., and Ohdo, S. (2007). Molecular basis for rhythmic expression of CYP3A4 in serum-shocked HepG2 cells. Pharmacogenet. Genomics 17, 1047–1056.

Taubel, J., Naseem, A., Harada, T., Wang, D., Arezina, R., Lorch, U., and Camm, A.J. (2010). Levofloxacin can be used effectively as a positive control in thorough QT/QTc studies in healthy volunteers. Br. J. Clin. Pharmacol. 69, 391–400.

Thummel, K.E., O'Shea, D., Paine, M.F., Shen, D.D., Kunze, K.L., Perkins, J.D., and Wilkinson, G.R. (1996). Oral first-pass elimination of midazolam involves both gastrointestinal and hepatic CYP3A-mediated metabolism. Clin. Pharmacol. Ther. 59, 491–502.

Tomalik-Scharte, D., Suleiman, A.A., Frechen, S., Kraus, D., Kerkweg, U., Rokitta, D., Di Gion, P., Queckenberg, C., and Fuhr, U. (2014). Population pharmacokinetic analysis of circadian rhythms in hepatic CYP3A activity using midazolam. J. Clin. Pharmacol. 54, 1162–1169.

Tsunoda, S.M., Velez, R.L., von Moltke, L.L., and Greenblatt, D.J. (1999). Differentiation of intestinal and hepatic cytochrome P450 3A activity with use of midazolam as an in vivo probe: effect of ketoconazole. Clin. Pharmacol. Ther. 66, 461–471.

Voogel, A.J., Koopman, M.G., Hart, A.A., van Montfrans, G.A., and Arisz, L. (2001). Circadian rhythms in systemic hemodynamics and renal function in healthy subjects and patients with nephrotic syndrome. Kidney Int. 59, 1873–1880.

Vrijens, B., Vincze, G., Kristanto, P., Urquhart, J., and Burnier, M. (2008). Adherence to prescribed antihypertensive drug treatments: longitudinal study of electronically compiled dosing histories. BMJ 336, 1114–1117.

Watanabe, J., Suzuki, Y., Fukui, N., Ono, S., Sugai, T., Tsuneyama, N., and Someya, T. (2012). Increased risk of antipsychotic-related QT prolongation during nighttime: a 24-hour holter electrocardiogram recording study. J. Clin. Psychopharmacol. 32, 18–22.

Wertheimer, A.I., Santella, T.M., Finestone, A.J., and Levy, R.A. (2005). Drug delivery systems improve Pharmaceutical profile and facilitate medication adherence. Adv. Ther. 22, 559–577.

Westerhout, J., Smeets, J., Danhof, M., and de Lange, E.C.M. (2013). The impact of P-gp functionality on non-steady state relationships between CSF and brain extracellular fluid. J. Pharmacokinet. Pharmacodyn. 40, 327–342.

Xie, L., Kang, H., Xu, Q., Chen, M.J., Liao, Y., Thiyagarajan, M., O'Donnell, J., Christensen, D.J., Nicholson, C., Iliff, J.J., et al. (2013). Sleep drives metabolite clearance from the adult brain. Science 342, 373–377.

Yoshida, M., Ohdo, S., Takane, H., Tomiyoshi, Y., Matsuo, A., Yukawa, E., and Higuchi, S. (2003). Chronopharmacology of analgesic effect and its tolerance induced by morphine in mice. J. Pharmacol. Exp. Ther. 305, 1200–1205.

Zhang, R., Lahens, N.F., Ballance, H.I., Hughes, M.E., and Hogenesch, J.B. (2014). A circadian gene expression atlas in mammals: Implications for biology and medicine. Proc. Natl. Acad. Sci. 111, 16219–16224.

**SUMMARY**
**SAMENVATTING**
**CURRICULUM VITAE**
**LIST OF PUBLICATIONS**
**DANKWOORD**

# SUMMARY

Organisms across all kingdoms of life have evolved an endogenous timing system that entrains them to the 24-hour light-dark cycles present on the Earth. This allows them to anticipate to daily, predictable changes in the environment, such as variations in light intensity, temperature and food availability.

At the single-cell level, this so-called circadian timing system is regulated by a transcriptional/ translational feedback loop that generates 24-hour rhythms in gene expression levels in nearly all cell types. In mammals, synchronization of these cell-autonomous rhythms is coordinated by neuronal and humoral signals from the suprachiasmatic nuclei (SCN) in the hypothalamus. The rhythms generated by the SCN are entrained to the environmental light/dark cycle by photic input that is transmitted from the retina to the SCN.

Because of the circadian timing system, many physiological processes, including those involved in the absorption, distribution, metabolism, elimination, pharmacodynamics and toxicity of therapeutic drugs, show profound fluctuations over the course of the day, leading to time-of-day dependent changes in the exposure and effect of drugs. Chronopharmacology is the discipline that investigates the effect of daily variations in physiology on the exposure, therapeutic effect and toxicity of drugs.

In **Chapter 1**, it was discussed that the field of chronopharmacology could benefit from the development of a systematic approach to analyse and integrate the findings obtained in the many studies that investigate the effect of time of day on drug exposure and effect. PKPD modelling was introduced as a promising approach that could overcome some of the limitations encountered within this field of research.

As described in **Chapter 2**, the aim of this thesis was to provide a structured framework for the analysis of chronopharmacological studies, while touching upon several critical issues encountered during the development and optimization of new and existing drug treatments. The general approach taken in this thesis was put forward in Chapter 2, which consists of 1) the use of model compounds; 2) a strict study design with sufficient number of dosing times; and 3) the use of PKPD modelling.

The clinical trial is described in **Chapter 3** was designed to study 24-hour variation in the pharmacokinetics of midazolam, a benzodiazepine used in the treatment of insomnia and a model compound to study CYP3A-mediated metabolism. Midazolam was administered to twelve healthy male subjects at six different time-points throughout the 24-hour cycle in a randomized crossover design. A semi-simultaneous dosing regimen was used in which oral and intravenous dosing was combined in order to assess all pharmacokinetic parameters within one study occasion. It was found that oral bioavailability and absorption rate constant showed considerable daily variation, while the clearance of midazolam showed minor fluctuations over the day and night. Using simulations, it was shown that time of drug administration affects concentration-time profiles after oral dosing but not after

intravenous dosing. This indicates that 24-hour variation in CYP3A-mediated metabolism is of limited clinical relevance, while time-of-day dependency in absorptive processes does influence the exposure to midazolam.

The aim of the clinical trial described in **Chapter 4** was to identify potential 24-hour variation in the pharmacokinetic parameters of an oral dose of levofloxacin administered to twelve healthy male subjects. The pharmacokinetic properties of levofloxacin are characterized by solubility and permeability-independent absorption and passive renal elimination. We found that the absorption rate constant could be described as a cosine function with a period of 24 hours, a relative amplitude of 47% and a peak around 8:00 in the morning. Other pharmacokinetic parameters, including clearance, did not show significant daily variation. Despite the variation in absorption rate constant of levofloxacin, simulations of a once-daily dosing regimen show that the exposure and maximal concentration, two parameters important for the effectiveness of levofloxacin as an antibiotic, are not affected by time of drug administration. From these findings, we concluded that in terms of its pharmacokinetics, levofloxacin can be dosed without taking into account time of day. However, these findings are relevant for drugs with similar physicochemical properties as levofloxacin but with a narrower therapeutic index.

In the clinical trial described in Chapter 4, the effect of levofloxacin on the QT interval, a read-out of ventricular repolarization on the electrocardiogram, was also recorded. It is known that levofloxacin, like many other cardiac and non-cardiac drugs, slightly prolongs the QT interval due to an inhibitory action on a type of potassium channel in cardiomyocytes. This is a negative side-effect of many drugs, which, in combination with other predisposing factors, can lead to cardiac arrhythmias and death. However, it was unknown whether the magnitude of the effect of levofloxacin on the QT interval depends on the time of drug administration. In **Chapter 5**, the effect of time of day on the relationship between the concentration of levofloxacin and length of the QT interval was explored. A pharmacokinetic-pharmacodynamic model was developed to account for variations in pharmacokinetics, heart rate and daily variation in baseline QT. It was found that the effect of levofloxacin on the QT interval varies considerably and systematically over the course of the day. As a result, clinical trial simulations show that levofloxacin-induced QT prolongation depends on dosing time, with the largest effect predicted at 14:00 and the smallest effect at 06:00. These findings indicate that current approaches to assess drug-induced QTc prolongation, in which drugs are typically administered in the morning, may be biased and potentially misjudge the risk to patients.

Knowledge of a drug's concentration at the target site is an important aspect in the development and optimization of pharmacological treatments, especially when their target is in tissues that are hard to reach, such as the central nervous system. In addition to the structural protection provided by the tightly connected cells of the blood-brain barrier, the central nervous system is also protected by specialized efflux transporters such as P-glycoprotein. These efflux transporters function to expel potentially toxic molecules, including therapeutic drugs, from the brain back into the blood. The objective of the study

described in **Chapter 6** was to determine 24-hour variation in the distribution of the P-gp substrate quinidine to the brain. After administration of an intravenous dose of quinidine at six separate time-points in a pre-clinical animal model, we found that the exposure to quinidine in the brain is affected by time of drug administration, but only when P-gp transport is fully functional. Subsequent intracerebral microdialysis experiments and data analysis using physiologically-based pharmacokinetic modelling revealed that this time-of-day dependency is primarily due to higher activity of P-gp mediated transport from the deep brain compartment to the plasma compartment during the night. This study shows that taking into account time of day may be an important determinant of drug distribution to the brain and thereby offers a potential novel strategy to optimize drug treatments targeted at the brain.

In **Chapter 7**, daily variation in the blood and brain pharmacokinetics of morphine, a substrate of various transporters that are expressed in the blood-brain barrier, were studied in a preclinical animal model. The use of two inhibitors of the transporters that affect morphine exposure allowed us to determine the relative contribution of active and passive processes in the pharmacokinetic parameters. It was found that the active processes that regulate the clearance of morphine and its metabolite M3G from plasma shows considerable 24-hour variation. Moreover, the efflux of morphine from the brain back into the blood is characterized by a 24-hour rhythm. The lowest efflux occurs at the two light-dark transitions. Simulations reveal that as a result of this, the exposure to morphine in the brain and to M3G in plasma depends on the time of drug administration. We conclude that time of day is a source of variation in the systemic pharmacokinetics and brain distribution of morphine, which may partly explain the daily rhythms in its analgesic properties that have been reported in earlier studies.

The research described in this thesis was discussed in **Chapter 8**. Taken together, these studies show that time of day can present a considerable source of variation in the pharmacokinetic and pharmacodynamic parameters of a drug, which can be identified and quantified through modelling and simulation. Understanding the effect of time of day on the exposure and effect of drugs is required to account for this source of variation. More importantly, chronopharmacological aspects should not be overlooked in order to benefit from the systematic fluctuations in physiological processes during the development and optimization of drug treatments.

# SAMENVATTING

Organismen in alle rijken van het leven hebben een intern tijdssysteem ontwikkeld dat hen aanpast aan de 24-uurs licht-donker cyclus op aarde. Deze biologische klok zorgt ervoor dat ze kunnen anticiperen op de dagelijkse, voorspelbare veranderingen in hun omgeving, zoals schommelingen in lichtintensiteit, temperatuur en in de beschikbaarheid van voedsel.

Op het niveau van de cel wordt dit zogenoemde circadiane systeem gereguleerd door een moleculair terugkoppelingsmechanisme dat 24-uurs ritmes genereert in genexpressie niveaus. In zoogdieren worden deze cel-autonome ritmes gecoordineerd door neuronale, endocrine and paracrine signalen vanuit de suprachiasmatische nuclei (SCN) in de hypothalamus. Deze door de SCN gegenereerde ritmes worden gesynchroniseerd met de licht-donker cyclus in de omgeving door middel van lichtsignalen die via het netvlies wordt doorgegeven aan de SCN.

Door het bestaan van het circadiane systeem vertonen veel fysiologische processen, waaronder processen die betrokken zijn bij de opname, verdeling, afbraak, uitscheiding, effect en toxiciteit van medicijnen, grote verschillen gedurende de loop van de dag. Dit leidt tot tijdsafhankelijke veranderingen in de blootstelling en effectiviteit van geneesmiddelen. Chronofarmacologie is de wetenschappelijke discipline die het effect van dagelijkse ritmes in fysiologie op de blootstelling, therapeutic effect en toxiciteit van medicijnen bestudeert.

In **Hoofdstuk 1** werd gesteld dat er binnen de chronofarmacologie behoefte is aan de ontwikkeling van een systematische aanpak om de bevindingen van de vele studies naar het effect van het tijdstip van de dag op de blootstelling en het effect van medicijnen te analyseren en te integreren. Farmacokinetisch/farmacodynamisch modeleren werd in dit hoofdstuk naar voren gebracht als een veelbelovende aanpak die enkele beperkingen binnen de chronofarmacologie kan wegnemen.

Zoals beschreven in **Hoofdstuk 2** was het doel van dit proefschrift om een structureel raamwerk te creëren om de resultaten van chronofarmacologische onderzoeken te kunnen analyseren, terwijl we enkele belangrijke kwesties aanstippen die van belang zijn in de ontwikkeling en optimalisatie van nieuwe en bestaande medicinale behandelingen. De algemene aanpak die is gebruikt in dit proefschrift werd beschreven in Hoofdstuk 2, welke bestaat uit 1) het gebruik van modelstoffen; 2) een strikte studieopzet met een voldoende aantal doseertijdstippen en 3) het gebruik van farmacokinetisch/farmacodynamisch modelleren.

Het doel van de klinische studie beschreven in **Hoofdstuk 3** was om 24-uurs variatie in de farmacokinetiek van midazolam te bestuderen in twaalf gezonde mannelijke proefpersonen. Midazolam is een slaapmiddel dat wordt gebruikt voor de behandeling van slapeloosheid en is een modelstof om CYP3A-gemedieerd metabolisme te bestuderen. Op zes verschillende tijdstippen gedurende de dag en nacht werd midazolam oraal en intraveneus semi-simultaan toegediend om alle farmacokinetische parameters te kunnen meten binnen één studiedag. De resultaten wijzen uit dat de biologische beschikbaarheid

en de absorptie snelheidsconstante grote verschillen vertonen afhankelijk van het tijdstip van de dag, terwijl de klaring van midazolam beperkte schommelingen vertoont over de loop van de dag. Door middel van simulaties toonden we aan dat het tijdstip van toedienen de concentratie-tijd profielen alleen beïnvloedt na orale dosering, maar niet intraveneuze toediening. Dit wijst erop dat 24-uurs variatie in CYP3A-gemedieerd metabolism beperkte klinsche relevantie heeft, terwijl tijdsafhankelijke variatie in de processen betrokken bij absorptie wel van invloed zijn op de blootstelling aan midazolam.

Het doel van het onderzoek beschreven in **Hoofdstuk 4** was om 24-uurs variatie in de farmacokinetiek van een orale doses levofloxacine te onderzoeken in twaalf gezonde mannelijke proefpersonen. De farmacokinetische eigenschappen van dit medicijn worden gekenmerkt door absorptie die onafhankelijk is van de oplosbaarheid en permeabiliteit en door passieve renale klaring. Onze resultaten lieten zien dat de absorptie snelheidsconstante kon worden beschreven door een cosinus functie met een periode van 24 uur, een relatieve amplitude van 47% en een piek om 8 uur 's ochtends. Andere farmacokinetische parameters, waaonder klaring, vertoonden in dit onderzoek geen significante variatie over de tijd van de dag. Ondanks de variatie in de absorptie snelheidsconstante van levofloxacine lieten simulaties van een eenmaal-daags doseerscheme zien dat de blootstelling aan en de maximale concentratie van levofloxacine, twee parameters die van belang zijn voor de effectiviteit van het middel als antibiotica, niet worden beïnvloed door het tijdstip van de dag. Op basis van deze bevindingen hebben we geconcludeerd dat levofloxacine gedoseerd kan worden zonder rekening te houden met het tijdstip van de dag, in ieder geval wat betreft de farmacokinetiek. Desalniettemin zijn deze resultaten van belang voor medicijnen met vergelijkbare fysicochemische eigenschappen als levofloxacine maar met een nauwere therapeutische index.

In de klinische studie beschreven in Hoofdstuk 4 hebben we ook het effect van levofloxacine op het QT interval gemeten. Het QT interval is een marker voor ventriculaire repolarisatie dat is af te lezen van het electrocardiagram. Het is bekend dat levofloxacine, net als veel andere medicijnen, het QT interval in beperkte mate verlengt omdat het een kaliumkanaal in de hartspiercellen blokkeert. Dit is een negatieve bijwerking van veel geneesmiddelen, dat in combinatie met andere risicofactoren in zeldzame gevallen kan leiden tot aritmie en hartdood. Het was onbekend of het effect van levofloxacin op het QT interval afhangt van het tijdstip van de dag. In **Hoofdstuk 5** hebben we het effect van het tijdstip van de dag op de relatie tussen de concentratie van levofloxacine en de lengte van het QT interval onderzocht. Een farmacokinetisch-farmacodynamisch model is ontwikkeld om te kunnen controleren voor variaties in de farmacokinetiek, hartslag en 24-uurs ritmes in de basislijn van het QT interval. We vonden dat het effect van levofloxacine op het QT interval grote en systmatische variatie vertoont over de loop van de dag. Uit het gebruik van simulaties blijkt dat, als een gevolg van deze variatie, levofloxacine-geïnduceerde QT interval verlenging afhangt van het tijdstip waarop de medicatie wordt toegediend. Het grootste effect wordt voorspeld om 14:00 uur en het kleinste effect om 6:00 uur. Uit deze bevindingen blijkt dat huidige aanpak waarmee het effect van medicijnen op het QT interval

wordt onderzocht kan leiden tot een onjuiste beoordeling van het risico voor de patient.

Kennis verwerven van de concentratie van medicijnen op de plek waar ze hun effect uitoefenen is een belangrijk aspect voor de ontwikkeling en optimalisatie van farmacolgische behandelingen. Dit geldt met name wanneer hun doelgebied zich bevindt op een plek die voor medicijnen moeilijk te bereiken is, zoals de hersenen. Naast de structurele bescherming die geboden wordt door de bloed-hersen barrière, worden de hersenen ook beschermd door gespecialiseerde efflux transporter-eiwitten zoals P-glycoproteïne (P-gp). Deze transporters pompen potentieel giftige stoffen, zoals medicijnen, uit de hersenen terug naar het bloed. Het doel van het onderzoek beschreven in **Hoofdstuk 6** was om de 24-uurs variatie te bepalen in de verdeling van het P-gp substraat quinidine naar de hersenen. In een preklinische diermodel hebben we gevonden dat de blootstelling aan quinidine in de hersenen na intraveneuze toediening afhankelijk is van het tijdstip van de dag. Vervolgens hebben we intracerebrale microdialyse experimenten uitgevoerd en de data geanalyseerd door middel van semi-fysiologisch modelleren. Uit deze experimenten bleek dat de tijdsafhankelijke transport van quinidine naar de hersenen wordt veroorzaakt door een hogere activiteit in P-gp gemedieerd transport van hersenweefsel naar plasma tijdens de nacht. Deze resultaten laten zien dat het tijdstip van de dag een belangrijke rol speelt bij de verdeling van P-gp substraten naar de hersenen. Dit biedt een potentiële nieuwe strategie om de dosering van medicijnen voor hersenziektes te optimaliseren.

In **Hoofdstuk 7** hebben we de 24-uurs variatie in bloed- en brein farmacokinetiek van morfine in een preklinisch dier model onderzocht. Morfine is een substraat voor verschillende transport eiwitten die tot expressie komen in de bloed-hersenbarrière. Het gebruik van twee stoffen die de activiteit van deze transport eiwitten remmen stelde ons in staat om de relatieve bijdrage van actief en passief transport van de farmacokinetische processen te onderzoeken. We vonden dat de actieve processen die betrokken zijn bij de regulatie van de klaring van morfine en de metaboliet M3G vanuit plasma aanzienlijke 24-uurs variatie vertoont. Bovendien blijkt dat de efflux van morfine uit de hersenen terug naar het bloed gekenmerkt wordt door een 24-uurs ritme met de minste efflux tijdens de schemerperiodes. Simulaties laten zien dat als een gevolg hiervan de blootstelling aan morfine in de hersenen en aan M3G in plasma afhangt van het tijdstip waarop morfine wordt toegediend. Hieruit kan geconcludeerd worden dat het tijdstip van de dag een bron van variatie is in de farmacokinetiek van morfine. Dit kan een verklaring zijn voor de dag- en nachtritmes die zijn gevonden in de pijnbestrijdende effecten van morfine die zijn waargenomen in eerdere onderzoeken.

Het onderzoek dat wordt beschreven in dit proefschrift werd besproken in Hoofdstuk 8. Samenvattend laten deze onderzoeken zien dat tijdstip van de dag een belangrijke bron van variatie kan zijn in de farmacokinetische en farmacodynamische parameters van medicijnen, die door middel van wiskundige modellen en simulaties kunnen worden geïdentificeerd en gekwantificeerd. Meer begrip van het effect van tijdstip van de dag op de blootstelling en het effect van medicijnen is noodzakelijk om deze bron van variatie te kunnen verklaren. Bovendien zouden chronofarmacologische aspecten niet over het hoofd

gezien moeten worden om te kunnen profiteren van de systematische schommelingen in fysiologische processen tijdens het ontwikkelen en optimaliseren van medicijnen.

# CURRICULUM VITAE

Laura Kervezee was born on the 26th of January 1989 in The Hague, the Netherlands. In 2007 she completed her secondary bilingual education (tvwo) at the Alfrink College in Zoetermeer and obtained the International Baccalaureate English A2 certificate.

She continued her studies at the University College Utrecht, where she majored in Biomedical Science and Neuroscience. In 2009, she spent a semester at Monash University in Melbourne (Australia) as part of an exchange program. Her interest in chronobiology developed during her bachelor's studies and was strengthened by an internship at the Academic Medical Center in Amsterdam on circadian rhythms in adipose tissue and by writing a literature review on the circadian clock in health and disease. In 2010, she received her Bachelor of Science degree summa cum laude from the University of Utrecht. In 2011, she obtained her master's degree in Neuroscience with distinction from University College London in England.

In January 2012, she started her PhD research within the STW OnTime consortium under the supervision of Prof. Johanna H. Meijer at the laboratory of Neurophysiology, Department of Molecular Cell Biology of the Leiden University Medical Center (LUMC) in collaboration with Dr. Elizabeth C.M. de Lange at the Leiden Academic Centre of Drug Research (LACDR) and Prof. Koos Burggraaf at the Center for Human Drug Research (CHDR) in Leiden. The results of this research are described in this thesis. During this period, she has been involved with the development of teaching material on chronobiology for secondary schools on behalf of the STW OnTime committee and wrote regular columns in the independent university newspaper Mare in 2015 and 2016. In 2015, she was awarded with the first prize in an essay competition from the Royal Holland Society for Sciences (KHMW) and the Dutch national newspaper NRC Handelsblad for an essay on the busyness of modern life. In 2016, she worked temporarily for the graduate school of the LUMC.

Currently, she is working as a postdoctoral researcher at the McGill University in Montreal, Canada, on a project addressing circadian maladaptation in shift workers in the groups of Prof. D. Boivin and Dr. N. Cermakian.

# CURRICULUM VITAE

Laura Kervezee werd geboren op 26 januari 1989 in 's Gravenhage, Nederland. In 2007 voltooide zij haar tweetalig-vwo opleiding cum laude aan het Alfrink College in Zoetermeer en behaalde ze haar International Baccalaureate English A2 certificaat.

Ze zette haar studie voort aan het University College Utrecht, waar ze als hoofdrichting biomedische wetenschappen en neurowetenschappen koos. In 2009 studeerde zij aan de Monash University in Melbourne (Australië) als onderdeel van een uitwisselingsprogramma. Haar interesse in chronobiologie ontwikkelde zich tijdens deze bachelor opleiding en werd versterkt door een stage bij het Academisch Medisch Centrum in Amsterdam onder begeleiding van Prof. A. Kalsbeek naar circadiane ritmes in vetweefsel en door het schrijven van een literatuuroverzicht over de circadiane klok in gezondheid en ziekte. In 2010 behaalde ze haar Bachelor of Science diploma summa cum laude van de Universiteit van Utrecht. In 2011 voltooide ze haar master opleiding in neurowetenschappen met het predicaat distinction van University College London in het Engeland.

In januari 2012 begon zij met haar promotieonderzoek in het kader van het STW OnTime consortium onder begeleiding van Prof. Johanna H. Meijer in de sectie Neurofysiologie van het Leids Universitair Medisch Centrum (LUMC), in samenwerking met Dr. Elizabeth C.M. de Lange van het Leiden Academic Centre for Drug Research (LACDR) en Prof. Koos Burggraaf van het Center for Human Drug Research (CHDR) in Leiden. De resultaten van dit onderzoek worden beschreven in dit proefschrift. Gedurende deze periode is zij betrokken geweest bij de ontwikkeling van lesmateriaal over chronobiologie voor middelbare scholieren namens de STW OnTime commissie en schreef zij vanaf 2015 regelmatig columns voor het onafhankelijke universitaire weekblad Mare. In 2015 won zij de eerste prijs in een essay wedstrijd van de Koninklijke Hollandse Maatschappij der Wetenschappen (KHMW) en het NRC Handelsblad voor een essay over drukte in het hedendaagse leven. In 2016 heeft ze tijdelijk gewerkt voor de graduate school van het LUMC.

Momenteel doet ze als postdoc onderzoek aan de McGill University in Montreal, Canada, naar circadiane maladaptatie als gevolg van werken in nacht- en ploegendiensten in de groepen van Prof. D. Boivin en Dr. N. Cermakian.

# LIST OF PUBLICATIONS

**Kervezee L**, Stevens J, Birkhoff W, Kamerling IMC, de Boer T, Dröge M, Meijer JH, Burggraaf J (2016): Identifying 24-hour variation in the pharmacokinetics of levofloxacin: a population pharmacokinetic approach. Br. J. Clin. Pharmacol. 81: 256–268.

**Kervezee L**, Gotta, V, Stevens J, Birkhoff W, Kamerling IMC, Danhof M, Meijer JH, Burggraaf J: Levofloxacin-induced QTc prolongation depends on the time of drug administration. CPT Pharmacometrics Syst. Pharmacol. doi: 10.1002/psp4.12085

**Kervezee L**, Hartman R, van den Berg, DJ, Shimizu S, Emoto-Yamamoto Y, Meijer JH, de Lange ECM (2014): Diurnal Variation in P-glycoprotein-Mediated Transport and Cerebrospinal Fluid Turnover in the Brain. AAPS J. 16: 1029–1037.

van Rongen A*, **Kervezee L**\*, Brill M, van Meir H, den Hartigh J, Guchelaar HJ, Meijer JH, Burggraaf J, van Oosterhout F (2015): Population Pharmacokinetic Model Characterizing 24-Hour Variation in the Pharmacokinetics of Oral and Intravenous Midazolam in Healthy Volunteers. CPT Pharmacometrics Syst. Pharmacol. 4: 454–464.
*These authors contributed equally

**Kervezee L**, Hartman R, van den Berg DJ, Meijer JH, de Lange ECM (2016): Daily variation in the pharmacokinetics and brain distribution of morphine. *Submitted*

*Publications not in this thesis*
**Kervezee L** (2015): Een drukte van belang? in: Koninklijke Hollandsche Maatschappij der Wetenschappen bekroonde essays 2015. ISBN 978-90-78396-17-8. Tevens gepubliceerd in NRC Handelsblad onder de titel We hebben het druk druk druk. Maar het is oké om nee te zeggen (10 oktober 2015).

Blom ML, **Kervezee L** (2014): Het verminderen van negatief gedrag in de gymles. Lichamelijke opvoeding 102: 38-40

# DANKWOORD

Een promotietraject is als een triathlon: het vereist een lange adem en, al moet je het uiteindelijk alleen afleggen, het was lang niet zo leuk geweest zonder de steun, hulp en afleiding van de mensen om je heen. Nu de eindstreep echt in zicht is, een woord van dank aan iedereen die van dichtbij of veraf betrokken is geweest bij de totstandkoming van dit proefschrift.

Prof. Meijer, beste Joke, bedankt voor het vertrouwen dat je me vanaf het begin hebt gegeven. Je enthousiasme en positiviteit heb ik altijd erg gewaardeerd. Prof. Burggraaf, beste Koos, jouw nuchtere kijk en jouw vermogen om – in mijn hoofd ingewikkelde – zaken een stuk makkelijker te maken waren erg verhelderend. Ik ben je erg dankbaar voor de kans om mijn project uit te voeren bij het CHDR: het was een erg leerzame ervaring waar ik de rest van mijn leven profijt van zal hebben. Beste Liesbeth, je gedrevenheid voor het onderzoek en je oog voor detail zijn erg inspirerend. Bedankt voor de fijne samenwerking.

Onderzoek uitvoeren in samenwerking met drie verschillende afdelingen maakt de lijst van collega's die mij hebben geholpen, gesteund of van de nodige gezelligheid hebben voorzien, te lang om iedereen op deze plek persoonlijk te bedanken. Collega's bij Neurofysiologie, in zo'n fantastische chronobiologie groep kon ik mij niet anders dan meteen thuis voelen. Bedankt voor alle gezelligheid door de jaren heen en vooral ook de geslaagde congresbezoeken.

Collega's bij het CHDR, bedankt voor alle hulp die jullie mij hebben gegeven bij de voorbereiding en (nachtelijke) uitvoer van mijn studie. Willem, ik waardeerde het erg dat je tijdens de uitvoer van mijn onderzoek bij het CHDR dag en nacht voor me klaar stond, dankjewel. Jasper, onder jouw hoede zette ik mijn eerste stapjes in de wereld van het modelleren. Bedankt voor al je geduldige uitleg, leuke discussies en prettige samenwerking.

Collega's bij Farmacologie, met een glimlach kijk ik terug op de fijne tijd die ik bij jullie heb gehad als "adoptie-promovendus". Ik heb veel geleerd (en gelachen)! Bedankt ook voor alle sportieve en minder sportieve gezelligheid. Robin, jij was vaak letterlijk een lichtpuntje tijdens lange, donkere, experimentdagen en ik heb veel bewondering voor je vakkundigheid. Bedankt! Dirk-Jan, bedankt voor al je (HP)LC(/MS) hulp!

Dank aan alle mensen buiten het lab die mijn promotietraject een stuk leuker hebben gemaakt. Alle etentjes, fietstochten, borrels, vakanties, triathlons en lange gesprekken vormden een welkome en onuitputtelijke bron van afleiding waar ik altijd naar uitkeek. Het STW OnTime consortium wil ik bedanken voor de kans om bij te dragen aan de bekendheid van chronobiologie onder middelbare scholieren en hun leraren. Het universitair weekblad Mare dank ik voor de kans om mijn hersenspinsels te mogen delen met het Leidse publiek.

Paranimfen, bedankt dat jullie er voor me willen zijn. Ivo, je kent me langer dan wie dan ook en je vult me aan, dus met jou naast me moet die verdediging wel goed komen. Juul, ik waardeer je humor, gezelligheid en (wetenschappelijke) gedrevenheid en ik ben er trots op dat je mijn paranimf wil zijn.

Pap en mam, jullie hebben me altijd de vrijheid en het vertrouwen gegeven om mijn eigen weg te vinden. Bedankt voor alle kansen die ik dankzij jullie heb kunnen aangrijpen. Oma, tijdens mijn hele promotietraject was u een vast rustpuntje in mijn week. Ik kon altijd bij u terecht voor een kopje soep, een luisterend oor en wijze woorden, dankuwel.

Als laatste: Super Mario! Ik bewonder je om wie je bent en ik ben je heel dankbaar voor het mooier maken van mijn leven.

LAURA